UAV AND FIELD SPECTROMETER BASED REMOTE SENSING FOR MAIZE PHENOTYPING, VARIETAL DISCRIMINATION AND YIELD FORECASTING

Walter Chivasa

A thesis submitted to the College of Agriculture, Engineering and Science, at the University of KwaZulu-Natal, in fulfilment of the academic requirements for the degree of Doctor of Philosophy in Environmental Science

Academic Supervisor: Professor Onisimo Mutanga

Academic Advisor: Dr. Chandrashekhar Biradar

Pietermaritzburg,

South Africa

July 2020

ABSTRACT

Maize is the major staple food crop in the majority of Sub-Saharan African (SSA) countries. However, production statistics (croplands and yields) are rarely measured, and where they are recorded, accuracy is poor because the statistics are updated through the farm survey method, which is error-prone and is time-consuming, and expensive. There is an urgent need to use affordable, accurate, timely, and readily accessible data collection and spatial analysis tools, including robust data extraction and processing techniques for precise yield forecasting for decision support and early warning systems. Meeting Africa's rising food demand, which is driven by population growth and low productivity requires doubling the current production of major grain crops like maize by 2050. This requires innovative approaches and mechanisms that support accurate yield forecasting for early warning systems coupled with accelerated crop genetic improvement.

Recent advances in remote sensing and geographical information system (GIS) have enabled detailed cropland mapping, spatial analysis of land suitability, crop type, and varietal discrimination, and ultimately grain yield forecasting in the developed world. However, although remote sensing and spatial analysis afforded us unprecedented opportunities for detailed data collection, their application in maize in Africa is still limited. In Africa, the challenge of crop yield forecasting using remote sensing is a daunting task because agriculture is highly fragmented, cropland is spatially heterogeneous, and cropping systems are highly diverse and mosaic. The dearth of data on the application of remote sensing and GIS in crop yield forecasting and land suitability analysis is not only worrying but catastrophic to food security monitoring and early warning systems in a continent burdened with chronic food shortages. Furthermore, accelerated crop genetic improvement to increase yield and achieve better adaptation to climate change is an issue of increasing urgency in order to satisfy the ever-increasing food demand. Recently, crop improvement programs are exploring the use of remotely sensed data that can be used cost-effectively for varietal evaluation and analysis in crop phenotyping, which currently remains a major bottleneck in crop genetic improvement. Yet studies on evaluation of maize

varietal response to abiotic and biotic stresses found in the target production environments are limited.

Therefore, the aim of this study was to model spatial land suitability for maize production using GIS and explore the potential use of field spectrometer and unmanned aerial vehicles (UAV) based remotely sensed data in maize varietal discrimination, high-throughput phenotyping, and yield prediction. Firstly, an overview of major remote-sensing platforms and their applicability to estimating maize grain yield in the African agricultural context, including research challenges was provided. Secondly, maize land suitability analysis using GIS and analytical hierarchical process (AHP) was performed in Zimbabwe. Finally, the utility of proximal and UAV-based remotely sensed data for maize phenotyping, varietal discrimination, and yield forecasting were explored.

The results showed that the use of remote sensing data in estimating maize yield in the African agricultural systems is still limited and obtaining accurate and reliable maize yield estimates using remotely sensed data remains a challenge due to the highly fragmented and spatially heterogeneous nature of the cropping systems. Our results underscored the urgent need to use sensors with high spatial, temporal and spectral resolution, coupled with appropriate classification techniques and accurate ground truth data in estimating maize yield and its spatio-temporal dynamics in heterogeneous African agricultural landscapes for designing appropriate food security interventions. In addition, using modern spatial analysis tools is effective in assessing land suitability for targeting location-specific interventions and can serve as a decision support tool for policymakers and land-use planners regarding maize production and varietal placement.

Discriminating maize varieties using remotely sensed data is crucial for crop monitoring, high-throughput phenotyping, and yield forecasting. Using proximal sensing, our study showed that maize varietal discrimination is possible at certain phenological growth stages at the field level, which is crucial for yield forecasting and varietal phenotyping in crop improvement. In addition, the use of proximal remote sensing data with appropriate pre-processing algorithms such as auto-

scaling and generalized least squares weighting significantly improved the discrimination ability of partial least square discriminant analysis, and identify optimal spectral bands for maize varietal discrimination. Using proximal sensing was not only able to discriminate maize varieties but also identified the ideal phenological stage for varietal discrimination. Flowering and onset of senescence appeared to be the most ideal stages for accurate varietal discrimination using our data.

In this study, we also demonstrated the potential use of UAV-based remotely sensed data in maize varietal phenotyping in crop improvement. Using multi-temporal UAV-derived multispectral data and Random Forest (RF) algorithm, our study identified not only the optimal bands and indices but also the ideal growth stage for accurate varietal phenotyping under maize streak virus (MSV) infection. The RF classifier selected green normalized difference vegetation index (GNDVI), green Chlorophyll Index (CIgreen), Red-edge Chlorophyll Index (CIred-edge), and the Red band as the most important variables for classification. The results demonstrated that spectral bands and vegetation indices measured at the vegetative stage are the most important for the classification of maize varietal response to MSV. Further analysis to predict MSV disease and grain yield using UAV-derived multispectral imaging data using multiple models showed that Red and NIR bands were frequently selected in most of the models that gave the highest prediction precision for grain yield. Combining the NIR band with Red band improved the explanatory power of the prediction models. This was also true with the selected indices. Thus, not all indices or bands measure the same aspect of biophysical parameters or crop productivity, and combining them increased the joint predictive power, consequently increased complementarity.
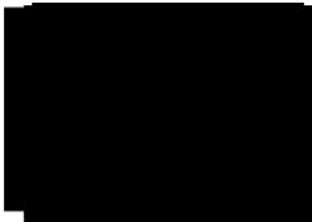
Overall, the study has demonstrated the potential use of spatial analysis tools in land suitability analysis for maize production and the utility of remotely sensed data in maize varietal discrimination, phenotyping, and yield prediction. These results are useful for targeting location-specific interventions for varietal placement and integrating UAV-based high-throughput phenotyping systems in crop genetic improvement to address continental food security, especially as climate change accelerates.

PREFACE

The research work described in this thesis was carried out in the School of Agricultural, Earth and Environmental Sciences (SAEES), University of KwaZulu-Natal, Pietermaritzburg, South Africa, from July 2016 to June 2020, under the supervision of Prof. Onisimo Mutanga (School of Agricultural, Earth and Environmental Sciences, University of KwaZulu Natal, South Africa).

I would like to declare that the research work reported in this thesis has never been submitted in any form to any other university. It therefore represents my original work, except where due acknowledgments are made.

Walter Chivasa Signed: Date: 31 July 2020

As the candidate's supervisor, I certify the above statement and have approved this thesis for submission.

Prof. Onisimo Mutanga Signed   Date: _11 Aug 2020_____

DECLARATION 1 – PLAGIARISM

I, **Walter Chivasa**, declare that:

1. The research reported in this thesis, except where otherwise indicated, is my original research,

2. This thesis has not been submitted for any degree or examination at any other university,

3. This thesis does not contain other persons' data, pictures, graphs, or other information, unless specifically acknowledged as being sourced from other persons,

4. This thesis does not contain other persons' writing, unless specifically acknowledged as being sourced from other researchers. Where other written sources have been quoted, then:

   a. Their words have been re-written, but the general information attributed to them has been referenced;

   b. Where their exact words have been used, then their writing has been placed in italics and inside quotation marks, and referenced.

5. This thesis does not contain text, graphics, or tables copied and pasted from the Internet, unless specifically acknowledged and the source being detailed in the thesis and in the References section.

Signed:
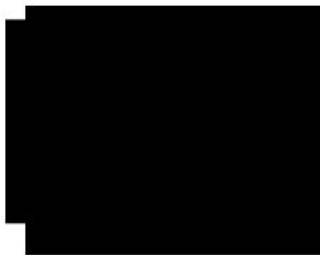
DECLARATION 2 – PUBLICATIONS AND MANUSCRIPTS

1. **Chivasa, W.**, Mutanga, O., Biradar, C. M. **2017**. Application of remote sensing in estimating maize grain yield in heterogeneous African agricultural landscapes: A review. *International Journal of Remote Sensing* 38 (23), 6816-6845. http://doi.org/10.1080/01431161.2017.1365390

2. **Chivasa, W.**, Mutanga, O., Biradar, C. M. **2019**. Mapping land suitability for maize (*Zea mays* L.) production using GIS and AHP technique in Zimbabwe. *South African Journal of Geomatics*, 8(2), 265-281. http://dx.doi.org/10.4314/sajg.v8i2.11

3. **Chivasa W.**, Mutanga, O, Biradar, C.M. **2019**. Phenology-based discrimination of maize (*Zea mays* L.) varieties using multi-temporal hyperspectral data. *Journal of Applied Remote Sensing* 13(1), 017504 (**2019**). http://dx.doi.org/10.1117/1.JRS.13.017504.

4. **Chivasa W.**, Mutanga, O., Biradar, C. M. **2020**. UAV-based multispectral phenotyping for disease resistance to accelerate crop improvement under changing climate conditions. *Remote Sensing* 2020, 12, 2445. http://dx.doi.org/10.3390/rs12152445

5. **Chivasa W.**, Mutanga, O., Burgueño, J. **2020**. UAV-based high throughput phenotyping to increase prediction and selection accuracy in maize varieties under artificial MSV inoculation. *Computers and Electronics in Agriculture* (**in review**).

Signed:
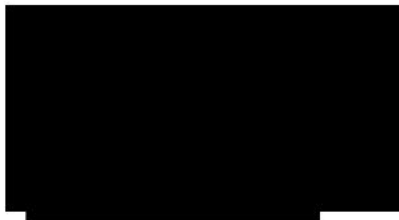
DEDICATION

To my wife (Vongai) and children (Tatenda, Tadiwanashe, Makomborero and Masimba).

ACKNOWLEDGEMENTS

TABLE OF CONTENTS

LIST OF FIGURES

LIST OF TABLES

SECTION I: GENERAL INTRODUCTION AND THEORETICAL PERSPECTIVE

Source: Seed Co Photo Library

CHAPTER 1: GENERAL INTRODUCTION

1.1 Maize and food security

Maize (Zea mays L.) is the second most commonly grown crop worldwide and the number one staple food in Africa where it accounts for more than 50% of the energy requirements and grown on more than 27 million ha in Sub-Saharan Africa (SSA). Planted area and yield information are critical for food security planning. Globally, food requirement is expected to double current demand by 2050 due to population and socio-economic growth (Ray et al., 2012). Meeting food requirements by 2050 in Africa requires doubling the current grain production of major grain crops like maize, wheat, and rice by 2050 (Tilman *et al*., 2011; Tubiello, 2012; Valin *et al*., 2013). The human population in Africa is forecasted to double by 2050 (Ezeh *et al*., 2012). Ironically, Africa is one of the hardest hit by food shortages, yet 75 % of its population depends on agriculture for subsistence and work. Furthermore, agricultural statistics (croplands and yields) in Africa are rarely measured, and where they are recorded, accuracy is poor (Carletto *et al*., 2015).

The pressure for increased food production is also compounded by the impending threats of climate change that alters water availability due to droughts, floods, poor soil fertility due to floods-induced soil erosion, and outbreaks of pests and diseases. These challenges are reducing crop productivity. In order to meet food requirements, farmers end up expanding crop fields by converting environmentally-sensitivity areas into croplands. Mitigating these challenges and be able to meet food security by 2050 will require innovative approaches and mechanisms that support accurate yield forecasting for early warning systems, land suitability analysis, good agronomic practices, and accelerated crop genetic improvement.

Recent advances in remote sensing and geographical information system (GIS) have enabled detailed cropland mapping, spatial analysis of land suitability, crop type, and varietal discrimination, and ultimately grain yield forecasting. However, the challenge of crop yield forecasting using remote sensing in Africa is a daunting task because agriculture is highly fragmented, cropland is spatially heterogeneous, and cropping systems are highly diverse and mosaic (Delrue *et al*., 2013; Vancutsem *et al*., 2013). Yet improving the continent's food security requires strong early warning systems that depend on precise and current data on

the maize spatial distribution, land suitability analysis, and yield estimates. In addition, due to climate change, there is an urgent need to accelerate crop genetic improvement as a mitigation measure, which can be achieved by combining genomics, rapid cycling, and phenomics (systematic study of phenotypes).

1.2 Spatial analysis of land suitability for maize production

Geospatial technology (remote sensing, GIS, and global positioning system) has found many applications in agriculture, particularly cropland mapping, land suitability analysis, above-ground biomass, and grain yield estimation, precision farming, and recently high throughput crop phenotyping in plant breeding. The advantages of geospatial technology over conventional ground-based methods include timely, cost-effective, precise, and multi-temporal measurements over large areas, among others. For example, GIS offers the power of storing, manipulation, analysis, and visualizing different spatial and non-spatial data, including land-use/land-cover. Thus geospatial technology provides cost-effective methods for cropland analysis (condition, productivity, and spatial extent). Although the importance of geospatial technology in agriculture is becoming widely recognized, their application in highly fragmented African agriculture is limited, especially land suitability analysis and remote sensing of maize. Yet maize productivity is decreasing due to climate change causing some land to be unsuitable for maize production without interventions like irrigation development. GIS can be effective in spatial analysis of land suitability for targeting location-specific interventions and can serve as a decision support tool.

1.3 Remote sensing for maize phenotyping, varietal discrimination and yield prediction

To satisfy the ever-increasing food demand, a better mechanism that supports the monitoring and forecasting of crop productivity is urgently needed. However, the mechanisms depend on precise and accurate information on the spatial distribution of maize and yield estimates. At the local scale, crop yield is variety-dependent. Therefore, techniques to discriminate maize varieties and estimate their productivity are needed. This is critical for a variety of reasons, including disease and pest assessments and yield forecasting. In addition, our ability to adapt maize production to future climates will not only depend on accurate prediction of future climate scenarios, but also on the development of robust adaptation strategies that address

the challenges associated with climate change. Such adaptation strategies include improved crop varieties that are resilient to biotic and abiotic stresses. Fortunately, breeders can now generate large numbers of new varieties due to advances in technologies (Phillips et al., 2010; Poland et al., 2015). However, plant phenotyping remains a major bottleneck for improving the selection efficiency in breeding (Furbank and Tester, 2011; Araus and Cairns, 2014). Phenotyping is the measurement of individual plant traits and physiology at the plant- or canopy-scale (Hickey *et al*., 2019). Recent advances in remote sensing tools are promising to accelerate screening, selection, and advancement of varieties in plant breeding. Remote sensing is the measurement of the physical properties of distant objects and their environments using reflected and emitted energy (Moore, 1979). In plant sciences, remote sensing is used to record plants or crop parameters in a non-invasive manipulation or without direct contact. Recently, the concept has encompassed proximal (close-range) sensing of plants (Mahlein *et al*., 2012; Oerke *et al*., 2014).

1.4 Remote sensing platforms

Remote sensing-based methods can be classified into three platforms: proximal, aerial, and space-borne satellites (Wójtowicz et al., 2016). Each platform has its own advantages and disadvantages depending on the task at hand. Therefore, the selection of which platform to use depends on the intended use and desired outputs. For example, satellite sensors are suitable for large-scale yield estimation and cropland mapping but they lack plot-level precision required in data collection in plant breeding for variety analysis due to their low spectral and temporal resolution. On the other hand, proximal sensing is labor-intensive, of limited scalability, and unsuitable when fields are too wet to allow traffic movement (Tattaris et al., 2016). Options from manned aerial, high spectral resolution remote sensing platforms are costly and are limited by operational complexity for application in small breeding plots (Hoffer et al., 2014; Jimenez-Berni et al., 2009). Consequently, there is a need to evaluate affordable alternative platforms with acceptable accuracy like unmanned aerial vehicles (UAVs) that are applicable at plot-level.

Therefore, there is an urgent need to: (1) apply spatial analytical tools based on GIS to model land suitability for maize production and varietal placement; (2) test the potential of field spectrometer for proximal sensing of maize in varietal discrimination and field-based

phenotyping; and (3) explore aerial remote sensing using UAVs for high-throughput phenotyping in maize and yield prediction under different biotic stresses like maize streak virus disease. These are the focuses of this thesis.

1.5 Aim and objectives

1.5.1 Aim

The aim was to model spatial suitability for maize production using GIS and explore the utility of remotely sensed data in maize varietal discrimination, high-throughput phenotyping, and yield prediction.

1.5.2 Objectives

The specific objectives were:

1. To review and synthesize different yield forecasting methods in maize using conventional approaches and remote sensing and highlight the inherent challenges when applied in heterogeneous agricultural landscapes;
2. To evaluate the potential use of GIS in modeling land suitability for maize production using physical environmental and climatic factors for spatial decision-making support in maize crop placement in Zimbabwe;
3. To explore *in situ* maize varietal discrimination using field spectrometer based proximal sensing and multivariate techniques in order to identify the ideal phenological stage(s) for varietal discrimination;
4. To assess the utility of UAV-derived remotely sensed data for image-based high-throughput plant phenotyping in maize varieties under artificial maize streak virus (MSV) inoculation;
5. To develop prediction models based on multi-temporal UAV-based remote sensing data in maize under artificial MSV inoculation and identify the most ideal phenological stage(s) for yield prediction to increase selection accuracy in maize breeding.

1.6 Study area

The research work was conducted at the Rattray Arnold Research Station (RARS) in Zimbabwe, Longitude 31⁰12' 41.35" E, Latitude 17⁰40' 20.07" S, located at an altitude of 1360 meters above sea level (Figure 1.1). The climate is sub-tropical with an average monthly temperature range of 28–32 °C from November to April, with mean annual precipitation of 865mm per annum received between November and April. RARS is located in the mid-altitude moist environments, representing the major maize growing environments in Southern Africa.
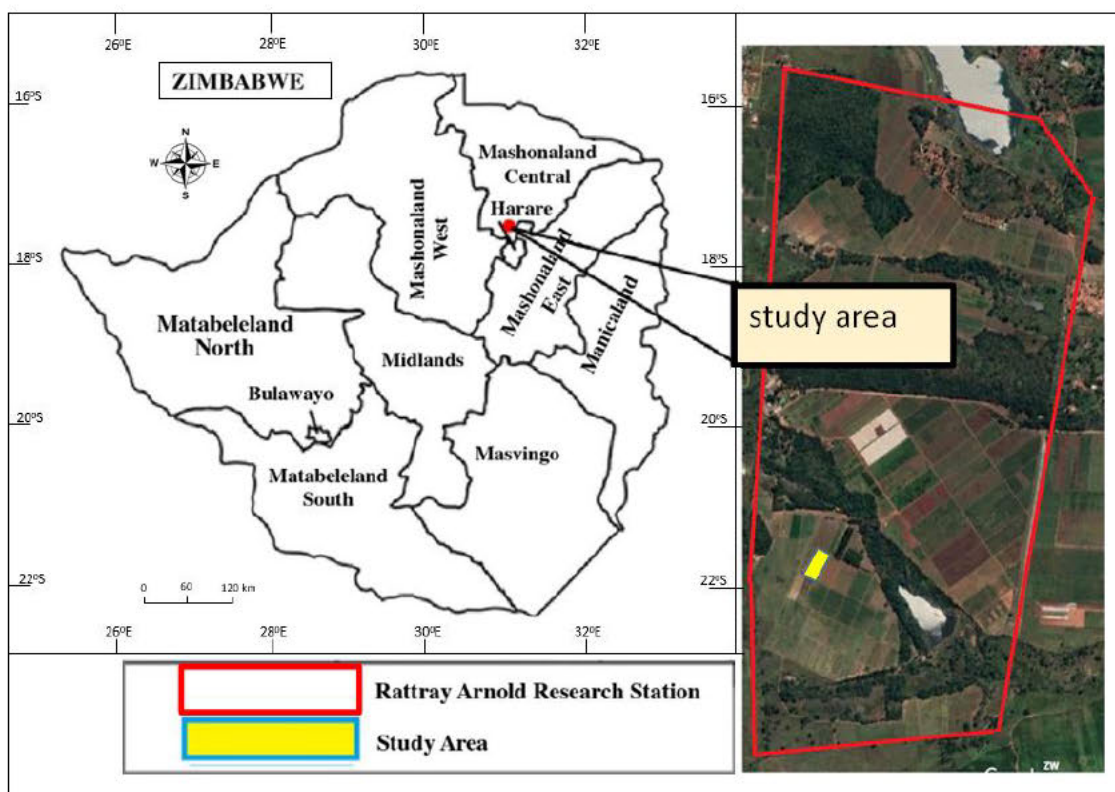
Figure 1.1. The location of the study area at Rattray Arnold Research Station. The figure on the right is the aerial image of Rattray Arnold Research Station (Source: Google Earth images).

1.7 Structure of the thesis

This thesis is divided into four sections. Section I is made up of two chapters: Chapter one is a general introduction to the study; and Chapter two gives a theoretical overview of remote sensing application and associated challenges in maize grain yield estimation using remote

sensing in fragmented and highly heterogeneous agricultural landscapes. Section II details the spatial analysis and proximal sensing of maize. Section III explores innovative aerial remote sensing of maize and yield prediction using UAV-based multispectral data under one of the major biotic stresses found in the major maize growing regions of sub-Saharan Africa (SSA). Section IV presents the synthesis. Chapter two to six are made up of manuscripts published or under consideration in peer-review international scientific journals. The contents and structures of these manuscripts have been maintained and therefore individual chapters have distinct abstract, introduction, materials and methods, results, discussion, and conclusion sub-sections. As such, some overlaps and repetitions may be found in some instances, especially in the introduction and methodology sections of these chapters. However, the overlaps are presumed to be of very limited consequence because the chapters are meant to be standalone yet interrelated peer-reviewed journal articles, which can be read separately, without losing the overall context of the study. Thus, the thesis is made up of seven chapters, split into four sections: general introduction and theoretical perspective (Section I); spatial analysis and proximal sensing of maize (Section II); UAV-based aerial remote sensing and yield prediction of maize (Section III); and synthesis (Section IV).

1.7.1 Section I: General introduction and theoretical perspective

1.7.1.1 Chapter One: General introduction

Chapter one is a brief introduction that gives an outline and general statement of the problem, ideas, motives, and justification for the study. It gives a brief overview of the importance of maize production, its role in fulfilling food security, challenges associated with maize production as climates change accelerates, and how this can be mitigated using combined innovative approaches like geospatial analysis, remote sensing, and crop genetic improvement. The chapter further highlights the scarcity of information on maize yield estimates in highly fragmented and heterogeneous African agricultural landscapes and limited studies using remote sensing in maize. The study's aim and objectives are provided.

1.7.1.2 Chapter Two: Theoretical perspective

This chapter gives a state-of-the-art review of the use of remotely sensed data in estimating maize grain yield in highly fragmented African agricultural landscapes. The chapter highlights the challenges faced by researchers and policymakers when forecasting maize yields using conventional ground-based survey methods and remote sensing in highly fragmented and heterogeneous agricultural landscapes. This review represents the first step to identify information gaps that require further investigation in estimating maize yield in heterogeneous agricultural systems in order to increase our understanding of African agriculture and improve food security through early warning systems, spatial analysis, and accelerated crop improvement.

1.7.2 Section II: Spatial analysis and proximal sensing of maize

1.7.2.1 Chapter Three: Spatial analysis of land suitability using GIS and AHP

This chapter evaluates land suitability for maize production using geographic information system (GIS) and analytic hierarchy process (AHP) using a multi-criteria evaluation (MCE) process. It integrates four thematic maps (rainfall, temperate, soil type, and slope) through an overlay technique to produce a maize production suitability map. The final maize suitability map was divided into highly suitable, suitable, moderately suitable, marginally suitable, and not suitable land for maize production. The maize suitability classes were validated using long-term maize grain yield. This land suitability analysis is crucial in understanding the land suitability shifts due to climate change and for targeting location-specific interventions for maize production. The resultant suitability map is an important decision support tool in land use planning and policymaking.

1.7.2.2 Chapter Four: Discriminating maize varieties using proximal remote sensing

In this chapter, we used proximal (close-range) sensing to explore in situ maize varietal discrimination using a field spectrometer and multivariate techniques in order to identify the ideal phenological stage(s) for varietal classification. A growing body of literature shows how the proximal sensing approach enhances the automation of high-throughput field-based phenotyping methods with improved precision and accuracy (Berger *et al*., 2010; Munns et al.,

2010; Araus and Cairns, 2014). Proximal sensing provides higher resolution data for varietal discrimination in phenotyping studies and it allows data collection at multiple view-angles, easy to control illumination and distance from the sensors to plants (White *et al*., 2012).

1.7.3 Section III: Aerial remote sensing and yield prediction of maize

1.7.3.1 Chapter Five: UAV-based multispectral imaging of maize

One of the emerging platforms in aerial remote sensing is the UAVs, developed recently and are proving to be effective sensor bearing platforms in plant phenotyping (Haghighattalab *et al*., 2016; Hu *et al*., 2020). Chapter five explores the utility of a cost-effective multi-temporal UAV-based multispectral data for phenotyping maize varieties in plant breeding. This chapter was premised on the hypothesis that multi-temporal UAV-derived multispectral imaging data is sensitive to MSV disease symptoms that cause distinct discoloration of the aerial parts of maize varieties, and are able to discriminate varieties on the basis of their response to disease infection. MSV is one of the major diseases of maize in sub-Saharan Africa. In this chapter, maize varieties were evaluated for their response to one of the major biotic stresses (MSV) using UAV-derived multispectral band settings and derived vegetation indices using the Random Forest algorithm.

1.7.3.2 Chapter Six: UAV-based yield estimation in maize

The growth in population that is projected to reach 10 billion by 2050 coupled with the effects of climate change on crop diseases poses some of the greatest challenges to achieving global food security. There is an urgent need to accelerate crop genetic improvement as a mitigation measure. This can be achieved by combining genomics, rapid cycling, and field-based high-throughput plant phenotyping. This chapter presents results of an evaluation of the utility of multi-temporal UAV-derived multispectral data in predicting maize streak virus (MSV) disease and grain yield. Modeling grain yield using UAV-derived multispectral data is presented as a useful and reliable phenotyping and selection tool in maize breeding and varietal evaluation.

1.7.4 Section IV: Synthesis

1.7.4.1 Chapter 7: UAV and field spectrometer based remote sensing of maize: a synthesis

Chapter seven summarizes the results, conclusions, and the contribution of this research work in field spectrometer and UAV-based remote sensing for maize phenotyping, varietal discrimination, and yield forecasting. It gives a synthesis of the major highlights of the study and their significance for the spatial analysis and remote sensing of maize at both large-scale and as emerging decision support tools for crop varietal targeting and plant phenotyping in crop genetic improvement. Conclusions are also drawn about the current status, limitations, and future prospects of spatial analysis and remote sensing in modern agriculture. All references cited in this work are provided as a single list at the end of the thesis.

CHAPTER 2: CROP YIELD ESTIMATION: A THEORETICAL PERSPECTIVE

This Chapter is based on:
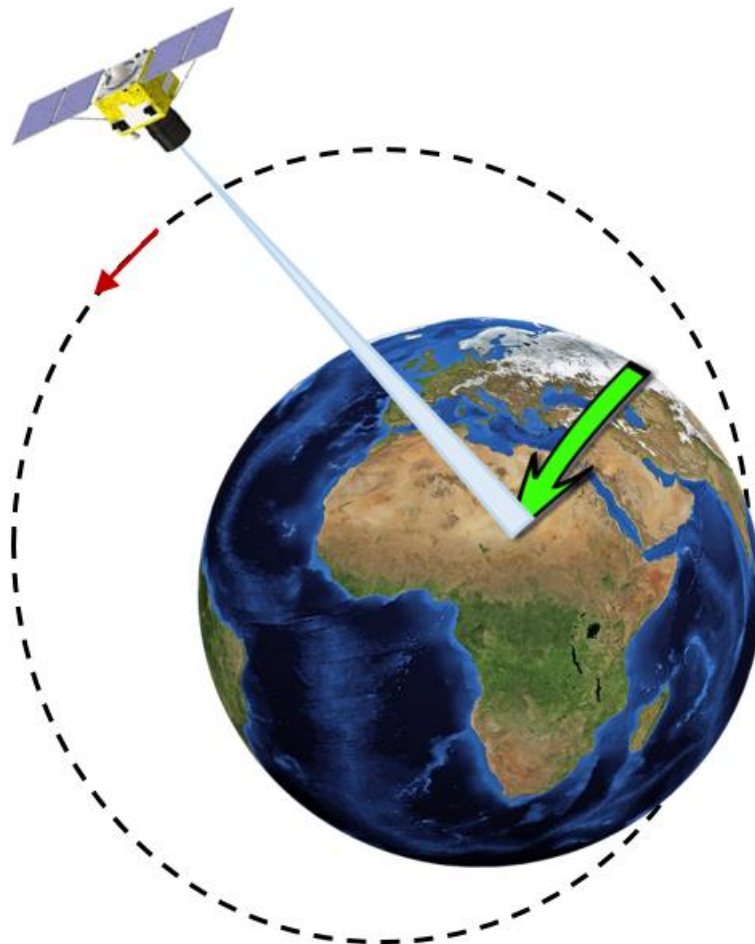
Abstract

Maize (*Zea mays* L.) is the second most commonly grown crop world-wide and number one staple food in Africa where it accounts for more than 50% of the energy requirements. However, despite its widespread cultivation and the significance of maize information in Africa, maize crop maps and yield forecasts are hardly available. Yet systematic area, spatial distribution and maize yield estimates are important in understanding and addressing food security in Africa. Objective monitoring of maize yield statistics in a systematic way is possible with remotely-sensed data. However, absence of maize yield forecasts using remote sensing in Africa has been attributed to the cost of acquiring satellite imagery and the heterogeneity of agricultural landscapes. The recent advances in sensors technology and availability of free high resolution (spatial and temporal) multispectral satellite images affords an opportunity to forecast maize yield as well as mapping its spatial distribution in near real time basis. This review gives an overview of maize yield estimation using remotely-sensed information and its potential application in a fragmented and highly granular agricultural landscapes in Africa, including inherent challenges and research needs. The review was motivated by challenges faced by researchers and national agricultural statistical services agents when forecasting maize yield using conventional ground-based survey methods. These problems include, but are not limited to, restricted accuracy, and cost and time spent resulting in missed opportunities in food security early-warning systems and proper developmental interventions. We conclude that by picking multispectral sensors with high spatial, temporal and spectral resolution, as well as appropriate classification techniques and accurate ground-truthing data, remote sensing can be a practical option for estimating maize grain yield and its spatio-temporal dynamics in heterogeneous African agricultural landscapes for designing appropriate developmental interventions and technological out scaling.

Keywords: remote sensing; heterogeneous agricultural landscapes; maize grain yield forecasting; Africa.

2.1 Introduction

Maize planting area and yield information is crucial in Africa. Maize plays a central role in fulfilling the staple food requirements, because it accounts for more than 50% of the energy

requirements in the continent. Agricultural activities constitute the major part of the African economies, absorbing 70% of workforce and account for 30% of gross domestic product (GDP) (Livingstone *et al*., 2011; World Bank, 2010). To satisfy the ever increasing food demand due to the forecasted doubling of Africa's population by 2050 (Ezeh *et al*., 2012), better mechanism that supports the monitoring and forecasting of food security are urgently needed. National trade, agricultural policies and timely response to food shortages, rely on accurate and timely maize production data. Crop yield information is needed by many users, such as governments, national and international organizations, insurance companies, input manufacturers, commodity brokers, humanitarian organizations, and farmers (Rembold *et al*., 2013). However, despite the importance of maize to food security, its productivity is rarely measured and where production statistics are available, they are often unreliable or not readily available (Biradar and Xiao, 2011; Carletto *et al*., 2015). Preparedness to deal with food security at national and continental level is a function of accurate, accessible and timely crop monitoring information. The role played by accurate and easily accessible maize yield forecasts cannot be over-emphasized. Understanding and responding to food shortages require knowledge of how much grain is available and where. Timely production estimates also depends on accurate mapping of crop area, because total production is a function of total crop area and yield per unit area. Systematic monitoring of maize yield statistics can be achieved using remotely sensed based big-data analytics.

Significant progress has been made in maize yield forecasting using remotely sensed data (Battude *et al*., 2016; Johnson, 2014; Lobell *et al*., 2003; Prasad *et al*., 2006; Shanahan *et al*., 2001). The power of remote sensing in maize yield prediction has been exploited fully by developed nations in agricultural production statistics management. In Africa, the use of satellite imagery in forecasting maize yield is very limited. The recent review by Mutanga *et al*. (2016) noted significant growth in the use of remotely-sensed data in South Africa. However, there is limited application in agriculture, especially on staple food crops. Significant applications in South Africa have been carried on grass (Adjorlolo *et al*., 2012; Adjorlolo *et al*., 2014; Mutanga and Skidmore, 2004; Mutanga *et al*., 2015), plantation forest (Abdel-Rahman *et al*., 2014; Adelabu *et al*. 2014; Dube *et al*., 2014; Dube *et al*., 2015), wetlands (Adam and Mutanga 2009), indigenous forest mapping (Malahlela *et al*., 2014) as well as pests and disease monitoring in plantation forests (Ismail and Mutanga, 2010; Oumar and Mutanga, 2013; 2014).

The dearth of information on application of remote sensing in maize yield estimates in Africa is not only worrying but catastrophic to food security monitoring and early warning systems in a continent burdened with chronic food shortages. Satellite remote sensing monitoring can play a pivotal role in providing the much needed information on maize yield at field, country and continental level (Lobell, 2013).

Recent enhancements in the spatial, temporal and spectral resolution of satellite sensors are making their application a practical option in crop yield monitoring in heterogeneous agricultural systems (Manatsa *et al.*, 2011; Kuri *et al.*, 2014; Wahab *et al.*, 2018) including crop type discrimination (Sibanda and Murwira, 2012). Remotely-sensed yield prediction offers a practical possibility because of quick and large area measurements at relatively low cost (Aronoff, 2005; Lillesand *et al.*, 2014) and its recurrent nature in coverage (Becker-Reshef *et al.*, 2010). Yield prediction in maize using remote sensing has been adequately demonstrated (Battude *et al.*, 2016; Johnson, 2014; Lobell *et al.*, 2003; Prasad *et al.*, 2006; Shanahan *et al.*, 2001). However, this demonstration has largely been in homogeneous agricultural systems (Lobell, 2013), and research has rarely been conducted in heterogeneous agricultural landscapes. Africa is characterized by highly fragmented agricultural systems (Pender *et al.*, 2006; You *et al.*, 2007) that limit the application of low to medium resolution remotely-sensed data in crop yield prediction. Small-scale farming systems dominate African agriculture, yet form the bedrock of the continent's food security (Sweeney *et al.*, 2015). Critical to the improvement of food security in Africa and understanding the system depends on accurate information of crop area and yield thereof. Remotely-sensed data can provide robust information on crop area as well as yield estimates. However, the challenge of discriminating crops in such heterogeneous agricultural landscapes remains to be resolved (Sweeney *et al.*, 2015). Challenges in estimating yield in such systems are caused by small cultivated fields, smallholder farmers' desire to preserve large fruit trees within their fields and crop diversity within one field (intercropping) magnifying the within-class variability of crop field (Sweeney *et al.*, 2015). Furthermore, distinguishing cropland from savanna using remote sensing in African agriculture is a major challenge (Hannerz and Lotsch, 2008; Leroux *et al.*, 2014). However, the presence of such challenges makes the use of remote sensing in fragmented African agriculture topical.

Therefore, Africa offers a new frontier for testing new generations of high resolution multispectral sensors in crop yield prediction. Limited use of remotely-sensed data in African agriculture is also attributed to cost of imagery acquisition. Consequently, maize crop yield forecasting in highly heterogeneous African agricultural landscapes has been neglected by past scholars. Previously, the United States Geological Survey (USGS) has been providing remote-sensed data at a cost, until recently data from Landsat series have become free (Wulder *et al.*, 2012). Also recent availability of free high spatial, temporal and spectral resolution data from Sentinel 2 and 3 series will support the use of remote sensing in investigating heterogeneous agricultural landscapes (Belward and Skøien, 2015).

The application of remotely-sensed data in crop yield estimation involves the use of various vegetation indices (VIs) related to crop yield (Petropoulos and Kalaitzidisz, 2012). Early studies by (Tucker 1979, 1980) confirmed that crop canopy spectral reflectance properties, especially computed VIs, are suitable for predicting their yield. The most preferred index – the Normalized Difference Vegetation Index (NDVI) proposed by Rouse Jr *et al.* (1974) first as Band Ratio Parameter (BRP) and later adopted by other researchers like Tucker (1979), Jackson *et al.* (1983) and Sellers (1985) has revolutionized our understanding of the VIs/crop yield relationship. The gradual refinement in the use of VIs to predict crop yield continues in modern studies (Basnyat and McConkey, 2001; Shanahan *et al.*, 2001; Johnson, 2014; Gitelson, 2011). NDVI is an indirect measure of above ground biomass because of its quasi-linear relation to fraction of absorbed photosynthetically active radiation (Prince, 1990; Los, 1998).

The benefits of remote sensing can be replicated in Africa's heterogeneous agricultural landscapes without compromising the quality of the output, if the appropriate remote sensors with high spatial, temporal and spectral resolution are chosen. Previous review of low to medium resolution sensors by Rembold *et al.* (2013) concluded that spatial patterns in agriculture, like field size, are crucial in determining the resolution to use. The new generation of high resolution sensors, such as the recently launched Sentinel 2 with pixel size smaller than most fields common to farmers in Africa, will resolve the challenge of pixel contamination. Consequently, yield monitoring in highly fragmented agricultural systems like Africa is now possible, when such high spatial resolution sensors are adopted. This review focuses on Africa's heterogeneous agricultural systems and will attempt to answer the

questions: what previous studies have been done; what challenges are there; and what are the outstanding research issues in estimating maize yield using remote sensing in Africa's heterogeneous agricultural systems? The authors of this review are convinced that the information contained in this manuscript is critical and timely to both the African and global scientific community, given that the use of remote sensing technology in Africa is still at its infancy (Mutanga *et al.*, 2016).

The review will assess some major remote sensing applications and their applicability to estimating maize grain yield in the African agricultural context, including research challenges. Previous studies applying remote sensing in forecasting maize yield in Africa and elsewhere will be reviewed. The primary focus of this review is three-fold: first, to review and synthesize different maize yield estimation methods, using conventional and remotely-sensed data, and highlight the inherent challenges when applied in heterogeneous agricultural landscapes; second, to compare, using evidence from literature, the capability of available sensors to predict crop yield in highly fragmented agricultural systems; and third, to identify and recommend areas for further research relevant to African agricultural context. In order to address these aims, firstly an overview is presented of different conventional methods for estimating maize yield vis-à-vis advanced remote sensing yield estimation methods. Examples will be drawn from both homogeneous and heterogeneous agricultural systems. Challenges to the use of remote sensing-based methods and sensor suitability are highlighted and implications for research given.

2.2 Conventional yield estimation methods

Several methods for yield forecasting exist, ranging from the traditional ground-based surveys to more advanced remote sensing-based techniques (Rembold *et al.*, 2013). However, in Africa, yield data on staple crops like maize have rarely been collected using more advanced remote sensing-based methods. Quite often, wherever the data is collected, old traditional conventional ground-based survey methods are used based on minimum sampling techniques. Accuracy and precision of such methods are affected by many factors: expert opinion, quality of sampling kit used, sampling methods, sampled locations, road access, data analysis methods used and self-reported data where farmers tend to over-report yield and crop area, among others. Furthermore, results from field-based surveys are difficult

to scale to large areas (Burke and Lobell, 2017). Ground-based survey methods take a lot of manpower and are costly, contain errors and involve inconsistent methods. The time required to complete ground-based surveys is generally long. Survey coverage of certain sites is practically impossible due to inaccessibility. Since ground-based surveys are based on sampling methods, some areas of significant production may be overlooked. Furthermore, the generally long time taken to complete ground-based surveys affects specific and timely information needs by, for example, food security early warning systems.

The commonly used ground-based survey methods have quality- and quantity-related problems in the crop yield information generated (World Bank, 2010; See *et al.*, 2015). For example, during the 2008/09 season in Malawi, cropland area was overestimated by 30% using conventional ground-based survey methods (Dorward *et al.*, 2010; Jayne and Rashid, 2010; Dorward and Chirwa, 2011). In Ethiopia, ground-based surveys overestimated different crop production by between 29% and 44% (Alemu *et al.*, 2008). In Uganda, official yield estimates and FAO figures in 2006 varied by 15% in maize and 75% in soybeans (Uganda Bureau of Statistics, 2007; FAO, 2012). Under- and over-estimation of crop yield at country and regional level cause price fluctuations, wrong national policy decisions and food insecurity among others. For example, Jayne and Rashid (2010) reported how surplus estimates in maize by Malawi government caused maize prizes to reach record levels, when the estimated surplus was not achieved. In Zimbabwe, late importation of maize by the government after the 1991/92 drought was caused in part by inaccurate and delayed yield estimates provided by the national early warning unit. Consequently, this costed the country close to US$ 340 million, about 10% of the then GDP when the government resorted to crisis grain imports (Rukuni *et al.*, 2006). The costs could have been kept to a minimum had the grain been acquired early using accurate and timely yield estimates and early warning systems. Walker (1989) indicated that for any information system to be authentic, it should be clear, accurate, significant, timely, adequate and valid. Thus, the information provided to decision makers in Zimbabwe's situation failed to meet Walker's attributes and affected the decisions made leading to food insecurity in the country in 1992.

Apart from ground-based methods, traditional crop yield assessment approaches include models that integrate the effect of weather, soil, temperature and other environmental

variables on crop growth, photosynthesis and evapotranspiration (Wiegand and Richardson, 1990). These models are based on crop physiological concepts, but are complicated in design and hence are imprecise in yield prediction at large spatial scales as they are affected by spatial variability in both soil management and soil-crop-atmospheric interactions (Wiegand and Richardson, 1990). Regression models have been used extensively by several researchers (Lynch *et al.*, 2007; Roberts *et al.*, 2012; Schlenker and Roberts, 2006; Tannura *et al.*, 2008; Thompson, 1969, 1970, 1988). Of note is work by Thompson (1969, 1970, 1988) using multiple regression models to measure the relationship between technology, monthly rainfall and temperature, to estimate maize yield in the USA. Using such models, maize yields were found to be greatly influenced by adequate rainfall.

However, while these regression models have been used in forecasting crop yields by other researchers (Dixon *et al.*, 1994; Tannura *et al.*, 2008), limitations are apparent. For example, using average monthly temperature or rainfall does not take their distribution into account. Furthermore, when weather data is aggregated over large geographical area, it becomes inaccurate when used to represent local conditions. What also complicates the use of weather data in the models is the sparse distribution of weather stations, especially in developing countries like Africa (Unganai and Kogan, 1998). This inadequate geographical coverage limits wider application of weather-based regression models in crop yield forecasting. Crop simulation models only approximate the reality on the ground and majority of the models do not take weeds, diseases, insects, tillage and minor nutrients into account (Jones *et al.*, 2001). Furthermore, the choice of the model to use is determined by data availability. In majority of the cases, simple rather than complex models are used for crop yield estimation. Simple models estimate crop yield across large geographical area based on climatic and historical yield records and rarely take into account soil-plant-atmospheric interactions. Complex mechanistic models offer detailed explanation of the soil-plant-atmospheric interaction, but require large amounts of input data, which is rarely available (Báez-González *et al.*, 2005).

Two types of models exist – deterministic models (those that give specific outcome assuming uniformity of plant and soil within the simulation space) and stochastic models (those that model outcomes under uncertainty). Uncertainties in crop production are caused by spatial variation of production factors (soil, weather, biotic and abiotic) unaccounted for by

deterministic models. Crop growth systems are more dynamic due to the heterogeneity of the agro-ecosystems. Crop simulation models that incorporate crop growth dynamics have not been developed yet to be applicable in crop yield estimation. Furthermore, data fidelity and availability for model calibration is an issue in African agricultural systems (Gommes, 1998). Although the literature states that models can be run using minimum data sets, models are still limited by being point-based, and are inadequate to run at regional or national scales, despite attempts by Bondeau *et al*. (2007) and Challinor *et al*. (2004) to develop simple crop simulation models that handle regional or national level crop yield simulation with minimum data inputs. Alternative approaches to crop yield estimation methods like remote sensing can offer plausible option compared to crop simulation models. Furthermore, a combination of satellite remote sensed data and crop production models recommended by Wiegand *et al*. (1986) is possible with the necessary modifications.

In the developed world, research in yield forecasting using remotely sensed-data as a substitute or complement to models has been successful (Benedetti and Rossini, 1993; Hayes and Decker, 1996; Quarmby *et al*., 1993). Such studies have demonstrated that crop yield potentials can be expressed in the spectral reflectance of their canopies and that crop's growing conditions can thus be quantified (Tucker, 1979; Wiegand *et al*., 1990). However, in Africa, limited use is being made of remote sensing to support research and for crop yield forecasting (Burke and Lobell, 2017). Remote sensing involves measurement of distinctive attributes or aspects of the earth by satellite sensors on-board aircraft, space-craft, or ground-based handheld sensors. The sensors' ability to detect objects on the earth's surface is a function of their spatial, radiometric, spectral and temporal resolutions. Sensors are designed to attain certain degree of accuracy and therefore they also need accurate ground truthing data. The interaction of sensors with crop canopy forms the basis for yield estimation and quantification of other crop biophysical parameters like leaf area index (LAI) and above ground biomass.

2.3 The basis of yield estimation using remote sensing

All photosynthesizing plants, including maize canopies, absorb light in the blue and red wavelengths for photosynthesis. Plant health and productivity are a function of various biophysical and biochemical factors interacting with spatial variations of nature (topography,

climatic, soil biophysical properties and conditions) and management. The spectral properties of maize, like any other vegetation, are determined by its biophysical and biochemical properties, like LAI, biomass, chlorophyll, water content and canopy structure (Asner, 1998). The main surface of maize canopy is made up of leaves where energy and gas exchange occurs. The influence of biophysical and biochemical properties on the reflectance properties of plants help to define the three distinguishable spectral domains (visible, near-infrared and middle-infrared) shown in Figure 2.1.
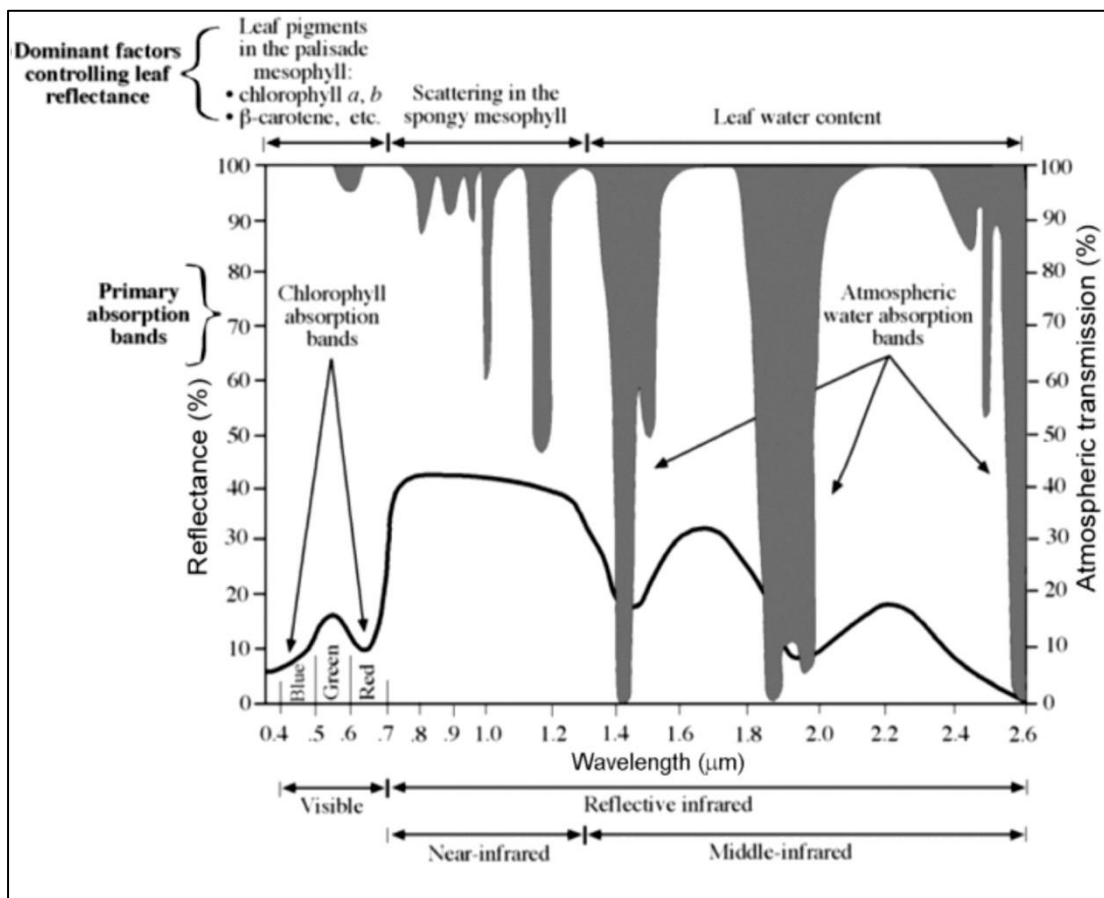
Figure 2.1. Classical reflectance profile of crop leaves (source: Jensen, 2009).

The interaction of solar radiation and plant leaves is shown in Figure 2.2. When light reaches the maize canopy, some is reflected, absorbed, or transmitted, and the pattern is influenced by the maize crop canopy and external factors such as background soil (Baret and Guyot, 1991; Major *et al.*, 1990). Factors that affect spectral response of the maize plant are canopy structure, biophysical and bio-chemical properties, agronomic factors, the geometry of data acquisition and the state of the atmosphere. Canopy geometrical structure is the major determinant of

optical properties of maize, with higher reflectance in planophile than erectophile leaf structure.
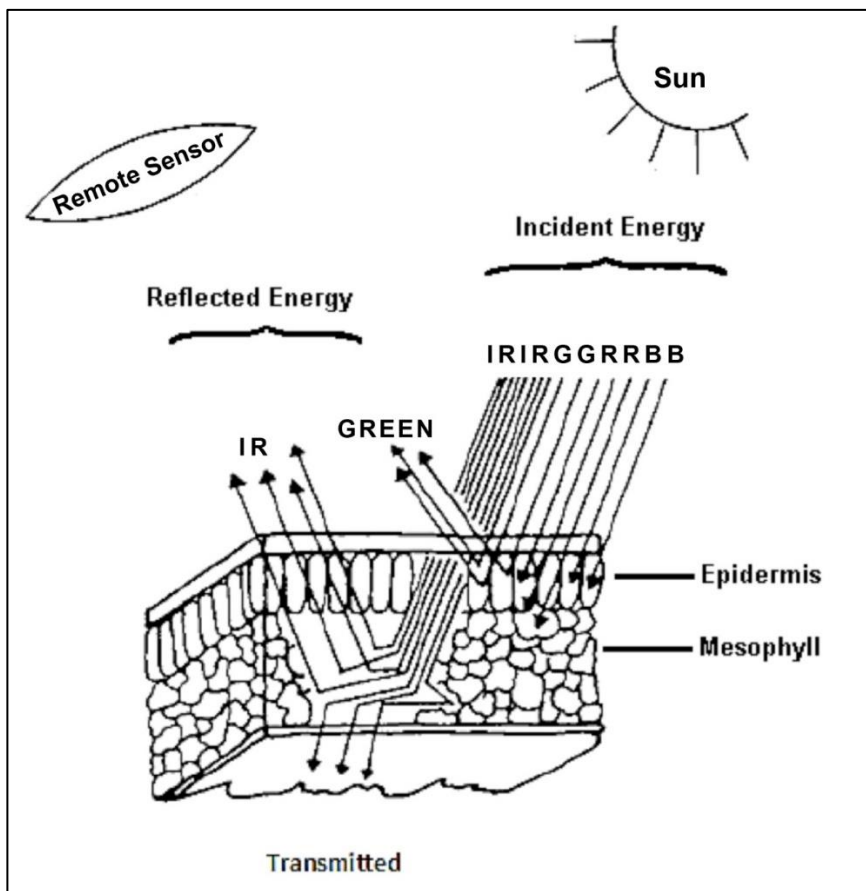
Figure 2.2. Cross-section of a leaf showing interactions between leaf structure and solar radiation (adapted from Campbell and Wynne, 2011 and modified by the authors).

Leaf pigments also affect the reflectance response of maize. Green leaves' chlorophyll strongly absorbs red light (low reflectance) and highly reflect and transmit (low absorption) in the near-infrared (NIR) range (Avery and Berlin, 1992). In the visible domain (400 – 700nm), leaf pigments are the main light-absorbing pigments with overlapping absorption features. In higher plants like maize, Chlorophyll *a* is the dominant pigment and together with *b* constitutes two thirds of the pigments. Chlorophyll *a* peak light-absorption is between 0.41 – 430nm and 600 – 690nm, while the range for *b* is 450 – 470nm and together they peak at about 650nm (visible red). Carotenoids absorption is in the range 440 – 480nm and polyphenols' (brown pigments) absorption intensity decrease from the blue to red (dead leaf) (Jensen, 2009). NIR and red (R) have been used to compute different VIs including the popular NDVI.

Reflectance is also higher between 700 and 1000nm (NIR) in the spongy mesophyll cells. The strength of reflectance from green leaves is usually higher compared to inorganic materials, and hence vegetation looks bright in the NIR wavelengths. These characteristics account for a vegetation's tonal signature on spectral images and form the basis for discrimination of vegetation from inorganic materials using remote sensing.

Other factors include foliar nutrient status, which affects spectral response either directly by absorption or indirectly through their effects on crop physiological processes that define plant health. For example, the Nitrogen (N) amount can affect the spectral reflectance depending on whether it is deficient or adequate (Burke and Lobell, 2017). The water status of the plants also affects the spectral response of the maize crop. Furthermore, leaf diseases and pests attack can alter the reflectance response of maize plants. A healthy plant reflects much more than diseased or pest damaged foliage. When plants are attacked by diseases or pests, LAI is reduced. The radiometric data obtained from such reflectance patterns are used to compute different VIs, which form the basis for estimating grain yield.

The relationship between VIs and biomass enables estimation of yield, since yield of maize is a function of the photosynthetic activity of the plant during its growth (Benedetti and Rossini, 1993). Generally, VIs are used as independent variables and the relationship appears to be strong in grasses or crops, whose dry matter is the final harvestable yield (Rembold *et al*., 2013). If the above ground biomass is not the final yield, the spectra/yield relationship is only indirect (Rudorff and Batista, 1990). Studies have also established that the correlation between crop yield and VIs fluctuates with crop phenology (Hayes and Decker, 1996). Furthermore, several studies have suggested that accumulated VIs rather than instantaneous measurements are more closely related to the final yield (Meroni *et al*., 2013; Pinter Jr *et al*., 1981). Pinter Jr *et al*. (1981) further suggested that integration of VIs like NDVI, performs better when taken at specific growth stages (e.g. at flowering stage). These VIs are measured by remote sensors ranging from hand-held to satellite-based with diverse spatial, temporal and spectral resolution, which affects the final output. The section below gives details of different available sensors and their capabilities in estimating maize grain yield.

2.4 Remote-sensing platforms for yield estimation

Remote-sensing-based methods are classified into three platforms: ground-based, airborne and space-borne satellites (Wójtowicz *et al*., 2016). Accordingly, each category has its own merits and demerits. The choice depends on the desired output and intended use. Here, we review the three platforms and sensor combinations.

The ground-based remote sensing method uses handheld remote sensors which are applicable at field-scale for monitoring crop status, including biotic and abiotic stresses (Wójtowicz *et al*., 2016). The advantages include better spectral, temporal and spatial resolution as compared to airborne and satellite-based remotely sensed data. Ground-based remote sensing instruments have been used successfully in yield forecasting in other crops. For example, Walsh *et al*. (2013), used ground-based remote sensing successfully to forecast winter wheat grain yield. However, the major limiting factors are that of scale, efficiency and labor involved, when compared to airborne and satellite remote sensing, which are suitable for larger geographical areas.

Airborne remote sensing involves the use of manned aircrafts and unmanned aerial vehicles (UAVs, often called "drones"), and provides an instant visual crop inventory. The choice of which one to use is governed by cost implications with UAVs being low cost, light weight and low speed instruments. In modern times, manned aircrafts are being replaced by UAVs. Two platforms of UAVs exist: the 'fixed wing' and the 'rotary wing' types (Wójtowicz *et al*. 2016). Fixed wings can fly at high speed and do not require a runway or a launcher. The rotary wing can hover over a target, but generally have a shorter flight time due to high battery power consumption. UAVs can be quick and can take repeated measurements at different heights and times, producing high resolution imagery. They can observe individual plant, patches, gaps and patterns (Franklin *et al*., 2006; Laliberte *et al*., 2006), allowing studies of within-field variation. Chang *et al*. (2003) used airborne remote sensing to estimate maize yield and found that they can substantially improve crop yield estimates. In rice, Swain and Zaman (2012) found a high correlation with a coefficient of determination (R^2) of 0.76 between yield and VIs.

The third platform is space-borne based remote sensing. Satellite remotely-sensed data are applicable over larger areas (Lamb and Brown, 2001), and hence can monitor crops globally,

regionally or locally providing important crop coverage, mapping, classification and yield forecasts (Simone *et al.*, 2002; Wójtowicz *et al.*, 2016). However, satellite remote sensors are affected by weather conditions (Stafford, 2000), atmospheric noise and obtaining data from them can be costly. Getting accurate yield predictions in heterogeneous agricultural landscapes using satellite remotely sensed data depends on the sensors' resolution and other exogenous factors. The most commonly used satellite-based multispectral sensors to estimate maize yield include the National Oceanic and Atmospheric Administration (NOAA)'s advanced very high resolution radiometer (AVHRR), Moderate Resolution Imaging Spectroradiometer (MODIS), Landsat series, ASTER, SPOT, among others. Each sensor offers specific features that make it more or less appropriate for a specific application. The spatial and temporal resolutions of these sensors are discussed below and also shown in Figure 2.3.
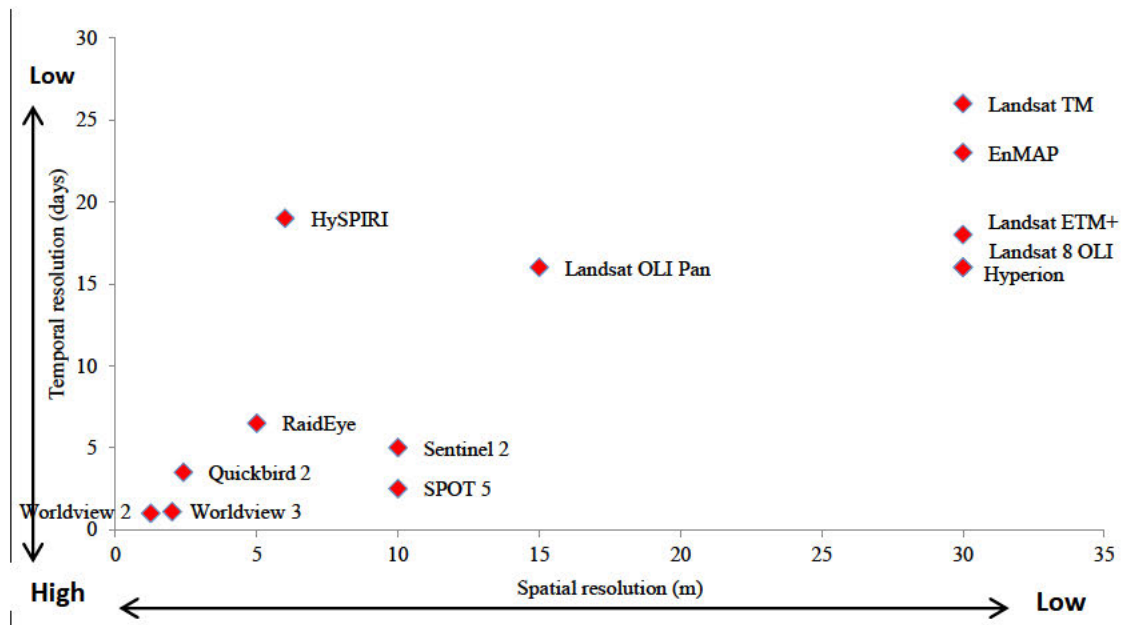
Figure 2.3. Selected satellite sensors and their spatial and temporal resolutions.

Freely available sensors like AVHRR are suitable for monitoring vegetation changes because of high temporal resolution (daily), but are limited by their low spatial resolution (>8 km) which is too coarse for yield estimation in heterogeneous agricultural landscapes. This makes AVHRR difficult to use to estimate yield in African agricultural context. The pixel size is far larger than most of the farmers' fields. In addition, the sensor itself cannot provide adequate spectral information with low noise. Advances in remote sensing technology have seen successor sensors like MODIS as improvements to AVHRR (Fensholt and Sandholt, 2005;

Huete *et al*., 2002), especially in terms of spectral and spatial resolutions because MODIS was specifically targeted for land related observations (Justice *et al*., 2002). Yield estimates using MODIS data have been more precise than AVHRR data in fairly homogeneous fields (Johnson 2014). MODIS has an improved spectral resolution (36 spectral bands), nevertheless, the 250m spatial resolution is still coarser for fragmented agricultural systems. Because of such limitations, sensors with enhanced spatial, temporal and spectral resolutions like Landsat series were developed.

When Landsat sensors were used, they offered a suitable alternative to MODIS and AVHRR in predicting crop yield, in particular the Landsat 8 OLI with a ground sample resolution of 30m. Although the swath width of Landsat 8 OLI (185 × 185km) is considered relatively narrow, it offers a plausible option to AVHRR and MODIS. The major drawback of Landsat 8 OLI is its somewhat long revisit period (16 days) which severely limits the number of observations within a typical growing season, especially when factoring in the likelihood of clouds, which would limit successful sensing (Johnson, 2014). Nevertheless, despite this limitation, yield estimates from other Landsat series (e.g. TM and ETM+) with similar temporal resolution to Landsat 8 OLI, have been reported to be fairly accurate in homogeneous cropping systems (Doraiswamy *et al*., 2003; Gitelson *et al*., 2012; Liu *et al*., 2010; Lobell *et al*., 2005). Furthermore, maize phenological stages can easily be captured by the 16 days revisit, making sensors like Landsat 8 OLI appropriate for highly fragmented African agricultural landscapes. Continuous improvements of multispectral remote sensors have led to the launch of new generation of free sensors like Sentinel 2 with high temporal (5 days), spectral (13 bands) and spatial (10m) resolution (Drusch *et al*., 2010), which can be applicable in highly fragmented agricultural landscapes.

The resolution of Sentinel 2 is much better than its predecessors, making it well suited for complex, spatially variable, diverse and dynamic African agricultural systems. Its high spectral resolution may allow discrimination of maize from other crop types, while its high spatial resolution captures "pure" pixels (= 0.04 ha). This advanced multispectral sensor also has a much improved signal-noise-ratio (SNR). The availability of free data from Sentinel 2 and 3 provides a unique opportunity to apply remote sensing in heterogeneous agricultural landscapes (Belward and Skøien, 2015). Other sensors with high spatial and temporal

resolutions in the range of Sentinel and Landsat series exist and include sensors like ASTER and ALI, which offer resolutions similar to Landsat series (Nikolakopoulos and Tsombos, 2009). ASTER has higher spatial (15m) and spectral resolution (14 bands) than Landsat. ALI has high spatial resolution, but is limited by a narrow scanning area (35 x 35km). The Indian Remote Sensing (IRS - Series) system scans with high spatial resolution (5.8m) with a width of 141km. SPOT offers a combination of high spatial resolution for large areas (60 x 60 or 60 x 120 km) and high revisit frequency (1 day). Some optical sensors like KOMOS, EROS, CARTOSAT-1, WorldView-1 and GeoEye-1 with high spatial resolution (1m) record data only in panchromatic mode while sensors like FORMOSAT-2, IKONOS, OrbView-3, QuickBird, and KOMPSAT-2 record a combination of panchromatic and multispectral regimes. There are several other high resolution sensors like WV 2 and 3, Space station cameras, URTHECAST DEIMOS IMAGING, and the recently launched 88 Doves, among others. However, data from most of these sensors can only be used for local-scale applications and most of these sensors are available on a commercial basis, and their use is restricted by the costs involved.

Therefore, for estimating maize yield using remotely sensed data in spatially heterogeneous agricultural landscapes, sensors with high spatial, temporal and spectral resolution are needed that are capable of accounting for such spatial heterogeneity. As mentioned earlier, multispectral sensors like Sentinel and Landsat series offer a plausible option. In future, where higher spectral resolution is needed, we envisage that hyperspectral remote sensors might become convenient once hyperspectral data becomes readily available. Hyperspectral sensors have higher spectral resolution than multispectral sensors (Erives and Fitzgerald, 2005; Lawrence *et al.*, 2006; Turner *et al.*, 2003). Hyperspectral, variously termed imaging spectroscopy, imaging spectrometry or ultra-spectral imaging in remote sensing (Clark 1999; Lillesand *et al.*, 2014), allows detailed analysis of crops, which cannot be achieved with broadband multi-spectral sensors (Cochrane, 2000; Govender *et al.*, 2007; Mutanga *et al.*, 2003). Hyperspectral remote sensors have more narrow contiguous spectral bands between 400 – 2500nm (Govender *et al.*, 2007; Vaiphasa *et al.*, 2005). However, hyperspectral sensors generate high volumes of data that complicate data collection, transmission, storage, processing and may be costly, thus prohibiting their application to larger geographical areas (Lillesand *et al.*, 2014). Currently hyperspectral data from sensors like Hyperion is not readily available and is still unreliable for large-scale application. Furthermore, the development of hyperspectral

satellite systems has been very slow compared to the rapid development of multispectral satellite systems and very few hyperspectral sensors are available (Lillesand *et al*., 2014). Several early attempts to develop or launch satellites with hyperspectral sensors ended in failure or cancellation, leading to missed opportunities for hyperspectral remote sensing from space (Lillesand *et al*., 2014). Due to this sluggish development, very few space-borne hyperspectral sensors like Hyperion, LEISA AC, CHRIS, HyspIRI and EnMAP are available. However, LEISA AC imagery was coarser with a spatial resolution of 250m and was meant to correct imagery from other sensors for atmospheric noise and was abandoned after first year.

The EO-1 Hyperion imaging spectrometer is one of the earliest and successfully launched hyperspectral satellite sensors, providing 242 spectral bands of data over the 360 – 2600nm range (Lillesand *et al*., 2014). However, only 198 of the 242 bands are usable because the rest, especially those at the lower and upper ends have a poor SNR. Hyperion has high spatial resolution (30m) with a swath width of 7.5km. Previous studies have shown the utility of Hyperion data over multispectral remotely-sensed data (Datt *et al*., 2003; Wu *et al*., 2010). Thenkabail *et al*. (2011) also demonstrated the ability of hyperspectral remotely sensed data to significantly characterize, discriminate, map and predict crop yields compared to broadband multispectral remotely-sensed data. This development might enable future studies to investigate remote sensing applications in crop yield estimation in spatially heterogeneous agricultural systems. Nevertheless, significant knowledge gaps still exist that require further investigation. For example, hyperspectral narrowband VIs suitable for predicting maize yield are not known. Furthermore, data dimensionality (commonly termed Hughes phenomenon or 'the curse of dimensionality') and data redundancy associated with hyperspectral sensors remain a challenge. Studies by Thenkabail *et al*. (2004) and Thenkabail *et al*. (2014) using hyperspectral field spectrometer data have identified 15 optimal bands for use in maize. However, further studies are needed to identify band ratios or combinations that best predict maize yield from these 15 bands in order to reduce data redundancy.

Other hyperspectral remote sensors like CHRIS and the upcoming EnMAP and HyspIRI also promise high spatial (30m) and temporal resolution hyperspectral imagery with a 30km swath width and different angle hyperspectral measurements of the same target, which assist in crop characterization (Thenkabail *et al*., 2011). CHRIS is a small light weight sensor with 62 narrow

spectral bands and a spatial resolution of 34m. CHRIS can also be operated at a spatial resolution of 17m with a swath width of 13 x 13km and capture data from 18 bands at this high resolution (Lillesand *et al*., 2014). The sensor operates in the visible/NIR range of 400 – 1050nm. EnMAP is a satellite-based hyperspectral sensor with a total of 244 spectral bands over the range of 240 – 2450nm (Lillesand *et al*., 2014). The spatial resolution is 30m and a swath width of 30km at nadir with a temporal resolution of 23 days for nadir pointing images and as short as 4 days, when 30° pointing is employed (Guanter *et al*., 2015).

The aforementioned hyperspectral sensors afford relatively high spatial, spectral and temporal resolution capabilities hitherto missing in the conventional multispectral sensors. It is likely that data from these sensors will have application in crop yield estimation in highly fragmented agro-ecosystems. Literature shows considerable application of conventional multispectral sensors in yield prediction in homogeneous agricultural systems (Báez-González *et al*., 2005; Guindin-Garcia, 2010; Sakamoto *et al*., 2013; Johnson, 2014; Battude *et al*., 2016). Studies using satellite-based high resolution hyperspectral sensors to estimate maize yield in heterogeneous agriculture are scant. Research needs to be conducted to test their capabilities in estimating yield in fragmented agricultural systems. Some examples of maize yield estimation using multispectral and hyperspectral remote sensors are given below.

Examples of large-scale application of remotely sensed data to estimate maize yield are drawn from homogeneous and heterogeneous cropping systems. To guide the readers, examples will be discussed under two sub-divisions: homogeneous and heterogeneous agricultural systems. The two subdivisions are convenient and relevant as the two systems are different. What works in one system may not necessarily work in the other. Case studies from homogeneous agricultural systems are given to demonstrate the utility of remote sensing in maize yield estimation. Furthermore, the scarcity of studies on maize yield estimation in heterogeneous agricultural systems has also necessitated drawing examples from where comprehensive studies have been conducted.

2.5 Yield estimation in homogeneous agricultural systems

The literature shows that studies using satellite imagery to estimate maize yield continue to be mostly conducted in more advanced agricultural systems (Battude *et al*., 2016; Johnson,

2014; Lobell *et al*., 2003; Prasad *et al*., 2006; Shanahan *et al*., 2001). The availability of this body of information makes it necessary to review what worked in these systems and can be replicated or improved upon in fragmented agricultural systems, and also to identify gaps that need further research and inherent challenges. Previous reviews on crop yield estimation using remote sensing include those by Rembold *et al*. (2013), who discussed the use of low resolution sensors in combination with crop yield models in homogeneous agricultural systems. Atzberger (2013) gave a broad summary of the application of satellite imagery in crop yield estimation. However, these reviews did not give an in-depth analysis of sensors that are applicable in fragmented agricultural systems. This section will review case studies in homogeneous agricultural systems and highlight their relevance to heterogeneous systems. Homogeneous agricultural systems are mainly those found in advanced agricultural systems like the USA, Brazil, Mexico, Australia and some parts of Europe and Asia. In these systems, low to medium resolution sensors are applicable due to the size of the fields versus pixel sizes of low to medium resolution sensors and reliable ground data are often available to validate satellite-derived yield estimates (Farmaha *et al*., 2016; Lobell, 2013). Several of these examples are briefly discussed below.

Maize yield estimation studies using remotely sensed data continue to be undertaken at different spatial scales, contingent to the objective and data availability. At large area, Báez-González *et al*. (2002) used NDVI from NOAA's AVHRR images in Mexico to develop and validate a maize yield estimating method with relatively high accuracy under irrigated (R^2 = 0.89) and non-irrigated (R^2 = 0.76) regimes. The methodology was robust in estimating maize yield in large-scale systems. Prasad *et al*. (2006) combined NDVI, VCI and TCI from NOAA-AVHRR as input variables into their maize yield prediction model to estimate maize yield using piecewise linear regression method. They used a non-linear Quasi-Newton multi-variate optimization method to reduce variation and inaccuracies in estimated yield, and found a good positive correlation (R^2 = 0.78) between maize yield and VIs in Iowa, USA. They concluded that their methodology can be replicated in other geographical areas to predict maize production under rainfed conditions. However, we emphasize here that these results are more applicable in homogeneous than heterogeneous agricultural systems due to the coarse resolution sensors used.

Guindin-Garcia (2010) compared green LAI recorded at peak grain filling period with maize final grain yield and found a high positive correlation ($R^2 = 0.75$). The author further demonstrated the utility of the MODIS's Wide Dynamic Range Vegetation Index (WDRVI), recorded at peak grain formation in Nebraska, Iowa, and Illinois, to accurately predict large-scale maize grain yield. Johnson (2014) used NDVI, land surface temperature (LST) from MODIS and precipitation to predict maize yield in the corn belt of USA. Using NDVI and daytime temperature, Johnson (2014) obtained a high correlation ($R^2 = 0.93$) with maize yield. Sakamoto *et al.* (2013) used time-series MODIS WDRVI, incorporating the crop phenological detection 'Shape-Model Fitting Method', and found that WDRVI taken a week before maize flowering correlated strongly with grain yield locally and regionally, with a coefficient of variation less than 10% for 18 major maize producing states in USA. However, these results again were obtained using coarse resolutions applicable in homogeneous cropping systems, and therefore, are not applicable in spatially heterogeneous agricultural systems.

Báez-González *et al.* (2005) used both ground- and satellite-measured LAI derived from Landsat ETM+ and AVHRR data, and predicted maize grain yield with very low mean errors in Sinaloa, Mexico. Their study concluded that AVHRR and Landsat ETM+ sensors can be used to forecast large-scale maize yields. Li *et al.* (2014) combined Landsat ETM+ data with a WOFOST-HYDROUS coupled-model and found good estimates of regional maize yield in Northwest China. However, as mentioned above, these sensors in their current form are not applicable to fragmented systems that require high spatial, temporal and spectral resolution. Therefore, the potential of high spatial, temporal and spectral resolution sensors like Sentinel 2 to estimate yield in fragmented systems need to be tested. Their potential to account for high spatio-temporal variability in crops has already been demonstrated in homogeneous agricultural systems. For example, Battude *et al.* (2016) tested the capabilities of Sentinel 2 in combination with a Simple Algorithm For Yield (SAFY) estimates model with remotely sensed data from SPOT 4, FORMOSAT 2, Landsat 8 and Deimos 1 resampled to Sentinel 2 sensor in temperate France. The study found good correlations for maize yields at both local scale ($R^2 = 0.86$) and regional scale ($R^2 = 0.96$). The study confirmed the potential of Sentinel 2 remotely-sensed data as a plausible option over medium resolution sensors, which can be replicated in fragmented agricultural systems.

A comparison of actual measured maize yield or government yield estimates with remotely sensing-based yield estimates is given in Table 2.1 using yield data extracted from studies by Prasad *et al*. (2006), Fang *et al*. (2008) and Guindin-Garcia (2010) in the USA, Ferencz *et al*. (2004) in Hungary and Battude *et al*. (2016) in France. The original data was used to calculate the deviations of predicted yield from the actual measured yield or government estimates and relative deviations were determined by dividing the difference by measured yield or government estimates and converted to percentages. On average the study by Prasad *et al*. (2006) using NOAA-AVHRR achieved accuracies above 90% in maize. Despite an overestimation in 1993, their results demonstrate that remotely sensed data can be used to forecast crop yield with acceptable accuracy before harvesting (Table 2.1). Ferencz *et al*. (2004) in Hungary used NOAA-AVHRR data and estimated maize yield from 1991 to 2000 with high reliability of above 95%. Fang *et al*. (2008) on the other hand combined CERES maize crop model and MODIS data to estimate maize yield and also achieved high accuracy in the USA's 110 counties in 2000 (Table 2.1). Guindin-Garcia (2010) using MODIS data also estimated maize yield with high accuracies except for 2006 where there was a slight overestimations with both MODIS 8 and 16 day revisit data. The low deviations from the results in Table 2.1 reinforced the conclusion that remote sensing can be a robust method to estimate maize grain yield before harvesting.

Furthermore, the results also show high accuracies in maize yield estimates in France when Sentinel 2-like data was used (Battude *et al*., 2016). Although an overestimation of rainfed maize yield occurred at Gers in 2013, their results showed high accurate predictions in both rainfed and irrigated maize. Results by Battude *et al*. (2016) demonstrate the capability of high spatio-temporal resolution remotely-sensed data in forecasting maize yield prior to harvesting. Such accuracies are encouraging and open the avenues for future yield forecasting in fragmented and highly granular agricultural landscapes like Africa. However, though results from these studies are encouraging, application and demonstration studies should be carried in Africa's heterogeneous agriculture to refine and test capabilities of remotely sensed data in forecasting maize yield. These studies need to be conducted in collaboration with end-users to demonstrate the possibilities of estimating crop yield from space, to permit remote sensing technology to graduate from a research tool for specialists to become an important

31

decision support tool to end users like farmers, governments and agricultural commodity traders.

Table 2.1. Maize yield forecasting using remote sensing-based (RS-based) methods versus actual yield measurements or government yield estimates

Period	Crop	Actual yield* (t ha⁻¹)	RS-based estimates* (t ha⁻¹)	Deviation (t ha⁻¹)	Relative deviation (%)	Reference
1982	Maize	7 53	6 69	0 84	11 22%	Prasad *et al* (2006)
1983	Maize	5 46	5 26	0 20	3 73%	Prasad *et al* (2006)
1984	Maize	7 03	6 44	0 59	8 35%	Prasad *et al* (2006)
1985	Maize	7 91	8 69	-0 78	-9 90%	Prasad *et al* (2006)
1986	Maize	8 47	8 17	0 30	3 57%	Prasad *et al* (2006)
1987	Maize	8 16	8 27	-0 11	-1 32%	Prasad *et al* (2006)
1988	Maize	5 27	6 19	-0 92	-17 36%	Prasad *et al* (2006)
1989	Maize	7 41	7 77	-0 37	-4 94%	Prasad *et al* (2006)
1990	Maize	7 91	8 57	-0 66	-8 38%	Prasad *et al* (2006)
1991	Maize	7 34	6 95	0 40	5 41%	Prasad *et al* (2006)
1992	Maize	9 23	8 73	0 49	5 33%	Prasad *et al* (2006)
1993	Maize	5 02	6 62	-1 60	-31 77%	Prasad *et al* (2006)
1995	Maize	7 72	6 88	0 84	10 93%	Prasad *et al* (2006)
1996	Maize	8 66	8 76	-0 10	-1 19%	Prasad *et al* (2006)
1997	Maize	8 66	8 60	0 06	0 68%	Prasad *et al* (2006)
1998	Maize	9 10	8 75	0 35	3 81%	Prasad *et al* (2006)
1999	Maize	9 35	9 33	0 02	0 23%	Prasad *et al* (2006)
2000	Maize	9 04	9 07	-0 04	-0 39%	Prasad *et al* (2006)
2001	Maize	9 16	8 69	0 47	5 13%	Prasad *et al* (2006)
		Measured yield (t ha⁻¹)	**RS-Based MODIS 8 day (t ha⁻¹)**	**(t ha⁻¹)**		
2006	Maize	10 36	11 92	-1 55	-14 99%	Guindin-Garcia (2010)
2007	Maize	12 92	12 25	0 67	5 18%	Guindin-Garcia (2010)
2008	Maize	12 67	13 21	-0 54	-4 26%	Guindin-Garcia (2010)
2009	Maize	12 43	12 91	-0 48	-3 82%	Guindin-Garcia (2010)
		Measured yield (t ha⁻¹)	**RS-Based MODIS 16 day (t ha⁻¹)**	**(t ha⁻¹)**		
2006	Maize	10 36	11 75	-1 39	-13 39%	Guindin-Garcia (2010)
2007	Maize	12 92	11 94	0 98	7 59%	Guindin-Garcia (2010)
2008	Maize	12 67	12 98	-0 31	-2 47%	Guindin-Garcia (2010)
2009	Maize	12 43	12 75	-0 32	-2 57%	Guindin-Garcia (2010)
		Hungary CSO (t ha⁻¹)	**RS-Based estimates (t ha⁻¹)**	**(t ha⁻¹)**		
1991	Maize	6 48	6 71	-0 23	-3 55%	Ferencz *et al* (2004)
1992	Maize	3 60	3 65	-0 05	-1 39%	Ferencz *et al* (2004)
1993	Maize	3 37	3 50	-0 13	-3 86%	Ferencz *et al* (2004)
1996	Maize	5 81	5 61	0 20	3 44%	Ferencz *et al* (2004)
1997	Maize	6 42	6 41	0 01	0 16%	Ferencz *et al* (2004)
1998	Maize	6 17	5 95	0 22	3 57%	Ferencz *et al* (2004)
1999	Maize	6 18	6 38	-0 20	-3 24%	Ferencz *et al* (2004)
2000	Maize	4 20	4 15	0 05	1 19%	Ferencz *et al* (2004)
		USA NASS (t ha⁻¹)	**RS-Based estimates (t ha⁻¹)**	**(t ha⁻¹)**		
2000 in 43 counties	Maize	9 08	9 77	-0 69	-7 54%	Fang *et al* (2008)
2000 in 67 counties	Maize	9 19	9 48	-0 29	-3 16%	Fang *et al* (2008)
		Government estimates (t ha⁻¹)	**RS-based estimates (t ha⁻¹)**	**(t ha⁻¹)**		
2013 in Gers	Irrigated maize	7 10	7 40	-0 30	-4 23%	Battude *et al* (2016)
2013 in Gers	Rainfed maize	3 70	5 10	-1 40	-37 84%	Battude *et al* (2016)
2013 in Gers	All maize	6 50	6 60	-0 10	-1 54%	Battude *et al* (2016)
2013 in Haute Garonne	Irrigated maize	8 80	9 10	-0 30	-3 41%	Battude *et al* (2016)
2013 in Haute Garonne	Rainfed maize	6 00	5 70	0 30	5 00%	Battude *et al* (2016)
2013 in Haute Garonne	All maize	8 30	7 80	0 50	6 02%	Battude *et al* (2016)
2014 in Gers	Irrigated maize	9 50	8 80	0 70	7 37%	Battude *et al* (2016)
2014 in Gers	Rainfed maize	8 60	8 80	-0 20	-2 33%	Battude *et al* (2016)
2014 in Gers	All maize	9 30	8 80	0 50	5 38%	Battude *et al* (2016)
2014 in Haute Garonne	Irrigated maize	9 60	9 50	0 10	1 04%	Battude *et al* (2016)
2014 in Haute Garonne	Rainfed maize	7 70	7 70	0 00	0 00%	Battude *et al* (2016)
2014 in Haute Garonne	All maize	9 30	8 90	0 40	4 30%	Battude *et al* (2016)

* Yields from Prasad *et al*. (2006) were converted from bushel per acre to t ha-1

The existing substantial body of studies using satellite imagery to estimate maize yield in homogeneous cropping systems has led to significant insights into these production systems. On the contrary, studies in Africa using remote sensing in agriculture are limited and this has led not only to poor insights into the productivity and yield gaps of these systems, but also missed opportunities to improve food security through early warning systems (Burke and Lobell, 2017). Limited effort has been made in estimating grain yield in staple food crops like maize. The absence of studies linking VIs to maize yield in Africa was the motivation for this review. Due to limited studies on forecasting maize yield using remote sensing in Africa, examples given in the section below also include those conducted on different crops other than maize. These are elaborated below.

2.6 Yield estimation in fragmented agricultural systems

In east Africa, Lewis *et al.* (1998) used a correlation model using NDVI derived from NOAA's AVHRR as the independent variable to estimate maize production. They applied a simple regression model approach using median NDVI to estimate maize production in Kenya and obtained a significant correlation ($R^2 = 0.75$) between NDVI and maize production. Recently, Rojas (2007) used the land cover weighted NDVI (CNDVI) derived from SPOT-VEGETATION in Kenya to estimate maize grain production and obtained better correlations between CNDVI and yield ($R^2 = 0.83$; root mean square error [RMSE] = 0.33 t ha^{-1}) than previously obtained by Lewis *et al.* (1998). However, both studies used production estimates obtained from government statistics and no ground truth data was used. Therefore, their results need to be interpreted with care.

In southern Africa, Unganai and Kogan (1998) used the NOAA-AVHRR-based Vegetation Condition Index (VCI) and temperature condition index (TCI) to estimate maize production approximately six weeks prior to harvesting time in Zimbabwe. The study established that VCI and TCI were strongly correlated with maize production ($R^2 = 0.70 - 0.95$) in all the 41 districts of Zimbabwe included in their study. They identified two peak periods where maize yield had a strong correlation with the VCI as well as TCI, one sensitive to thermal conditions (at maximum biomass accumulation) and a second sensitive to water stress (during grain filling). They concluded that NOAA-AVHRR derived indices can be used for maize production forecasting. In Swaziland, Mkhabela *et al.* (2005) used NDVI from NOAA-AVHRR

to forecast maize yield in four agro-ecologies of the country and found good correlation in three agro-ecologies (R^2 = 0.51 – 0.68). Svotwa et al. (2013), used a hand-held sensor (MR-5, 450 – 1750nm) in Zimbabwe and obtained a high correlation (R^2 = 0.79) between tobacco yield and NDVI. Vergara-Díaz et al. (2016), using VIs obtained using UAVs and red-green-blue (RGB) imagery, found maize grain yield to be strongly predicted by RGB indices (with R^2 = 0.70). However, studies by Svotwa et al. (2013) and Vergara-Díaz et al. (2016) did not compare the relationship of ground-based and airborne NDVIs with those from satellite platforms for validation purposes, and their results are thus of limited use when wider area application of these indices are sought. Studies by Unganai and Kogan (1998) and Mkhabela et al. (2005) did not use ground truth data either, and hence their results should be interpreted with care as well.

In west Africa, Maselli et al. (1992), using NDVI from NOAA-AVHRR, obtained a high positive correlation (R^2 = 0.85) between NDVI and grain yield in millet and sorghum in Niger. Before standardizing NDVI, a low correlation (R^2 = 0.57) was found, but after standardizing NDVI to VCI, as proposed by Kogan (1990), the correlation (R^2 = 0.85) improved tremendously. They concluded that the use of remotely sensed NDVI allows monitoring and yield forecasting in millet. Rasmussen (1992), in Burkina Faso, used integrated NDVI (iNDVI) from NOAA-AVHRR data to estimated millet yield, and found NDVI recorded during the reproductive phase to be critical for estimating millet yield. Rasmussen (1992) further used iNDVI to estimate area planted in addition to crop yield. Maselli et al. (2000) used Global Area Coverage (GAC) NDVI maximum value composites to forecast millet and sorghum yield in Niger. After geo-standardizing NDVI, they also found a strong correlation (R^2 = 0.85) between measured and estimated grain yield with a RMSE of less than 72kg ha^{-1}. They further demonstrated that the best time to obtain NDVI is during millet's and sorghum's grain filling period. The accuracy of their estimation results were comparable to results by Hayes and Decker (1996) in the USA, and showed improvement in predictive power from a previous study in Africa by Groten (1993). Maselli et al. (2000) concluded that such results permit the use of satellite remotely sensed data in yield estimation and early warning systems. However, Groten (1993) in Burkina Faso found a high correlation (R^2 = 0.87) between crop yield and NDVI recorded at the end of growing season. Such conflicting findings need further

investigations to determine the best phenological stage to record NDVI for purposes of yield estimation.

The major ambiguity in most of the studies conducted in heterogeneous environments is on the methodologies used. Most of these studies predicted maize production using national governments production statistics. In most cases, no field training data was used to validate the estimates. It was reported earlier in this review that maize production statistics from national governments can be very unreliable (Carletto *et al*., 2015; Dorward *et al*., 2010; Dorward and Chirwa, 2011). Therefore, these results need to be interpreted with caution. Future yield predictions in Africa need ground truthing through precise determination of field training data, as this affects the accuracy and efficacy of satellite-based estimates. For example, a recent study by Burke and Lobell (2017) using a commercial high spatial resolution satellite Terra Bella (formerly Skybox, a Google subsidiary) estimated maize yield in smallholder farmers' fields in western Kenya using extensive training data. They found good agreement between measured yield and satellite-based yield estimates. Furthermore, their predictions were scalable to large geographical areas. They concluded that high spatial sensors can be used in heterogeneous cropping systems to estimate maize yield.

2.7 Challenges of yield estimation using remote sensing and research needs

One crucial restriction on the use of yield/VIs regression is that most of the studies above were carried out in specific environments governed by local climatic conditions. Therefore, they may not be widely applicable in other geographical areas, where the climate is different. In most cases the studies were also limited by the available data from low resolution sensors obtained from fairly homogeneous cropping systems. Furthermore, locally calibrated models cannot be extended to other geographical areas or other scales (Rembold *et al*., 2013). Addressing the accuracy of predicted yield is critical and it is a matter of choice between accuracy and cost. From the above examples, accuracy varies from one study to another. At the small area level, robust statistical measures are available and are generally known. However, gaps remain in predicting yield accurately at regional and national levels. Furthermore, when crop acreage is unknown, the yield/NDVI relationship will not give insight into the final production, yet total production is critical for many users. Another challenge with satellite remote sensing systems in crop yield estimation is the availability of

usable imagery recorded frequently at consistent intervals during the crop growing season. Most available high spatial resolution sensors have temporal resolutions that are not adequate enough to record important maize phenological changes and this is compounded by frequent cloud cover, leading to missing data.

Crop yield estimation accuracy is also affected by non-crop vegetation signals. Sensors with high spectral resolution are needed to discriminate such non-crop vegetation signal or signals from non-target crop. Maselli *et al*. (2000) suggested the use of crop masking to discard irrelevant signals. Freund (2005) found crop masking to improve accuracy of crop yield estimation. However, Atzberger (2013) argued that during image masking, some important pixels might be discarded and this compromises the precision of crop yield forecasting. Furthermore, reflectance from different crops or vegetation can be highly correlated (causing spectral confusion) with the target crop due to similarities in their biochemical and biophysical properties. In addition, yield estimation in intercropped fields is nearly impossible, yet a substantial number of small-scale African farmers intercrop maize with legumes. Pixels from intercropped fields will be classified as contaminated. Therefore, the production from these fields in most cases is not accounted for when using remotely sensed data, leading to under estimation of total production.

Crop reflectance properties are directly affected by environmental and management factors thereby altering the known unique spectral signatures (Price, 1994). Different stresses like N deficiencies (Burke and Lobell, 2017), drought, and pest and disease infestation also affect the spectral properties of maize. Other factors that affect maize reflectance properties include age of the crop due to different planting dates, local weather, edaphic factors, water, rainfall and landscape (Adam *et al*., 2010). Different maize varieties produce different spectral reflectance signatures due to different canopy structures and biochemical properties. Furthermore, VIs from broadband sensors are known to be unstable, as they tend to saturate reducing accuracy of measurements (Gao *et al*., 2000; Mutanga and Skidmore, 2004; Thenkabail *et al*., 2000). However, despite these limitations, remotely-sensed data can still play a crucial role in estimating maize yield accurately in fragmented agricultural systems. This can be achieved by choosing sensors with high spatial, temporal and spectral resolution coupled with appropriate analysis techniques, backed up by model training using ground truthing data.

This review, however, identified several areas that still remain unresolved from a research point of view.

Firstly, most of the studies on maize yield estimation have been undertaken in developed countries with highly homogeneous agricultural systems, often with large fields of monoculture crops. These studies used broad band sensors like AVHRR, MODIS, Landsat series, SPOT, among others, which are of limited use in heterogeneous agricultural systems with small farm fields. Conclusions derived from such studies cannot be replicated in highly fragmented cropping systems common in Africa. Therefore, research applying remotely sensed data to estimate maize yield is urgently needed in Africa. The heterogeneity nature of Africa agricultural systems require detailed testing of available high resolution multispectral and hyperspectral sensors with capabilities to discriminate maize from other crops to improve accuracy of yield estimates.

Secondly, literature on studies applying remote sensing in Africa lacked information on mapping of maize area and distribution. This affects area calculation, a crucial input in estimating final production figures. There is a need to test available high resolution multispectral sensors' capabilities in mapping maize distribution with the ultimate objective of calculating maize area as an input in the final production estimates. Recent work by Fritz *et al*. (2015) mapping cropland at global, continental and national levels, including African countries, achieved encouraging accuracies using innovative approaches like crowdsourced data at national level. Furthermore, advances in global high resolution land cover mapping studies by Gong *et al*. (2013) and Zhao *et al*. (2014) have achieved high accuracies at 30m level. However, crop type discrimination still remains a challenge and the human and computing resources required are massive.

Thirdly, this review also shows a glaring gap in comparative studies between multispectral broadband (MBB) and hyperspectral narrow band (HNB) reflectance data in modelling maize yield and discriminating crop type, in order to improve final estimates. Furthermore, studies show that the quantification of maize biophysical parameters using hyperspectral data can be achieved using as few as 15 bands (Chan and Paelinckx, 2008; Thenkabail *et al*., 2004). However, to the best of our knowledge no studies have been conducted to explore

hyperspectral vegetation indices' (HVIs) capabilities to model maize yield in Africa. Comprehensive analysis of the HVIs from the 15 narrow bands is required to conclusively confirm the ideal wavebands, in order to understand their contribution to maize characterization. Fewer bands will also help to reduce data dimensionality.

Fourthly, there is lack of studies and information in Africa on how different maize biophysical parameters like LAI correlate with grain yield. Previous studies elsewhere (Báez-González *et al*., 2005) showed that LAI measured either on the ground or satellite-derived can be used to predict maize yield. Therefore, there is a need to undertake detailed studies to demonstrate the utility of remotely derived LAI to estimate yield over large areas.

Fifthly, as alluded to, different varieties within the same crop, in this case maize, may have different morphologies and even physiologies. Experienced crop experts can tell them apart visually. This means that it would appear feasible that a combination of morphological and reflectance parameters could uniquely describe individual varieties remotely through distinct signatures. Future studies with hyperspectral sensors should test their ability to distinguish individual varieties within a crop (intra-species). This would create invaluable opportunities for rapid phenotyping at low costs and accelerate maize genetic improvement as well as yield estimation.

Finally, in addition to the evolutionary development of methods to estimate yield in fragmented agricultural systems through use of freely available high resolution imagery from different satellite sensors, integrating remotely sensed data with crop growth models may improve yield estimates. Maas (1988) indicated that integrating remotely sensed data with crop growth models can be a good alternative given the ability of remote sensing to quantify crop status synoptically, while crop growth models are capable of describing crop growth daily throughout the season.

2.8 Conclusion

Our review shows that the use of satellite imagery to estimate maize yield offers possible and cost-effective options vis-a-vis conventional ground-based surveys, which are laborious, error-prone, expensive, inefficient and often unsuitable due to terrain inaccessibility. Yet the utilization of remotely sensed data in predicting maize yield in Africa is scant. The review

further established that in applying remote sensing in maize yield estimation, we should not overlook the intrinsic limitations caused by low and medium resolutions sensors in transferring these methodologies to fragmented agricultural systems. Spatial patterns in these heterogeneous agricultural systems like field size and shape define the appropriate spatial, temporal and spectral resolution to use. Mixed pixel problems will remain a challenge with low to medium resolution sensors in fragmented agricultural systems. However, significant improvements in yield estimation are expected with multispectral sensors like Sentinel 2, Landsat 8 OLI and other commercial high resolution sensors like WV, Dove, among others, whose pixel sizes are several times smaller than the field sizes prevalent in heterogeneous cropping systems. Likewise, one day distinguishing individual varieties within crops remotely through unique signatures seems at least in theory feasible. We, therefore, conclude that further studies are necessary to investigate the use of high resolution multispectral remote sensing in estimating maize yield in heterogeneous agricultural systems in order to increase our understanding of African agriculture and improve food security through early warning systems.

SECTION II: SPATIAL ANALYSIS AND PROXIMAL SENSING
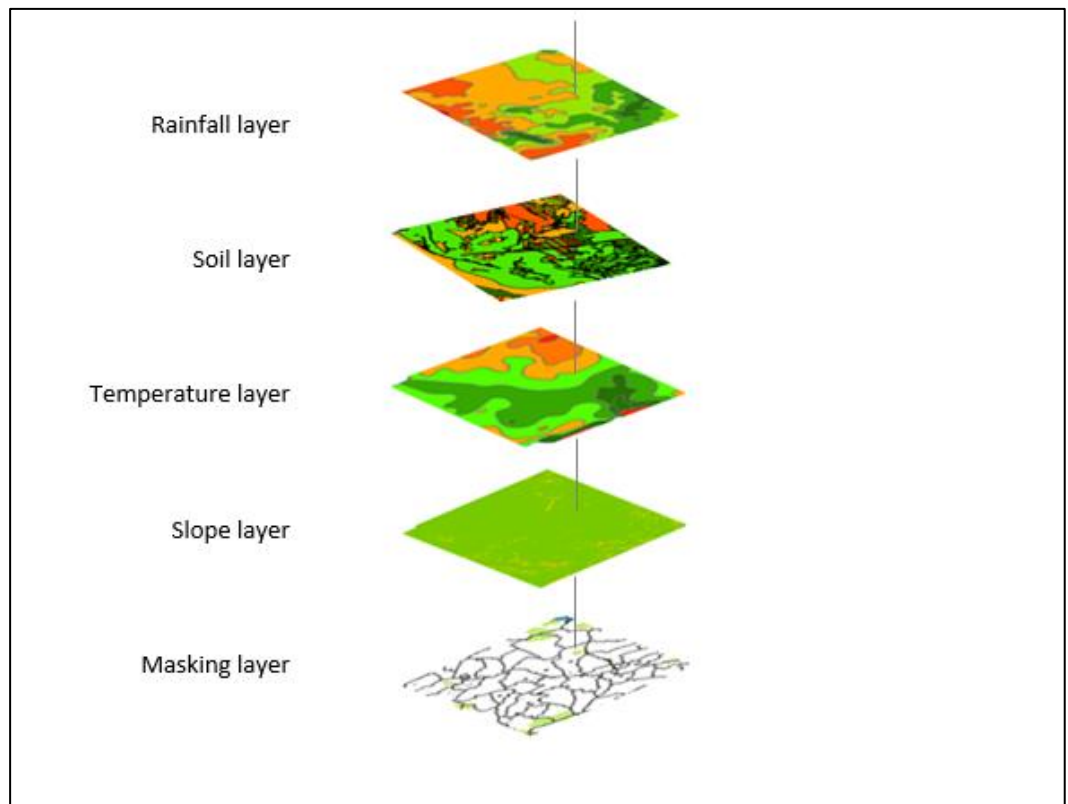
Spatial Analysis

CHAPTER 3: SPATIAL ANALYSIS OF LAND SUITABILITY FOR MAIZE PRODUCTION

This Chapter is based on:

Chivasa W, Mutanga, O., Biradar, C.M. **2019**. Mapping land suitability for maize production using GIS and AHP technique in Zimbabwe. *South African Journal of Geomatics* 8 (2), 265-281. http://dx.doi.org/10.4314/sajg.v8i2.11.

Abstract

Maize (*Zea mays* L.) is the major staple food crop in Zimbabwe, grown by 80% of the farmers and provides more than 50% of the population's dietary requirements. Understanding land suitability for maize production is critical in detecting environmental limits to sustainable maize production systems and variety deployment. The objective of this study was to integrate geographic information system (GIS) and analytic hierarchy process (AHP) to evaluate land suitability for maize production in Zimbabwe using multi-criteria evaluation (MCE) process. The assessment used four criteria (rainfall, temperature, soil type and slope gradient), each with six sub-criteria, to make a total of 24 factors. Four thematic maps were georeferenced, digitized and integrated through the overlay technique in a GIS environment to produce maize production suitability map. Finally, we overlaid the map of constraints (forestry and national parks, obtained from Surveyor General's office) with the maize suitability map to 'mask out' all protected areas and non-agricultural land (water bodies and built-up areas). The final maize suitability map shows that 3.20% of the total land is highly suitable, 16.56% is suitable, 25.34% is moderately suitable, 32.33% is marginally suitable and 9.57% is not suitable for maize production in its current form. The maize suitability classification was validated by regression analyses using measured maize grain yield of 5 key maize varieties representing 5 different maturity groups. Grain yield was regressed against suitability index (SI) of each land suitability class. There were significant positive correlations between maize grain yield and land suitability classes ($R^2 = 0.63 - 0.85$). This shows that land suitability is closely correlated to maize yield in Zimbabwe. Integrating GIS and AHP with MCE was effective in assessing land suitability for targeting location specific interventions for maize production and the result is the first comprehensive suitability map for Zimbabwe, incorporating several critical environmental factors affecting maize adaptation. We recommend the use of this suitability map as a decision support tool in land use planning and policy making regarding maize varietal placement.

Keywords: Mapping maize land suitability; Geographical Information System; Multi-criteria evaluation; Analytic hierarchic process; Zimbabwe.

3.1 Introduction

Maize (*Zea mays* L.) is the most preferred staple food crop in Zimbabwe and is currently cultivated by more than 80% of the farmers and provides more than 50% of the calorie requirements of the people (Rukuni *et al*., 2006). Understanding land suitability for maize production is the basis for sustainable land utilization and increased productivity. Land suitability evaluation involves the determination of the level of suitability of a given piece of land for a certain type of use (Akinci *et al*., 2013). Steiner *et al*. (2000) defined land suitability in terms of how close the properties of the land unit satisfy the requirements for a specified purpose when all the relevant critical factors are considered. FAO (1976), Beek *et al*. (1987) and Al-Shalabi *et al*. (2006), described land suitability analysis as a specific-purpose system for appraising and mapping specific land areas into distinct classes according to defined uses when limiting factors are considered simultaneously. Currently, Zimbabwe is classified into five agro-ecological zones based on mean annual rainfall as the main determinant. The demarcation of the country into agro-ecological regions was conducted in the 1960s by Vincent and Thomas (1960) and is still being used for decision making in terms of maize placement.

As yet, no land suitability assessment integrating most of the critical factors has been done (to the best of our knowledge) in Zimbabwe that informs the farmers, crop breeders, researchers and policy makers as to which area offers the most ideal conditions for maize production. Complete land suitability analysis takes into account all relevant physical environmental, climatic and socio-economic factors. However, socio-economic conditions can readily be manipulated and modified by human interventions and therefore are more time dependent. The physical environmental and climatic factors are known to be more stable over time (Dent and Young, 1981; Van Lanen, 1991; Triantafilis *et al*., 2001; Zhang *et al*., 2015). Accordingly, land suitability analysis for producing maize is largely based on environmental and climatic factors (Van Ranst *et al*., 1996). Comprehensive land suitability evaluation integrates three factors of an area (location, environmental constraints and uses) and provides a more integrated view of their interactions (Al-Shalabi *et al*., 2006). In such land suitability assessment, all factors affecting suitability are considered simultaneously (Keshavarzi *et al*., 2010), although they may influence crop growth and ultimately land suitability unequally,

and are themselves interactive with confounding feedback loops. This more inclusive but also compound approach presents some challenges since the level of significance of factors affecting land suitability are not equal (Elsheikh *et al.*, 2013). The need to consider different factors of varying importance simultaneously makes land suitability assessment a more complex exercise (Duc, 2006; Bandyopadhyay *et al.*, 2009; Akıncı *et al.*, 2013).

In practice on-the-ground, the relative importance of factors affecting land suitability is determined based on expert knowledge (Saaty, 1977, Eastman, 2012). GIS-based land suitability evaluation has been proven to be a powerful tool in integrating physical environmental factors of varying level of importance with expert knowledge into land suitability mapping (Carver, 1991; Malczewski, 2004). The process of combining physical environmental factors and expert knowledge to produce crop suitability maps with high explanatory power, and how assessments are compared and used, is known as the decision rule, which can either be simple or complex depending on the number of factors involved and included in the model (Eastman *et al.*, 1995). Because several factors and various criteria are involved, land suitability analysis is best described as a multi-criteria evaluation (MCE) problem (Reshmidevi *et al.*, 2009). Decision rules involve processes that combine factors into a single composite index using MCE processes. The most commonly used procedures in MCE are weighted linear combination (WLC) (Eastman *et al.*, 1995), concordance-discordance analysis (Voogd, 1983; Carver, 1991) and Boolean overlay technique (Malczewski, 2004). However, concordance-discordance analysis is computationally impractical when many factors are involved. On the other hand, Boolean land suitability classification procedures have many challenges (Banai, 1993). For example, Boolean overlay only classifies land units based on a precise, often binary definition (suitable or not suitable). Land units that do not satisfy a given definition will be excluded in the classification. In Boolean logic, an element is either in or out and does not allow part-membership. Membership is limited to two definitions, 0 (if element is not in set) and 1 (if element is in the set) (Banai,1993). WLC is now the most widely used procedure in MCE, where factors are assigned weights and combined through summation to yield a balanced suitability map in a GIS environment.

Several methods to determine the relative weights of factors exist. However, pairwise comparison known as the analytic hierarchy process (AHP) suggested by Saaty (1977) and

applied in several studies (Akinci *et al.*, 2013; Zhang *et al.*, 2015; Mu and Pereyra-Rojas, 2017), has been found to be the most suitable for handling multi-criteria data, which are heterogeneous in nature. Saaty (1977) indicated that AHP is a decision-making theory concerned with measurement of intangibles utilizing pairwise comparisons. The theory requires expert knowledge to derive priority measurements of complete judgements that show exactly by how much one factor dominates the other with respect to a given attribute (Saaty, 1977; Saaty, 2008). However, the judgements might be inconsistent. Measuring inconsistency in order to improve the judgements is the strength of the AHP approach. AHP enables us to understand complex problems through decomposing them into hierarchical structures depicting the connection of the goal, criteria and sub-criteria. The criteria and sub-criteria are pairwise compared to obtain a measure of relative importance and comparative scales. Pairwise comparison creates a ratio matrix, which simplifies an otherwise complex process and calculates reliability or discrepancy of the comparisons through a consistency ratio (CR). The CR measures consistency (CR < 10%) or inconsistency (CR > 10%) (Saaty 2002). If CR is greater than 10%, then the data used to construct the scale might need to be re-examined and additional information added to improve consistency. Once the factors are rated and weighted using AHP, they are analyzed in a GIS environment using the overlay technique (Malczewski, 2004).

In this study we integrated GIS and AHP in a MCE process to map land suitability for maize production in Zimbabwe using 24 factors. Rainfall, temperature, soil type and slope gradient were considered as sub-criteria, each with six classes for the suitability evaluation. The study seeks to address the question: which land areas are suitable for maize production in Zimbabwe? To be grown by farmers, the maize crop, at a minimum, have to be adapted to the farmers' area. The result of this study will enable farmers, crop breeders and policy makers to make informed decisions about maize crop placement, seed deployment and sustainable land utilization using spatially detailed information based on the land suitability map.

3.2 Materials and Methods

3.2.1 Study area

The study was conducted in Zimbabwe (Figure 3.1). Zimbabwe lies between latitudes $15^0$37'S to $22^0$24'S and longitudes $25^0$14'E to 33^0 04'E. The country is classified into five agro-ecological zones termed Natural Regions (NR). NR I is the wettest (>1050 mm per annum (p.a.)) and covers just 1% of the country. NR II receives 750 – 1000mm p.a. and covers 15% of Zimbabwe. NR III averages 650 – 800mm p.a., covering 19% of the total area. NR IV has an annual rainfall of 450 – 650mm p.a., covering about 38%. NR V's poorly distributed rainfall is usually less than 450mm p.a. and covers about 27% of the country's land area. Mashonaland West Province is the largest maize producer (23.40% in 2014) among the eight maize growing Provinces, and has four maize producing agro-ecological zones (II, III, IV and V). Manicaland Province has five agro-ecological zones but ranks only 4th in maize production (12.10%) after Mashonaland West (23.40%), Mashonaland Central (16.90%) and Midlands (16.40%). Zimbabwe has two clearly defined seasons: a rainy season (November – April) and a dry season (May – October). The steps followed in this study to generate a land suitability map are summarized in Figure 3.2 and briefly described below:
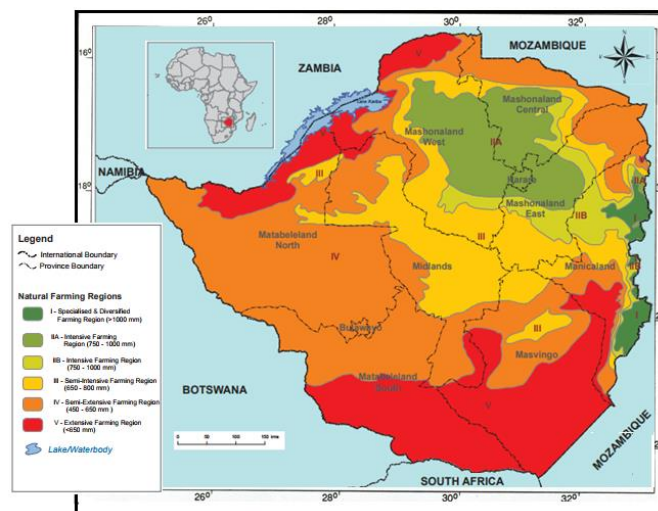
Figure 3.1. The location of study area (Zimbabwe) showing agro-ecological regions (natural farming regions) and Provinces. Insert shows the location of study area in Africa.
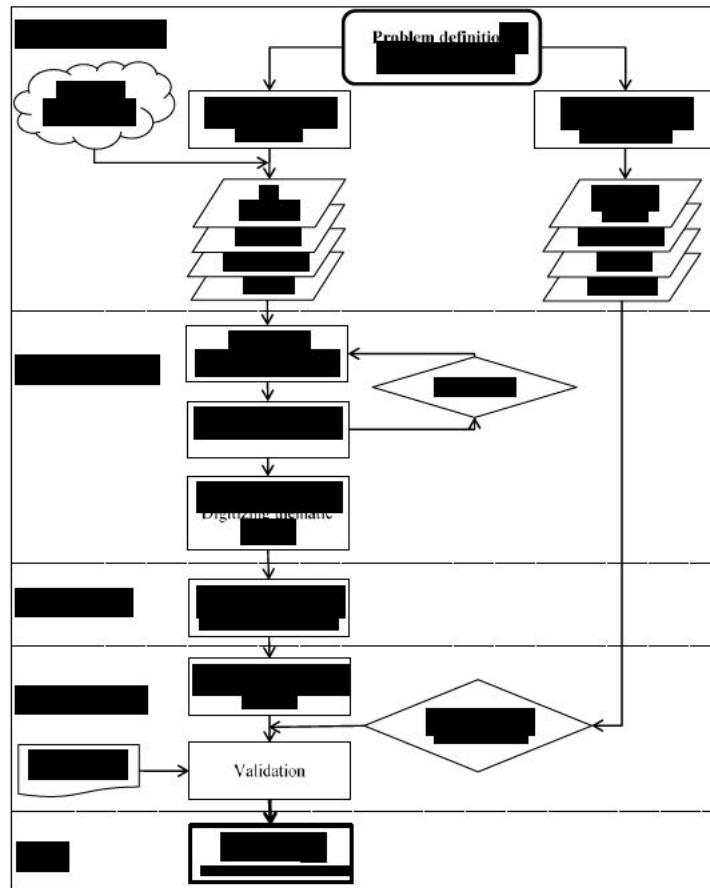
Figure 3.2. Land suitability analysis workflow used in this study

3.2.2 Establishing the criteria: factors and constraints

In land suitability analysis, criteria must be established including constraints. In this study, criteria were established from the literature and expert knowledge and were identified as environmental (soil type and slope gradient) and climatic (rainfall and temperature). Literature and experts identify rainfall (Huajun and Van Ranst, 1992, Elsheikh *et al.*, 2013), temperature (Herrero and Johnson, 1980; Schoper *et al.*, 1987; Dupuis and Dumas, 1990; Hatfield and Prueger, 2015), soil type (Braimoh *et al.*, 2004; Albaji *et al.*, 2009) and slope gradient (Bandyopadhyay *et al.*, 2009; Bagherzadeh and Mansouri Daneshvar, 2011) as major factors determining maize growth. These factors were used in this study to analyze land suitability for maize production. National parks, forests, etc. were identified as constraints, that is, the maize suitability areas should be outside protected areas (e.g. forestry and national parks) and non-agricultural lands (water bodies and built-up areas). Factors such as aspect, elevation, day length, relief, growing degree days, soil pH were not considered in this study.

47

Accurate pH data is not readily available. Aspect and day length are not major limiting factors to land suitability for maize production in Zimbabwe because most parts of the country receive sun exposure for almost equal hours because of the sun position during crop growing period. Equally, elevation was omitted because areas classified as highlands in Zimbabwe are insignificant. Relief plays a significant role in rugged terrains or in areas characterized by rapid changes in elevation. However, most of Zimbabwe is plateau with three distinct areas: the Highveld with altitudes ranging from 1 200 to 1 675m, the Middleveld with altitudes ranging from 600 to 1 200m, and the Lowveld with altitudes below 600m. Research has shown that, when rainfall, soil and temperature are not limiting, all the three areas are suitable for maize production. Therefore, relief was considered insignificant factor in the analysis. Selected factors are briefly explained below.

Rainfall amount is critical in maize growth, adaptation and variety placement. Higher values in rainfall indicate increasing suitability. Highly suitable areas for maize production in Zimbabwe are those receiving above 900mm per season (November to April) with above 18 rain pentads. Rainfall suitability classes were done according to Vincent and Thomas (1960). Very suitable areas were classified as those receiving rainfall in the 800 – 900mm range with 16 – 18 rain pentads. Suitable areas will be those receiving 700 – 800mm with 14 – 16 pentads, while moderately suitable are areas receiving 600 – 700mm with probability of mid-season dry spells. Areas receiving 500 – 600mm per season are prone to mid-season droughts and are thus classified as marginally suitable. Finally, areas receiving less than 500mm per season are classified as not suitable in their current form for maize production without supplementary irrigation. These rainfall classes are given in Table 3.1.

Temperature affects maize growth and evapotranspiration. Higher temperatures above the optimum upper limit indicate decreasing suitability. Maize growth is highly sensitive to high temperature at the pollination stage (Hatfield and Prueger, 2015). Maize pollen viability declines at temperatures above 35^0C (Herrero and Johnson, 1980; Schoper *et al*., 1987; Dupuis and Dumas, 1990). Furthermore, during grain filling, temperatures above 35^0C reduce grain formation and kernel sizes are reduced (Jones *et al*., 1984). Muchow *et al*. (1990) reported the highest grain yields at mean temperatures between 26 – 29^0C in warm tropical environments

and a decrease of 5 to 8% per every 2^{0}C temperature increase above 29^{0}C. The temperature suitability ranges used in this study are given in Table 3.1.

Soil types are important as they determine crop productivity in general and maize crop suitability, in particular. In crop suitability analysis, it is critical to know the dominant soil types and their characteristics. The soil type map was obtained from the Surveyor General of Zimbabwe's office. Soil types were placed into six groups (Table 3.1) according to suitability classification by Thompson (1965) and Nyamapfene (1992), where class I was designated highly suitable, Class II was designated very suitable, class 3 was designated suitable, class IV was moderately suitable, class V was marginal suitable, and class VI was not suitable. Suitability classes for soil type were determined based on soil types.

Slope is an important determinant of land suitability for maize production (Bandyopadhyay, Jaiswal *et al*. 2009, Bagherzadeh and Mansouri Daneshvar, 2011). Soil depth decreases with an increase in slope. Steep slopes are prone to erosion and are associated with soils that are relatively shallow and low in fertility thus affecting crop productivity indirectly through affecting soil properties. Furthermore, steep slopes affect crop production directly by restricting machine use in soil tillage and management operations such as irrigation and drainage. Therefore, higher values in slope indicate continuously decreasing suitability. In this study, slope was divided into six classes based on slope percentage. Slope suitability was classified (Bandyopadhyay *et al*., 2009; Bagherzadeh and Mansouri Daneshvar, 2011) as follows: I = highly suitable, II = very suitable, III = suitable, IV = moderately suitable, V = marginally suitable and VI = not suitable (Table 3.1). Current protected areas and non-agricultural lands (water bodies and built-up areas) were identified as "constraints" to maize suitability classification. The land suitability for maize production was obtained using overlay thematic maps of the four parameters (rainfall, temperature, soil type and slope).

3.2.3 AHP approach

The AHP model was made up of goal, criteria and sub-criteria (Figure 3.3), where the overall objective is the suitability map. In MCE process, the weight of each factor needs to be defined. Different approaches to assign weights to factors can be used, such as principal component analysis, regressions and AHP. A review of literature shows that AHP is quite robust in

determining the weights of the assessment factors in comparison with other methods (Saaty, 1977; Malczewski, 2004; Akinci *et al*., 2013; Zhang *et al*., 2015; Mu and Pereyra-Rojas, 2017). Relative importance of criteria were assigned using Saaty's scale (Table 3.2) (Saaty, 1977).

Table 3.1. Criteria used in suitability mapping and their brief descriptions

Level 1		Level 2			
Criteria	Sub-criteria	Class	Suitability range	Description	Reference
Rainfall	Rain1	I	≥ 901 mm	High rainfall ranging from 900 mm and above. Rainfall in this area is well distributed during maize growth period (Nov - April). Receives above 18 rain pentads per season and is very reliable	Vincent & Thomas 1960
	Rain2	II	801 - 900 mm	Recives rainfall in the range of 801 - 900 mm. Receives on average 16-18 rain pentads per season and reliable	Vincent & Thomas 1960
	Rain3	III	701 - 800 mm	Rainfall ranges from 701- 800 mm per annum. Receives 14 - 16 rain pentads per season.	Vincent & Thomas 1960
	Rain4	IV	601 - 700 mm	Receives moderate in total amount. The area is also subject to mid season dry spells	Vincent & Thomas 1960
	Rain5	V	501 - 600 mm	Receives low rainfall, prone to periodic droughts and severe dry spells during the season	Vincent & Thomas 1960
	Rain6	VI	400 - 500 mm	Rainfall in this area is too low and erratic for reliable production of even drought-resistant grain crops	Vincent & Thomas 1960
Soil type	Soil1	I	Fersiallitic group	Moderate - very deep reddish, brown granular clays formed on mafic rocks.	Thompson 1965; Nyamapfene 1992
	Soil2	II	Fersiallitic group	Moderate shallow, geryish brown, relatively silty sandy loams	Thompson 1965; Nyamapfene 1992
	Soil3	III	Paraferrallitic group	Sandy soils with substential ferralitic characteristics	Thompson 1965; Nyamapfene 1992
	Soil4	IV	Siallitic group	Prodominantly illite or illite-montmorillonoid clay soil, with or without calcareous in the underlying material.	Thompson 1965; Nyamapfene 1992
	Soil5	V	Rigosol/Lithosol groups	Sand soils with less than 10% silt + clay above 2 m. Very low silt/clay ratios (so called Kalahari sands).	Thompson 1965; Nyamapfene 1992
	Soil6	VI	Sodic group	Soils containing significant amounts of exchangeable sodium within 80 cm of the surface horizons	Thompson 1965; Nyamapfene 1992
Temperature	Temp1	I	24 - 28°C	Optimal temperature = highly suitable	Muchow *et al*. 1990; Hatfield and Prueger 2015
	Temp2	II	28 - 30°C	Sub-optimal - very suitable	Muchow *et al*. 1990; Hatfield and Prueger 2015
	Temp3	III	31 - 32°C	Beyond this growth is affected - still suitable	Muchow *et al*. 1990; Hatfield and Prueger 2015
	Temp4	IV	33 - 34°C	Five consecutive days at this results in > 2% yield loss	Muchow *et al*. 1990; Hatfield and Prueger 2015
	Temp5	V	35 - 36°C	Leaf firing & pollen death result in large yield losses	Muchow *et al*. 1990; Hatfield and Prueger 2015
	Temp6	VI	> 36°C	More than 5 days at this = permanent wilting & death	Muchow *et al*. 1990; Hatfield and Prueger 2015
Slope gradient	Slope1	I	0.0 - 5.0 %	Highly suitable	Bandyopadhyay et al. 2009
	Slope2	II	5.1 - 10.0 %	Very suitable	Bandyopadhyay et al. 2009
	Slope3	III	10.1 - 15.0 %	Suitable	Bandyopadhyay et al. 2009
	Slope4	IV	15.1 - 20.0 %	Moderately	Bandyopadhyay et al. 2009
	Slope5	V	20.1 - 25.0 %	Marginally suitable	Bandyopadhyay et al. 2009
	Slope6	VI	$\geq 25.1\%$	Not suitable	Bandyopadhyay et al. 2009

I = highly suitable, II = very suitable, III = suitable, IV = moderately suitable, V = marginally suitable and VI = not suitable.
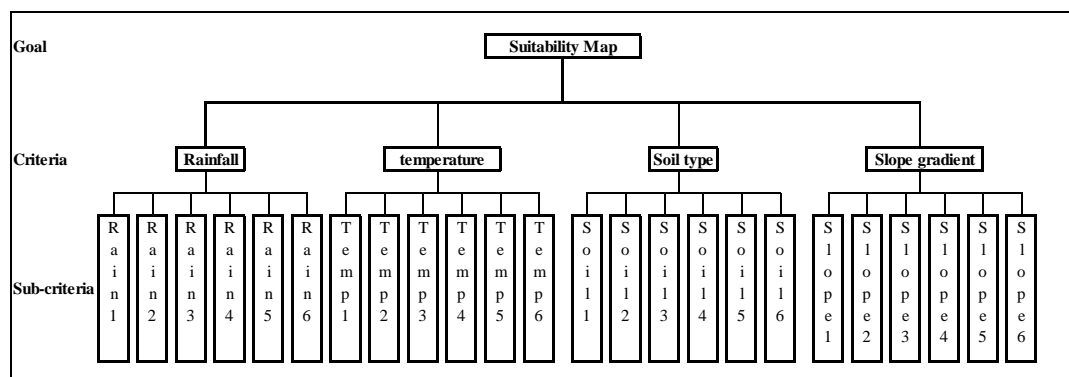
Figure 3.3. Decision tree model for land suitability analysis using AHP

The pairwise comparison matrix for criteria and sub-criteria were constructed. Saaty (1977) recommended a scale for evaluation comprising of values from 1 to 9, describing the relative importance of factors over one another. To arrive at relative importance of each factor, 28 scientists were requested to give the importance of the factors through consensus. These scientists included crop breeders, agronomists, soil scientists and climatologists following a similar methodology used in other land suitability studies (Eastman, 2012; Zhang *et al.*, 2015)

A pair-wise comparison matrix for the sub-criteria was constructed, which was normalized to obtain the suitable weights and the consistency ratio (CR) was determined (Table 3.3). The 4 × 4 matrix comprises all the pair-wise comparisons for the four criteria. Different methods of calculating weights and eigenvalues in AHP exist (Saaty, 1983). This study used the geometric mean suggested by Saaty (1983) to calculate the factor weights. Using the geometric mean, the nth root of the product of the pair-wise comparison values in each row of the matrices was determined. The nth root was then normalized by dividing each nth root value by their sum to obtain the corresponding weights. If a matrix is of the order n (total elements in comparison), then the total number of judgements needed is given by $(n^2 - n)/2$ with diagonal elements being equal to unity since it is a reciprocal (Saaty, 1987). When comparing a pair of factors *(i,j)* in a matrix, with *i* on the left side of the matrix and *j* on top of the matrix, the objective is to see which factor is more important and by how much, using the scale developed by Saaty (1977) (Table 3.2). This gives a_{ij} (or a_{ji}), while the reciprocal value is entered for the transpose, where a_{ij} is relative importance value of factor *i* relative to factor *j* in the matrix.

Table 3.2. The scale for pair-wise comparison

Intensity of importance	Description
1	Equally important
2	Equally to moderately important
3	Moderately important
4	Moderately to strongly important
5	Strongly important
6	Strongly to very strongly important
7	Very strongly important
8	Very strongly to extremely important
9	Extremely important

Source: Saaty and Vargas (1991)

Lambda-max (λ_{max}) was determined by adding the columns of the matrix of judgements and multiply the resulting vectors by the priority vector (weight) then sum the products (Table 3.3) following Saaty's method (Saaty, 2002). The sum yielded the eigenvalue denoted by λ_{max}. The consistency index (CI) was determined using Saaty's (1977; 2012) equation [3.1]:

$$CI = \frac{(\lambda max - n)}{n - 1} \qquad [3.1]$$

Where λ_{max} is the largest or principal eigenvalue of the matrix, and *n* is the number of criteria or factors being compared. The CI equation has been applied in similar work by Akinci *et al*. (2013), Zhang *et al*. (2015) and Mu and Pereyra-Rojas (2017), among others. The consistency ratio (CR) was calculated using Saaty (1996)'s equation [3.2]:

$$CR = \frac{CI}{RI} \qquad [3.2]$$

Where RI is the Random Index (Table 3.4), determined by Saaty and Tran (2007). CR is a measure of the decision maker's consistency when rating the factors used in the pair-wise comparisons. It is the measure of departure of λ_{max} from *n*. It shows the likelihood that the ratings were developed by chance. The ideal CR is zero (0). However, in practice achieving zero is difficult. To be accepted the CR must be < 10%, and if CR > 10% then the decision maker should re-evaluate the pair-wise comparison to identify the source of inconsistency and resolve it and repeat the analysis until CR reaches an acceptable level (Saaty, 1996).

Table 3.3. Pair-wise comparison of relative importance of sub-criteria

	Rainfall	Soil type	Temperature	Slope gradient	Weight
Rainfall	1	5	7	9	0.652
Temperature	0.143	1	5	7	0.231
Soil type	0.125	0.143	1	5	0.085
Slope gradient	0.111	0.125	0.143	1	0.033

Max. Eigenvalue (λ_{max}) = 4.1772; n = 4; Consistency Index (CI) = ($\lambda_{max} - n$)/(*n*-1) = 0.0591; RI = 0.89; Consistency Ratio (CR) = CI/RI = 0.07

Table 3.4. The Random Indices

N	1	2	3	4	5	6	7	8	9	10	11	12	13	14	15
RI	0.00	0.00	0.52	0.89	1.11	1.25	1.35	1.40	1.45	1.49	1.52	1.54	1.56	1.58	1.59

Source: Saaty and Tran (2007)

The second step of AHP involved determination of relative ratings of each class for each criterion. As indicated earlier, each criterion had six classes (Figure 3.2). Therefore each matrix of the classes was of the order of 6 × 6. Pair-wise comparison for each class was constructed (Table 3.5) and λ_{max} determined. The CI and CR were determined using equations [3.1] and [3.2], respectively. Finally, the land suitability index (SI) was obtained by combining each factor weight (W_i) with factor score (X_i) to get a suitability value for each land unit following a similar approach used by Bagheri *et al*. (2013), Malczewski (2004) and Feizizadeh and Blaschke (2013) using equation [3.3]:

$$ SI \quad = \quad (\sum_{i=1}^{n} W_i \times X_i) \times \Pi C_i \qquad [3.3] $$

Where SI is the suitability value, W_i is the weight of factor i, X_i is the criterion score of factor i, C_i is the constraints (Boolean value), and Σ is the sum and Π is the product. SI lies between 0 and 1 because values of both W_i and X_i are between 0 and 1. In this case values near zero represent unsuitable areas, while those near one indicate highly suitable areas. Since C_i is the land use constraint, it only takes a value of either 0 or 1 (Boolean logic), where zero was assigned to protected land (national parks and forests) and non-agricultural land (built-up areas and water bodies) and 1 represents current and potential croplands.

3.2.4 Digitizing and overlay of thematic maps

Thematic maps for rainfall, temperature, soil type and slope gradient were obtained from the Surveyor General's office of Zimbabwe. Spatial databases were created by geo-referencing, digitization, vectorization and rasterization of thematic maps of rainfall, soil type, temperature and slope gradient. The thematic maps were digitized using ArcGIS (ArcGIS 10.3) and each reclassified into six different land suitability classes (Figure 3.4).

Table 3.5. Pair-wise comparison of relative importance of classes

(a) Rainfall

	Rain1	Rain2	Rain3	Rain4	Rain5	Rain6	Weight
Rain1	1	3	5	7	8	9	0.4559
Rain2	0.333	1	3	5	7	8	0.2632
Rain3	0.200	0.333	1	3	5	7	0.1423
Rain4	0.143	0.200	0.333	1	3	5	0.0744
Rain5	0.125	0.143	0.200	0.333	1	3	0.0410
Rain6	0.111	0.125	0.143	0.200	0.333	1	0.0232

(b) Temperature

	Temp1	Temp2	Temp3	Temp4	Temp5	Temp6	Weight
Temp1	1	2	3	4	5	6	0.4014
Temp2	0.500	1	2	3	4	5	0.2364
Temp3	0.333	0.500	1	2	3	4	0.1689
Temp4	0.250	0.333	0.500	1	2	3	0.0886
Temp5	0.200	0.250	0.333	0.500	1	2	0.0600
Temp6	0.167	0.200	0.250	0.333	0.500	1	0.0448

(c) Soil type

	Soil1	Soil2	Soil3	Soil4	Soil5	Soil6	Weight
Soil1	1	2	3	4	5	7	0.3870
Soil2	0.500	1	2	3	4	5	0.2493
Soil3	0.333	0.500	1	2	3	4	0.1587
Soil4	0.250	0.333	0.500	1	2	3	0.1000
Soil5	0.200	0.250	0.333	0.500	1	2	0.0639
Soil6	0.143	0.200	0.250	0.333	0.500	1	0.0410

(d) Slope gradient

	Slope1	Slope2	Slope3	Slope4	Slope5	Slope6	Weight
Slope1	1	1	3	4	5	6	0.3518
Slope2	1	1	1	3	4	5	0.2610
Slope3	0.333	1	1	1	3	4	0.1662
Slope4	0.250	0.333	1	1	1	3	0.1047
Slope5	0.200	0.250	0.333	1	1	1	0.0669
Slope6	0.167	0.200	0.250	0.333	1	1	0.0495

(a) Max. Eigenvalue (λ_{max}) = 6.5068; n = 6; Consistency Index (CI) = 0.1014; Consistency Ratio (CR) = 0.08;

(b) Max. Eigenvalue (λ_{max}) = 6.1934; n = 6; Consistency Index (CI) = 0.0387; Consistency Ratio (CR) = 0.03;

(c) Max. Eigenvalue (λ_{max}) = 6.0217; n = 6; Consistency Index (CI) = 0.0043; Consistency Ratio (CR) = 0.04;

(d) Max. Eigenvalue (λ_{max}) = 6.1075; n = 6; Consistency Index (CI) = 0.0215; Consistency Ratio (CR) = 0.02; Random Index (RI) = 1.24.

The Digital Elevation Model (DEM) (20m contour interval) was used to generate a slope gradient layer (Figure 3.4d). The thematic maps were aggregated to produce a maize suitability map using the overlay technique in a GIS environment (Eastman *et al*., 1995). For further details on overlay techniques, readers are referred to Collins *et al*. (2001) who gave a more detailed review of the historical development of overlay technique in land suitability analysis.

The maize suitability map produced by overlaying different thematic maps was integrated with the constraints map to "mask out" all protected areas (national parks and forests) and

non-agricultural land (water bodies and built-up areas). After "masking out" constraints, the size of each land suitability class was determined including the size of protected areas and non-agricultural land.

3.2.5 Validation using maize yield responses

Finally, linear regression analyses were carried out to validate the final maize suitability classification. Saaty (1977), Bagheri *et al*. (2013) and Zhang *et al*. (2015) suggested that the actual validation of derived suitability classes rests with statistical measures. Long-term maize yield for key varieties were obtained from Seed Co's multi-environment trials (METs) conducted over a period of 10 years. Measured long-term yields of five key and popularly grown maize varieties representing five different maturity groups (ultraearly ≤100 days, very early = 101 – 120 days, early = 121 – 130 days, medium = 131 – 140 days and late = 141 – 150 days) were regressed against the SI value of each land suitability class to validate the classification. The Kolmogorov-Smirnov test was conducted to test for normal distribution of the land classes (Zhang *et al*., 2015).
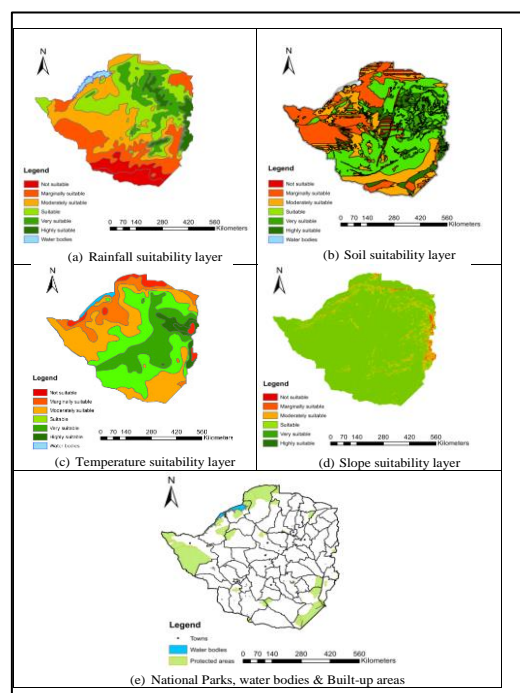
Figure 3.4. Maps for the significant layers used to generate the maize land suitability map: (a) rainfall, (b) soil type, (c) temperature, (d) slope gradient and (e) Parks, water bodies and built-up areas.

3.3 Results

The pairwise comparison matrix produced weights shown in Table 3.3 for annual rainfall, temperature, soil type and slope gradient. The consistency ratio was 0.07, which is less than 10% and therefore acceptable (Saaty, 1977; Saaty, 2002). Furthermore, the pairwise comparison of classes (Table 3.4) yielded normalized weights shown in Table 3.5 giving CRs of 0.08, 0.03, 0.04 and 0.02 for rainfall, temperature, soil type and slope gradient, respectively, which are below the acceptable limit of 10% (Saaty, 1977; Saaty, 2008).

3.3.1 Rainfall Suitability

The size of land area and distribution in terms of rainfall suitability is shown in Figure 3.4a and Table 3.6. The results showed that only 5.28% of the total land is highly suitable, 12.11% is very suitable and 25.28% is suitable for maize production. About 10.49 % in its current form is not suitable without further human intervention. The remainder comprise 26.13% and 20.70% classified as moderately and marginally suitable, respectively.

3.3.2 Temperature Suitability

Temperature suitability map is shown in Figure 3.4b, while Table 3.6 shows the calculated area for each suitability class. For a total area of 386 850km², only 5.08% is highly suitable, 18.80% is classified as very suitable and 30.03% as suitable. Moderately suitable and marginally suitable are made of 29.94% and 12.05% of the total area, respectively. About 4.10% is not suitable for maize production in its current form.

3.3.3 Soil type suitability

A land suitability map in terms of soil type is shown in Figure 3.4c and suitability area distribution is shown in Table 3.6. The results showed that 11.73% is highly suitable, 38.05% is very suitable, 4.01% is suitable and only 2.91% is not suitable for maize production. About 18.88% and 24.43% of the total land were classified as moderately and marginally suitable, respectively.

3.3.4 Slope gradient suitability

Land suitability for maize production can be influenced by topographical factors such as relief, aspect, elevation and slope. However, in this study only slope was considered while the other factors are not considered for the reasons given earlier. A land suitability map in terms of slope is shown in Figure 3.4d and area distribution is shown in Table 3.6. The results showed that 63.69% of the total area was highly suitable while 23.58% is very suitable together constituting more than 87.27% of the total area. Insignificant amounts were classified as moderately suitable (3.24%), marginally suitable (1.24%) and not suitable (0.35%).

3.3.5 Overall suitability

Criteria modelling produced different thematic maps, one for each criterion. Figure 3.4 shows different thematic maps reclassified into six land suitability classes. Integration of all the thematic layers (Figure 3.4a-d) and masking out the constraints in Figure 3.4e produced a detailed and complete maize suitability map (Figure 3.5). The map was classified into five suitability classes: *highly suitable, suitable, moderately suitable, marginally suitable and not suitable*. The highly suitable class represents land with negligible limitations that are insignificant to affect maize growth. Thus, maize productivity is expected to decrease continuously from highly suitable to marginally suitable land until it is no longer feasible to grow maize (not suitable area) under purely rain-fed conditions. The unsuitable land is that which cannot support maize growth in its current state.

The size of the final suitability land classes are given in Table 3.6. The result shows that only 12,383.50km^2, representing about 3.20% of the total land is highly suitable. Suitable areas occupy 64,065.03km^2, which represents 16.56% of the total area. Together, highly suitable and suitable areas take about 19.76% of the total area. The areas are mainly situated in the north-eastern parts of the country. The mean annual temperatures of these highly suitable and suitable areas range from 24 to 30^{0}C, while their average rainfall per year is between 801 and 900mm and receives an average of 14 – 16 rain pentads per crop growing season. These are areas characterized by fersiallitic soils with moderate to very deep reddish, brown granular clays soils (Thompson, 1965; Nyamapfene, 1992) and slopes of 0 – 15%, with excellent drainage.
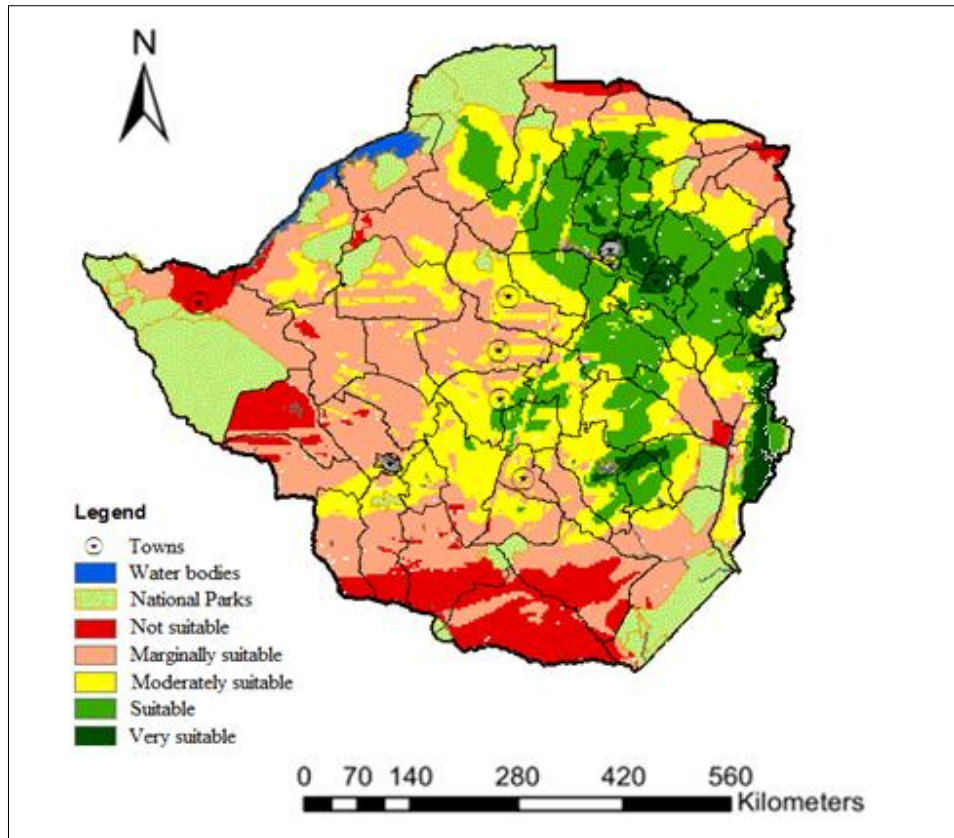
Figure 3.5. Final land suitability map for maize production in Zimbabwe

Land areas classified as moderately suitable are those with slope from 15.1 – 20.0%. The areas covered an area of 98,032.32km² and accounted for 25.34% of the total area. These areas are scattered around the periphery of suitable areas and receive 701 – 800mm annual rainfall, with mean temperatures of 30 – 32⁰C, and are characterized mainly by loamy and clay loamy soils. Marginally suitable areas constitute 125,051.38km², which represent 32.33% of the total area. These are areas, which receive 501 – 600mm rainfall per annum and experience frequent droughts and prolonged dry spells during the crop growing season. The soils of the areas are deep sands with extremely low silt/clay ratios. These are mainly distributed in the south and south-west of the country. Non-suitable areas cover an area of 37,027.27km² and represent 9.57% of the total area. The areas are mainly found in the south and west of the country. Most of the soils in these areas are sodic, containing significant amount of exchangeable sodium within 80cm of the surface horizon. Average temperatures are above 35⁰C and rainfall is below 500mm per annum. The areas experience very erratic rainfall for reliable crop production of even drought resistant varieties.

Protected land, built-up areas and water bodies defined as constraints in this study constituted about 13.00% of the total land area. The overall suitability distribution is shown in Figure 3.6. The Kolmogorov-Smirnov test shows that it is not a normal distribution but exhibits a slight left skewness. Land suitability for maize production generally decreases from north-east to south-west of the country. Suitability is high in the north-eastern parts of the country due to high rainfall, deep fertile soils, favorable temperatures and gentle slopes. The bulk of the study area is made up of moderately and marginally suitable areas, together constituting 57.67% of the total potential area available for maize production.

Table 3.6. Suitability areas and their distribution for each thematic layer.

Suitability	Area (Km^2)	Area (%)
Rainfall		
Highly suitable	20441.19	5.28%
Very suitable	46856.21	12.11%
Suitable	97794.18	25.28%
Moderately suitable	101098.01	26.13%
Marginally suitable	80081.42	20.70%
Not suitable	40578.99	10.49%
Total	386850.00	100.00%
Temperature		
Highly suitable	19667.45	5.08%
Very suitable	72746.75	18.80%
Suitable	116154.08	30.03%
Moderately suitable	115817.86	29.94%
Marginally suitable	46616.99	12.05%
Not suitable	15846.88	4.10%
Total	386850.00	100.00%
Soil type		
Highly suitable	45362.15	11.73%
Very suitable	147200.06	38.05%
Suitable	15509.40	4.01%
Moderately suitable	73034.95	18.88%
Marginally suitable	94492.48	24.43%
Not suitable	11250.95	2.91%
Total	386850.00	100.00%
Slope gradient		
Highly suitable	246369.08	63.69%
Very suitable	91226.21	23.58%
Suitable	30565.93	7.90%
Moderately suitable	12538.11	3.24%
Marginally suitable	4814.29	1.24%
Not suitable	1336.38	0.35%
Total	386850	100.00%
Overall Suitability		
Very suitable	12383.50	3.20%
Suitable	64065.03	16.56%
Moderately suitable	98032.32	25.34%
Marginally suitable	125051.38	32.33%
Not suitable	37027.27	9.57%
Others (Parks, etc.)	50290.50	13.00%
Total	386850.00	100.00%
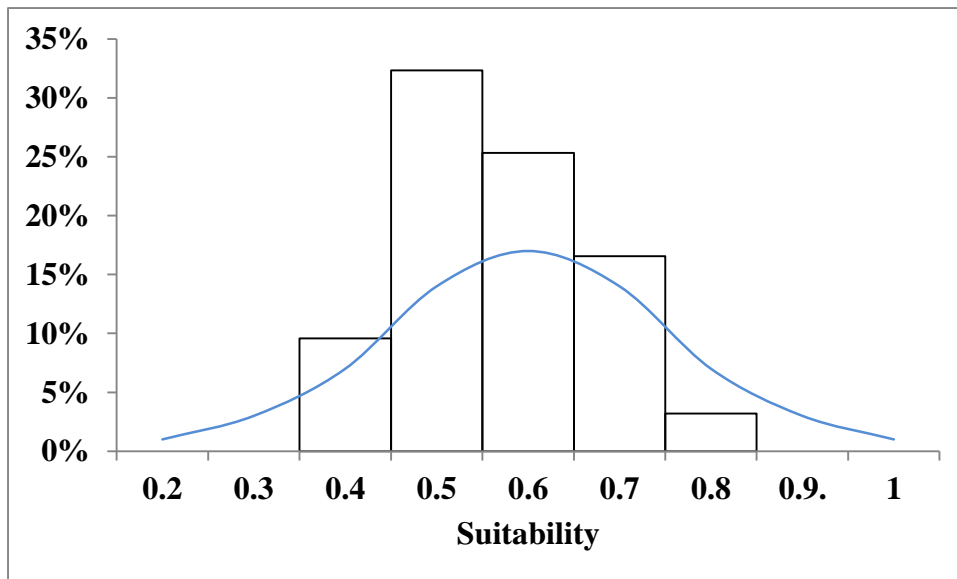
Figure 3.6. Overall distribution of the land suitability classes (from not suitable to highly suitable). The line graph shows the expected normal distribution.

3.3.6 Validation of classification results

The validity of the results of the classification was verified using regression analysis of measured maize grain yield and land suitable indices (Figure 3.7). All regressions coefficients were statistically significant, indicating that land suitability is directly linked to maize yield in Zimbabwe. The coefficients of determination (R^2) ranged from 63 to 85%. The correlations between grain yields (Figure 3.7) and suitability classes (Figure 3.5) is critical in placement of varieties of different maturity groups. Obtaining high yield in maize is largely a matter of matching land capability with varieties of suitable maturities. In most parts of Zimbabwe, rainfall, temperature, soil type and slope gradient are the major determinant factors. The correlation analyses confirmed the accuracy of classification and showed good agreement between ranked land suitability classes and maize yield, which is a measure of genotypic adaptation. Braimoh *et al*. (2004) used maize grain yield to validate a suitability map in Ghana and found a high positive correlation ($R^2 = 0.87$) between ranked land suitability classes and maize yield. They concluded that land suitability classes were closely associated with maize yield in Ghana. Huajun and Van Ranst (1992) also used maize grain yield to validate land suitability mapping in Aitai County, China and found maize grain yield to be highly correlated with ranked land suitability classes.
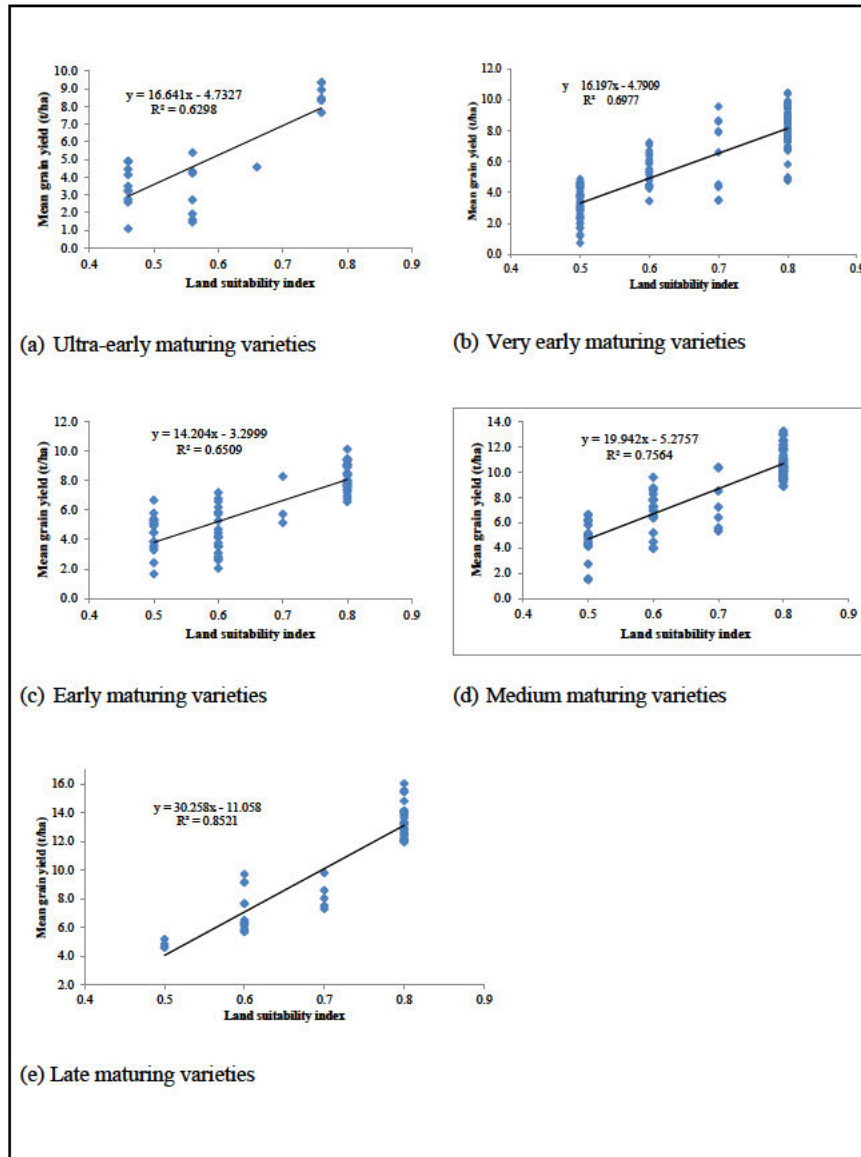
Figure 3.7. Regression analysis of maize grain yield vs land suitability index (a) late, (b) medium, (c) early, (d) very early, and (e) ultraearly maturing maize varieties

3.4 Discussion

The primary focus of this study was to map land suitability for maize production in Zimbabwe using MCE process. Understanding land suitability for maize production is critical in detecting environmental limits to sustainable maize production systems and variety deployment. Using GIS and AHP in land suitability appraisal and mapping systems produce quick but general suitability maps. This is helpful as a first appraisal, but detailed quantitative

61

information is needed to validate the classification against reality (Van Lanen and Bouma, 1989; Rossiter, 1990). For example, empirical data of crop performance from each land suitability class is needed to validate the classification. The land suitability map should only be considered valid if suitability indices correlate well with empirically derived crop yield response (Huajun and Van Ranst, 1992).

In the present study, validation of land suitability classification was performed using 10 years data from multi-environmental trials conducted in each land suitability class. The high correlation (with R^2 ranging from 0.63 to 0.85) observed between maize yield and suitability indices reflect the accuracy of the classification. The results show that combining GIS and AHP in assessing land suitability was effective in producing a land suitability map for maize production in Zimbabwe. Utilizing actual yield response of the intended crop in validation of land suitability classification provides a more detailed assessment of potentials of each land class. Previous studies recommended the use of actual crop yield in validating the suitability classification to confirm whether indeed lands deemed highly suitable from the classification analysis produce high yields (Zhang *et al*., 2015). Researchers elsewhere also found good correlation between land suitability and crop yield. For example, Braimoh *et al*. (2004) in maize ($R^2 = 0.87$) and Keshavarzi *et al*. (2010) in wheat ($R^2 = 0.91$). In the current study, the validation results fully confirmed the suitability classification, with low yields being highly correlated with less suitable land classes and highly suitable land classes associated with high yields.

The AHP procedure used in this study served as a useful tool in decomposing an otherwise complex land suitability problem, where factors were arranged in a descending hierarchical from the overall goal, criteria and classes in successive levels. This reduced a multidimensional problem into a unidimensional one. Once the decision structure was decomposed into its finer distinguishable details, pairwise comparison judgements were used to capture the reality on the ground for our understanding in order to aid decision making process. The strength of AHP in measuring consistency or lack thereof, improved the authenticity of the results of this study. For each hierarchical level of criteria and classes, the consistency ratios were acceptable (< 10%) as proposed by Saaty (1977; 2012).

Our results agree with findings by other land suitability analysis studies integrating GIS and AHP in a MCE process to map land suitability for agricultural use (Akıncı *et al.*, 2013), irrigated and rainfed agriculture (Feizizadeh and Blaschke, 2013), tobacco (Zhang *et al.*, 2015), wheat (Mendas and Delali, 2012), and maize (Braimoh *et al.*, 2004). The land suitability classes in this study are given in relative importance, which are decreasing in suitability from highly suitable to non-suitable. Van Lanen (1991) indicated that there is a priority of sequence of land use built into a suitability system, with a downward sequence of suitability. This agrees with Wang (1994) who discussed relative suitability. This study mapped land into relative suitability for maize production, and therefore, land with the highest suitability class, would be expected to produce relatively high maize grain yield and naturally be best suited for high yield-potential maize varieties under intensive culture (optimum inputs and management). The less suitable areas will be best suited for decreasing maturity varieties. Land classified as marginally suitable will likely still be suited for short-season varieties, capable of escaping major environmental stresses, or put to other land use types such as drought tolerant crops, livestock, national parks or recreational purposes. Thus, this land suitability mapping explored the potential land use options in an integrated approach incorporating the major limiting factors.

The final maize suitability map is a result of GIS-based land suitability analysis converting data into information that transform and adds value to the original data, which in its original form may not be useful to the end users (farmers, crop breeders and policy makers). This study has shown that GIS-based land suitability analysis is a powerful tool with the ability to incorporate both hard (physical environmental factors) and soft (expert knowledge) data into new information in the form of single suitability map (Carver, 1991; Malczewski, 2004). Hence, when integrated with AHP in a MCE process, GIS transforms and combines geographical data and value judgements into decision making information (Malczewski, 2006a; 2006b).

However, while the regression analyses of measured maize grain yield against land suitability classes showed significant positive correlations (R^2 = 0.63 - 0.85), the analysis does not incorporate different crop management practices. Therefore, the analysis only shows the probable suitable areas for producing maize in different land areas. The fact that an area is highly suitable does not entail that high yields would be obtained without employing proper

farming practices, which include time of planting, fertilizer application, weed control and appropriate variety choice. Successful maize production systems largely depend on precise matching the target crop and variety with land suitability and good agronomic practices. Consequently, future studies need to quantify genetic correlations of different varietal maturity and land suitability classifications obtained in this study in order to support varietal placement decisions.

A challenge in using MCE analysis lies in the definition of weights for a given set of criteria. One approach to resolving this is to use AHP (Saaty, 1977), which was used in this study. In addition, another challenge is how to specify the criteria performance scores, which often becomes subjective in their determination (Lamelas et al., 2012). Data that have been recorded directly will certainly be more reliable than estimates, interpolations, extracted from a map, or simply interpreted. Therefore, the criteria data collection approach is important (Marinoni, 2005). A stochastic approach, which uses probability distributions for the input variables as compared to the use of single values takes into account the uncertainty of input values is one way to solve this dilemma (Lamelas et al., 2012).

Nevertheless, the integrated land suitability map and the individual criterion thematic maps obtained in this study are crucial in supporting government land use planning and farmers' decision making process in maize production. All the maps from the primary thematic maps showing partial suitability to synthesized (integrated) overall suitability map can be used as decision making tools. For example, the primary factor(s) responsible for low suitability index can be readily identified and managed to raise suitability index. Therefore, the final maize land suitability map and each thematic layer are valuable decision making tools, which can be used to evaluate and understand local, regional and national land dynamics and structure.

3.5 Conclusion

In this study, we set to integrate GIS and AHP to assess land suitability for maize production in Zimbabwe using multi-criteria evaluation (MCE) process. The spatial data of the land evaluation criteria and their weights were derived using GIS and AHP. From the results, it was concluded that:

- Integrating GIS and AHP with computer-captured expert knowledge was useful as a decision support tool in land suitability classification and mapping for maize production;

- The integration allowed us to manage the factors, create thematic layers, compute criterion weights, combine decision criteria through modelling, perform validation analyses and the production of maize suitability map needed for spatial decision-making support in maize crop placement;

- Significant positive correlation between maize yield and suitability indices is an indication that land suitability is directly linked to maize yield in the study area;

- AHP is a powerful method that is able to deal with inconsistent judgements and provides a measure of the inconsistency.

The results of the study can serve as a basis for decision support management tool for policy makers and land-use planners regarding maize production in Zimbabwe. However, this land suitability analysis does not incorporate management decisions. Therefore, good farming practices, such as time of planting, fertilizer application, weeding and variety choice need to be employed in order to get maximum yields. The success of maize production systems largely depend on precise matching of the target crop and variety with land suitability. Consequently, future studies need to quantify genetic correlations of different varietal maturity and these land suitability classes.

CHAPTER 4: FIELD SPECTROMETER BASED REMOTE SENSING OF MAIZE

This Chapter is based on:

Chivasa W, Mutanga, O., Biradar, C.M. **2019**. Phenology-based discrimination of maize (*Zea mays* L.) varieties using multi-temporal hyperspectral data. *Journal of Applied Remote Sensing* 13(1), 017504 (2019), http://dx.doi.org/10.1117/1.JRS.13.017504.

Photo: Testing the Apogee spectrometer, 2017

Abstract

Discriminating maize varieties is crucial for crop monitoring, high-throughput phenotyping, and yield forecasting. Crop experts discriminate maize varieties using morphological and biophysical characteristics. However, visual classification suffers from inconsistency, low throughput, and is only applicable in small-scale. A cost-effective and accurate *in situ* varietal discrimination using multi-temporal hyperspectral data and multivariate techniques is explored with threefold objectives, namely, to (1) discriminate maize varieties, (2) define suitable spectral bands, and (3) determine the optimum phenological stage(s) for varietal discrimination. Spectral data in 0.5nm discrete narrow bands between 400 and 900nm range are taken from 25 varieties measured using Apogee spectrometer at five phenological stages. Prior to discrimination analysis using partial least squares-discriminant analysis (PLS-DA), three preprocessing transformations are performed: autoscaling, Savitzky–Golay smoothing, and generalized least squares weighting. Ten optimal bands are identified for maize varietal discrimination across the visible and near-infrared section of the wavelength. The significant bands are located in the Blue (400 and 455nm), Green (545nm), Red and Red-edge (625, 680, 705, and 720nm), and near-infrared (765, 840, and 895nm) ranges of the spectrum. Flowering and onset of senescence are identified to be the most ideal phenological stages for accurate maize varietal discrimination. The overall discrimination accuracy improves by 52% and 63% with autoscaling at flowering and senescence, and by 55% and 62% with generalized least squares weighting at flowering and onset of senescence, respectively, compared to no preprocessing transformation. Of the three preprocessing transformations used, autoscaling and generalized least squares weighting are the most effective. Therefore, with appropriate preprocessing transformation, hyperspectral data and PLS-DA are effective in discriminating maize varieties.

Keywords: Maize variety discrimination, partial least squares discriminant analysis, multi-temporal hyperspectral data, pre-processing transformation, remote sensing.

4.1 Introduction

More than 75% of the human population in Africa relies on agriculture both in terms of subsistence and work (World Bank, 2010; Livingston *et al.*, 2011; Carletto *et al.*, 2015). Maize

remains the major staple food crop for the continent, occupying 30% of total land under cereal production and contributes more than 50% of the daily calorie requirements (FAO, 2010; Masuka *et al.*, 2012). Improving the continent's food security therefore requires strong early warning systems that depend on precise and current data on the spatial distribution of maize and yield estimates. At local scale, crop yield is variety-dependent (Pfeiffer, 1996). Therefore, techniques to discriminate different maize varieties and estimate their productivity are crucial. Variety-level discrimination is critical for a number of reasons: firstly, for assessing disease and pest spreads as influenced by susceptible varieties; secondly, to confirm correct variety placement in their area of adaptation domains to improve productivity; thirdly, to map actual varietal acreage and quantify their yields; fourthly, for precision crop management and yield forecasting; and finally, to map crop variety in real-time as they are actually being grown using their distinctive spectral signatures. The latter is immensely important for monitoring and evaluation of varietal adoption by farmers as this will provide insights on varietal adaptation that will inform breeding programs on how to improve their breeding and testing methodologies. The ability to discriminate maize varieties *in situ* also facilitates high-throughput phenotyping in plant breeding for comprehensive data-driven variety selection and release (Sankaran *et al.*, 2015)**.**

Crop experts discriminate crop varieties based on their different morphological and biophysical characteristics. However, such techniques are costly and time consuming (Van Niel and McVicar, 2004; Wilson *et al.*, 2014; Sobhan, 2017) and only applicable at small-scale. Cost-effective and accurate *in-situ* varietal discrimination can be achieved using remotely sensed data (Galvão *et al.*, 2005; 2006; Galvão *et al.*, 2009; Rajah *et al.*, 2015). However, remotely sensed data from multi-spectral satellite-based sensors such as Landsat series, Spot, MODIS, etc., cannot give precise estimates of biophysical features of agricultural crops (Wiegand and Richardson, 1990; Wiegand *et al.*, 1991; Thenkabail *et al.*, 1994; Fassnacht *et al.*, 1997), nor quantify intra-species variation in order to discriminate varieties. Hyperspectral sensors offer high spectral resolution capable of inter- and intra-species discrimination (Galvão *et al.*, 2005; Zhang *et al.*, 2012; Mariotto *et al.*, 2013; Rajah *et al.*, 2015; Li *et al.*, 2016) . Hyperspectral data provides crucial information available in specific narrow bands required to accurately discriminate crops and quantify subtle differences within species (Blackburn, 1998; Thenkabail *et al.*, 2000). Reflectance spectroscopy in the VIS (400 – 700nm) and NIR (700 –

1100nm) provide rich data regarding the composition of vegetation in general, and agricultural crops, in particular (Thenkabail *et al*., 2000; Mariotto *et al*., 2013; Rajah *et al*., 2015; Li *et al*., 2016; Chemura *et al*., 2016). However, hyperspectral sensors record large amount of information within a short space of time leading to problems of data dimensionality and redundancy (Thenkabail *et al*., 2004).

Different discriminant techniques have been used by different authors to reduce data dimensionality and multi-collinearity through band selection. Such techniques include, but are not limited to, principal component analysis (PCA) (Cheriyadat and Bruce, 2003; Hobro *et al*., 2010), artificial neural network (Hinton and Salakhutdinov, 2006) partial least squares discriminant analysis (PLS-DA) (Cochrane, 2000; Schmidt and Skidmore, 2001; Schmidt and Skidmore, 2003; Thenkabail *et al*., 2004; Vaiphasa *et al*., 2007; Rajah *et al*., 2015), and discriminant analysis (Zhang *et al*., 2012; Sibanda *et al*., 2015). However, PCA is weak in reducing data dimensionality using remotely sensed data and merely show group structure when difference within-species is less than between group variation (Cheriyadat and Bruce, 2003; Hobro *et al*., 2010; Worley and Powers, 2013; Rozenstein *et al*., 2014). Wold *et al.* (2001) and Dorigo *et al*. (2007) note that PLS is an effective multivariate statistical technique capable of addressing the problems related to high data dimensionality and is capable of reducing data redundancy in classification process. PLS achieves a dual purpose of reducing overfitting as well as eliminating non-sensitive wavebands (Dorigo *et al*., 2007; Cho *et al*., 2007; Abdel-Rahman *et al*., 2014). Classification with PLS is called PLS-DA, wherein DA means discriminant analysis.

PLS-DA have shown potential in reducing spectral dimension and have proved to be invaluable in defining useful wavebands in hyperspectral data (Peerbhay *et al*., 2014; Rajah *et al*., 2015). For example, Rajah *et al*. (2015) used PLS-DA to discriminate bean (*Phaseolus vulgaris* L.) varieties using hyperspectral data. In forestry studies, Peerbay *et al*. (2013) managed to demonstrate the potential use of PLS-DA in reducing hyperspectral data dimensionality and determination of optimal subset wavebands for accurate species discrimination. However, while PLS-DA can reduce overfitting and remove insensitive wavebands (Huang *et al*., 2004; Cho *et al*., 2007; Dorigo *et al*., 2007), on its own cannot give insight on the best wavebands ideal for accurate variety discrimination (Menze *et al*., 2009; Peerbay *et al*., 2013). For example,

Peerbay *et al.* (2013) have shown that PLS-DA alone cannot clearly identify redundant wavebands nor select the ideal number of wavebands. In fact, when PLS-DA was used in combination with variable importance in the projection (VIP) method, Peerbay *et al.* (2013) could determine the optimal wavebands and accurately discriminate and classify forestry species. Chemura *et al.* (2016) applied PLS-DA and VIP and identified optimal wavebands to discriminate diseased coffee (*Coffea Arabica* L.) plants. Preprocessing transformations (PPTs) have also been used to improve discrimination power of PLS-DA using spectroscopy (Kinoshita *et al.*, 2012; Gholizadeh *et al.*, 2013; Herrmann *et al.*, 2013). Spectral PPTs are used to eliminate somewhat inconsistent information, which might not be properly analyzed by the model. PPTs aim to linearize variable response and eliminate unnecessary causes of variance, which are not of importance in the analysis. PPTs serve to increase the variation within class, permitting better discrimination. Subjecting spectra data to various PPTs prior to classification has become quite common in recent studies using spectroscopy (Kinoshita *et al.*, 2012; Herrmann *et al.*, 2013; Rotbart *et al.*, 2013; Schwartz *et al.*, 2013).

As yet, no studies known to the authors have been conducted to discriminate different maize varieties using hyperspectral data. Most remote sensing studies in maize are related to crop-type discrimination and mapping (Mingwei *et al.*, 2008; Wardlow and Egbert, 2008; Zhang *et al.*, 2012; Mariotto *et al.*, 2013; Wilson *et al.*, 2014; Waldner *et al.*, 2015;), crop management (Bausch and Duke, 1996; Bausch and Diker, 2001; Pinter *et al.*, 2003) and yield estimation (Ferencz *et al.*, 2004; Prasad *et al.*, 2006; Fang *et al.*, 2008; Guindin-Garcia, 2010; Battude *et al.*, 2016; Burke and Lobell, 2017;). Studies to discriminate crop varieties using remote sensing refer to other crops such as sugar cane (Galvão *et al.*, 2005; 2006; Fortes and Demattê, 2006), common dry bean (Rajah *et al.*, 2015), soya bean (Galvão *et al.*, 2005), wheat (Pinter *et al.*, 1985; Hansen and Schjoerring, 2003), rice, cotton, sugarcane and chillies (Rao, 2008), apple (Luo *et al.*, 2011) and pumelo (Li *et al.*, 2016). Furthermore, studies on crop varietal discrimination have been based on 'snapshot' (single phenological stage) datasets (Lin *et al.*, 2012). Yet, Rajah *et al.* (2015) showed that accurate crop varietal discrimination can be achieved using data measured at different crop phenological stages. Maize varietal discrimination is complicated by the inherent spectral similarities. As such, the overall goal in varietal discrimination is to identify the few features that uniquely define each variety. However, maize varieties are easily perturbed by experimental or environmental factors, for example, nutrient, phenological

stage, pH, temperature, pests and diseases, thereby altering their spectral signatures. Therefore, for accurate varietal discrimination, experiments should be grown under ideal conditions and spectral data collected at different phenological stages because varietal differences may be more apparent at certain stages of crop growth. Similarly, spectral collection methodology and sensors used can also introduce undesirable variations. Thus, varietal discrimination analysis requires a robust methodology to uncover the underlying subtle differences between the varieties.

In this study, we set to evaluate the potential of multi-temporal hyperspectral data in studying maize crop characteristics with threefold objectives: to (1) discriminate maize varieties; (2) define the spectral bands suitable for discriminating maize varieties; and (3) determine the ideal phenological stage for varietal discrimination. We explored different pre-processing algorithms to smooth (reduce noise) spectra data in order to extract subtle spectral features. The questions to be answered were: (1) can a cost-effective and accurate *in-situ* maize varietal discrimination be achieved using hyperspectral data?; (2) are there any statistically significant differences between spectral reflectance values of maize varieties that can be used for varietal discrimination; and (3) are there any optimal phenological stages at which varietal discrimination is most ideal? The hypothesis associated with this study is that maize varieties have different inherent canopy architecture because of genetic background that gives particular morphophysical characteristics, and therefore can be feasible to discriminate using multi-temporal hyperspectral data.

4.2 Materials and Methods

4.2.1 Study area

The study was conducted at Rattray Arnold Research Station (RARS) in Zimbabwe as explained in Chapter 1 section 1.6 of this thesis.

4.2.2 Crop varieties and experimental set-up

A set of five representative varieties from each of the five maturity groups (ultraearly = 100 – 120, very early = 121 – 130, early = 131 – 140, medium = 140 – 150 and late >150 days) were grown at RARS. Widely grown maize varieties were selected in each maturity group to assess

their spectral reflectance properties (Table 4.1). The experimental design was a 5 × 5 partially balanced alpha lattice laid out as a split-plot to minimize maturity effect, with maturity as the main plot and varieties as subplot. Four-row plots replicated three times were used. A total of 75 plots constituted the experimental area (five maturity groups × five varieties × five replications). Gross sub-plot area was 3m × 7m × 4rows. Maize seeds were sown at a spacing of 0.5m in-rows and 0.75m between rows. Sowing was done at a seeding rate of four seeds per station and thinned to final two plants per station after three weeks to achieve a target plant population of 53,000 plants ha^{-1}. The crop was fertilised at a rate of 450kg ha^{-1} of basal fertilizer containing nitrogen (13%), P_2O_5 (26%), K_2O (13%) at planting. Ammonium Nitrate (34.5% N) was applied as top dressing at a rate of 450kg ha^{-1}. The top dressing fertilizer was split into two equal applications – first at early vegetative after thinning and second at booting (preflowering) stage. Experimental plots were kept weed free through a combination of herbicides and hand weeding.

4.2.3 Spectral measurements

Hyperspectral data were measured by a 0.5nm wide narrowband field spectrometer Apogee VIS-NIR (Apogee Instruments, Inc., Logan, UT, USA) with a spectral range of 350.0 – 999.5nm. Spectral gathering involved integration time optimization, providing foreoptic data, recording dark current, collecting white reflectance, and then record the target reflectance. Readings were taken at canopy level. Three spectral scans were taken and averaged at nadir (30°) 30 cm above canopy of the target variety. Data was collected between 1000 and 1400 hours – the critical time of the day for maximum net sun radiation that is important for defining spectral signatures of plants. The spectrometer was connected to a personal computer for spectral data storage. Spectral data were measured and calculated as the fraction of energy reflected off the target genotype to energy incident on the target (Thenkabail *et al.*, 2000). Thus:

$$\text{Reflectance (\%)} \quad = \quad \frac{\text{target} - \text{dark current}}{\text{reference} - \text{dark current}} \times 100 \qquad\qquad [4.1]$$

Records of spectral data were taken at different crop phenological stages: early vegetative, midvegetative, flowering/tasseling, midgrain filling and onset of senescence resulting in several thousand hyperspectral data samples for 25 varieties. Spectra data were measured in

0.5nm discrete narrow bands between 350.0 and 999.5nm, yielding a total of 1300 bands. Data in 350 to 399 range and 900.5 to 999.5nm of the electromagnetic spectrum were not used due to low signal-to-noise ratio. Thus, spectral data in 400 to 900nm range was utilized, yielding a total of 1001 bands, which were averaged to 5nm to reduce dimensionality and finally giving 101 bands within the visible (VIS) and the NIR portions of the spectrum. However, one of the limitation of using 400 to 900nm range in this study was that variety discrimination was based on spectral reflectance from leaf pigments (visible range) and cell structure (NIR). This excluded reflectance as influenced by leaf water content and leaf biochemicals (protein, lignin and cellulose), which is measured when midinfrared section of the spectrum is used. This can be achieved when full spectral range of 350 to 2200nm is used.

Table 4.1. Maize varieties considered for PLS-DA and some of their distinguishing characteristics relevant to spectral reflectance [maturity duration and leaf angle distribution (LAD)].

VARIETY NAME	LAD
Ultra-early maturity (100 to 120 days) white grained hybrids	
SC 301	- Medium erectophile
SC 303	- Planophile
11C11501	- Planophile
13C0949	- Medium erectophile
PAN3M01	- Medium erectophile
Very early maurity (121 to 130 days) white grained hybrids	
SC 403	- Planophile
SC 417	- Planophile
SC 419	- Planophile
SC 423	- Medium planophile
PAN413	- Planophile
Early maturity (131 to 140 days) white grained hybrids	
SC 513	- Medium planophile
SC 529	- Planophile
SC 533	- Medium planophile
SC 537	- Medium planophile
PAN4M21	- Planophile
Medium maturity (141 to 150 days) white grained hybrids	
SC 627	- Planophile
SC 637	- Planophile
SC 643	- Medium planophile
SC 649	- Planophile
PAN53	- Medium planophile
Late maturity (> 150 days) hybrids	
SC 709	- Planophile
SC 719	- Medium planophile
SC 608	- Highly erectophile
SC 727	- Medium erectophile
PAN7M89	- Planophile

4.2.4 Statistical Data Analysis

A three-stage data analysis was adopted to discriminate maize varieties; PPTs using Microsoft Excel 2013, ANOVA using breeding View (BV) of BMS version 10 (IBP, 2018) and PLS-DA using XLSTAT for Microsoft Excel 2013 platform (EXLSTAT, 2013). The three-stage analysis was adopted to reduce high dimensionality associated with hyperspectral data and improve discrimination ability (Adam and Mutanga, 2009; Carvalho *et al*., 2013; Prospere *et al*., 2014; Rozenstein *et al*., 2014; Sibanda *et al*., 2015). Rozenstein *et al*. (2014) showed that PPTs increase the discrimination precision in spectroscopy data. Spectral PPTs were used to eliminate any unsuitable information, which the model cannot correctly handle. PPTs aim to linearize the response of the variables and to eliminate unnecessary sources of variance that affect the analysis. Adelabu *et al*. (2014) demonstrated the effectiveness of ANOVA in the classification process as a first step in selecting crucial variables for classification. Sibanda *et al*. (2015) used ANOVA to remove redundant wavelengths. Rozenstein *et al*. (2014) used different PPTs to improve the discrimination accuracy of spectroscopy data using PLS-DA. In this study, PPTs and ANOVA analyses were used as preliminary analysis before the data were subjected to PLS-DA during classification. The discriminatory power (or separability) between maize varieties was measured by Wilks' lambda (λ) and Pillai's trace (Wilks, 1935; Pillai, 1955).

4.2.4.1 Pre-processing Transformations (PPTs)

The three different PPTs used in this study to improve varietal discrimination are auto-scaling, modified Savitzky-Golay Smoothing (SGS) and generalized least squares weighting (GLSW). The selected PPTs are the most frequently used in spectroscopy (Madden, 1978; Tsai and Philpot, 1998; Wise *et al*., 2006).

Auto-scaling. Auto-scaling was applied by subtracting spectral signature of each sample from the mean spectral signature (mean-centering) followed by dividing each variable by their standard deviation. This process ensures that each variable is scaled so that the variable's useful signal has an equal footing with the other variables' signals (Wise *et al*., 2006).

Savitzky-Golay Smoothing. The modified Savitzky and Golay (Savitzky and Golay, 1864) equation was used for smoothing spectra data (Madden, 1978). Direct use of Savitzky and Golay (Savitzky and Golay, 1864) equation was avoided due to the limitations pointed by Tsai

and Philpot (1998). First, the Savitzky and Golay (1964) equation is only applicable to few combinations of derivatives and polynomial orders, and second, the look up tables provided by Savitzky and Golay, were limited to 25 points for a smoothing array (m = 12) (Madden, 1978). The smoothing in this study was based on computations based on a modified Savitzky-Golay equations given by Madden (1978) to overcome the limitations above. The equation can be rewritten as:

$$Y_j^* = \sum_{i=-m}^{m} P_i^{(0)} Y_{j+i} \qquad\qquad [4.2]$$

Where $P_i^{(0)}$ is the coefficient for the ith point of the filter in the zeroth order of derivative computation. Yj is the midpoint of the smoothing array (window).

Generalized least squares weighting. GLSW produced a filter matrix based on the differences between pairs or groups of samples that should otherwise be similar (Wise *et al*., 2006). The single adjustable parameter α that defines how strongly GLSW lowers weight interferences was set to 0.02 because larger values > 0.02 decreases filtering effects and smaller values apply more filtering.

4.2.4.2 ANOVA

After PPTs, spectra data was subjected to ANOVA in breeding View (BV) of BMS version 10 (IBP, 2018) to compare the 25 varieties. A test for significant differences in mean reflectance of the five groups of maturity used in this study was done. The wavebands that were significant ($p < 0.05$) were chosen and used as input variables for discrimination analysis using PLS-DA. The 25 varieties used for discrimination analysis are shown in Table 4.1.

4.2.4.3 Partial Least Squares Discriminant Analysis

PCA is applied prior to PLS-DA. Worley *et al*. (2013) suggested that for data exploration, subjecting the data to PCA provides an informative first look at the data structure and relationships between groups. Furthermore, separation between groups is observed in PCA scores when within-groups difference is not significantly less than between-groups variation. PLS-DA classification guided by well-separated PCA scores has a greater likelihood of producing relevant results. PLS-DA is an effective multivariate supervised pattern

recognition technique, which utilizes a training routine to allocate class membership to variables based on their known statistical parameters projected into latent variables (Wang *et al.*, 2011). The PLS-DA model can be represented as:

$$X = TP^T + E \qquad\qquad [4.3]$$

$$Y = UQ^T + F \qquad\qquad [4.4]$$

where *X* is the matrix of spectral data, *T* is a factor score matrix, *P* is the *X* loadings, *E* is the residual or a noise term, *Y* is a matrix of the categorical variable, *U* is the scores for *Y*, *Q* is the *Y* loadings, and *F* is the residuals (Wang *et al.*, 2011).

To ensure model reliability, validation was critical because PLS tends to overfit the models to data (Westerhuis *et al.*, 2008; Worley and Powers, 2013). Model validation entails partitioning data into training and validation set (Anderssen *et al.*, 2006; Broadhurst and Kell, 2006). The data was split into one-third test and two-thrid training sets. As indicated above, the separability between maize varieties was measured using Wilks' λ and Pillai's trace (Wilks, 1935; Pillai, 1955). The classification ability of PLS-DA improves as latent variables increase, because a combination of these various independent variables offered much more data as compared to less-latent variables. Nevertheless, to avoid model over fitting, the optimum quantity of latent variables was established that resulted in a lower misclassification error. The training datasets related to the model were used to assess its accuracies in discrimination based on a PLS-DA with a 10-fold cross validation. Cross validation has been long recognized as an accurate way of testing the model's significance whenever PLS was used (Wold *et al.*, 2001). In this study, PLS-DA model parameters were optimised by a 10-fold cross validation using training data set within 400 to 900nm range. The optimization process was done by adding each component to the PLSA-DA model in repetitive fashion and the model with the lowest cross-validation error was then used in the discrimination of the test data set.

4.2.5 Accuracy Assessment

For accuracy assessment, we used quantity disagreement and allocation disagreement according to Pontius and Millones (2011). Pontius and Millones (2011) demonstrated some shortcomings of kappa statistic in accuracy assessment because it gives misleading

information. Moreover, kappa was difficult to determine, comprehend, and interpret (Pontius and Millones, 2011). They recommended summarizing cross-tabulation matrix based on quantity disagreement and allocation disagreement. For calculating the agreement between the testing and training data, the two disagreements were subtracted from 100% and then the overall accuracy, user accuracy, and producer accuracy were calculated using confusion matrix, as suggested by Pontius and Millones (2011).

4.3 Results

4.3.1. Pre-processing Transformations and their effect on varietal discrimination

4.3.1.1 Early vegetative growth stage

Seasonal mean vegetation spectra (untransformed) of 25 maize varieties measured at different phenological stages and some photographs of the corresponding biomass growth are shown in Figure 4.1. Spectral measurements taken during early crop growth were largely influenced by soil characteristics. As the crop canopy developed, spectral reflectance characteristics were increasingly influenced by plant factors. For a better discrimination analysis of maize varieties, "true" spectra values attributed only to the varietal signal and free of any soil contamination were needed. Spectral data were transformed using different PPTs and were subjected to different analyses, including ANOVA, PLS-DA, Wilks' λ test (Rao's approximation), and Pillai's trace. However, no band was significant (p>0.05) in discriminating maize varieties at this stage.

Early vegetative
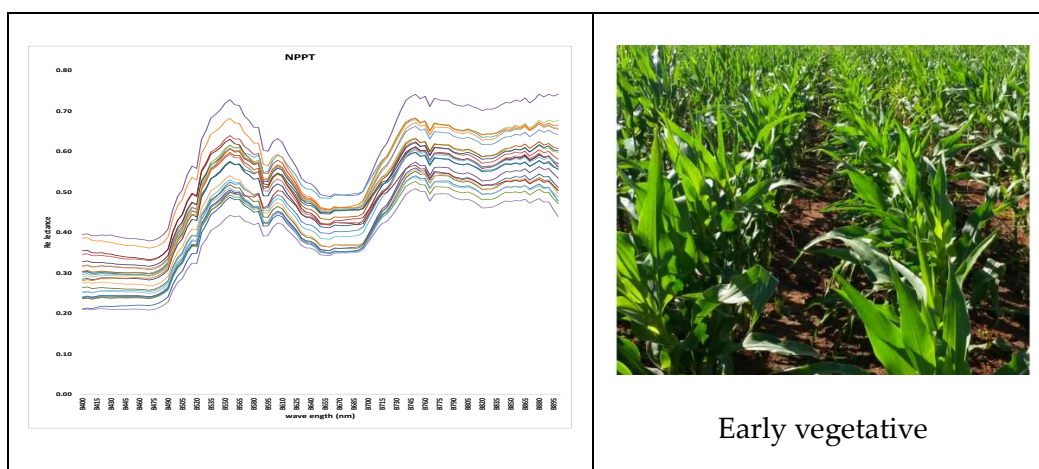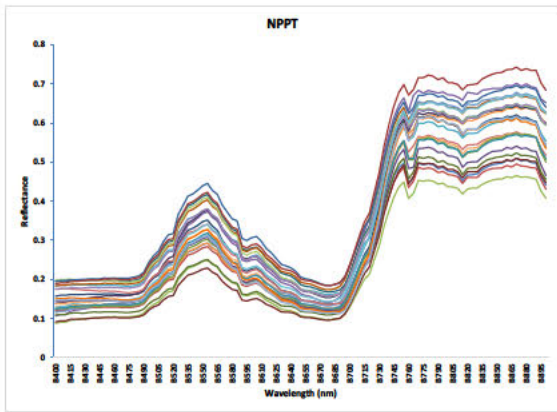
Midvegetative stage
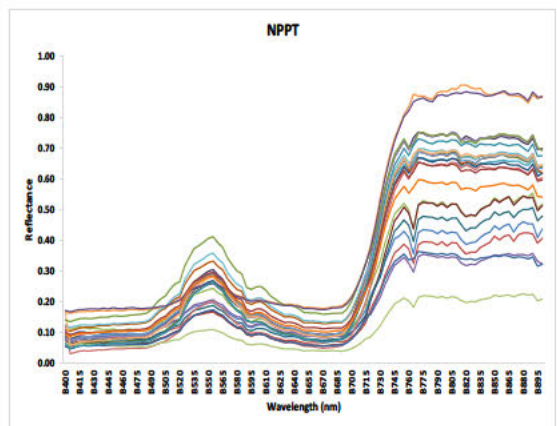
Flowering/Tasselling

Midgrain filling stage

Onset of senescence

11C11501	13C0949	PAN3M01	PAN413	PAN4M21	PAN53	PAN7M81
SC301	SC303	SC403	SC417	SC419	SC423	SC513
SC529	SC533	SC537	SC608	SC627	SC637	SC643
SC649	SC709	SC719	SC727			
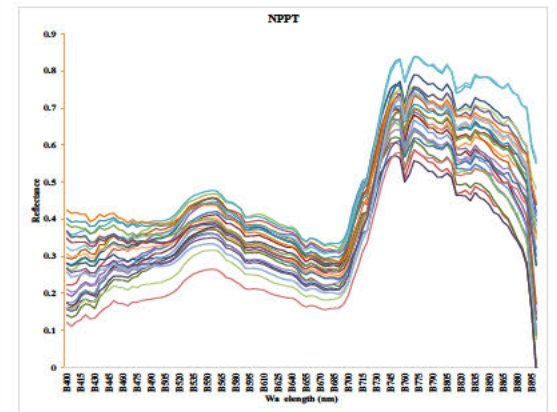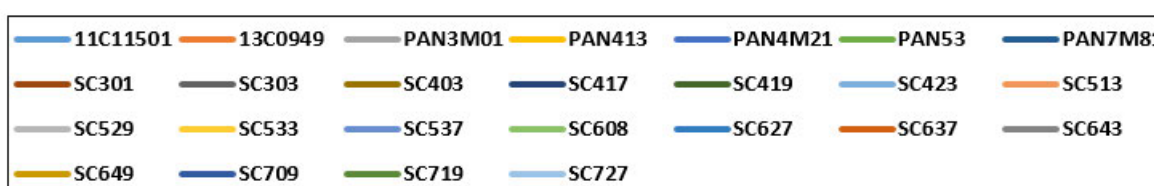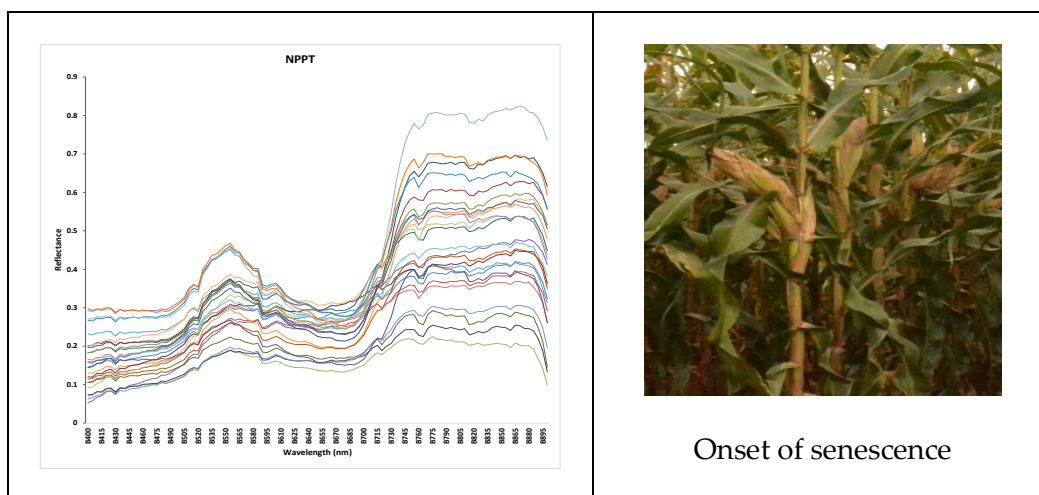
Figure 4.1. Seasonal mean vegetation spectra (untransformed) of 25 maize varieties measured at different phenological stages and some photographs of the corresponding biomass growth.

4.3.1.2 Midvegetative growth stage

Discrimination analysis at midvegetative stage after spectra data transformation showed no significant ($p > 0.05$) differences among wavebands. Only two bands (400 and 405nm) were found to be significant ($p < 0.05$) in discriminating maize varieties with no PPTs and when AS (710 and 715nm) was applied in the red-edge spectrum. Using GLSW did not yield any significant band and only one band (710nm) with SGS was significant ($p < 0.05$). There were no spectral differences among the varieties at midvegetative stage using ANOVA and Wilks' λ test. Wilks' λ values with and without PPTs were high (>0.5) showing no significant difference between wavebands in discriminating maize varieties at this phenological stage.

4.3.1.3 Flowering (tasseling) stage

After subjecting the data to PLS-DA, Wilk's λ test and Pillai's trace, different bands were found to be significantly ($p < 0.05$) different using each PPTs algorithm. Twelve bands (405, 440, 445, 490, 495, 595, 650, 705, 720, 765, 835 and 895nm) were found to be significant ($p < 0.05$) in discriminating maize varieties without PPT. However, significant improvements in

discrimination ability were obtained after subjecting spectral data to different PPTs. For example, 22 bands (400, 425, 455, 505, 520, 545, 590, 595, 605, 615, 660, 690, 700, 705, 725, 760, 765, 790, 830, 870, 895 and 900nm) were found to be significant ($p < 0.05$) after AS transformation, and 23 bands (400, 405, 425, 430, 445, 455, 500, 510, 545, 620, 655, 675, 680, 690, 715, 720, 740, 745, 765, 865, 880, 895 and 900nm) after GLSW, whereas 12 bands were significant with SGS (400, 480, 500, 565, 625, 670, 680, 690, 700, 720, 765 and 895nm) using Wilks' λ test. The Wilks' λ values were ranked in ascending order to determine which bands were contributing more to the discrimination function (the closer Wilks' λ is to 0, the more the variable contributes to the discriminant function). The spectral bands with significantly ($p < 0.05$) smaller Wilks' λ values were identified as the most ideal bands.

4.3.1.4 Midgrain filling stage

At midgrain filling stage, only two bands (400 and 405nm) in the blue range were significant ($p < 0.05$) in discriminating the varieties with no PPT. However, using GLSW, a total of 18 bands (415, 730, 735, 745, 750, 760, 770, 775, 780, 785, 790, 795, 800, 805, 820, 840, 850 and 845nm) were significant ($p < 0.05$) in discriminating maize varieties. These differences can be attributed to different morphological and biophysical attributes of these varieties and the power of GLSW PPT. Thus, with GLSW, the subtle differences among the spectral signatures were amplified. Smoothing alone using SGS did not allow better discrimination; only one band (710nm) was significant ($p < 0.05$), whereas only two bands (575 and 710nm) were significant ($p<0.05$) with AS.

4.3.1.5 Onset of senescence

The best discrimination was obtained at onset of senescence with all transformations yielding more significant bands in discriminating maize varieties. A total of 10 bands were significant without PPTs (400, 405, 475, 530, 580, 625, 680, 765, 870 and 900), 22 bands (400, 405, 440, 455, 515, 535, 545, 560, 665, 700, 705, 735, 760, 770, 815, 820, 840, 855, 885, 890, 895 and 900nm) with AS, 24 bands (400, 410, 430, 485, 525, 540, 570, 585, 600, 630, 650, 695, 715, 720, 740, 755, 760, 765, 770, 815, 860, 885, 895 and 900nm) with GLSW and 10 bands (400, 430, 480, 625, 680, 695, 720, 770, 895 and 900nm) were significant with SGS. The results suggest that AS and GLSW

PPTS were the most suitable for increasing the variance between varieties prior to discrimination.

4.3.2 Ideal number of hyperspectral bands, band centers and bandwidths

The frequency of occurrence of significant narrow bands is shown in Figure 4.2. Majority of the variety discrimination information is found in a few hyperspectral narrow bands, out of the 101 bands used. These are found in the blue portion (400 and 455nm), the green portion (545nm), the red portion (625nm), the red-edge portion (680, 705 and 720nm) and the NIR portion (765, 840 and 895nm) (Table 4.2). This makes up 10 optimal bands, made up of four (545, 680, 705 and 720nm) very narrowbands ($\leq$ 15nm bandwidth), three (625, 765 and 895nm) narrowbands (> 15 to < 30nm bandwidth), and three (400, 455 and 840nm) broadbands (> 30nm bandwidth) (Table 4.2). The band centers are rounded off to the nearest 5nm, and bandwidths shown in Table 4.2 are derived from the results in Figure 4.2. The results show that the ideal bands for discriminating maize varieties are spread across the VIS and NIR spectrum and are not just located in the red and NIR wavelengths. Thus, the ideal bands for discriminating maize varieties are located in the blue (20%), green (10%), red and red-edge (40%), and NIR (30%) range of the spectrum. The flowering and the onset of senescence are the most ideal phenological stages for accurate maize varietal discrimination using the data in this study.
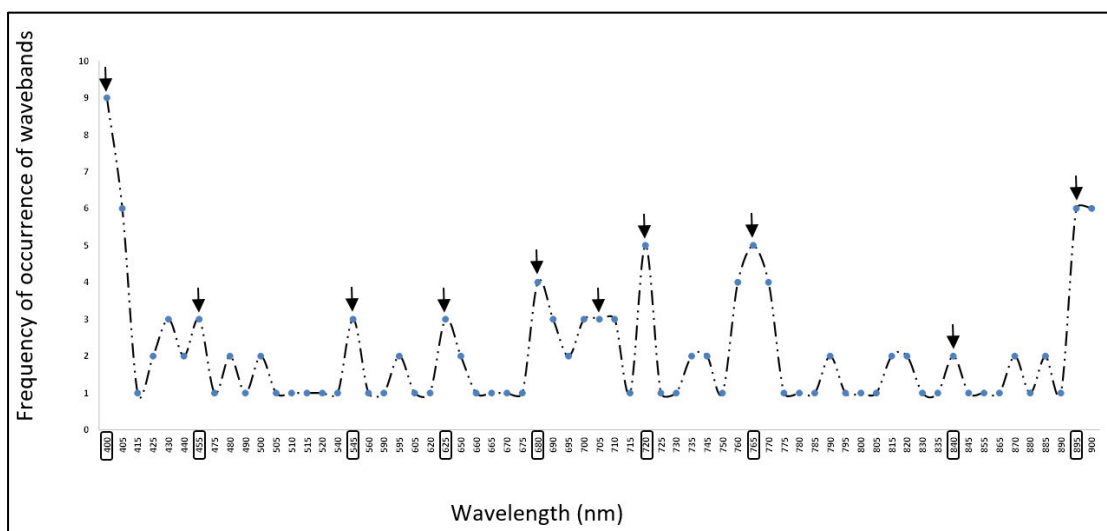
Figure 4.2. Frequency of Significant ($p < 0.05$) bands for discriminating maize varieties at different phenological stages based on Wilks' λ tests. Arrows and text box highlight the selected band centers.

4.3.3 Accuracy assessment

Components of quantity disagreement between the reference training data and the test data at different phenological stages using different PPTs were analyzed for the five phenological stages. The results of disagreements, agreements and discrimination accuracies are shown in Figures 4.3 – 4.5. The components of quantity disagreement between the reference training data and the test data were higher at early vegetative, midvegetative and midgrain filling phenological stages than at flowering and onset of senescence stages (Figure 4.3). Generally, spectral data subjected to no preprocessing transformations (NPPTs) and SGS produced higher disagreements (Figure 4.3) and low accuracies (Figure 4.5), as compared to AS and GLSW.

The classification agreements at each stage are shown in Figure 4.4. Comparing the three PPT algorithms used, AS and GLSW consistently produced higher agreements (Figure 4.4) and accuracies (Figure 4.5). On the other hand, low agreements (Figure 4.4) and low accuracies (Figure 4.5) were obtained with NPPT and SGS. Across all phenological stages, high discrimination agreements (Figure 4.4) and accuracies (Figure 4.5) were obtained after AS and GLSW using PLS-DA. However, the highest discrimination accuracies were obtained at flowering and onset of senescence stages. AS improved overall discrimination accuracy by 52% at flowering and 63% at onset of Senescence. With GLSW, the overall discrimination accuracy improved by 55% at flowering and 62% at onset of senescence compared to NPPT. Of the three PPTs used, AS and GLSW were the most effective.

Table 4.2. Ten optimal bands for discriminating maize varieties based on frequency of significant ($p < 0.05$) bands at different phenological stages

Waveband number	Waveband portion name	Waveband center: λ (nm)	Waveband width: $\Delta\lambda$ (nm)	Waveband explanation
1	Blue 1	400	30	Sensitive to chlorophyll loss, senescence, maturity, and soil background effects (Schepers *et al.*, 1996; Thenkabail *et al.*, 2000).
2	Blue 2	455	45	Very good estimator of grain yield
3	Green	545	10	Part of maximal reflectance in the visible spectrum and is directly related to chlorophyll (Schepers *et al.*, 1996).
4	Red	625	25	Chlorophyll absorption pre-maxima (reflectance minima (Schepers *et al.*, 1996; Blackburn, 1998).
5	Red-edge 1	680	15	Highest crop-soil contrast found at the start of Red-edge for most crops (Schepers *et al.*, 1996; Blackburn, 1998; Thenkabail *et al.*, 2000).
6	Red-edge 2	705	10	Chlorophyll absorption post-maxima sensitive to stress (Schepers *et al.*, 1996).
7	Red-edge 3	720	10	Sensitive to stress and good indicator of chlorophyll and nitrogen status of crop (Carter, 1994. Shaw *et al.*, 1998; Clevers, 1999).
8	NIR 1	765	25	Beginning of the NIR shoulder and Sensitive to water stress in crops.
9	NIR 2	840	105	Center of 'NIR shoulder.' Correlates well with total chlorophyll (Schepers *et al.*, 1996).
10	NIR peak	895	20	Highest reflectance for certain crop varieties and/or phenological stages. Sensitive to stress in maize (Thankbail *et al.*, 2000).
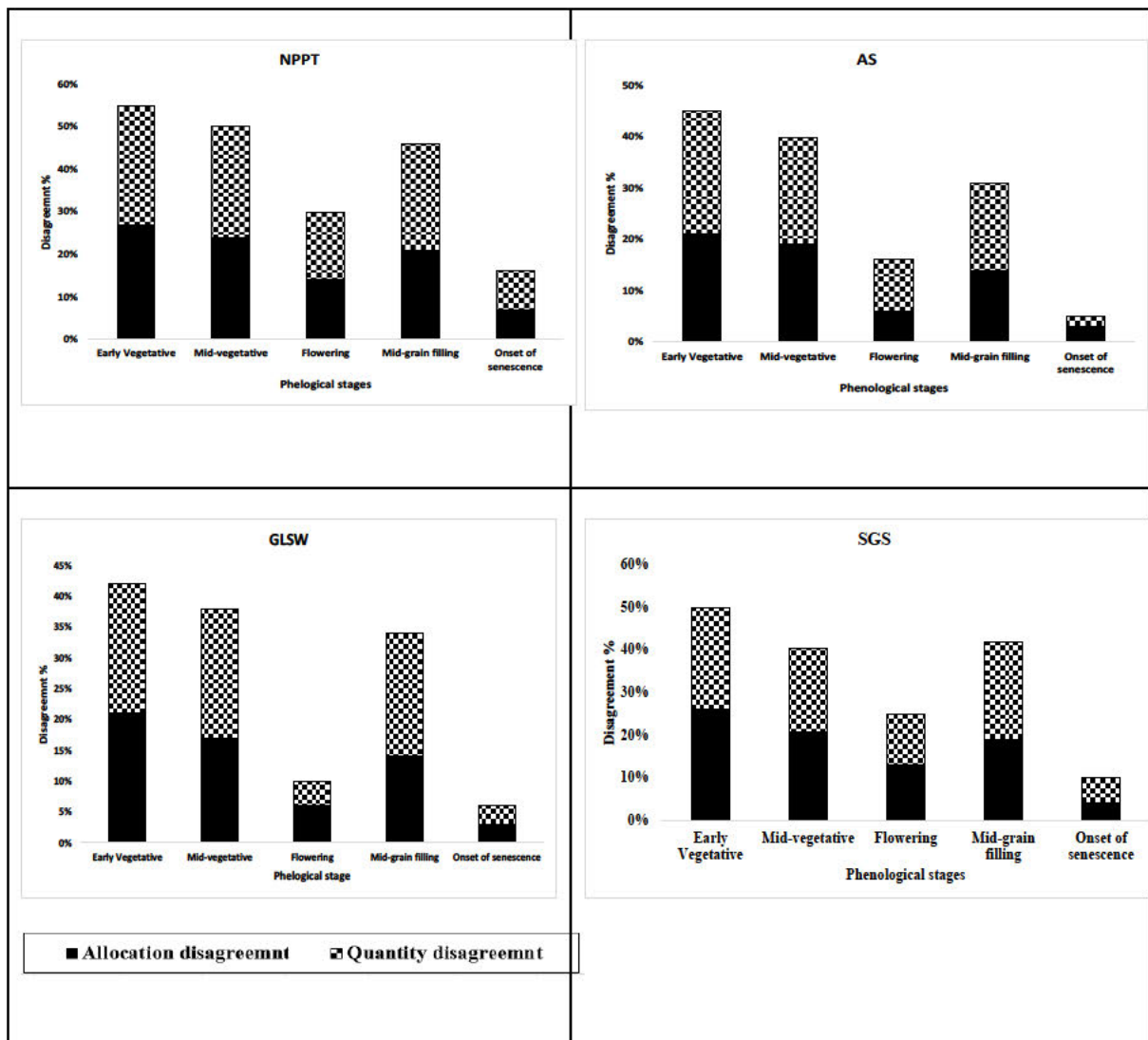
Figure 4.3. Components of disagreement between the reference training data and the test data at different phenological stages
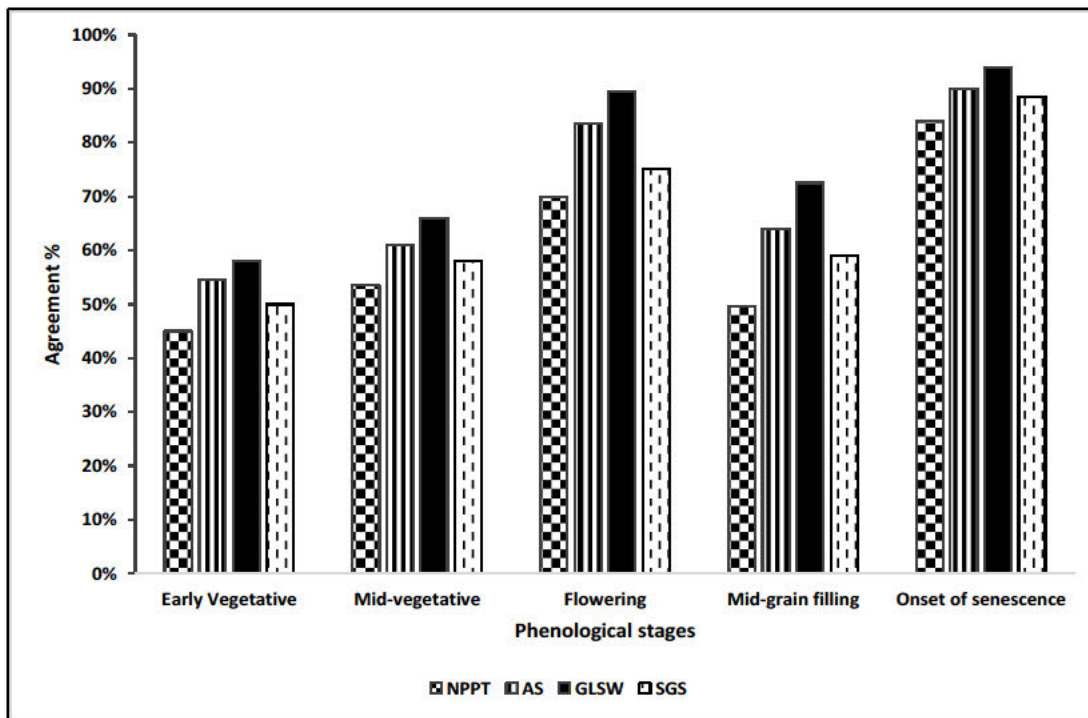
Figure 4.4. Agreement between the reference training data and the test data at different phenological stages
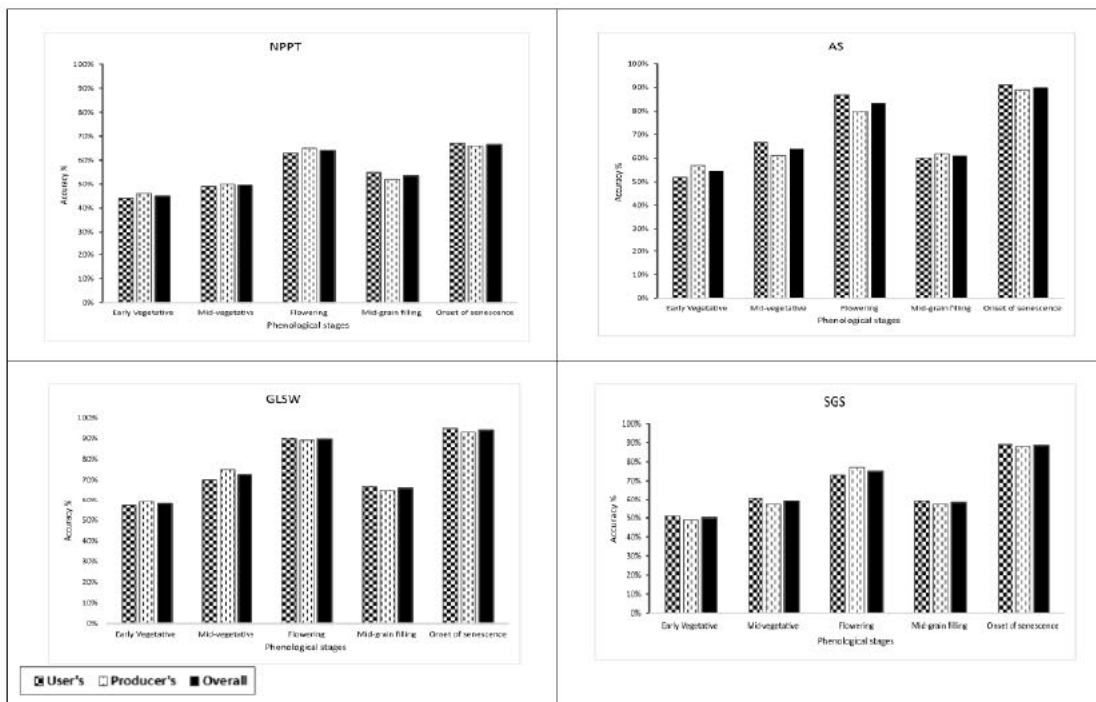
Figure 4.5. Discrimination accuracies using different PPTs at different phenological stages

4.4 Discussion

The absence of significant spectral difference at early vegetative stages could be attributed to spectral mixing as influenced by soil background. "Pure" maize varietal spectra are expected at closed canopies stages, which begin at full canopy closure because canopy scattering is insignificant when the crop is young and, conversely, the soil signal is negligent with full canopy cover. The results show low discriminating power of spectral data when PLS-DA is performed without PPTs. However, with some PPTs, particularly AS and GLSW, better varietal discrimination is achieved. This shows that PPTs can increase the variance within species and can lead to better discrimination precision. The analysis showed that hyperspectral data can be useful in maize varietal discrimination. The inherent spectral similarities among maize varieties did not pose a challenge for PLS-DA with appropriate PPTs. However, it is crucial to take care when applying PPTs to spectral data so that the PPTs will not affect the input to the classifier in such a way that can significantly alter the product of the discrimination (Worley and Powers, 2013). Therefore, caution must be exercised as significant discrimination might not be because of meaningful spectral variations but due to noise. Our results show that AS and GLSW are suitable PPTs because they increased the variance between varieties.

Evidence exists that shows that it may be difficult to know *a priori* the most suitable PPT method (Rozenstein *et al.*, 2014). Different PPTs may be more suitable for different data sets. The challenge is in finding the suitable PPT method to achieve accurate discrimination. Discrimination accuracy of maize varieties is affected by many factors, including the inherent spectral similarities, experimental or environmental factors, crop age, nutrient, growth phase, pH, temperature, pests, diseases, spectral collection methodology, and sensors used. These factors easily alter spectral signatures of varieties. Thus, when subtle differences between maize varieties are less obvious due to close spectral signatures, PPTs prior to classification may improve discrimination accuracy. The PPTs used in this study, such as AS and GLSW, have worked well with maize data at flowering and onset of senescence growth stages. Flowering stage of plants is one of the important phenological stage for crop-type mapping and also for varietal discrimination, as each variety flowers at a different time and so have a time-step variable in flowering, which triggers a good signal for large-scale discrimination

using remote sensing. However, the PPTs were applied at microscales. Their applicability in imaging spectroscopy using aerial and satellite sensors (macroscales) needs to be validated, under low signal-to-noise ratio, atmospheric interference, large data sets, among other challenges.

Ten bands (400, 455, 545, 625, 680, 705, 720, 765, 840 and 895nm) are found to be ideal for discriminating maize varieties using data in this study. The bandwidths of the seven ideal bands centers (545, 625, 680, 705, 720, 765 and 895nm) are very narrow ($\leq$ 15nm) to narrow (< 30nm) except for bands 400, 455 and 840nm with bandwidths of 30, 45 and 105nm, respectively, and are classified as broadband. The study shows that, of the 101 bands within 400 to 900nm range, spaced at 5nm, 91 bands are redundant in discriminating maize varieties. The results show that the optimal information on maize varieties is found in blue, green, red, red-edge and the moisture-sensitive NIR. These results clearly show the important wavebands as well as redundant wavebands. This is important for future generations of hyperspectral satellites and in overcoming the Hughes's phenomenon. Previous studies have showed that wavebands in the visible and NIR range of the spectrum show great potential in discriminating plant species (Vrindts and Baerdemaeker, 1997; Vrindts *et al.*, 2002). For example, Smith and Blackshaw (2003) and Cochrane (2000) suggested that irrespective of crop species, the red-edge wavelengths (680 to 730nm) are always significant for vegetation discrimination. Our findings have confirmed the red-edge importance in discriminating maize varieties at different phenological stages as three (680, 705 and 720nm) out of the ten bands are in the red-edge. Three bands in the NIR (765, 840 and 895nm) reflectance are significant in discriminating maize varieties. This can be attributed to leaf morphology and leaf structure as influenced by genotypic variations due to maturity differences among the varieties used in this study.

The performance of reflectance spectroscopy data in discriminating maize varieties varied across phenological stages of the varieties. For example, spectral data were able to discriminate maize varieties accurately at flowering, midgrain filling and onset of senescence than early and midvegetative growth stages. At early growth stages, soil background always affects the reflectance measured by the spectrometer. Variety discrimination is high at flowering and onset of senescence stages. Such results obviously show the importance of the

timing of remote sensing data acquisition for effective variety discrimation in maize. This is crucial as accurate prognosis of variety phenology is critical for prediction and calculating crop yield, using time series of normalized vegetation indices. The VIS spectrum is known to be sensitive to chlorophyll loss, senescence, and maturity (Smith and Blackshaw, 2003). This is confirmed by our results wherein during the flowering and onset of senescence, different varieties undergo different physiological process as a function of their maturity duration and genotypic differences. Such physiological processes affect the pigment content and chloroplast for these different maize varieties and cause subtle reflectance differences at certain bands that are sensitive to such changes (Nichol *et al*., 2000). The dramatic changes in spectral behavior form the basis for significant discrimination ability witnessed at flowering and onset of senescence. For example, as biomass increases, taking up most of the moisture in the plant, absorption in the moisture sensitive NIR portion also increases. Of the 101 bands used, four very narrowbands (545, 680, 705 and 720), three narrowbands (625, 765 and 895) and three broadbands (400, 455 and 840) are found to be ideal for maize variety discrimination at flowering, midgrain filling and onset of senescence stages. The significance of each of these wavelengths in crop research is explained as noted by other researchers (Table 4.2).

The results of this study are consistent with Rajah *et al.* (2015) who found higher discrimination accuracies at flowering and pod formation in common bean (*Phaseolus vulgaris* L.). Zwiggelaar (1998) indicated that spectral characteristics of plant canopies are a result of their physical condition and chemical attributes, which are influenced by the variety's phenological stages. In agreement with Misra (2012), a crop variety's phenological stage and vigor is critical in varietal discrimination. Using six herbaceous species, Sobhan (2007) found maximum species discrimination at flowering. Therefore, maize varieties' temporal dynamics (phenology) are crucial for individual variety characterization and discrimination (Turner *et al*., 2003; Underwood *et al*., 2003), which are both crucial for high-throughput phenotyping using remote-sensing technique. In our study, only 10 bands (400, 450, 545, 625, 680, 705, 720, 765, 840 and 895nm) provided optimal information to discriminate maize varieties at different phenological stages in the 400 to 900nm spectrum. Identification of these optimal bands is important in the selection of wavelengths for use and reduction of data redundancy in hyperspectral datasets for agricultural purposes at field, aerial and space-borne levels.

4.5 Conclusion

Our results have shown that PLS-DA was capable of accurately discriminating maize varieties using hyperspectral data at certain phenological stages. Our analysis further shows that, by using appropriate PPTs, the accuracy of discriminating maize varieties using hyperspectral data is significantly improves. The accuracy improved after the ideal PPT was applied, compared to data without PPT. Therefore, we conclude as follows:

1. The study identified the flowering and onset of senescence to be the most ideal phenological stages for accurate maize varietal discrimination.
2. This study also showed that, of the three PPTs algorithm used, AS and GLSW were the most suitable for improving the discriminating power of PLS-DA using our data set.
3. The study established that maize varieties can be discriminated using 10 optimal hyperspectral bands (400, 455, 545, 625, 680, 705, 720, 765, 840 and 895nm) out of the 101 hyperspectral bands each with 5nm width in the VIS and NIR spectral range of 400 to 900nm.

The study provided useful insights into the optimum growth stages and ideal bands to discriminate maize varieties using spectroscopy for agricultural applications at field level. However, there is a need for scaling-up the results to large area crop discrimination using aerial and space-borne remote sensing platforms. Discriminating maize varieties is crucial in plant breeding for high-throughput phenotyping using unmanned aerial vehicles (UAVs) mounted with hyperspectral sensors. Further studies should look into the potential use of UAVs mounted with hyperspectral sensors, not only for aerial crop variety discrimination but also for biotic and abiotic stress detection for improved high-throughput phenotyping. Thus, the applicability of our results in imaging spectroscopy using aerial and satellite sensors (macroscales) needs to be validated, under low signal-to-noise ratio, atmospheric interference, large data sets, among other challenges.

SECTION III: AERIAL REMOTE SENSING AND YIELD PREDICTION OF MAIZE

Aerial imagery (RGB)

Digital surface model

VIs landscape

90
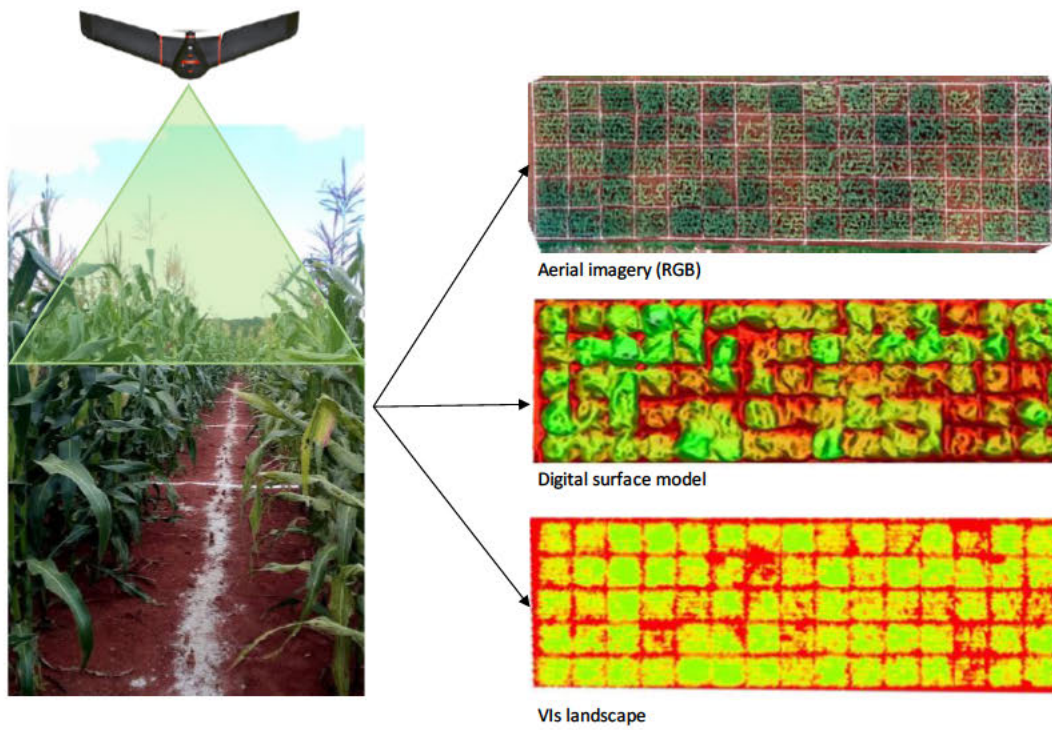
CHAPTER 5: UAV-BASED AERIAL REMOTE SENSING OF MAIZE

This Chapter is based on:
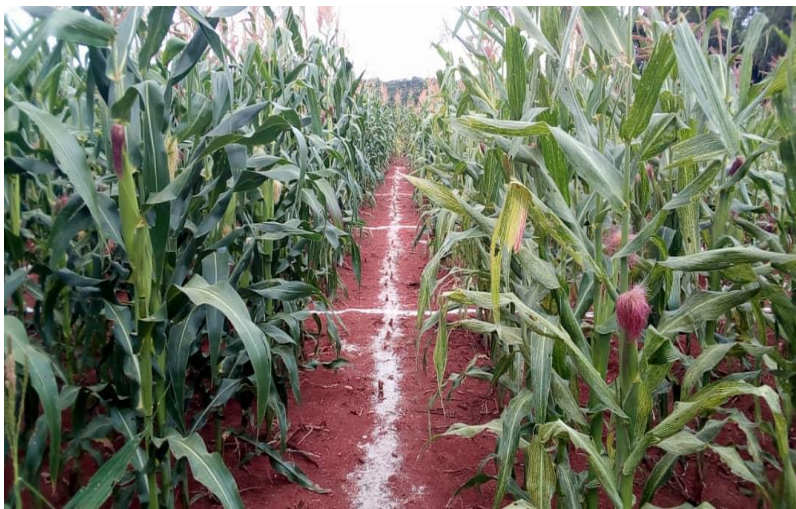
Flowering stage

Abstract

Accelerating crop improvement for increased yield and better adaptation to changing climatic conditions is an issue of increasing urgency in order to satisfy the ever-increasing global food demand. However, the major bottleneck is the absence of high-throughput plant phenotyping methods for rapid and cost-effective data-driven variety selection and release in plant breeding. Traditional phenotyping methods that rely on trained experts are slow, costly, labor-intensive, subjective, and often require destructive sampling. We explore ways to improve the efficiency of crop phenotyping through the use of unmanned aerial vehicles (UAVs)-based multispectral remotely sensed data in maize (*Zea mays* L.) varietal response to maize streak virus (MSV) disease. Twenty-five maize varieties grown in a trial with three replications were evaluated under artificial MSV inoculation. Ground scoring for MSV infection were carried out at midvegetative, flowering and midgrain filling on a scale of 1 (resistant) to 9 (susceptible). UAV-derived spectral data were acquired at these three different phenological stages in multispectral bands corresponding to Green ($0.53 - 0.57\mu m$), Red ($0.64 - 0.68\mu m$), Red-edge ($0.73 - 0.74\mu m$) and Near-infrared ($0.77 - 0.81\mu m$). The imagery captured was stitched together in Pix4Dmapper, which generates two types of multispectral orthomosaics: the NoAlpha and the transparent mosaics for each band. The NoAlpha imagery was used as input into QGIS to extract reflectance data. Six vegetation indices were derived for each variety: normalized difference vegetation index (NDVI), green normalized difference vegetation index (GNDVI), Red-edge NDVI ($NDVI_{red\text{-}edge}$), Simple Ratio (SR), green Chlorophyll Index (CI_{green}) and Red-edge Chlorophyll Index ($CI_{red\text{-}edge}$). The Random Forest (RF) classifier was used to evaluate UAV-derived spectral and VIs with and without variable optimization. Correlations between the UAV-derived data and manual MSV scores were significant ($R = 0.74 - 0.84$). Varieties were classified into resistant, moderately resistant and susceptible with overall classification accuracies of 77.3% (Kappa = 0.64) with optimized and 68.2% (Kappa = 0.51) without optimized variables, representing an improvement of ~ 13.3% due to variable optimization. The RF model selected GNDVI, CI_{green}, $CI_{red\text{-}edge}$ and the Red band as the most important variables for classification. Midvegetative was the most ideal phenological stage for accurate varietal phenotyping and discrimination using UAV-derived multispectral data with RF under artificial MSV inoculation. The results provide a rapid UAV-based remote sensing solution that offer a step-change towards data availability at high spatial

(submeter) and temporal (daily/weekly) resolution in varietal analysis for quick and robust high-throughput plant phenotyping, important for timely and unbiased data-driven variety selection and release in plant breeding programs, especially as climate change accelerates.

Keywords: Maize; unmanned aerial vehicles; high-throughput phenotyping; multispectral data; remote sensing; maize streak virus; Random Forest; climate change

5.1 Introduction

Maize (*Zea mays* L.) breeding success depends on developing adapted high-yielding varieties that are resistant or tolerant to both biotic and abiotic stresses found in the target production environments. Accelerated crop improvement to increase yield and better adaptation to changing climate conditions is an issue of increasing urgency to satisfy the ever-increasing global food demand (Alston *et al.*, 2009; Godfray *et al.*, 2010). Global warming is predicted to continue due to the increase in greenhouse gases, which affects the rainfall patterns in the 21st century (IPCC, 2014) increasing the threats of abiotic and biotic stresses. For example, the rising temperatures and altered rainfall patterns will affect the spatial distribution and development of crop diseases, as different diseases may respond differently to the changing climate conditions (Velásquez *et al.*, 2018).

The impact of climate change on crop diseases is well documented (Luo *et al.*, 1998; Coakley *et al.*, 1999; Garrett *et al.*, 2006). Certainly, climate change will directly influence plant disease epidemics (Garrett *et al.*, 2011). For instance, with particular reference to maize streak virus (MSV), changes that result in environmental factors, which cause the leafhopper vectors (*Cicadulina* species) that transmit MSV, to move long distances will spread virus populations and epidemics to non-endemic areas (Rose, 1978). Climate change prediction models have shown a general trend of increased rainfall in East Africa (EA), with a concurrent decrease in Southern Africa (SA) (IPCC, 2007). The increase in precipitation in EA will produce a conducive temporal overlap of seasons, which will provide a 'greenbridge' (Stanley *et al.*, 1999; Kloppers, 2005). The 'greenbridge' allows the leafhopper vectors that subsequently spread the virus to survive throughout the year. On the other hand, decreasing precipitation in SA will bring droughts, and MSV disease epidemics are frequently associated with droughts followed by erratic rainfall at the start of the season (Efron *et al.*, 1989), as occurred

93

in the savanna region of West Africa in the 1983 and 1984 seasons (Rossel and Thottappilly, 1985), and in Kenya in 1988-89 (Njuguna *et al.*, 1990). Furthermore, the prevalence of *Cicadulina* species that spreads the virus in the major crop growing regions of sub-Saharan Africa (SSA) is influenced by altitude, temperature, and rainfall (Dabrowski *et al.*, 1987). The tripartite biotic interaction involving plant × pathogen × environment due to climate change, strongly influences disease prevalence and/or severity, with the disease expected to have devastating effects in some years and being insignificant in others (Efron *et al.*, 1989). The tripartite interaction functions within a continuum – it can create conditions highly conducive to diseases (disease optima) or it may create those that totally discourage disease development. The resultant environments may make the same variety appear completely resistant in some situations and prove fully susceptible in others. Conversely, the pathogen itself might change from being virulent to being merely weakly pathogenic as it continues to evolve to local conditions. To address these various scenarios, there is a need to develop new phenotyping tools for the rapid evaluation of new varieties adapted to futures climates.

An increase in plant disease prevalence coupled with the growing human population poses one of the greatest challenges to achieving global food security in the face of climate change. Maize is one of the main staple food crops in SSA, grown on a total of about 27 million ha according to FAO data. Adapting maize production to future climates depends not only on our ability to precisely predict future climate scenarios, but also on the development of robust adaptation strategies that address the challenges associated with climate change. These adaptation strategies include, but are not limited to, improved germplasm with resistance to diseases, and tolerance to heat and drought. For plant breeders, the challenge is how to develop varieties resistant or tolerant to the major plant diseases affecting modern agriculture today and in the future. Fortunately, plant breeders have access to a plethora of cutting edge technologies to use to generate large numbers of superior new varieties for selection due to advances in genomics, doubled haploid technology, rapid cycling and molecular breeding (Phillips *et al.*, 2010; Poland *et al.*, 2015). Crop breeding programs around the world generate a larger number of new varieties each year for selection to meet the demand for new varieties to address multiple traditional stresses but also increasingly able to adapt to climate change. However, as these demands increase, the major bottleneck is rapid variety selection and the absence of high-throughput plant phenotyping tools for precise, cost-effective and quick

assessment of phenotypic expressions in the field (Bilder *et al.*, 2009; Araus and Cairns, 2014; Sankaran *et al.*, 2015; Ghanem *et al.*, 2015; Tardieu *et al.*, 2017).

Plant phenotyping is the measurement of individual traits and physiology at single plant-level or canopy-scale (Hickey *et al.*, 2019). High-throughput refers to the relative effort that is associated with the measurements. Image-based phenotyping tools are capable of imaging thousands of plants or plots within a few hours, and doing so at a very high level of accuracy (Fahlgren *et al.*, 2015). Phenotypes are a set of visible characteristics of the variety as a result of genotype × environment interaction, including light emission (fluorescence) properties of the photosynthetic machinery, growth rates, morphology, tolerance to abiotic and biotic stresses, yield, and yield components (Hickey *et al.*, 2019). Variety selection efficiency relies on accurate field-based phenotyping, which measures the relative genetic potential as influenced by the target production environment and expressed in terms of grain yield, biomass, and tolerance to abiotic and biotic stresses (White *et al.*, 2012; Araus and Cairns, 2014). Rapid and robust field phenotyping, which establishes superior trait performance by phenotypes at set levels of statistical significance, is key to plant breeding success and forms the basis for successfully discriminating field selection. Such improved rapid phenotyping methods must balance speed, cost, and accuracy (Hickey *et al.*, 2019).

The traditional phenotyping methods rely on trained experts to take crop records using visual assessment of crop vigor and other abiotic stresses (Zaman-Allah *et al.*, 2015). However, traditional crop phenotyping methods are comparatively slow, costly, laborious, not easily applicable over large areas and numbers of varieties, and frequently require destructive sampling (Furbank and Tester, 2011; Walter *et al.*, 2012; White *et al.*, 2012; Dhondt *et al.*, 2013; Cobb *et al.*, 2013; Fiorani and Schurr, 2013; Araus and Cairns, 2014). Furthermore, field data collection requires repeated measurements with a high risk of damaging the plants as researchers walk through fully developed canopies (Anthony *et al.*, 2017). The improvement in high-throughput plant phenotyping methods capable of accounting for environmental factors like rainfall, temperature, humidity, solar irradiation, soil nutrient levels, and biotic and abiotic stresses will increase selection efficiency in plant breeding (Sankaran *et al.*, 2015). Recently, advances have been made in high-throughput crop phenotyping to accelerate variety selection and advancement in plant breeding using sensing and imaging systems

(Deery *et al.*, 2014; Prashar and Jones, 2014; Araus and Cairns, 2014; Zaman-Allah *et al.*, 2015; Mahlein, 2016; Anthony *et al.*, 2017). Satellite remote sensing technology has shown to delivers accurate, timely, and cost-effective measurements at large-scale, especially in grain crops like wheat (Casadesús *et al.*, 2007; Hosoi and Omasa, 2009; Römer *et al.*, 2011), maize (Trachsel *et al.*, 2011; Weber *et al.*, 2012; Yang *et al.*, 2014), and rice (Tanabata *et al.*, 2012; Hairmansis *et al.*, 2014). However, current generations of satellite sensors are limited by their spectral and temporal resolution for plot level variety analysis and data collection in plant breeding. High spectral resolution remote sensing options from manned aerial platforms are costly and are limited by operational complexity for application in small breeding plots (Jimenez-Berni *et al.*, 2009). Despite progress made so far in sensing systems, there are limited studies on disease phenotyping in maize varieties.

Recently, field-based high-throughput plant phenotyping studies are exploring UAV-derived data at submeter resolution and accurate products that can be used effectively at low cost for agriculture and environmental analysis (Lelong *et al.*, 2008; Zhou *et al.*, 2017; Maimaitijiang *et al.*, 2017; Jin *et al.*, 2017; Yue *et al.*, 2018). Using proximal sensing we have shown in Chapter 4 that it is possible to discriminate maize varieties using multi-temporal hyperspectral data. The ability to discriminate crop varieties using their spectral reflectance showed the potential of proximal remote sensing in crop phenotyping. A lot of studies to estimate crop parameters used the characteristic spectra in the visible and Near-infrared (NIR) range (Rouse Jr *et al.*, 1974; Rondeaux *et al.*, 1996; Jiang *et al.*, 2008). Nevertheless, while proximal sensing eliminates bias that can be introduced by visual scoring, it still remains labor-intensive to collect data from each breeding plot (Tattaris *et al.*, 2016). While phenotyping using satellite-derived data can cover large areas instantaneously, it does not match the spatial (submeter) and temporal (daily/weekly) resolution that can be achieved with UAV-based phenotyping. Such a higher degree of resolution is required for distinguishing small changes in plant response, such as for example, due to disease infection, heat and drought stress, or mineral deficiencies. The resolution of UAV-based phenotyping is at plot level and provides the possibility of instantaneous records of single or multiple plots and is therefore applicable to plant breeding (Chapman *et al.*, 2014; Araus and Cairns, 2014). Therefore, the potential application of UAVs mounted with hyperspectral and multispectral sensors needs to be investigated, not only for

aerial crop variety classification but also for biotic and abiotic stress detection and varietal classification on disease reaction for improved selection accuracy in plant breeding.

UAVs are relatively small and cheap to operate for the crop remote sensing community (Yue *et al.*, 2018). The usage of UAVs mounted with high spectral sensors is an emergent and affordable tool for high-throughput crop phenotyping community (Frank *et al.*, 2015). UAVs are flexible and have the ability to fly and hover over the area of interest making them a desirable tool for plot-level data collection (Anthony *et al.*, 2017). Nevertheless, the ability of the UAV sensors to discriminate crop varieties based on their response to target production environmental constraints for adequate field phenotyping remains to be tested. Grenzdörffer *et al.* (2008) indicated that remotely sensed data for agricultural analysis needs to come from high temporal resolution imagery. Obtaining high temporal and spatial resolution images in small varietal plots commonly used in plant breeding is even more difficult and expensive using traditional remote sensing platforms, and therefore UAVs seem a very attractive alternative (Hunt *et al.*, 2008; Nebiker *et al.*, 2008; Perry *et al.*, 2012; Zhang and Kovacs, 2012).

Several studies using UAV-based remote sensing have been conducted to evaluate morpho-physical characteristics of crops including crop growth, height, and vigor in plant breeding as indicators of crop performance (Wei *et al.*, 2010; Ilker *et al.*, 2013; Alheit *et al.*, 2014; Njogu *et al.*, 2014). The potential of UAVs based remote sensing of crops has been demonstrated in yield estimation (Swain and Zaman, 2012), pest damage detection (Nebiker *et al.*, 2008), physiological condition assessment (Zarco-Tejada *et al.*, 2012; Zarco-Tejada *et al.*, 2013), and stress detection (Jimenez-Berni *et al.*, 2009), including low-nitrogen stress (Zaman-Allah *et al.*, 2015). Therefore, plant phenotypic responses to biotic and abiotic stress, growth, and yield prediction can be evaluated using remotely sensed data (Zhang and Kovacs, 2012). For example, in a study of low nitrogen response in maize, Zaman-Allah *et al.* (2015), using UAV-derived multispectral data, found significant correlation between maize yield and nitrogen stress index (R = 0.40 – 0.79) and between crop senescence index and NDVI values (R = 0.84). Their findings confirmed the utility of using UAV-derived remotely sensed data in field-based crop phenotyping. Hairmansis *et al.* (2014) used UAVs to evaluate rice varieties for tolerance to salinity. Calderón *et al.* (2013) and Garcia-Ruiz *et al.* (2013) used UAV-based remote sensing to monitor citrus disease with up to 85% accuracy. UAVs have also been used to monitor crop

germination (Sankaran *et al*., 2014), vigor, and leaf area index (Hunt *et al*., 2008; Sugiura *et al*., 2005). Recently, Sankaran *et al*. (2014) used UAV in assessing emergence of spring wheat and found a high correlation (R = 0.86) with ground-based measurements. UAV-based remote sensing can also be effective in detecting crop maturity (Khot *et al*., 2014), a key trait in variety selection. Similarly, UAV-derived data can be used for such traits like plant height, canopy development, chemical damage, nutrient deficiency or toxicity, insect damage, disease damage, and presence of weeds (Sankaran *et al*., 2015).

Evidence from previous studies has stimulated research interests to further refine the utility of UAV-derived remotely sensed data in crop phenotyping. For UAV-derived remotely sensed data to be useful in plant breeding and varietal selection, the ability to discriminate different varieties using their spectral reflectance as they respond to disease infection is critical. Using proximal sensing, Dhau *et al*. (2018) demonstrated the potential of hyperspectral data to detect MSV infection in maize. MSV (Genus *Mastrevirus*, Family *Geminiviridae*) is found throughout SSA, causing the most severe viral crop disease on the continent (Shepherd *et al*., 2010; Jourdan-Ruf *et al*., 1995). MSV is obligately transmitted by leafhoppers in the Genus *Cicadulina*, mainly by *C. mbila* Naudé and *C. storeyi*. MSV causes extensive damage to maize in the tropics (Africa and South America). This is exacerbated by the rising temperatures, which promote development of vector populations (Jourdan-Ruf *et al*., 1995). Breeding for resistant or tolerant varieties is the most economic way to combat the disease due to lack of effective agronomic and chemical control techniques. MSV stressed plants are less able to effectively use light, leading to reduced grain yield. Therefore, crop stresses may be sensed remotely due to temporal or spatial variation in reflectance (Barton, 2012). The spectral reflectance is controlled by the absorption properties of leaf pigments (Chlorophyll *a*, *b* and carotenoids). Therefore, any change in pigment concentrations relates strongly to the physiological status of the plant's health status and productivity. In MSV-infected plants, the leaves become streaked with narrow, broken, white, or yellow chlorotic stripes reducing the photosynthetic area of the leaves. As the disease level increases, complete foliar chlorotic can occur in susceptible varieties because of chloroplast destruction (Engelbrecht, 1982). Therefore, individual variety pigments at canopy-level holds tremendous potential for facilitating detection of MSV stress for varietal classification and estimating productivity by measuring and interpreting their reflectance properties. Potential use of remotely sensed data

to detect plant diseases have been shown through comprehensive reviews (e.g., Barton, 2012; Sankaran *et al.*, 2010) and empirical evidence using multispectral and hyperspectral remote sensing. Examples of diseases detection include head blight in wheat caused by fusarium (Bauriegel *et al.*, 201; Dammer *et al.*, 2011) and soyabean root rot (Wang *et al.*, 2004. Yet, studies on the classification of maize varietal response to disease (e.g. MSV) using UAV-derived remotely sensed data are limited (to the best of our knowledge).

This study sets out to assess the utility of UAV-derived remotely sensed data for phenotyping maize varietal response to maize streak virus (MSV) disease. We hypothesized that UAV-derived multispectral imaging data is sensitive to MSV disease symptoms that cause distinct discoloration of the aerial parts of maize varieties, and are able to discriminate varieties on the basis of their response to disease infection.

5.2 Materials and Methods

5.2.1 Study area

The study was conducted at Rattray Arnold Research Station (RARS) in Zimbabwe as indicated in section 1.6 of this thesis. The trial was planted on 23 November 2018. The vegetative stage of the crop was in December 2018 and January 2019. Figure 5.1 shows the monthly rainfall, heat units, maximum, minimum and mean temperatures during the crop growing period. The weather data was recorded using an advanced automatic weather station Pro (supplied by Dacom Farm Intelligence, Netherlands). The weather station Pro was installed outside the experimental plots in the study area to record temperature, relative humidity, rainfall, wind speed, wind direction and radiation. Plant and insect growth and development depend on temperature, often described as heat units (HU). HU were calculated using equation [5.1]:

$$HU = ((Maxi. Temp. + Min. Temp.)/2) - Threshold/Base Temp. \qquad [5.1]$$

Were HU = heat units; base temperature = 10^0C.
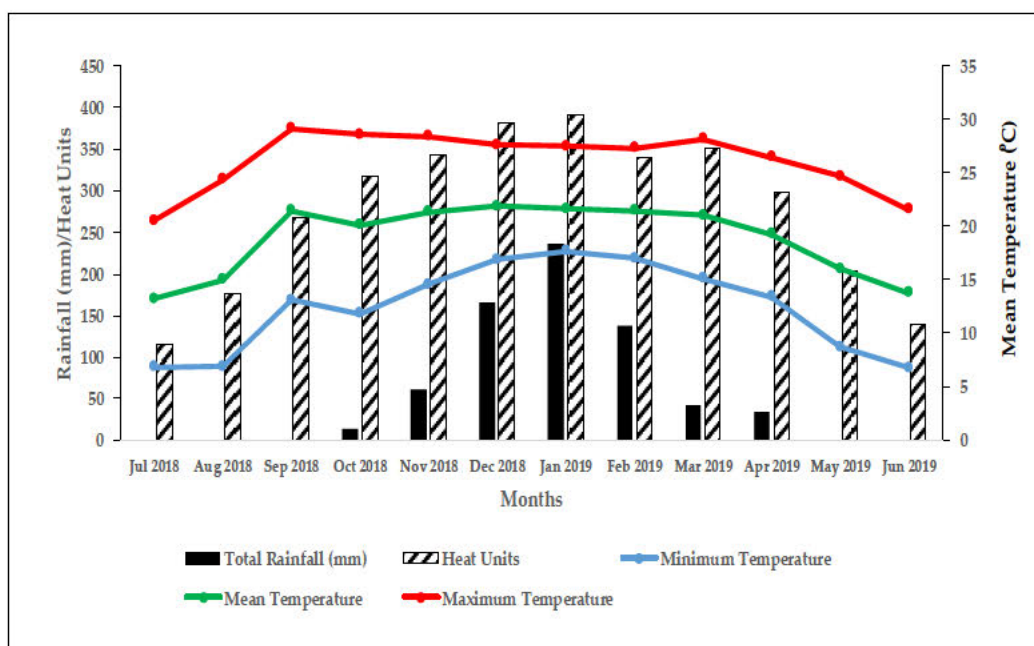
Figure 5.1. Monthly rainfall, heat units, mean, maximum and minimum monthly temperatures during the crop growing season (November 2018 – April 2019).

5.2.2 Crop varieties, experimental set-up and ground truth data

Twenty-five maize varieties were grown in a 5 × 5 partially balanced alpha lattice design (Figure 5.2). Six-row plots replicated three times were used. A total of 75 plots constituted the experimental area (25 varieties × 3 replications). Three known check varieties representing resistant, moderate and susceptible responses to MSV were included. Gross plot area was 7.5m × 4.5m × 6 rows. Maize seeds were sown on a flat soil surface at a spacing of 0.5m within rows and 0.75m between rows. Sowing was done at a seeding rate of four seeds per station and after germination thinned to a final two plants per station at 21 days after sowing to achieve a target plant population of 53,000 plants ha^{-1}. Uniform management was applied to all varieties. Fertilizer was applied at a rate of 450 kg ha^{-1} basal (13:26:13 – N: P: K) at planting and 450kg ha^{-1} ammonium nitrate (34.5% N) top dressing split into two applications. The first half (225kg ha^{-1}) of the top dressing was applied at early vegetative and the second half (225kg ha^{-1}) at booting (pre-flowering) stage. A combination of manual hand weeding and herbicide application was done to keep the experimental plots free of weeds.

To evaluate resistance to MSV, varieties need to be assessed under artificial inoculation where the whole procedure is controlled. Every plant was artificially infested when four leaves had

100

fully expanded with mass reared viruliferous leafhoppers (*Cicadulina mbila*) (Rodier, 1995) previously fed with MSV infected maize plants. To achieve maximum infestation, spreader rows of a susceptible variety were planted around the experimental area.
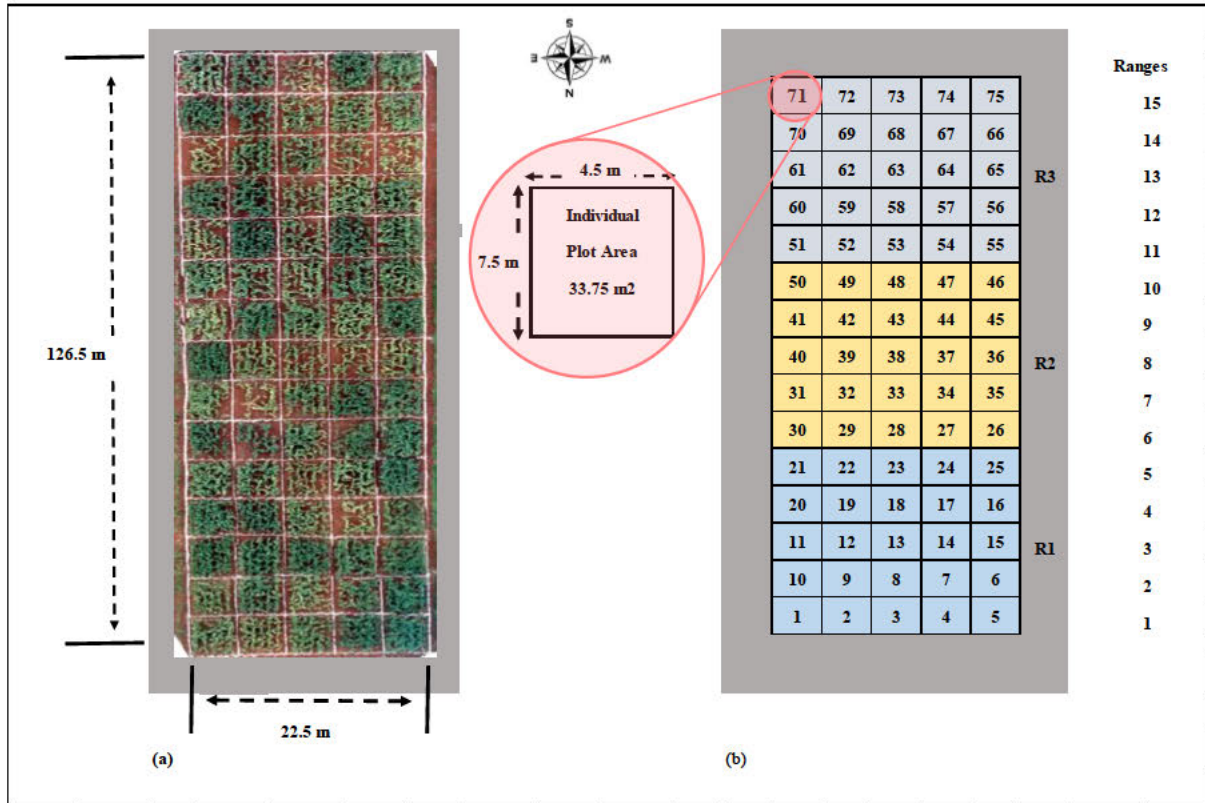
Figure 5.2. Field layout showing (a) the experimental area (aerial image to the left with plots demarcated using agricultural lime – white lines) taken using the UAV RGB camera and (b) the experimental layout (right) of 25 varieties × 3 replications (R1 – 3) in different colors. The insert shows individual plot dimensions.

The white lines on the left image of Figure 5.2 indicate plot divisions into 75 plots. The individual gross plot area was 7.5m × 4.5m × 6 rows, and the whole experimental area was 126.5m × 22.5m planted to 25 varieties. The ground truth MSV scores were taken on all 25 maize varieties in all replications. Each plot was rated for MSV using visual scoring at midvegetative, flowering, and midgrain filling growth stages on a scale of 1 to 9, where 1 denotes resistant (zero or very slight symptoms) and 9 is susceptible (very severe symptoms).

5.2.3 UAV platform, imagery acquisition and processing

5.2.3.1 The UAV platform

The imagery was acquired using a Parrot Sequoia Multispectral camera mounted on eBee SQ UAV (manufactured by Swiss Geo Consortium Sensefly, Cheseaux-Lausanne, Switzerland) (Figure 5.3). The UAV is a Delta Fixed Wing craft with greater speed and superior aerodynamics compared to multi-rotor craft. It is designed strictly for agricultural purposes. The Parrot sequoia sensor is made up of 5 cameras, with 4 discreet bands: Green $(530-570nm)$, Red $(640-680nm)$, Red-edge $(730-740nm)$ and NIR $(770-810nm)$. The fifth camera functions as a composite color capture sensor (red, green, and blue (RGB)). The sensor unit has a sunshine sensor with GPS, sunshine detection unit and the Inertial Measuring Unit (IMU). The GPS unit receives positional information so that the imagery produced is subsequently georeferenced. The IMU captures the attitudes of the sensor at the times of image capture (through rotations about the X, Y and Z axes). The sunshine unit captures and records the sunshine radiance value to allow for radiometric correction of the imagery. The imagery was captured using a single grid mapping pattern, with flight plan designed to map an area in excess of the area of interest to minimize the effects of radial distortion around the periphery of the area of interest. The flight plan had the following parameters: 42.5m altitude, with a ground sampling distance of 8cm in the RGB and 11.5cm in the multispectral; 75% forward overlap and 75% side overlap as per Sensefly's recommendation. Table 5.1 shows some of the sensor parameters and spectral ranges for the Red (R), Green (G), Red-edge (RE), and Near-infrared (NIR) bands of the camera used in this study.

Figure 5.3. The Unmanned Aerial Vehicle (UAV) used in this study

Table 5.1. UAV sensor parameters and spectral ranges for the Red (R), Green (G), Red-edge (RE), and Near-infrared (NIR) bands of the camera used in this study.

Sensor specifications	Spectral features
Sensor type	Multispectral sensor + RGB camera
Multispectral sensor	4-band
RGB resolution	16 mega-pixel (MP), 4,608 x 3,456 px
Single-band resolution	1.2 MP, 1,280 x 960 px
Multispectral bands	Green (550nm ± 40nm); Red (660nm ± 40nm); Red-edge (735nm ± 10nm); Near-infrared (790nm ± 40nm)
Field of view	64°
Data spectral resolution	Green, Red, Red-edge, NIR
Image spatial resolution	8cm at 42.5m altitude

5.2.3.2 Image acquisition and processing

Aerial imagery was collected at three different phenological stages (midvegetative, flowering and midgrain filling) using a UAV-mounted multispectral camera (Figure 5.3). The imagery was processed using Sensefly's Pix4D Structure from Motion (SfM) software (Cheseaux-Lausanne, Switzerland in collaboration with Pix4D SA, Lausanne, Switzerland). SfM works by finding correspondence between images, features and coordinates by tracking one imagery to the next using the scale-invariant feature transform (SIFT). The SIFT uses the maxima from a difference-of-Gaussians (DOG) pyramid as features. The precise mechanics of Pix4d's structure from motion are proprietary and therefore cannot be described further. These steps were followed during image processing:

a) Initial processing involved key points identification, extraction and matching; camera model optimization – calibration of the internal (focal length) and external parameters (orientation) of the camera; and geolocation GPS/GCP (Ground Control Points).

b) Point cloud and mesh: this step builds on the automatic tie points, which entail point densification and creation of 3D textured mesh.

c) Digital Surface Model (DSM) creation to determine orthomosaics and vegetation indices maps. Orthomosaics creation was based on orthorectification to remove perspective distortions from the images to produce vegetation index maps with the value of each pixel with true-to-type reflectance from the area of interest.

Comprehensible mosaics at high spatial resolution (11.5cm × 11.cm) were produced using four multispectral bands: Green (530 – 570nm), Red (640 – 680nm), Red-edge (730 – 740nm) and NIR (770 – 810nm). Spectral reflectance values were extracted and vegetation index (VI) values were calculated per each variety. Maps of VIs were produced at all UAV flight/data acquisition dates (phenological plant stages), showing the evolution of the maize varieties throughout the different phenological stages (Figure 5.4). The maps are crucial in analyzing the differences between varietal responses to environmental conditions. They provide rich information about the biotic stress that was affecting the varieties. The prevalent biotic stress that was recorded was MSV. The maps generated at the pixel scale allow obtaining precise data to examine the varietal variation for rapid assessment of maize varieties in breeding programs to improve the selection process. Comparison of VIs maps provide excellent visual analysis at different phenological stages (Figure 5.4).

5.2.3.3 Reflectance data extraction

The imagery captured over the study site was stitched together in Pix4D mapper, which generates two types of multispectral Orthomosaics: the NoAlpha and the transparent mosaics. These were generated for each band of the imagery (Green, Red, Red-edge, and NIR). The NoAlpha imagery was used as input into QGIS for reflectance data extraction. A shape file was created by converting a Google earth Key Markup Language (KML) file of the mapped area. The shape file was then used to clip the imagery of the mosaic to the extent of the study area. Shape files were then drawn for each of the compartments (individual plots) according to the experimental layout shown in Figure 5.3. The "Clip Multiple Layers" plugin was used to simultaneously clip each of the band images using the shapefile for each plot. Once the shapefile compartments were extracted for each shapefile, the maximum, weighted mean, minimum reflectance, and their standard deviations were generated for each plot in each layer. The average reflectance for each plot was determined by considering a buffer of 25cm on each of the four plots sides to restrict the analysis to the center of the plot, making the net plot area 7.0m x 4.0m. Ground-truth biophysical measurements for each micro-plot were taken from the center of the plot, consistent with UAV data. Extracted reflectance data were exported into excel spreadsheet format for each of the phenological stages. Vegetation indices were calculated from the plots' mean reflectance values.

VIs	Midvegetative	Flowering	Grain filling
NDVI			
NDVI$_{red-edge}$			
GNDVI			
SR			
CI$_{green}$			
CI$_{red-edge}$			
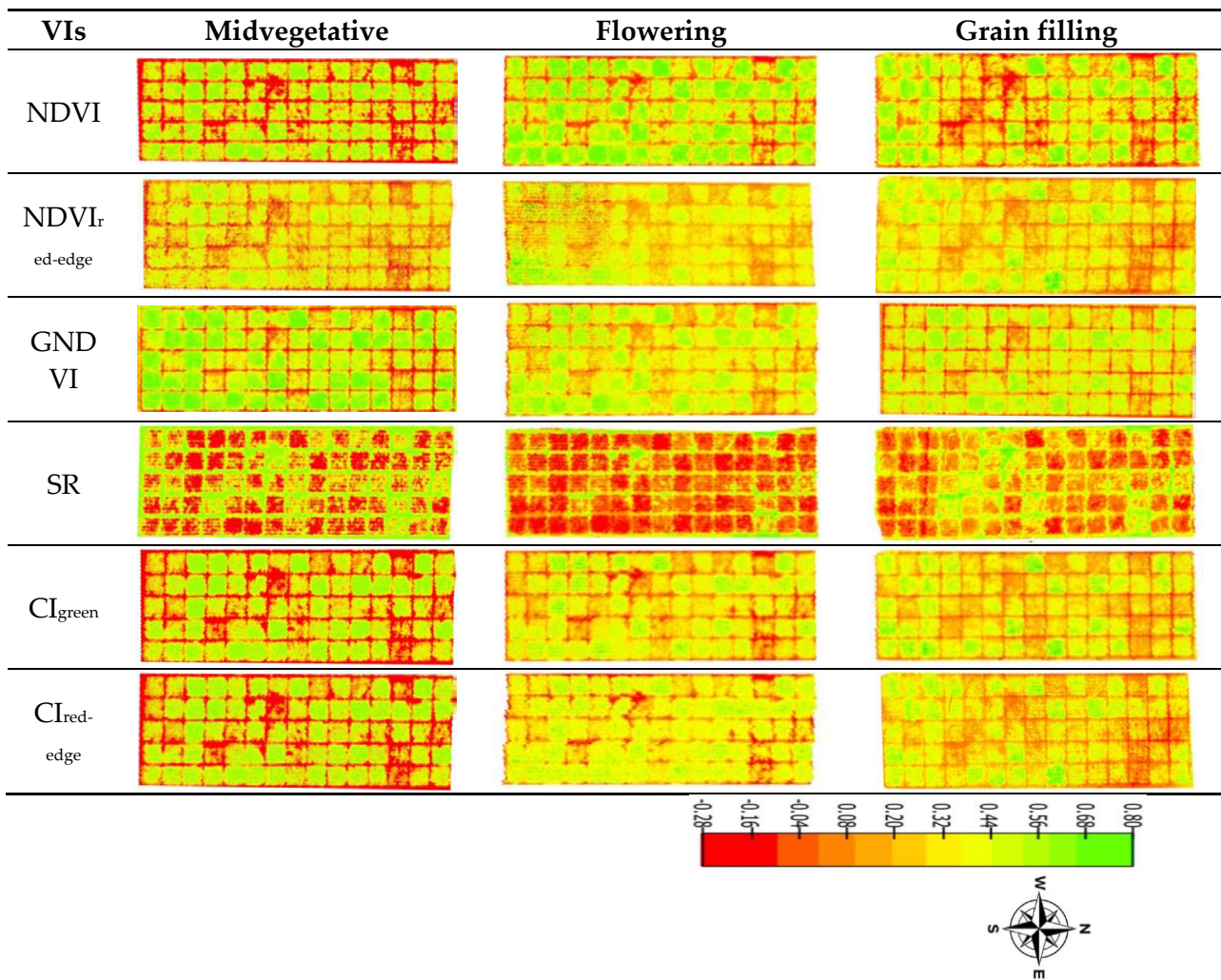
Figure 5.4. UAV-based multispectral images at different phenological plant stages. VIs = Vegetation Indices; NDVI = Normalized Difference Vegetation Index; GNDVI = Green Normalized Difference Vegetation Index; NDVI$_{red-edge}$ = Red-edge Normalized Difference Vegetation Index; SR = Simple Ratio, CI$_{green}$ = Green Chlorophyll Index; CI$_{red-edge}$ = Red-edge Chlorophyll Index

5.2.3.4 Vegetation indices

For complete phenotyping, this study used reflectance values in multispectral bands corresponding to Green (530 – 570nm), Red (640 – 680nm), Red-edge (730 – 740nm) and NIR (770 – 810nm) taken at midvegetative, flowering and grain filling stages. The reflectance values were used to derive the normalized difference vegetation index (NDVI), green normalized difference vegetation index (GNDVI), Red-edge NDVI (NDVI$_{red-edge}$), Simple Ratio

(SR), green Chlorophyll Index (CI$_{green}$) and Red-edge Chlorophyll Index (CI$_{red-edge}$). Table 5.2 shows the VIs used in this study.

Table 5.2. List of VIs and their formulas used in this study

Indices	Equation	Reference
NDVI	$\dfrac{NIR - Red}{NIR + Red}$	Rouse Jr *et al.* (1974)
GNDVI	$\dfrac{NIR - Green}{NIR + Green}$	Gitelson *et al.* (1996)
NDVI$_{red-edge}$	$\dfrac{NIR - RedEdge}{NIR + RedEdge}$	Gitelson and Merzlyak (1994)
SR	$\dfrac{NIR}{Red}$	Baret nad Guyot (1991)
CI$_{green}$	$\dfrac{NIR}{Green} - 1$	Gitelson *et al.* (2005)
CI$_{red-edge}$	$\dfrac{NIR}{RedEdge} - 1$	Gitelson *et al.* (2005)

5.2.4 Varietal classification

Prior to varietal classification, we ran descriptive and correlation analyses of ground truth and spectral data. For determining classes, we used the Jenks natural breaks algorithm, which divides a dataset into homogenous classes (Jenks, 1977). One of the requirements of the Jenks method is that the number of desired classes be specified prior to applying the algorithm to the dataset. In this study, the mechanism for determining the classes was based on the fact that for disease evaluation in plant breeding, the main objective is to classify varieties into either resistant or susceptible. However, there are certain varieties that fall in between the two classes. Thus, a third class (moderately resistant) was included and the visual MSV scores were divided into three categories: resistant (1 – 3.4), moderately resistant (3.5 – 5.4), and susceptible (5.5 – 9) for analysis.

The Random Forest model was used to classify varietal response to MSV under artificial inoculation. RF was chosen for this classification task due to its proven robustness and effectiveness found in other studies for vegetation condition classification in comparison to other supervised parametric and machine learning (ML) classifiers (Rogan *et al.*, 2008; Nitze *et al.*, 2012; de Almeida *et al.*, 2013; Lebedev *et al.*, 2014; Chemura *et al.*, 2016). The RF algorithm also has in-built functionalities for optimizing variables, making it more suitable for classifications that require selection and ranking important variables (Pal, 2005; Chemura *et*

al., 2016). Furthermore, this study required a robust method suitable for sample sizes that are relatively small and well suited for cross-validation in accuracy assessment (Chemura *et al*., 2016). The data were split randomly into training (70%) and validation (30%) sets (Duro, *et al*., 2012). The general rule that applies to remote sensing is also important for ML, that one should assess classification accuracy using data not used in training the classifier (Maxwell *et al*., 2018). Raw data was used for analysis without any correction for experimental design or spatial variability. This was done to increase variability in the data and make it easier to fit the models. In addition, it is important to predict each plot and then run the classical analysis using predicted values. While it is possible to predict the mean of each variety directly, this might affect the precision of the model. RF utilizes a specified number of variables (*mtry*) drawn at each individual node from a random subset of the variables and compute the best split where a subset of variables are used without pruning (Breiman, 2001; Lin *et al*., 2010; Genuer *et al*., 2010). Classification accuracy is improved through RF parameter optimization (*mtry* and *ntree*) (Breiman, 2001; Mutanga *et al*., 2012). The RF classification model was developed using the "caret" package within R version 3.6.1 (R Development Core Team, 2019).

5.2.4.1 Variable optimization

The selection of bands and VIs to use in varietal classification was done using the RF variable importance measure. The most important variables were determined and those found important for varietal classification were then used in the model. RF classifier estimates the importance of each input variable to the classification by comparing the magnitude of out-of-bag (OOB) error when a variable is excluded, while retaining others (Breiman and Cutler, 2007; Gislason *et al*., 2004). Thus, RF ranks the variables according to the average error reduction as a result of inclusion of that variable in the classification. Variables with high mean decrease in errors are deemed important for classification and are therefore selected. The tuning of the parameters (*n*tree and *m*try) of RF guarantees high classification accuracy. The default *n*tree (n = 500) was used. The *m*try was optimized by trying all possible values (Breiman, 2001; Lin *et al*., 2010; Genuer *et al*., 2010).

5.2.4.2 Accuracy assessment

Confusion matrices were used to assess classification accuracies (Story and Congalton, 1986; Congalton and Green, 2009). The overall accuracy (OA) denotes the likelihood that a randomly selected variety is correctly classified according to its reaction to the MSV disease. On the other hand, producer's accuracy (PA) shows the probability that the algorithm has correctly categorized the variety's response to MSV. Ground-truth MSV scores were used to assess classification accuracy. The term resistant here was defined as varieties showing no symptoms to very slight symptoms with no effect on final yield; moderately resistant refers to a variety that exhibits symptoms of a partially suppressed virus multiplication and with fewer symptoms than the susceptible. The OA, user accuracy (UA), and PA were determined using the following equations,

$$OA = \frac{1}{N} \sum_{i=1}^{r} n_{ii} \times 100\%$$

(5.2)

where, N is the total number in a confusion matrix, r is the number of rows and n_{ii} is the number of varieties correctly classified in a category.

$$PA = \frac{n_{ii}}{n_{icol}} \times 100\%$$

(5.3)

$$UA = \frac{n_{ii}}{n_{irow}} \times 100\%$$

(5.4)

The Kappa coefficient (Kc), which is also a measure classification accuracy was computed as follows (Congalton, 1991; Jensen, 1996):

$$Kc = N \sum_{n=1}^{r} \frac{n_{irow} n_{icol}}{N^2} - \sum_{i=1}^{r} n_{irow} n_{icol}$$

(5.5)

where n_{ii} is element at position i^{th} row and i^{th} column, n_{icol} is column sums and n_{irow} is row sums.

5.3 Results

5.3.1 Varietal response to MSV

Significant levels of MSV developed on susceptible varieties by midvegetative stages. MSV measurements at the different stages were highly correlated (R = 0.88 – 0.95), thus subsequent models were developed using average MSV severity. Figure 5.5 represents the mean disease severity scores. Response among varieties differed significantly (p < 0.001) with maximum severity mean score of up to 7.3 for most susceptible variety on a scale of 1 – 9. Conversely, the most resistant variety had a mean score of 1.8. Using ground-truth data, of the 25 maize varieties tested, six varieties were classified, in order of increasing mean MSV score, as resistant (V15, V9, V16, V13 V19, and V17), twelve as moderately resistant (V20, V12, V8, V18, V6, V24, V7, V21, V23, V25, V10, and V14) and seven varieties as susceptible (V22, V4, V3, V5, V11, V2, and V1) (Figure 5.5). The most resistant varieties (top six) had mean MSV scores ranging between 1.8 and 3.4.
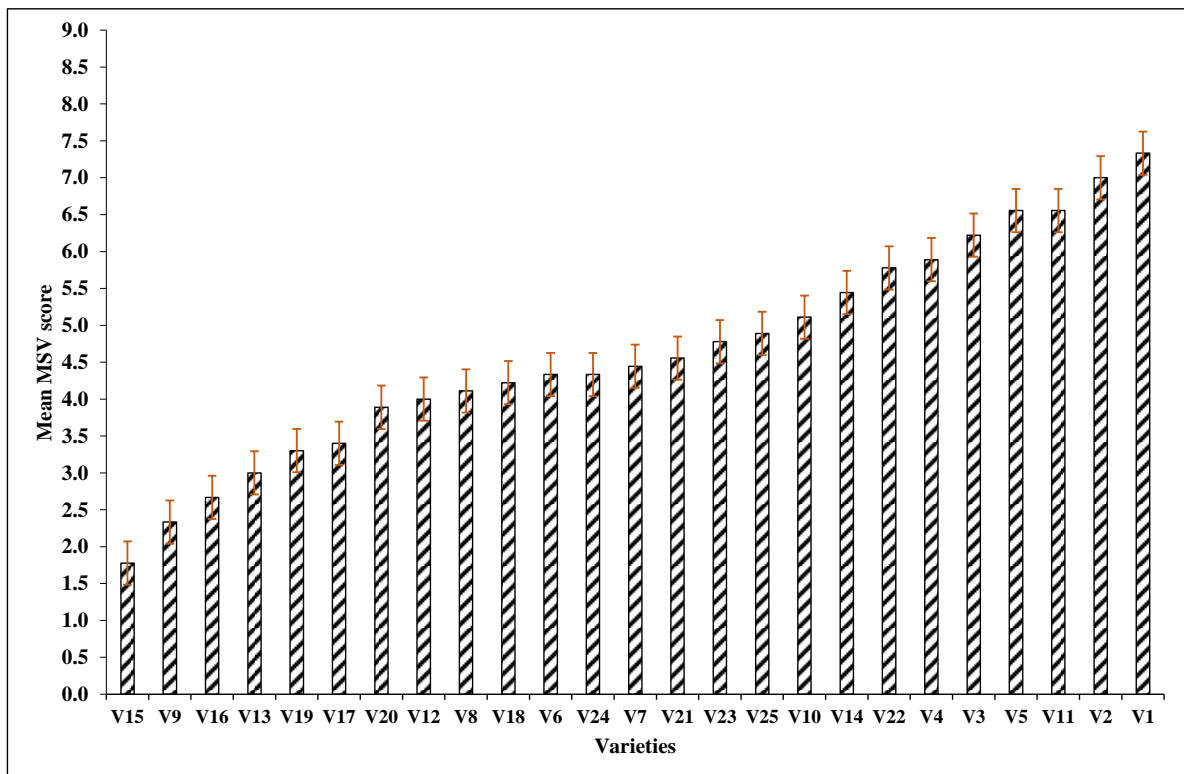
Figure 5.5. Mean disease response of the 25 varieties evaluated. The disease was rated on a score of 1 – 9, where a mean score of 1 – 3.4 (resistant), 3.5 – 5.4 (moderately resistant) and 5.5 – 9 (susceptible). (V1 to V25 = Varieties 1 to 25).

5.3.2 Comparison of UAV-derived and ground truth data

A descriptive analysis, including descriptive statistics and correlation of ground truth measurements and UAV-derived data, follows. The analysis shows that there are no outliers in any variable. Figure 5.6 shows phenotypic correlations between ground truth (manual) scoring and UAV-derived data at each phenological stage. Correlations between the UAV-derived data and manual MSV scores are significant for the shown variables. In absolute terms, the highest correlations between UAV-derived and manual scoring were Red band (R = 0.78), NDVI (R 0.75), SR (R = 0.74), CI_{green} (R = 0.83), $CI_{red-edge}$ (R = 0.78) and GNDVI (R = 0.84). These significant agreements between UAV-derived and ground truth data suggest that UAV-based phenotyping of MSV in maize is feasible. This is critical because, to be effective, image-based phenotyping methods need to achieve a level higher or equivalent to the accuracy achieved using traditional phenotyping methods, and in a shorter time and at lower costs.
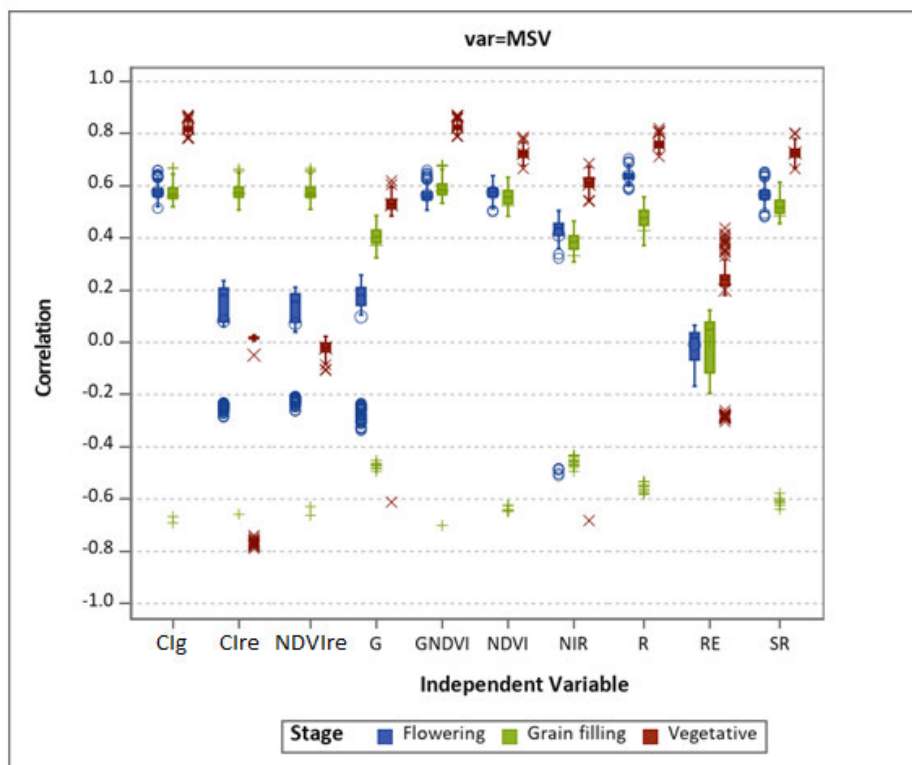
Figure 5.6. Box plots of correlations for ground truth average MSV measurements and UAV-derived multispectral data. CIg = Green Chlorophyll index; CIre = Red-edge Chlorophyll index; NDVIre = Red-edge Normalized Difference Vegetation Index; G = Green; R = Red; NIR = Near-infrared; RE = Red-edge; SR = Simple Ration

110

5.3.3 Phenology-based classification using UAV-derived data

5.3.3.1 The effect of RF input parameter on classification

Prior to evaluation of variable importance, we assessed the effect of the user-specified parameters (*m*try) using the default *n*tree (n = 500) on the classification accuracy. Figure 5.7 indicates that the default setting of *m*try (n = 14) was the best, beyond which no further improvement in classification accuracy was achieved. The advantage of using R statistical package is that it provides straightforward optimization techniques, which are not always available in most commercially available remote sensing software packages (Maxwell *et al.*, 2018). The results showed that when optimizing the RF model, the default settings of *m*try is sufficient (in this case *m*try = 14) and RF was not sensitivity to the chosen *m*try, agreeing with other studies by Liaw and Wiener (2002), Díaz-Uriarte and Alvarez de Andrés (2006), and Adam *et al.* (2014).
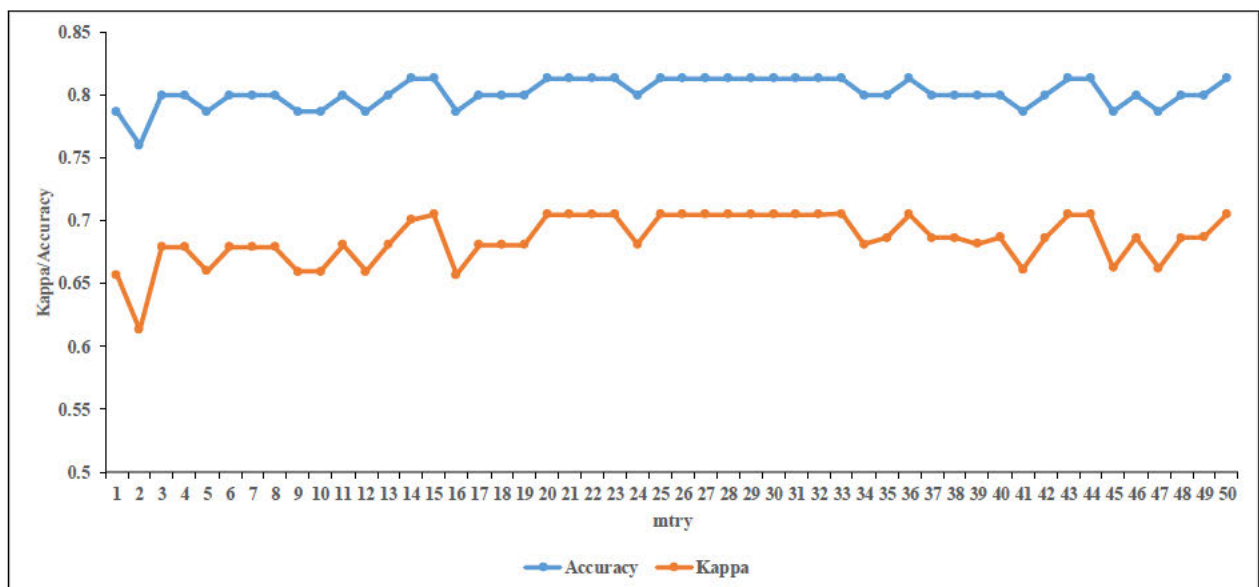
Figure 5.7. Impact of the number of variables tried at each node (*m*try) on RF classification performance

5.3.3.2 Classification with all variables

Figure 5.8 shows all variables used for classification. The different variables were ranked as a measure of their importance in the classification process. The determination of variable importance identified the band(s) and VI(s) that are significant in the classification. An

analysis of the four bands at different phenological stages indicates that only Red (vegetative and flowering) and Green (vegetative) bands were ranked in the top ten important variables as significant for classification process using our data. On the other hand, examination of the six VIs shows that five VIs (CI_{green}, GNDVI, $CI_{red-edge}$, NDVI, and SR) measured at vegetative stage were ranked as important variables in the classification of the varieties by the RF model (Figure 5.8). The overall accuracy of 68.2% (Kc = 0.51) was achieved using all variables. However, to improve the classification accuracy, variable optimization was implemented using RF.
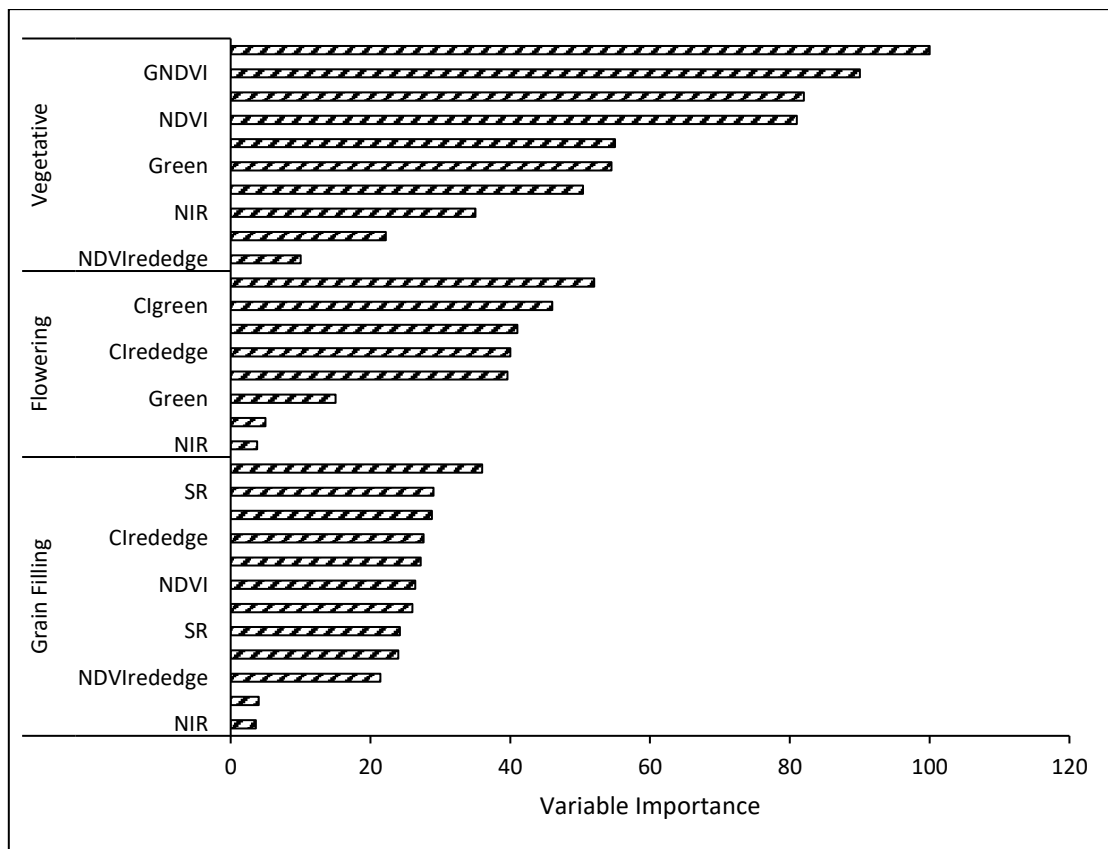
Figure 5.8. Variable importance at different phenological stages used in the classification process without optimization. NDVI = Normalized Difference Vegetation Index; GNDVI = Green Normalized Difference Vegetation Index; NDVIred-edge = Red-edge Normalized Difference Vegetation Index; SR = Simple Ratio, CIgreen = Green Chlorophyll Index; CIred-edge = Red-edge Chlorophyll Index

5.3.3.3 Variable optimization

Variable optimizing was implemented on all the thirty variables, and only seven variables (i.e. two bands and five VIs) were selected as important using the RF OOB error (Figure 5.9). During optimization the RF model dropped less important variables. Dropping less important variable has been confirmed in others studies to improve the performance of RF in classification (Adam *et al.*, 2014; Chemura *et al.*, 2016). When variable importance is very low, it either means the variable is not important or it is highly collinear with one or more other variables. The two spectral bands (Red and Green) at vegetative stage were retained as important. A total of five VIs (CI_{green}, GNDVI, $CI_{red-edge}$, SR and NDVI) at vegetative stage were selected. All the selected variables by the RF model for classifying different varieties were spectral bands or derived VIs measured at midvegetative stage (Figure 5.9). Therefore, midvegetative appeared to be the most ideal phenological stage for accurate classification of maize varietal response to MSV using UAV-derived multispectral data with RF under artificial MSV inoculation. This might be because after flowering, tassels could mask the detection of MSV by the multispectral cameras.

The variable importance approach used in this chapter considers each variable individually, assuming all variables are totally independent and not correlated in any way. However, two or more variables may be collinear. One important advantage of RF is that it has functionalities for dealing with collinear variables. To identify if variables are correlated, a correlation matrix was constructed in R at different phenological stages. Highly correlated variables indicates that the variable is completely predictable using the other variables, which means it could be dropped without affecting model accuracy. For example, the CI_{green} and GNDVI at vegetative stage were highly correlated (R = 0.991). Thus, similar classification results can be achieved using either one of the two. Similarly, SR and NDVI at vegetative stage (R = 0.966), $CI_{red-edge}$ and $NDVI_{red-edge}$ (R = 0.997) at flowering, CI_{green} and GNDVI (R = 0.997), and SR and NDVI (R = 0.988) at grain filling are highly correlated. The discussion of multicollinearity of these variable is beyond the scope of the thesis, therefore, the detailed matrix results of multicollinearity are not shown.

113

5.3.3.4 Classification using optimized variables

Table 5.3 shows the results of varietal classification after variable optimization. Use of optimized UAV-derived VIs resulted in increased varietal classification accuracies into different classes (resistant, moderately resistant, and susceptible) compared to variables without optimization. The results indicate a notable improvement in accuracy of varietal classification using optimized variables. The performance of the RF model in classifying the varieties was improved through variable optimization, with the RF model achieving overall varietal classification accuracies of 77.3% (Kc = 0.64) with optimized variables compared to 68.2% (Kc = 0.51) without variable optimization, representing an improvement of ~ 13.3%. Furthermore, optimization reduced the number of variables from thirty to seven, which were then used by the RF model (Figure 5.9). Improvement in classification accuracies obtained in this study agrees with previous work by Adam *et al*. (2014) and Chemura *et al*. (2016), who found improvements in classification accuracies when variables are optimized. Moreover, our results are comparable to the accuracies found by Sankaran *et al*. (2013) using ground-based sensors.
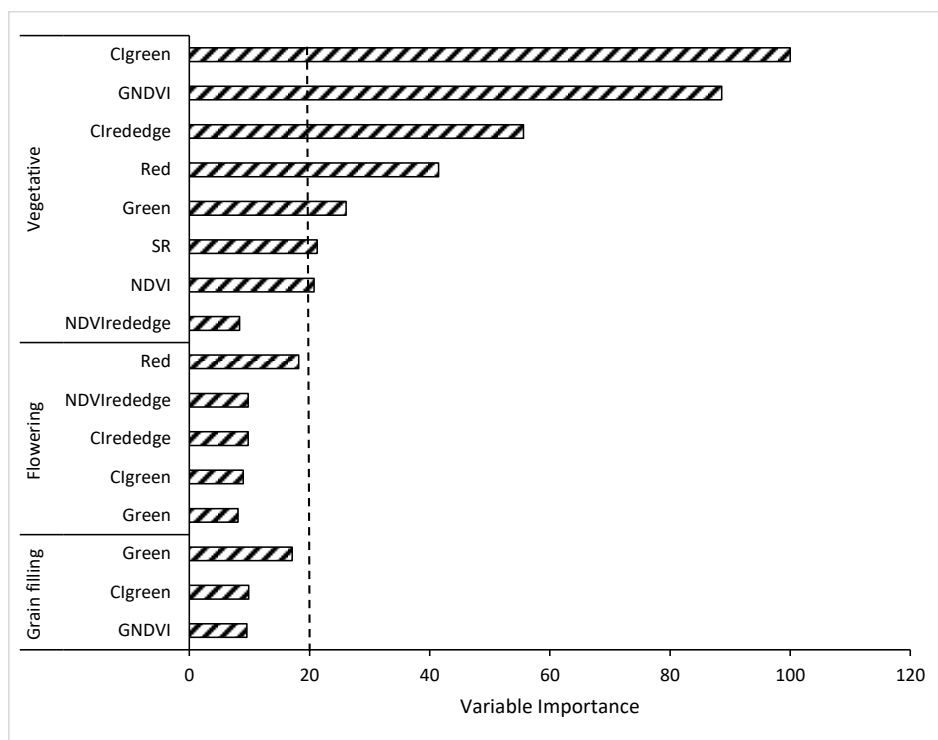
Figure 5.9. Optimization of variables for varietal classification using RF-OOB for different spectral bands and vegetation indices. The vertical dotted line indicates the cut-off point for

selected variables. NDVI = Normalized Difference Vegetation Index; GNDVI = Green Normalized Difference Vegetation Index; NDVIred-edge = Red-edge Normalized Difference Vegetation Index; SR = Simple Ratio, CIgreen = Green Chlorophyll Index; CIred-edge = Red-edge Chlorophyll Index

Table 5.3. Classification accuracies using optimized variables (all seven selected variables were at vegetative stage). PA and UA are Producer's and user's accuracy, respectively.

	Resistant	Moderate	Susceptible	Total	UA (%)
Resistant	4	1	0	5	80
Moderate	1	7	1	9	77.8
Susceptible	0	2	6	8	75
Total	5	10	7	22	
PA (%)	80	70	85.7		
Overall accuracy (%)	77.3				
Kappa coefficient	0.64				

5.4 Discussion

The recent progress in the use of sensing and imaging systems, including UAV-derived data with high spatial (submeter) and temporal (daily/weekly) resolution, present a step-change towards data availability and turnaround time in varietal analysis for quick and robust high-throughput plant phenotyping in plant breeding programs. This study set out to assess the utility of UAV-derived multispectral data for improved phenotyping of maize varietal response to MSV disease under field conditions. The UAV-derived VIs maps produced using UAV-derived data show comprehensive temporal and spatial variations at varietal level (Figure 5.4), providing significant information about the variability in varietal response that can be explained by varietal interaction with the MSV disease. Although UAV-derived multispectral imageries have limited spectral range and resolution, they offer robust spatial and temporal resolutions that allow variation associated with different varieties to be quantified. Maize varieties are evaluated for disease resistance to select appropriate varieties for the target production environment, to address global food demand and responding to changing climate conditions. Undoubtedly, the continuing climate changes are threatening the currently vulnerable global food security in a number of ways, as well as exacerbating major crop diseases and creating weather conditions conducive for the emergence of new

devastating diseases in major food-producing regions. Therefore, the call for intensified crop breeding efforts and the need to bring phenotyping up to speed with genomics by harnessing the power of computing, robotics, machine learning (ML), artificial intelligence, and image analysis is urgent, if we hope to meet the global food demand to feed 10 billion people by 2050.

5.4.1 Comparison of UAV-derived data and ground truth measurements

There was generally strong correlations between UAV-derived imagery and ground-based MSV measurements in this study, suggesting the value of UAV-derived data in plant phenotyping. These are encouraging results given the bottlenecks experienced in manual phenotyping, especially in plant breeding where screening of a large number varieties is needed before suitable ones are selected for advancement, release, and commercialization. Our results agree with Garcia-Ruiz *et al.* (2016) who found significant correlation between UAV-based data and the ground-truth measurements for detection of Huanglongbing (Citrus Greening) disease in citrus trees. Jarolmasjed *et al.* (2019) compared UAV-derived multispectral imaging data and found significant correlation with ground-truth disease rating of fire blight disease (*Erwinia amylovora*) in apples. Similarly, Mahlein *et al.* (2013) also reported a significant agreement ($R^2 = 0.89$) between NDVI and ground-truth leaf disease severity with a classification accuracy of 80% in sugarbeet *Cercospora* leaf spot. Jansen *et al.* (2014), using noninvasive spectral phenotyping to screen *Cercospora* disease resistance in sugar beet, similarly established significant correlations between spectral data and ground-truth scores confirming the potential use of remotely sensed data in disease resistance phenotyping.

However, most of these studies were based on snapshot (single phenological stage) spectral data collection. Our approach in this study was based on multi-temporal spectral data. For example, Garcia-Ruiz *et al.* (2012) recommended that future work should study temporal effects in aerial remote sensing of plant diseases. Thus, using multi-temporal data, we identified not only the optimal bands and indices, but also the ideal growth stage for accurate varietal phenotyping. The results demonstrated that VIs measured at vegetative stage are the most important for classification of maize varietal response to MSV. The MSV disease symptoms on a susceptible variety result in changes in color, size and shape. Our results show

116

that these morpho-physical changes can be measured accurately using spectral data at the vegetative stage. Furthermore, measurements after flowering could suffer from masking effects by the flowers (tassels) and old senescing leaves at midgrain filling.

5.4.2 RF classification performance using spectral bands and VIs

The results of this study show that UAV-derived VIs produced plausible varietal classification and majority of selected important variables were VIs compared to spectral bands (Figure 5.9). This agrees with previous studies, for example, Chemura *et al*. (2016) who found vegetation indices to perform better than spectral bands in discriminating coffee (*Coffea arabica*) leaf rust (*Hemileia vastarix*) using RF. Furthermore, the overall classification accuracy results obtained in this study using UAV-derived multispectral VIs are comparable to similar studies. For example, Garcia-Ruiz *et al*. (2013), using UAV-based multispectral data from six bands and seven indices for classification and identification of citrus greening disease, obtained accuracies ranging from 62 – 82% using linear discriminant analysis and between 63 and 85% using support vector machines. As indicated above, our study further demonstrates that crop phenological stage is critical when assessing varietal variation in crop phenotyping using UAV remotely sensed data. Most of the selected variables were measured at vegetative stage (Figure 5.9). This is important in field-based high-throughput plant phenotyping for characterizing maize varieties at multiple scales, and at different levels of resolution and dimensionality using remote sensing. Thus, aerial imaging using UAVs can offer the plant breeding, research and remote sensing community the ability to quickly record high-temporal and spatial-resolution data for maize varietal analysis and allow rapid, cost-effective and comprehensive data-driven variety selection and release in plant breeding programs. Robust phenotyping is critical to plant breeding because it forms the basis for selection of new varieties. However, UAV do not provide a substitute for the breeder's eye, but augment the effort and inform better phenotype-based selections (Hickey *et al*., 2019). The advantage of the UAV-based imaging data is the high-throughput capability and ability to measure multiple traits instantaneously (Andrade-Sanchez *et al*., 2014; Crain *et al*., 2016). Furthermore, UAV-based phenotyping does not suffer from low repeatability associated with manual records (Condorelli et al., 2018). Thus, UAVs eliminate subjectivity and reduce labor costs, spatial singularity, and fatigue associated with manual methods (Chemura *et al*., 2016; Bock

et al., 2010). Additionally, the naked eye may not be able to identify physiological/metabolic differences caused by different stresses (Masuka *et al.*, 2016), which can be possible with imaging tools (Barbagallo *et al.*, 2010). For example, Nutter *et al.* (1993) found improved precision in characterizing bent grass dollar spot (*Agrostis palustris* Huds.) using spectral data compared to a visual scoring method. Condorelli *et al.* (2018) reported higher repeatability when screening drought-adaptive traits in wheat using UAV phenotyping methods compared to ground-based methods.

5.4.3 Variable optimization effect on RF algorithm classification

In this study, RF successfully ranked each variable importance both UAV bands and VIs on the classification output (Figures 5.8 and 5.9), providing an insight into which UAV-derived bands and VIs are critical in the classification process using our data. The classification improved by 13.3%, when optimized variables were used indicating that variable importance is efficient and improves RF modelling. There are various reasons why variable optimization achieves better classification results in comparison to using all available variables. For example, Chemura *et al.* (2016) reasoned that multispectral sensors are meant for multiple purposes that range from water, agricultural, forestry and urban applications, hence just a limited number of parameters may be useful for the intended purpose. Furthermore, several variables maybe correlated or may not provide useful information, and these are dropped in the classification and modeling process. The removal of these redundant variables enables the model to achieve better results, agreeing with studies by Pal and Foody (2010); Saeys *et al.* (2007) and Chemura *et al.* (2016).

Machine learning algorithms classification accuracy is affected by training data quality, sample size, user-specified parameters (Huang *et al.*, 2002). In this study, the sample size was relatively small (n = 75), split randomly into training (70%) and validation (30%), and a robust RF model suitable for such scenarios was used, consistent with recommendation by Maxwell *et al.* (2018). In parametric maximum likelihood classifiers, the rule of thumb requires that the number of training samples be at least 10 times the number of variables (Swain, 1978). However, for ML classifiers, literature is silent on the size of the training sample (Maxwell *et al.*, 2018). Huang *et al.* (2002) posit that in ML, the size of the training sample may depend on

the algorithm used and number of input variables. On the other hand Lu and Weng (2007) and Li *et al*. (2014) recommended a large training data set regardless of algorithm used. Indeed, Huang *et al*. (2002) showed that increased training sample size gave higher accuracy. However, in practice, there is a need to balance the size, quality, cost, and the limited time available. RF has been found to be less sensitive to training sample size compared to single decision trees methods (Ghimire *et al*., 2012; Rodríguez-Galiano *et al*., 2012), and has proved to be appropriate for small samples in disease classification in coffee leaf rust (Chemura *et al*., 2016), in *Sirex noctilio* infestation in pine trees (Ismail and Mutanga, 2010), and classification of alfalfa (14 training samples) and oats (with only 5 training samples) (Maxwell *et al*., 2018).

5.4.4 The utility of UAV-based multispectral data in high-throughput phenotyping

Most of the recent studies that systematically attempt to validate spectral indices in plant phenotyping at field scale are based on proximal measurements (Chemura *et al*., 2016; Tattaris *et al*., 2016). However, proximal sensing is associated with the challenges eluded to above. It is difficult to use when fields are under irrigation or pesticides applications, and not practical for rapid evaluation of multiple varieties at scale and high temporal resolution in breeding programs (Chapman *et al*., 2014; Araus and Cairns, 2014). Furthermore, proximal remotely sensed data can fail precision test for high-throughput because of fluctuations in weather conditions in between measurements (i.e. from start to finish), which may take one to several hours where large numbers of breeding plots are involved (Tataris *et al*., 2016). Extended time taken in manual scoring introduces variation due to phenological changes, environmental conditions, and recorder fatigue thereby affecting repeatability and leading to inaccurate data and even unjustified conclusions (Condorelli *et al*., 2018; Naik *et al*., 2017). Speed is therefore essential in achieving high precision in high-throughput phenotyping. Although this study did not compare the time difference between manual scoring and UAV-based phenotyping, researchers have found UAV-based phenotyping to be 10 times faster than manual scoring (Duddu *et al*., 2019). Similarly, Guan and Nutter (2003) found remote sensing to be 15 times faster in estimating alfalfa leaf disease. Therefore, UAV offers real-time and fast crop phenotyping and will reduce dependence on time consuming and resource-intensive manual phenotyping in plant breeding and varietal selection, leading to speeding up breeding and selection processes.

The opportunities presented by UAV-derived data have to take into account the practical limitations imposed by field conditions to the applications of the technology where a complex of different diseases are present in the same field or area of interest. The UAV-derived spectral bands and indices applied in this study are not disease-specific (to the best of knowledge), and therefore can only be useful in quantifying different levels of infestation or damage when a single disease affects the crop with no ability to distinguish between different types of diseases. This makes the current UAV-derived spectral data relevant in phenotyping of disease with a prior knowledge of the type of disease that exists in the target area of interest. Studies into development of disease-specific VIs have been reported (Mahlein *et al*., 2013; Rumpf *et al*., 2010; Mahlein *et al*., 2010). However, this is an area that needs further exploration. In addition, although VIs derived from multispectral data are informative, they utilize less than 1% of available spectra (Pauli *et al*., 2016), and as such may lack detail compared to, for example, hyperspectral data. Therefore, further investigations are necessary to refine the use of UAV-derived data in high-throughput crop phenotyping. It is also noteworthy to mention that the study only used one ML algorithm (RF), yet there several other classifiers, which can be used.

5.4.5 Leveraging high-throughput phenotyping to fast-track crop improvement under changing climate conditions

MSV disease can be controlled using systemic insecticides that control the vector through spraying or treatment of seed. However, spraying and use of seed treatments against MSV are expensive and beyond the reach of most of the resource-poor farmers. Furthermore, spraying and seed treatment options offer only temporary protection when disease pressure is severe. The development and cultivation of varieties tolerant or resistant to MSV is arguably the most cost-effective and climate-smart way of preventing MSV epidemics and protecting farmers' livelihoods. To breed for resistance, breeders evaluate large numbers of lines or varieties to select suitable ones for commercialization. However, as previously alluded to, rapid and accurate phenotyping of traits associated with grain yield is presently creating serious bottlenecks (Araus and Cairns, 2014; Furbank and Tester, 2011). Robust phenotyping is critical in plant breeding programs because it forms the basis for new variety selection. In this study, our method has demonstrated the utility of image-based high-throughput phenotyping to

relieve the breeding community of phenotyping bottlenecks. Image-based high-throughput phenotyping technology will help accelerate crop breeding in the face of changing climate conditions and associated new challenges. This will be achieved by screening large numbers of varieties for multiple traits with higher accuracy and at reduced costs (Mahlein, 2016). In addition, high-throughput image-based phenotyping will enable the evaluation of physiological/metabolic differences caused by different stresses (Masuka *et al*., 2016), which may not be possible with the naked eye but possible with imaging tools (Barbagallo *et al*., 2003; Rutkoski *et al*., 2016). This will help broaden the genetic variation in the germplasm pool if such traits are accumulated in the breeding pipeline. Furthermore, high-throughput phenotyping data can be combined with genomic data to further improve genetic gain (Rutkoski *et al*., 2016; Crain *et al*., 2018; Juliana *et al*., 2018). The key to the successful application of image-based high-throughput plant phenotyping for diseases and other stresses lies in our ability to develop reproducible protocols that are user-friendly, including image-based data retrieval, analysis, and interpretation. This will increase crop genetic improvement efficiency and our ability to satisfy future food requirements, especially as climate change accelerates.

5.5 Conclusion

This study assessed the utility of UAV-derived multispectral data with RF algorithm to classify different maize varieties under artificial MSV inoculation. The results showed that UAV-based multispectral data combined with advanced classifier RF analysis can be useful in field-based high-throughput maize phenotyping. Therefore, we conclude the following.

1. UAV-based remotely sensed data provides plausible accuracy, thereby offering a step-change towards data availability and turn-around time in varietal analysis for quick and robust high-throughput plant phenotyping in maize breeding and variety evaluation programs. To address the vagaries brought by climate change and meet global food security. Specifically, the study has demonstrated that VIs measured at vegetative stage are the most important for classification of maize varieties under artificial MSV inoculation using UAVs.

2. UAV-derived remotely sensed data correlate well with ground-truth measurements, confirming the utility of UAV approach in field-based high-throughput phenotyping in

breeding programs, where final varietal selection must be based on extensive screening of multiple genotypes. This will reduce selection bottlenecks caused by manual phenotyping and offers decision support tools for large-scale varietal screening.

3. Variable optimization improves classification accuracy when compared to the use of variables without optimization. Thus, RF classifier is a robust algorithm capable of determining the depth of variable importance and their rankings using our data.

4. Image-based high-throughput phenotyping can relieve the breeding community of phenotyping bottlenecks usually experienced when evaluating large populations of genotypes in order to accelerate crop breeding and selection addressing multiple stresses associated with climate change.

The study shows that cost-effective UAV-derived multispectral data is capable of classifying maize varieties affected by MSV with good accuracy, and therefore can complement and eventually replace visual ratings, especially for large-scale canopy-level measurements when multiple genotypes are evaluated in plant breeding. However, current VIs are not disease-specific and therefore can only be useful in different levels of infestation or damage due to a singly present disease with no ability to distinguish between complex types of diseases. This makes the current UAV-derived spectral data relevant in phenotyping of disease with a prior knowledge of the type of disease that exists in the target area of interest. Three research gaps have been identified for further inquiry: (i) comparison of multiple ML algorithms to identify the best performing classier(s); (ii) evaluation of whether UAVs mounted with hyperspectral high-resolution cameras improves detection and classification accuracies; and (iii) development of disease-specific VIs.

CHAPTER 6: GRAIN YIELD MODELLING USING UAV-DERIVED DATA

This Chapter is based on:

Chivasa W, Mutanga, O., Biradar C.M. **2020**. UAV-based high throughput phenotyping to increase prediction and selection accuracy in maize varieties under artificial MSV inoculation. *Computers and Electronics in Agriculture* (**in review).**

Early grain filling stage

Midgrain filling stage

Abstract

The increased usage of unmanned aerial vehicles' (UAV) remotely sensed data in crop evaluation is revolutionizing the field of plant phenotyping. This study was conducted to (1) develop protocol to predict maize streak virus (MSV) and grain yield using UAV-derived multispectral data; and (2) identify the suitable predictor variables (reflectance or indices) and ideal phenological stages for MSV and grain yield prediction. The study evaluated 25 maize varieties grown under artificial MSV inoculation. Manual scoring and multispectral imaging measurements were performed at midvegetative, flowering and midgrain filling stages. UAV-derived data were acquired in the multispectral bands of Green ($0.53 - 0.57\mu m$), Red ($0.64 - 0.68\mu m$), Red-edge ($0.73 - 0.74\mu m$) and Near-infrared ($0.77 - 0.81\mu m$). Ground-truth scoring of MSV infection was done using a 1 (resistant) to 9 (susceptible) scale. We performed accurate corrections of UAV-derived imagery and extracted multispectral data. Eight vegetation indices (VIs) were determined for each variety: NDVI (normalized difference vegetation index), $NDVI_{red-edge}$ (red-edge NDVI), GNDVI (green normalized difference vegetation index), SR (simple ratio), CI_{green} (green chlorophyll index), $CI_{red-edge}$ (red-edge chlorophyll index), SAVI (soil-adjusted vegetation index) and OSAVI (optimized SAVI). Finally, predictions of MSV and grain yield were performed with 36 models using multiple regression, decision trees and linear regression. The relevant statistics considered in MSV prediction were the Akaike Criterion corrected by small sample (AICC), the average square error in the validation set (ASE-Test) and the predicted residual sum of squares in the validation data set (CVEXPRESS). There were no significant differences ($p > 0.05$) between spectral data or indices in predicting MSV. However, for indices, the variability between models was larger than for spectral data, especially for the ASE-Test statistic. Frequently selected variables for MSV prediction were Green band at vegetative (61.5%), Red band at vegetative (68.4%) and flowering (80.4%), and GNDVI at midvegetative (88.7%). However, the best MSV predictors were GNDVI (r = 0.84; RMSE = 0.85,), CI_{green} (r = 0.83; RMSE = 0.86) and Red band (r = 0.77; RMSE = 0.99) measured at midvegetative stage. For grain yield prediction, six out of 36 models were selected as ideal for predicting maize grain yield: RF-REF-NIRF (r = 0.69; RMSE = 0.65); NDVIREG-GNDVIG (r = 0.74; RMSE = 0.56); RV-NIRV (r = 0.84; RMSE = 0.37); and the tree with the largest correlations are RV-NIRV-RF (r = 0.86; RMSE = 0.32); GNDVIV-OSAVIV (r = 0.84; RMSE = 0.36); GV-RV-NIRV (r = 0.84; RMSE = 0.35); the last two of which were at midvegetative stage. From these

results we conclude that UAV-based multispectral remote sensing is a reliable tool for phenotyping MSV disease and grain yield prediction, and midvegetative appear to be the most ideal phenological stage for MSV and grain yield prediction.

Keywords: maize; UAV multispectral data; remote sensing; maize streak virus; high-throughput phenotyping; yield prediction.

6.1 Introduction

Global food requirement is projected to double current demand by 2050 due to population and socio-economic growth (Ray *et al.*, 2012). Meeting this demand, particularly in developing countries requires doubling current grain production of major food crops like maize, wheat and rice by 2050 (Tilman *et al.*, 2011; Tubiello, 2012; Valin *et al.*, 2013). This requires genetic gain on grain yield of up to a 2.4% per year on non-compounding basis to meet global demand by 2050 (Ray *et al.*, 2013). However, the growth in human population that is projected to be 10 billion by 2050 (Ray *et al.*, 2012; Ray *et al.*, 2013) coupled with the effects of climate change on crop diseases (Luo *et al.*, 1998; Coakley *et al.*, 1999; Garrett *et al.*, 2006) poses some of the greatest challenges to achieving global food security. Because of a changing climate and its effects on pathogen and vector appearance and distribution, we urgently need to accelerate crop genetic improvement as a mitigation measure. This can be achieved by combining genomics, rapid cycling and field-based high-throughput plant phenotyping. Fortunately, plant breeders are now able to generate large numbers of new varieties for selection due to access to a plethora of cutting-edge technologies because of advances in genomics, doubled haploid technology, rapid cycling and molecular breeding (Phillips *et al.*, 2010; Poland, 2015). However, phenotyping of traits associated with grain yield is presently creating a serious bottleneck (Furbank and Tester, 2011; Araus and Cairns, 2014). Robust phenotyping is critical in crop improvement programs because it forms the basis for selecting new variety with high yield and improved resistance to multiple stresses.

The previous two decades have seen tremendous innovations in genomics, with significant reduction in costs while throughput and accuracy continued to improve (Tung *et al.*, 2010; Elshire *et al.*, 2011). Associated with the reduction in sequencing cost is the increasing usage of high-resolution genotyping in crop breeding, previously overlooked by the genomics

community (Bachlava *et al.*, 2012; Ferguson *et al.*, 2011; Hyten *et al.*, 2010). With the increase in low cost genomic data for major food crops, a major focus in variety evaluation is shifting towards addressing the scarcity of high-quality phenotypic data (Cobb *et al.*, 2013). Currently, phenotyping has become the major operational bottleneck in plant breeding. Compared to genotyping that is now highly automated and fundamentally uniform across crops, high-throughput phenotyping remains a cottage industry, crop-specific, laborious, and certainly environmentally-sensitive (Cobb *et al.*, 2013). Furthermore, whereas variation in sequence is finite in theory, and consequently all sequence variants can possibly be found for a specified crop, there is no prospect that the phenomes will ever be completely characterized (Houle *et al.*, 2010). The phenomes of crops are dynamic and respond to a multi-dimensional set of internal and external signals. Thus, phenotypic data can be seen as a dynamic set of information that changes throughout the crop growing season as a result of prevailing environmental conditions. As the phenotyping science evolves, attention is increasingly directed towards generating accurate and precise information at reasonable costs. Reduction in phenotyping costs even with slight precision decrease will maximize genetic gains through efficient utilization of financial resources that can be used to increase the number of varieties under evaluation, investment in doubled haploid technologies, among others. In this study we explore the use of UAV-based multispectral image-based high-throughput phenotyping to interrogate the complex tripartite interaction involving genotype × phenotype × pathogen (environment), as well as to develop prediction models based on spectral data in maize under artificial MSV inoculation. Image-based high-throughput phenotyping allows imaging of thousands of plots within a few hours and doing so at a very high level of accuracy and lower costs (Fahlgren *et al.*, 2015).

Maize is the preferred staple food crop in Africa, which contributes more than 50% of the daily calorie requirements and occupies over 27 million hectares in Sub-Saharan Africa (SSA) (FAO, 2010). However, maize production is being affected by many biotic and abiotic stresses. These multiple stresses impact on agriculture by reducing quality and quantity of products, posing a serious threat to food security and safety (Savary *et al.*, 2012; 2017). For example, maize streak virus (MSV) continues to be one of the major maize diseases (Bock *et al.*, 1974; Fajemisin *et al.*, 1984) found throughout SSA that threatens food security (Bosque-Pérez, 2000; Martin and Shepherd, 2009). The disease is caused by maize streak virus (Bock *et al.*, 1974), a geminivirus

(Bock *et al*., 1977). MSV is obligately transmitted by leafhoppers (*Cicadulina mbila* Naudé and *C. Storeyi*) (Storey, 1924; 1928; Webb, 1987) causing extensive damage to susceptible maize varieties in SSA (Shepherd *et al*., 2010). This is exacerbated by climate change, for example, rising temperatures promote the development of leafhopper populations (Jourdan-Ruf *et al*., 1995). Climate change predictions have indicated an overall trend of increased precipitation in East Africa (EA), with a concurrent decrease in Southern Africa (SA) (IPCC, 2007). Such increase in precipitation produces a conducive temporal overlap of seasons, providing a 'greenbridge' that allows leafhoppers to survive throughout the year (Stanley *et al*., 1999; Kloppers, 2005). On the other hand, less precipitation will cause droughts, and MSV disease epidemics have been shown to be associated with droughts followed by erratic precipitation at the beginning of the season (Efron *et al*., 1989), as occurred in West Africa in the 1983 and 1984 seasons (Rossel and Thottappilly, 1985), as well as in Kenya in 1988-89 (Njuguna *et al*., 1990). To offset future yield losses due climate change induced diseases, maize breeding for disease resistance is a priority.

MSV infected maize leaves show chlorotic streaks because of chloroplast destruction (Storey, 1925; Engelbrecht, 1982). In severe infections, susceptible varieties become totally chlorotic, leading to necrosis causing pre-flowering death and complete yield losses (Guthrie, 1978). In addition, MSV infections also result in stunted growth as a result of reduced carbohydrate production because of impairment of photosynthesis (Shepherd *et al*., 2010). Reduction in chlorophyll (photosynthetic capacity) and water (stomatal conductance) content have been linked to grain yield reduction in crops (Araus *et al*., 2002; Fischer *et al*., 1998). Systemic insecticides can be used to control leafhoppers, either through spraying or seed treatment. However, the probability of pesticide resistance and the possible negative impacts on the environment of these interventions underscore the urgent need to breed resistant varieties. Furthermore, pesticides options are expensive and beyond the reach of many resource poor farmers, who are the majority of maize producers in SSA. The severity of MSV disease, defined as the proportion of the maize leaves showing symptoms (Madden *et al*., 2007), is an important quantitative variable for evaluating new varieties in plant breeding. The disease can be quantified visually by giving a severity value/score to the symptoms as seen by the naked human eye. Recently, sensors are being deployed to quantify disease or stress signals based on remote sensing (Mahlein, 2016; Bock *et al*., 2010). However, most of the spectral sensor-

based disease phenotyping studies in field crops have been conducted in wheat head blight (*Fusarium graminearum*) and yellow rust (*Puccinia striiformis* f. sp. *tritici*) (Bravo *et al*., 2003; Huang *et al*., 2007), net blotch (*Pyrenophora teres*), brown rust (*Puccinia hordei*) and powdery mildew (*Blumeria graminis hordei*) in barley (Kuska *et al*., 2015; Wahabzada *et al*., 2015), and orange rust (*Puccinia kuehnii*) in sugar cane (Apan *et al*., 2004).

MSV disease symptoms on a susceptible variety result in changes in color, size and shape, therefore, these morpho-physical changes can be measured using multispectral imaging sensors (Bock *et al*., 2010; Bock and Nutter Jr, 2011; Barbedo, 2013; 2016). Image-based high-throughput plant phenotyping has advantages over visual phenotyping (Mahlein, 2016), because it is repeatable, reproducible, very accurate and scalable (Martin and Rybicki, 1998; Bock *et al*., 2008; Barbedo, 2014; Clément *et al*., 2015; Bock *et al*., 2020). Visual scoring by trained experts can provide accurate estimates but this is often very slow and expensive, and throughput is very low. Scalability using manual scoring is limited to plot level. On the other hand, UAV-based multispectral imaging offers high-throughput at much lower cost and fulfils the needs of high-throughput phenotyping at field scale, hitherto a major bottleneck in plant breeding (Cobb *et al*., 2013; Mutka and Bart, 2015; Simko *et al*., 2017). Recent advances in remote sensing tools, especially unmanned aerial vehicles (UAVs) is promising to bring phenotyping up to speed with genomics by harnessing the power of computing, robotics, machine learning, artificial intelligence and image analysis (Furbank and Tester, 2011). The advances in the use of automated image-based plant phenotyping systems afford the plant breeding community rapid and efficient screening of large numbers of varieties with significant accuracy (Araus *et al*., 2018; Hickey *et al*., 2019). UAV-derived data provide measurements that are close to reality or actual, commonly referred to as ground truth in remote sensing (Bock *et al*., 2020). Accurate phenotyping is crucial to understand yield loss relationships, and germplasm phenotypes are rated appropriately. UAVs are easy to operate and offer high spatio-temporal resolution and quick coverage (Geipel *et al*., 2016; Haghighattalab *et al*., 2017). Potentially, the throughput of UAVs is intrinsically higher compared to ground-based approaches due to the wider viewing angle, greater speed, non-invasive and are suitable in all soil conditions that may prevent ground traffic (Liebisch *et al*., 2012).

Remotely sensed data can be useful as selection decision tools due to their highly significant correlations with grain yield (Weber *et al*., 2012). For instance, Weber *et al*. (2012) assessed 300 maize varieties using hyperspectral data and reported a selection efficiency of 88 and 68%, using spectral reflectance measured at leaf- and canopy-level, respectively. Osborne *et al*. (2002) combined stepwise regressions and six wavelengths and managed to explain over 95% of grain yield variation in maize grown under optimum conditions. Most of the studies on maize yield prediction have been done at large-scale using satellite sensors (Báez-González *et al*., 2002; Battude *et al*., 2016) and using proximal sensing (Osborne *et al*., 2002; Weber *et al*., 2012). However, satellite sensors lack the plot-level precision required in data collection in plant breeding for variety analysis due to their low spectral and temporal resolution. On the other hand, proximal sensing is labor-intensive, of limited scalability and unsuitable when fields are too wet to allow traffic movement (Tattaris *et al*., 2016). Options from manned aerial, high spectral resolution remote sensing platforms are costly and are limited by operational complexity for application in small breeding plots (Hoffer *et al*., 2014; Jimenez-Berni *et al*., 2009). The ability to predict maize grain yield under MSV disease stress can be useful for selecting superior lines for crossing at flowering. This will increase selection gain and reduce the costs of phenotyping in plant breeding.

Despite recent advances in sensing systems, no significant advances have been made, to the best of our knowledge, in spectral-based MSV high-throughput phenotyping and yield prediction at plot level in maize using UAV-based imaging data. Yet the use of UAVs is becoming very important in supporting and accelerating breeding progress for generating data from increasingly large numbers of breeding plots. Enabling near real-time field-based yield predictions using UAV-derived imaging data is crucial for rapid cycling. This study explores the potential of UAV-derived multispectral data in image-based high-throughput phenotyping. The specific objectives were two-fold: to (1) develop protocol to predict MSV and grain yield using UAV-derived multispectral data; and (2) identify the suitable predictor variables (reflectance or indices) and ideal phenological stages for MSV and grain yield prediction. The additional objectives of chapter 6 are beyond what has already been established and reported in chapter 5 on MSV but reports on MSV and yield prediction using multi-temporal UAV-derived multispectral data

6.2 Material and methods

6.2.1 Study area

The research work was carried out at the Rattray Arnold Research Station (RARS) in Zimbabwe as explained in Chapter 1, section 1.6 of this thesis. RARS has also suitable facilities to run MSV inoculation experiment and offers ideal disease development conditions as shown in Chapter 5 Figure 5.1 of this thesis.

6.2.2 Field Trial Design and Management

A set of 25 varieties were grown in a 5 × 5 partially balanced alpha lattice design (as shown in Figure 5.2 in Chapter 5 of this thesis). Each plot was six rows replicated three times. The experimental area was made up of a total of 75 plots (25 varieties × 3 replications). Gross plot area was 7.5m × 4.5m (6 rows). Maize seeds were planted on the flat with a spacing of 0.5m in-row × 0.75m between rows. Four seeds were planted per station and later thinned to a final two plants per station at 21 days after sowing to attain a desired 53,333 plants ha^{-1}. Uniform management was applied to all varieties. Fertilizer was applied at a rate of 450kg ha^{-1} basal (13:26:13 – N:P:K) at planting and 450kg ha^{-1} Ammonium Nitrate (34.5% N) top dressing divided into two equal amounts of 225kg ha^{-1}, with the first half applied at early vegetative and the second at booting (pre-flowering) stage. Hand weeding and herbicides were used to keep the experimental area free of weeds.

The trial was planted on 23 November 2018. The vegetative stage of the crop was between December 2018 and January 2019. Figure 5.1 shows the monthly rainfall, heat units, maximum, minimum and mean temperatures during the crop growing period. The weather data was recorded using an advanced automatic weather station Pro (supplied by Dacom Farm Intelligence, Netherlands) that record wind direction, solar radiation, relative humidity, wind speed, temperature and rainfall,. Plant and insect growth and development depend on temperature often described as heat units (HU). HU were calculated using equation [5.1].

6.2.3 Ground truth data collection

To evaluate resistance to MSV, every plant was artificially inoculated when four leaves had fully expanded with mass reared viruliferous leafhoppers (*Cicadulina mbila* Naudé) (Rodier et al., 1995) previously fed with MSV infected maize plants. The ground truth MSV scores were taken on all 25 maize varieties in all replications. Each plot was rated using visual scoring (Figure 6.1a) for MSV at midvegetative, flowering and midgrain filling growth stages on a scale of 1 to 9. The ground truth MSV scores were taken on all 25 maize varieties in all replications. Each plot was rated for MSV using visual scoring at midvegetative, flowering and midgrain filling growth stages on a scale of 1 to 9. Grain moisture (%) and grain yield (t ha^{-1}) were measured after physiological maturity. Physiological maturity was defined as the time when 95% of the base tip of seeds on the cob turned black (commonly referred to as black layer). Grain yield (t ha^{-1}) was determined from the net plot area which comprised the 4 central rows of each plot, excluding one plant station from either end of the rows. Grain moisture content was taken using a Dickey-John high quality, instant reading moisture meter with a moisture range of 5 – 45% accurate to two decimal places. Grain yield was converted to t ha^{-1} and adjusted to an equivalent at 12.5% moisture content.

6.2.4 The UAV platform, image acquisition and processing

The imagery was acquired using a Parrot Sequoia Multispectral camera mounted on an eBee SQ UAV (manufactured by Swiss Geo Consortium Sensefly, Cheseaux-Lausanne, Switzerland) (Figure 6.1b). The UAV is a Delta Fixed Wing craft with greater speed and superior aerodynamics compared to multi-rotor crafts. It is designed strictly for agricultural purposes. The Parrot sequoia sensor is made up of 5 cameras with 4 discreet bands: Green (0.53 – 0.57μm), Red (0.64 – 0.68μm), Red-edge (0.73 – 0.74μm) and Near-infrared (0.77 – 0.81μm). The fifth sensor is a composite color capture camera (RGB). The sensor unit has a sunshine sensor with GPS, sunshine detection unit and the Inertial Measuring Unit (IMU). The GPS unit receives positional information so that the imagery produced is subsequently georeferenced. The IMU captures the attitudes of the sensor at the times of image capture (the rotations about the X, Y and Z axes). The sunshine unit captures and records the sunshine radiance value to allow for radiometric correction of the imagery. The imagery were acquired

between 10:00 to 14:00 GMT/UTC + 02:00. Figure 6.1 outlines the two methods used in data gathering, including a contrast of some aspects of each method.

MSV Disease Severity Phenotyping

Estimation   *Measurement*

(a)

Visual (scale) → **Ordinal** → **Quantitative** → **Scale**

(b)

Imaging (non-visual) → **Spectral Imaging** → **Multispectral Imaging** → **Spectral data and VIs**

Visual method	Aspect*	Imaging method
Yes	Training	Yes
No	Disease-specificity	Yes
Yes	Subjectivity	No
No	High-throughput	Yes
Medium	Technical expertise	High
Low	Cost of equipment	Low
High	Operational cost (personnel)	Low
Low	Scale (spatial coverage)	High
High	Canopy penetration	Low
Low	Operational speed	High

Figure 6.1. The major characteristics of (a) visual scoring (ground truth) and (b) multispectral UAV-based imaging system used in this study. *A comparison of visual scoring and multispectral imaging methods as used in this study in maize varieties disease severity phenotyping.

The imagery was captured using a single grid mapping pattern, with the flight plan designed to map an area in excess of the area of interest to minimize the effects of radial distortion around the periphery of the area of interest. The flight plan had the following parameters: 42.5 m altitude, with a ground sampling distance of 8 cm in the RGB and 11.5 cm in the multispectral; 75% forward overlap and 75% side overlap as per Sensefly's recommendation. The sensor parameters and spectral ranges for the Red (R), Green (G), Red-edge (RE), and Near-infrared (NIR) bands of the camera used are shown in Chapter 5 Table 5.1.

Data was collected at three phenological stages: midvegetative (pre-booting) stage; mid-flowering (when 50% of the plants had flowered); and midgrain filling. The imagery captured over the study site were stitched together in Pix4D mapper, which generates two types of

multispectral Orthomosaics: the NoAlpha and the transparent mosaics. These were generated for each band of the imagery (G, R, RE, NIR). The NoAlpha imagery was used as input into QGIS for reflectance data extraction. A shape file was created by converting a Google earth KML (Key Markup Language) file of the mapped area. The shape file was then used to clip the imagery of the mosaic to the extent of the study area. Shape files were then drawn for each of the compartments (individual plots) according to the experimental layout shown in Figure 5.2. The "Clip Multiple Layers" plugin was used to simultaneously clip each of the band images using the shapefile for each plot. Once the shapefile compartments were extracted for each shapefile, the maximum, weighted mean, minimum reflectance and their standard deviations were generated for each plot in each layer. The average reflectance for each plot was determined by considering a buffer of 50cm on all four sides of the plot to restrict the analysis to the center of the plot. Extracted reflectance data were exported into excel spreadsheet format for each of the three phenological stages. Vegetation indices were calculated from the plots' mean reflectance values.

6.2.5 Vegetation indices

For complete phenotyping, this study used reflectance values in multispectral bands corresponding to Green (0.53 – 0.57μm), Red (0.64 – 0.68μm), Red-edge (0.73 – 0.74μm) and Near-infrared (0.77 – 0.81μm) taken at the same three different phenological stages. The reflectance values were used to derive the normalized difference vegetation index (NDVI), Red-edge NDVI ($NDVI_{red-edge}$), green normalized difference vegetation index (GNDVI), Simple Ratio (SR), green Chlorophyll Index (CI_{green}) and Red-edge Chlorophyll Index ($CI_{red-edge}$) as shown in Chapter 5 Table 5.2. In addition, the soil-adjusted vegetation index (SAVI) and optimized SAVI (OSAVI) were calculated using equations [6.1] and [6.2] according to Huete (1988) and Rondeaux et al. (1996), respectively.

$$SAVI = \frac{NIR - R}{NIR + R + 0.5)(1 + 0.5)} \times (1.0.5) \qquad [6.1]$$

$$SAVI = \frac{NIR - R}{NIR + R + 0.16)} \qquad [6.2]$$

6.2.6 Statistical Analysis

Data was initially analyzed with a standard linear mixed model for a block design including variety as a random effect to estimate variance components and heritability of the different traits:

$$y_i = \mu + \beta_i + g_j + \varepsilon_{ij} \qquad\qquad [6.3]$$

Where, y_i is the response in the ith block with the jth variety, μ is the overall mean, β_i is the effect of the ith block, g_j is the effect of the jth variety, $g_j \sim N(0, \sigma_g^2)$, ε_{ij} is the experimental error in the ith block with the jth variety, $\varepsilon_{ij} \sim N(0, \sigma_a^2)$

Broad sense heritability (H^2), a measure of repeatability and precision, which is linked to higher predictive ability for secondary traits associated with grain yield (Crain *et al.*, 2017), was computed as follows:

$$H^2 = \frac{\sigma_g^2}{\sigma_g^2 + \dfrac{\sigma_\varepsilon^2}{r}} \qquad\qquad [6.4]$$

Where the variances are defined in equation [6.3] and r is the number of replicates.

Residual of the model were analyzed to identify outliers and normality. Good predictors should have stability across experiments, low coefficient of variation and high heritability, and preferably be genetically correlated with the trait of interest to perform indirect selection, therefore phenotypic and genotypic correlation between predictors and response variables (MSV and grain yield) were calculated.

A correlation matrix was constructed at different phenological stages to identify variables that are correlated. Highly correlated variables indicate that the variable is completely predictable using the other variables, which means it could be dropped without affecting model accuracy. Variable redundancy and multicollinearity increase modelling complexity and affects regression performance. Finding optimal subset of variables from the input reduces noise or select uncorrelated variables thereby improving performance of the prediction model and reduce runtime. Principal component analysis (PCA) based on phenotypic correlation were used to understand and describe data structure and general relationships.

Predictive models

Raw data was used to build predictive models. In plant breeding, breeders are most interested to classify genotypes into resistant or susceptible than considering MSV score directly. However, certain varieties may fall in between the two classes. Therefore, the visual MSV scale was divided into three categories: resistant (1 – 3.5), moderately tolerant (3.5 – 5.5), and susceptible (5.5 – 9) for analysis. Predictive variables were grouped in two groups: reflectance and indices data measured or derived at midvegetative (V), flowering (F), and grain filling (GF). Because MSV was measured at the same time that images were taken, predictive models considered as predictive variables those that were measured before or at the same time in which MSV was measured. For MSV at vegetative stage, only predictive variables measured at vegetative stage were considered, for MSV at flowering, vegetative and flowering predictive variables were used, and for MSV at grain filling, all predictive variables were considered. Because MSV measurements at the different stages were highly correlated (R = 0.88 – 0.95), we also considered average MSV in prediction. This measure is equivalent to the area under the disease progress curve (AUDPC) if days between measurements are equal. Three methods were used to predict MSV and grain yield using UAV-derived imaging data: multiple regression, decision tree, and linear regression with field calibration. Multiple regression method was selected because it is simple and allows predictor selection. However, inclusion of interaction effects is not easy, therefore decision tree was used as a second method that even when it does not include direct interactions between predictors, it uses predictors one after the other in data subsets. Finally, a third linear regression method with field calibration was considered because it can be applied in any situation and it is not necessary to define an *a priori* model since the model is calibrated for each trial.

Multiple regression model

Considering different combinations of the four response variables, that is, MSV at three vegetative stages and the average of them, the two sets of predictive variables (spectral data and indices), and the three vegetative stages at which these were taken, thirty-six different models were used. For example, for MSV at vegetative stage, only spectral data and indices measured at the same stage were considered as predictive variables, while for MSV average

we considered as predictors, different combinations of measures at the three stages. Three models used predictors variables measured at only one vegetative stage. The other models used combination of two vegetative stages data. Finally, one model combined predictors from the three vegetative stages. Half of the models use spectral data to do the prediction and the other half used indices. PROC GLMSELECT in SAS V9.4 was used to estimate and to select predictive variables, and the best predictive models. Selection of predictive variables was performed based on the LASSO (least absolute shrinkage and select operator) method and for the selection model we used the predicted residual sum of squares with external cross validation (CVEX). To measure the model precision, corrected Akaike's information criterion for small sample (Hurvich and Tsai, 1989), the average square error in the validation set (ASETest), and the predicted residual sum of squares in the validation data set (CVEXPRESS) were used. The importance of each variable was based on the frequency with which that predictive variable was included in the model for the 50 cross-validation (CV) sets. Because the main interest is to classify varieties in the three categories, for the best models identified in previous analyses, predicted values in the 1 – 9 scale were transformed into the three categories scale (resistant (1-3.5), moderately resistant (3.5-5.5) and susceptible (5.5-9) as explained in data collection section. Models were evaluated using the polychoric correlation and percentage of matching between the predicted and observed values in this scale.

The LASSO method obtains parameter estimations minimizing the residual sum of square penalized by the absolute size of the parameters, $\min \lVert \mathbf{y}_i - \mathbf{X}_i\boldsymbol{\beta} \rVert^2$ with the restriction that $\sum_{j=1}^{m} \lvert \beta_j \rvert \le t$. The formulas used for the evaluation statistics are:

$$AICC = n\log\left(\frac{SSE}{n}\right) + 2p + 2n + 2 \qquad [6.5]$$

Where n is the number of observations, p the number of parameters and SSE is the error sum of squares. The average square error (ASE) in the validation was computed using equation [6.6]:

$$ASE = \frac{SSE}{n} \qquad [6.6]$$

For cross validation, the predicted residual sum of squares (PRESS) statistics was calculated as follows:

$$PRESS = \sum_{i=1}^{n} \frac{r_i^2}{\left(1 - h_i\right)^2}$$ [6.7]

Where r_i is the residual at observation i and h_i the leverage of observation i, $h_i = \mathbf{x}_i \left(\mathbf{X'X}\right)^{-} \mathbf{x}_i'$.

The PRESS statistics considered the residual at each observation, weighted by the position of the point in the space of the predictor variables because it is known that predictions in the edge of the space are less precise.

Decision Tree

Decision Tree regression was fitted using PROC HPSPLIT of SAS V 9.4. Because the method is intrinsically a variable selection method, only one model for each response variables was used, i.e., one per stage in which MSV was measured, the average across stages, and grain yield. All predictive variables were included simultaneously. To fit the models, the maximum depth of the trees was fixed at 8 and the minimum leaf size at 3. Tree pruning was performed considering the cost complexity algorithm. Variable importance was calculated to identify best predictors.

Linear regression with field data calibration

In this approach to predict MSV, besides the indirect measurements (image data), nine plots were used for calibration, that is, one plot for each one of the three levels of response to infection (resistant, moderately resistant, and susceptible) per replicate. Image data or indices are obtained or calculated as usual for all the plots. The nine calibration plots are used to obtain a linear regression model that is used to predict the other plots. We mimic this procedure by simulation, considering each combination response to infection-replicate as strata, one plot for each stratum was selected by random to have the nine calibration plots. This procedure was replicated two hundred times and a linear regression model was estimated for each predictive variable to predict MSV at different stages and the average across stages. The remaining 66 of the 75 plots were predicted following this procedure and

the square root of the mean square error (RMSE) and the Pearson correlation were used to measure predictive accuracy.

The $RMSE = \sqrt{\dfrac{SSE}{n-p}}$ is comparable with the ASE except for the denominator in the RMSE considers the number of parameter p. Pearson correlation was calculated using equation [6.8] as shown in cross validation section below.

6.2.6.1 Cross Validation

To test the accuracy in prediction, we followed a random cross validation (CV) procedure. The data set was divided into a training and validation subset with 12 varieties in the training and 13 varieties in the validation set. We used a stratified selection procedure as described in Table 6.1, and the procedure was repeated 50 times. Varieties were assigned to strata according to the average of the scale level of MSV. The same 50 cross validation sets were used in all the models.

Table 6.1. Number of varieties by MSV susceptibility and in CV subsets

Strata	Total number of varieties	Training Set	Validation Set	
			n	%
Susceptible	7	3	4	30.8
Moderately resistant	12	7	5	38.5
Resistant	6	2	4	30.8

The correlation coefficient (*r*) and *RMSE* of cross validation were used as metrics to evaluate the model suitability and how well the models predict new data. Equations [6.7] and [6.8] were used to calculate *r* and *RMSE*, respectively:

$$r_{xy} = \frac{Cov\,(x,y)}{\sigma_x \sigma_y} \qquad\qquad [6.8]$$

Where: r_{xy} = correlation coefficient; Cov (*x,y*) = covariance of variables *x* and *y*; σ_x = standard deviation of *x*; σ_y = standard deviation of *y*.

$$RMSE = \sqrt{\frac{1}{N}\sum_{i=1}^{N}(y_i - \hat{y})^2}$$

[6.9]

Where N = sample size, y_i = observed values, $\hat{y}_i$ = predicted values.

6.3 Results

6.3.1 Data structure

The heritability as well as phenotypic and genotypic correlations for MSV and grain yield are high. The grain yield is negatively affected by the presence of MSV. Negative correlations are at least R = -0.82 for phenotypic correlation and R = -0.92 for genotypic correlation. Thus, most of the potential predictors showed high phenotypic and genotypic correlations with MSV and GY. However, there are five predictors that showed low phenotypic correlations below 0.6 in absolute terms with both response variables (MSV and grain yield). These are NDVIRE (R = 0.01 – 0.15) at vegetative and flowering stages, CIRE (R = 0.01 – 0.20) at vegetative and flowering stages, Green band (R = 0.34 – 0.45) at flowering, Red-edge (R = 0.18 – 0.46) at all three phenological stages and NIR (R = 0.52 – 0.58) at flowering and grain filling stages. However, three of these predictors had high genotypic correlations in absolute terms, for example, CIRE (R = 0.75 to 0.86) and NIR (R = 0.83 to 0.89) at flowering and NIR (R = 0.79 to 0.90) at grain filling stage. The five predictors also showed low heritability and large coefficient of variation, except Green at flowering time (H^2 = 71.5%, CV = 5.9%).

Figure 6.2 shows the relationship between grain yield and mean disease severity on different varieties under artificial maize streak virus (MSV) inoculation. Grain yield showed significant ($p < 0.001$) difference between susceptible and resistant varieties. Grain yield ranged from 1.1 (most susceptible) to 4.5 t ha^{-1} (resistant). Comparison of disease severity and associated grain yield shows a significant (R^2 = 0.74) decline in yield as the disease severity increases on susceptible varieties. The comparatively large differences observed in these varieties is largely attributed to differences in MSV resistance and susceptibility of the different varieties. The best variety (V16) produced 10% significantly ($p < 0.01$) higher grain yield than the most resistant commercial check (V9) and a mean MSV score of 2.7 out of 9. The commercial resistant check, V17 had slightly lower MSV score (2.3) than the highest yielding variety, V16 (2.7), but not significantly ($p > 0.05$) different. Relative yield difference between the highest

yielding resistant variety (V9) and the most susceptible (V1) was highly significant (p < 0.001) and was almost three-fold.
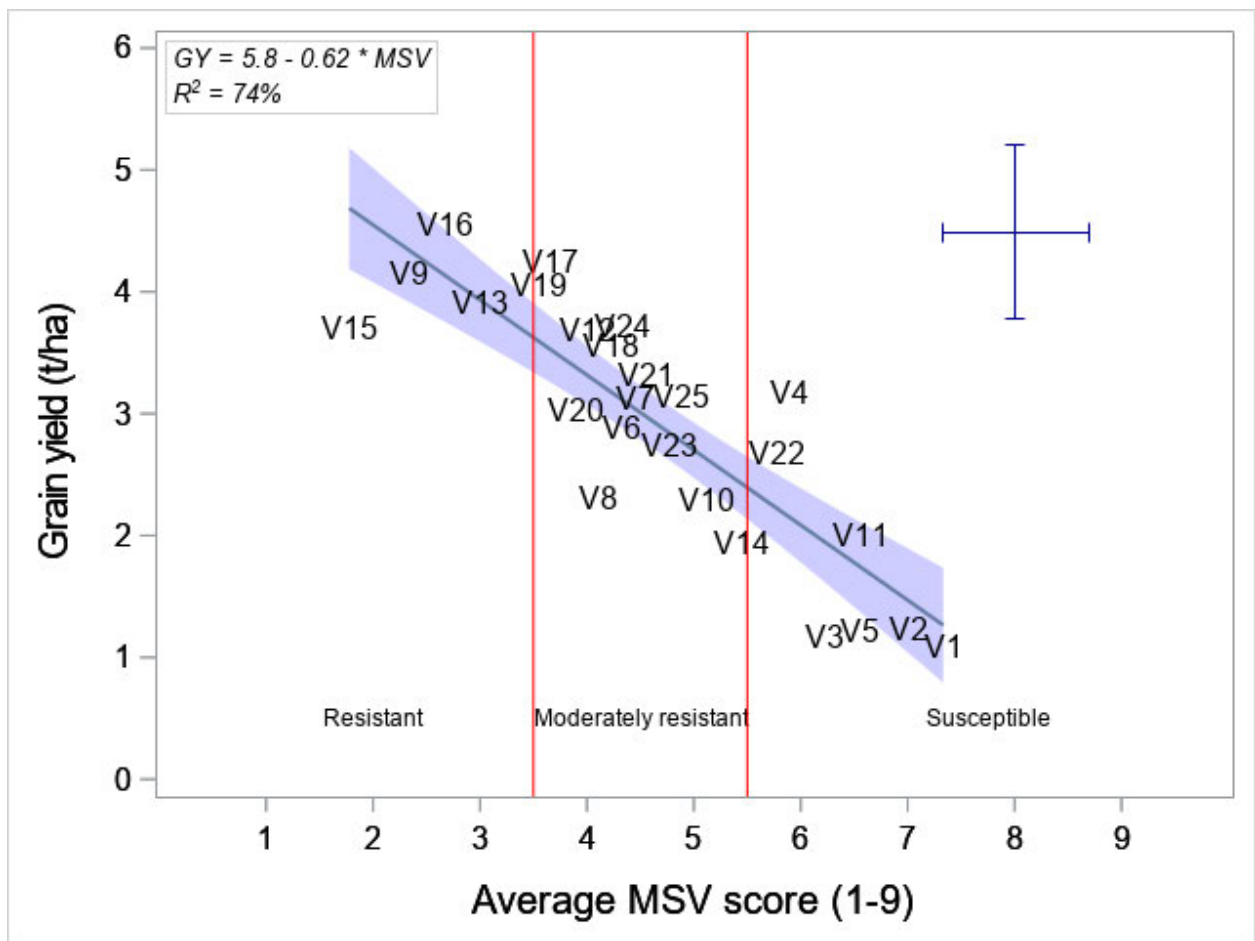
Figure 6.2. Relationship between grain yield and disease severity on mean varieties under artificial maize streak virus (MSV) inoculation. The vertical red lines demarcate the three classes (resistant, moderately resistant and susceptible). Blue cross represents the confidence interval (95%) for MSV (horizontal line) and GY (vertical line). Blue shadow is the 95% confidence interval for the mean model. V1 to V25 = Varieties 1 to 25

6.3.2 PCA Analysis

Correlation between predictive variables and PCA analysis was performed to describe their relationships and to establish which variables can be retained or removed to train the models. The strongest structure in the data is reflected in the largest proportions of variance explained by the first components. The first two components explain 69.1% of the variation in the data (Table 6.2). The first 10 cumulative components explain 96% of the variance (Table 6.2). Thus,

the most important components were PC1 and PC2, explaining 69.1% of total variance. Neither pair of variables showed a correlation of 1. The largest correlations, above 0.95 were found between pair of variables for which we can expect this large correlation because of their definition. Considering this result, no one variable was removed "*a priori*" from the training model especially because we then used variable selection procedures.

Table 6.2. The eigenvalues and total variance explained by components of PCA analysis considering all the variables

Component	Eigenvalue	Proportion	Cumulative
1	20.94	0.499	0.499
2	8.07	0.192	0.691
3	3.70	0.088	0.779
4	2.16	0.051	0.830
5	1.72	0.041	0.871
6	1.18	0.028	0.899
7	1.06	0.025	0.924
8	0.69	0.016	0.941
9	0.51	0.012	0.953
10	0.40	0.010	0.962

Multiple Regression

Thirty-six different models were considered as a result of the combination of the four response variables, MSV at different stages and the average MSV, and independent variables. Half of the models used multispectral data to predict and the other half used indices. Finally, the individual bands and indices were pooled together for predicting the response variables. The most relevant statistics are the AICC, the ASE-Test and CVEXPRESS (Figure 6.3). In all cases, the lowest values are indicative of higher accuracy. The AICC is related with the predictive accuracy of the models.

Considering the three fit statistics, data taken during the vegetative stage are better predictors than data from flowering and grain filling. There are no big differences in using spectral data or indices. However, the indices have more outliers than the spectral data, especially for the ASE-Test statistic. Prediction of MSV scale during grain filling shows poor results compared

to prediction at other stages or the average prediction across stages. Because these models include all the predictive variables, a selection procedure was run in order to select predictive variables and to reduce the complexity of the model. Based on this analysis, we identify those predictive variables that were more frequently included in the models (50 Cross Validation). We also compared the fit statistics of the selected model with the full model. For these analyses, we considered only models which fit. Thirty percent of the models using spectral data did not fit, while for indices it was 18%. For indices, the variability between models was larger than for spectral data. In the latter case, they ranged from 20% to 38% and for indices from 2% to 44%.
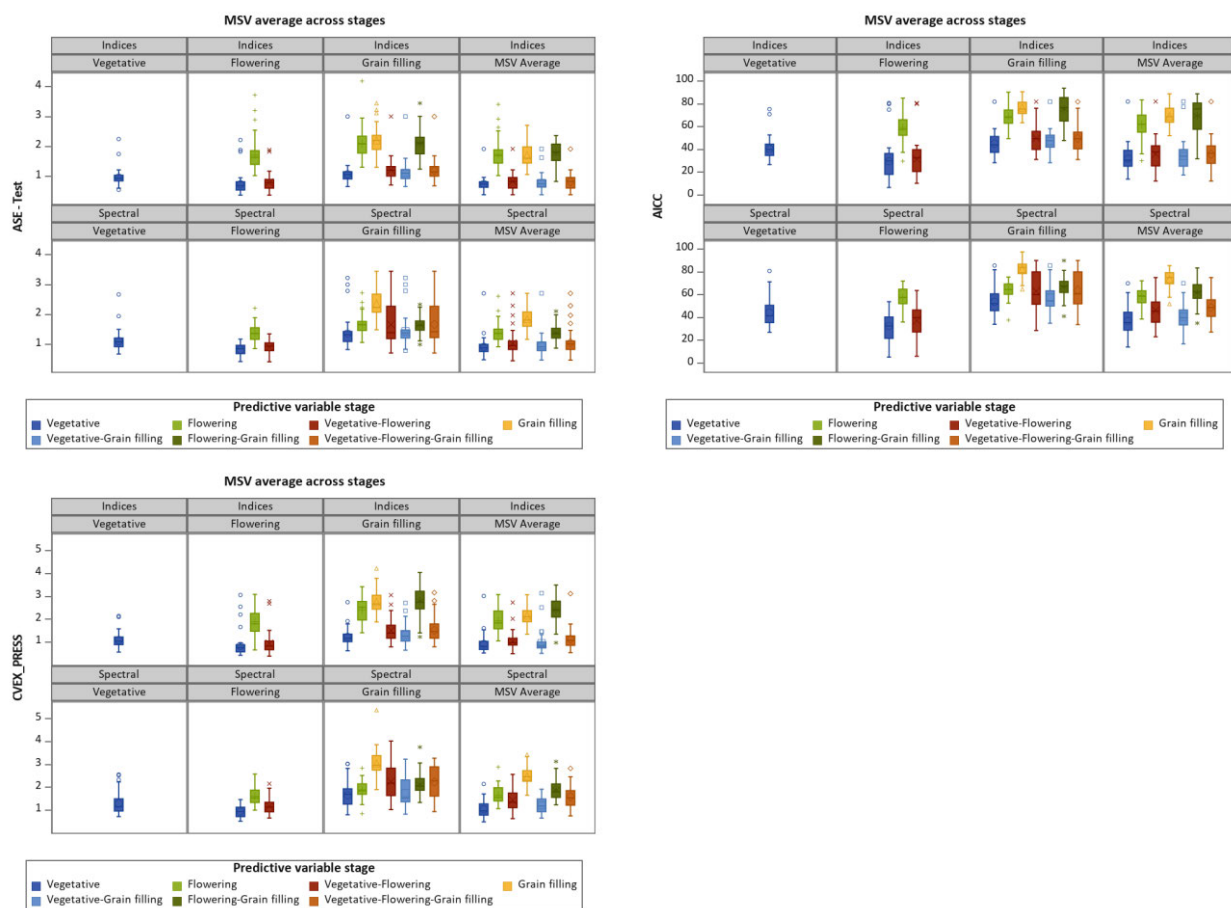
Figure 6.3. Boxplot for three fit statistics, arranged by set of variables (multispectral or indices), response variables (MSV at different stages and the average MSV) and inside each cell, the different sets (stages) of independent variables considered for prediction. V = vegetative, F = flowering, VF = combine vegetative and flowering, G = green filling, VG = vegetative-grain filling, FG = flowering-grain filling, VFG = vegetative-flowering-grain filling combined

Four variables were present in the models with percentages between 61.5 and 88.7. These variables are GV, RV, RF, and GNDVIV (Figure 6.4). Five variables (NIRV, CIGV DNVIREV, CIGF, and SRF) have percentages between 31.8 and 47.8; remaining variables have percentages lower than 20%. In general, phenotypic traits measured at vegetative are better predictors than those at flowering or grain filling. This might be because after flowering, tassels and old senescing leaves could mask the detection of MSV by the multispectral cameras.
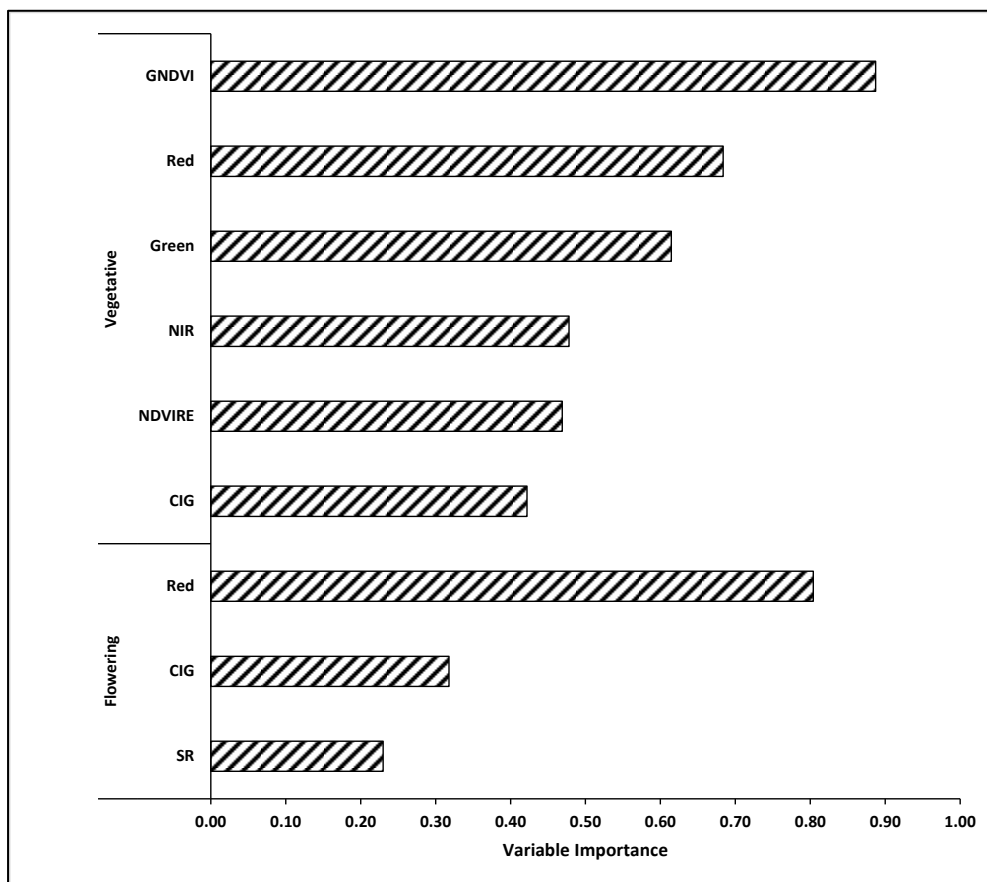
Figure 6.4. Variable importance. The bands or indices were measured at vegetative, flowering and grain filling. GNDVI = Green Normalized Difference Vegetation Index; NDVIred-edge = Red-edge Normalized Difference Vegetation Index; SR = Simple Ratio, CIG = Green Chlorophyll Index.

6.3.3 Decision Tree

Because the method is intrinsically a variable selection method, only one model for each response variables was used, that is, one per stage in which MSV was measured and the

average cross stages. All predictive variables were included simultaneously. Using variable importance (Figure 6.4), GNDVI at vegetative is the only variable with high importance to predict responses for all three vegetative stages and their mean. CIG at vegetative is important to predict the average MSV, and CIG at flowering is the most important to predict both, MSV at grain-filling and average MSV. Other variables that show importance are Red at vegetative and GNDVI at flowering to predict MSV at grain-filling. All the above predictive variables have large importance in both, training and validation sets. The variability in variable importance across cross-validation sets are shown in Figures 6.5a - c.
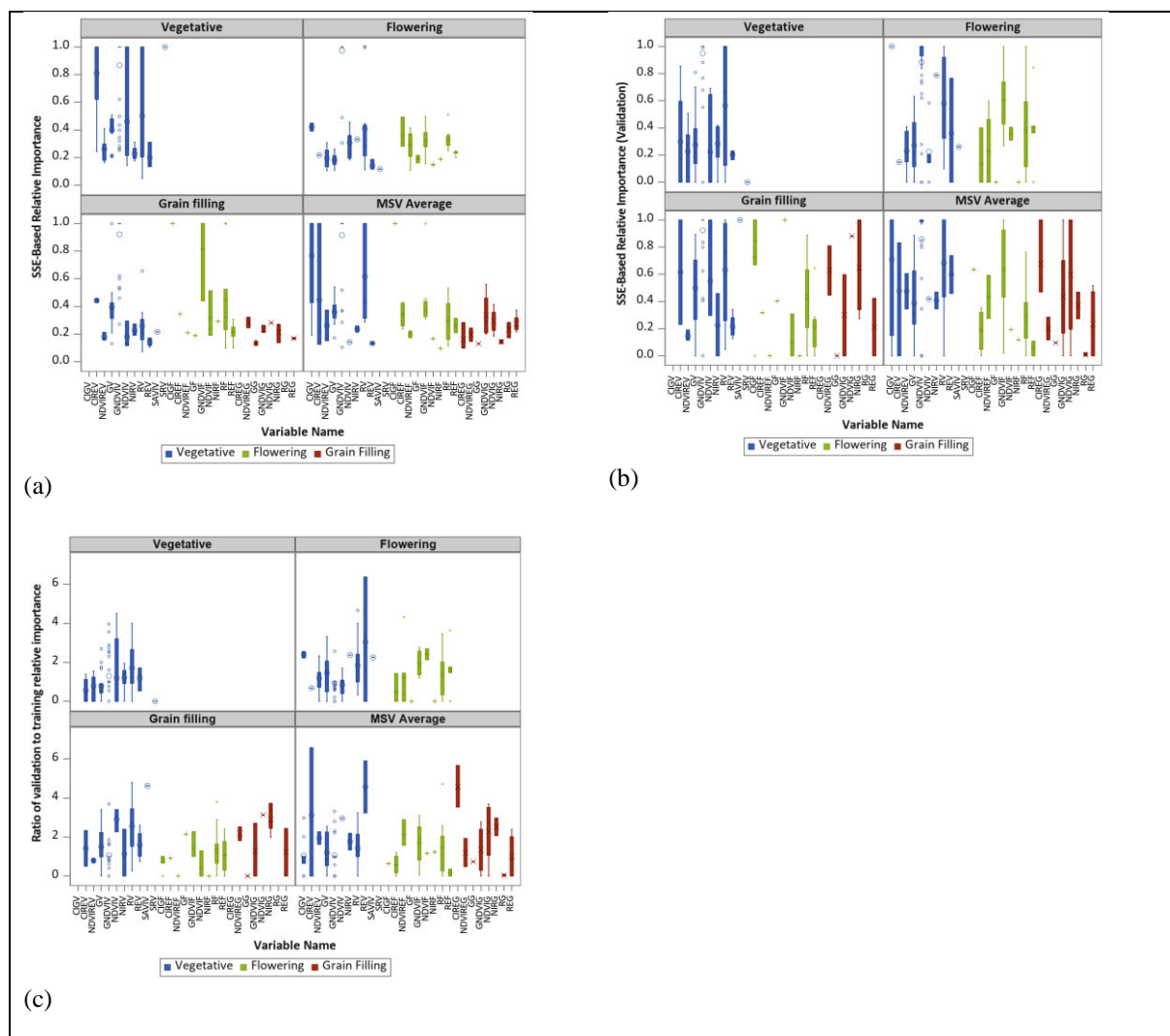
Figure 6.5. Boxplots of (a) relative importance of predictive variables in training set by response variable, (b) relative importance of predictive variables in validation set by response variable and (c) ratio of relative importance of predictive variables, validation/training by response variable. All the bands or indices were measured at V, F and G = vegetative,

flowering and grain filling. R = Red; G = Green; RE = Red-edge; NIR = Near-infrared; GNDVI = Green Normalized Difference Vegetation Index; NDVIRE = Red-edge Normalized Difference Vegetation Index; SR = Simple Ratio, CIG = Green Chlorophyll Index; SAVI = soil-adjusted vegetation index; OSAVI = optimized SAVI. Spectral bands or vegetation indices ending with V, F or G means it was measured at vegetative, flowering or grain filling stage, respectively.

Figure 6.6 shows (a) number of leaves in the tree per response variable and (b) Average Square Error (ASE) by response variable. The number of leaves per tree represents the complexity of the model (Figure 6.6a). Complexity is associated with the complexity of the problem and not with the accuracy in prediction. Figure 6.6b shows the average square error. As usual, the validation set has a lower predictability than the training set. Predictions at flowering stage and the average are similar while predictions at vegetative or grain-filling present the largest ASE. An average square error of 1.5 means a 1.2 average error in MSV scale.

| (a) Boxplot of number of leaves in the tree per response variable. | (b) Boxplot of average square error by response variable. |
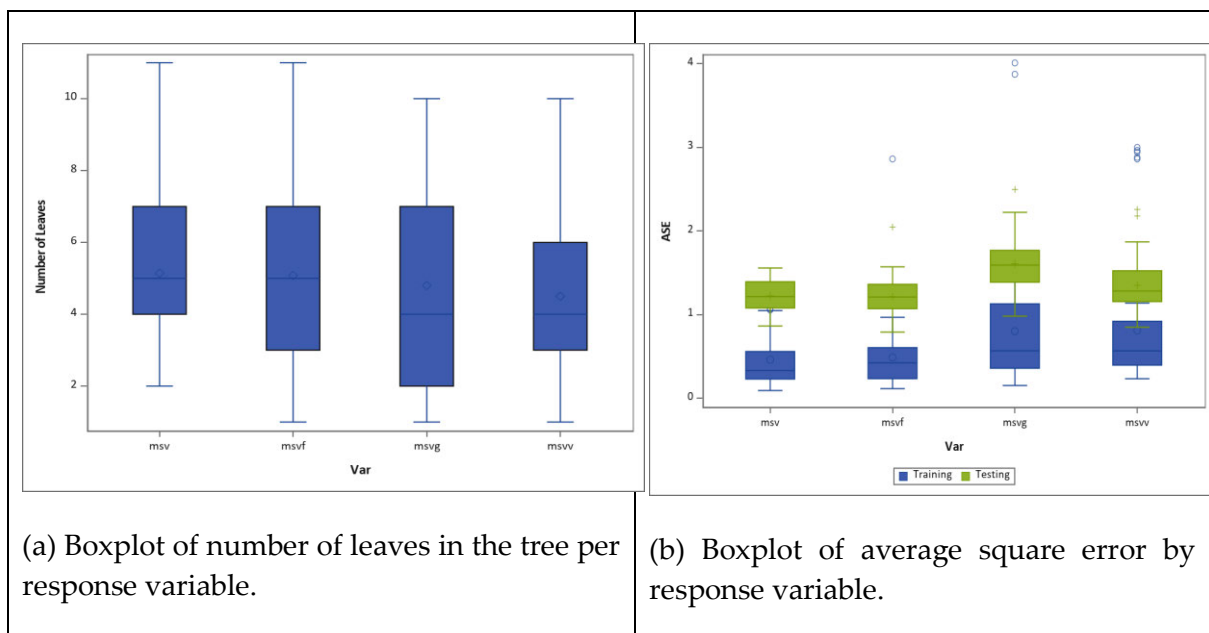
Figure 6.6. Boxplots of (a) number of leaves in the tree per response variable and (b) Average Square Error (ASE) by response variable. MSVV: MSV scale at vegetative stage, MSVF: MSV scale at flowering, MSVG: MSV scale at grain filling stage, MSV: Mean MSV

6.3.4 Linear regression with field data calibration

The best three models for MSV prediction (at any stage or the average) are those with GNDVI, CIG and Red band, all of them measured at vegetative stage, as predictive variables. Correlation goes from 0.713 (Red band at vegetative) to 0.84 (GNDVI at vegetative) (Figures 6.7a - d). In absolute terms, the highest correlations between UAV-derived and manual scoring (Figure 6.7d - average MSV as also reported in chapter 5) were Red band (R = 0.78), NDVI (r = 0.75), SR (r = 0.74), CIG (r = 0.83), CIRE (r = 0.78) and GNDVI (r = 0.84). These significant agreements between UAV-derived and ground truth data suggest that UAV-based phenotyping of MSV in maize is feasible. This is critical because to be effective, image-based phenotyping methods need to achieve a level higher or equivalent the accuracy achieved using manual phenotyping methods quickly at low costs.

a) Vegetative

b) Flowering

c) Grain filling

d) Average across three stages
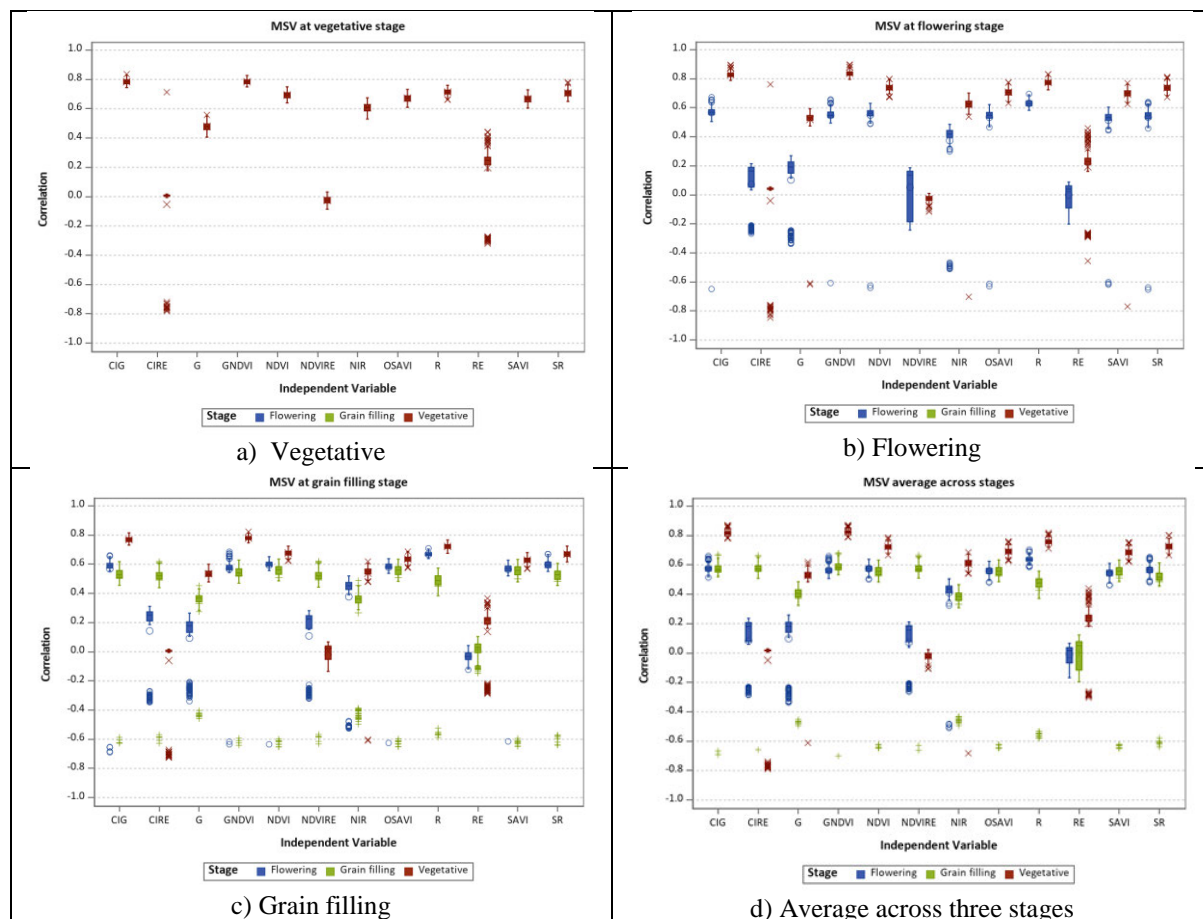
Figure 6.7. Boxplots of Correlation for MSV at (a) vegetative, (b) flowering, (c) grain filling (d) average MSV at three phenological stages by predictive variables for calibration by simple linear regression. R = Red; G = Green; RE = Red-edge; NIR = Near-infrared; GNDVI = Green Normalized Difference

Vegetation Index; NDVIRE = Red-edge Normalized Difference Vegetation Index; SR = Simple Ratio, CIG = Green Chlorophyll Index; SAVI = soil-adjusted vegetation index; OSAVI = optimized SAVI.

The best MSV predictors were GNDVI (r = 0.84; RMSE = 0.85, CIG (r = 0.83; RMSE = 0.86) and Red band (r = 0.77; RMSE = 0.99) at vegetative stage. The model that used GNDVI at vegetative to predict MSV at flowering was also the model with the lowest RMSE (0.847). The largest RMSE corresponds to the model that used Red band at vegetative (RMSE = 1.275) to predict MSV at grain filling. The better predictive variables were the same that showed largest correlation across all the data (Figure 6.8).
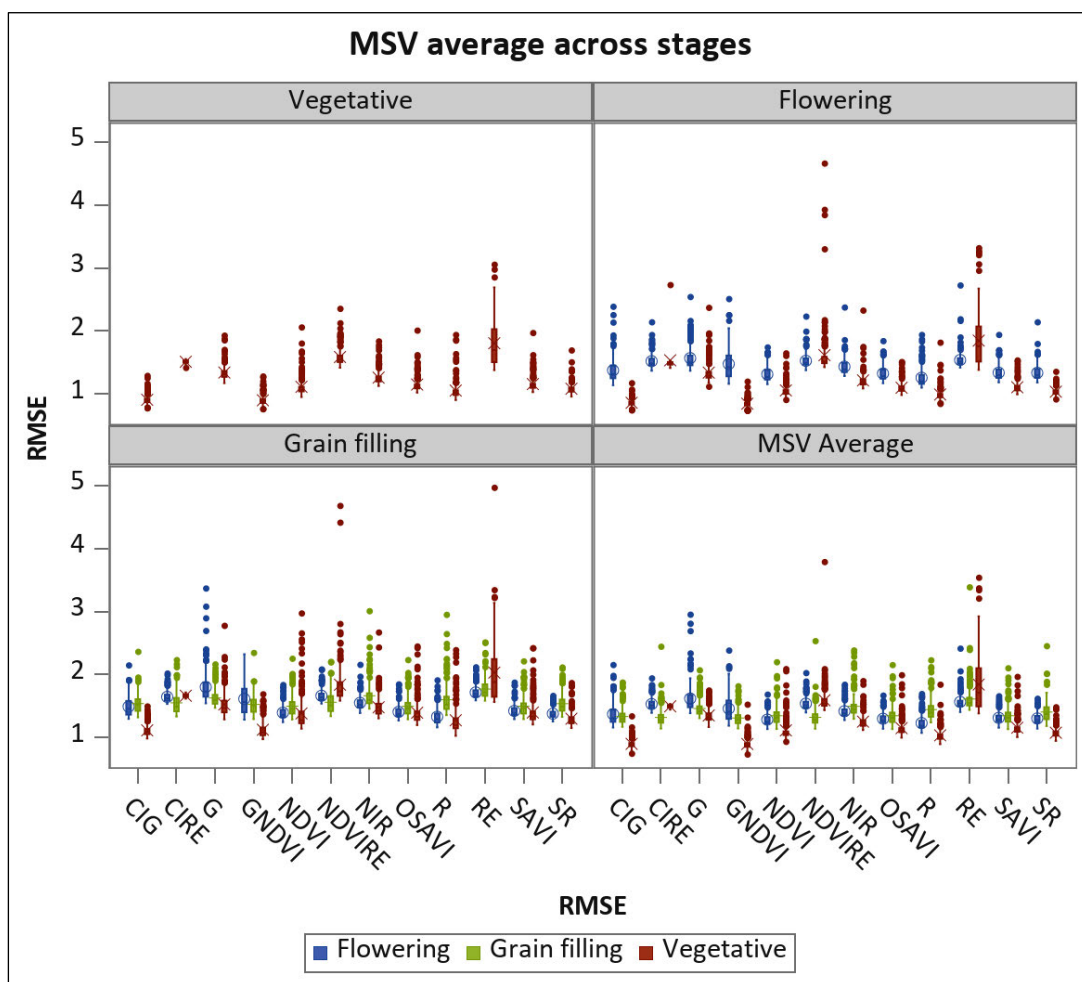
Figure 6.8. Boxplots of RMSE by response and predictive variables for calibration by simple linear regression. R = Red; G = Green; RE = Red-edge; NIR = Near-infrared; GNDVI = Green Normalized Difference Vegetation Index; NDVIRE = Red-edge Normalized Difference Vegetation Index; SR = Simple Ratio, CIG = Green Chlorophyll Index; SAVI = soil-adjusted vegetation index; OSAVI = optimized SAVI.

147

6.3.5 Grain yield prediction using selected best models

The models for maize grain yield predictions were based on UAV-derived multispectral data measured at three phenological stages. Out of 36 different model combinations of spectral bands and derived vegetation indices, six models were selected for prediction of grain yield (Figure 9). Of the selected models, grain yield was significantly correlated with UAV-derived data. The yield variability explained by models based on phenological stages of multispectral data ranged from $r = 0.69$ to 0.86 for the test data. Best regression for grain yield ($r = 0.86$; RMSE = 0.323) was obtained with a model combination of three spectral bands (RV-NIRV-RF) at vegetative and flowering stages. The most frequently selected bands by the model were Near-infrared ($0.77 - 0.81\mu m$), Red ($0.64 - 0.68\mu m$) and Red-edge ($0.73 - 0.74\mu m$). This indicates the importance of the use of spectral band combinations for maize grain yield under MSV disease. In this study, the spectral bands provided an overall better prediction or more models comprised of band combination compared to VIs. Using VIs, only two models GNDVI-OSAVI ($r = 0.84$; RMSE = 0.355) at vegetative and NDVIred-edge-GNDVI ($r = 0.74$; RMSE = 0.555) at green filling stages were selected for grain yield prediction. The four out of six selected models were those based on Red and NIR bands.

Evidently, our results show that most of the models selected use UAV-data measured at the vegetative stage, indicating this to be the critical phenological stage for predicting MSV and grain yield using our data. Combining spectral bands at the same phenological stage or across stages significantly improved the model predictions (Figure 6.9). These results demonstrate the capability of UAV-derived multispectral imaging data to predict MSV and estimate maize grain yield with reasonable accuracy. In addition, there was no model selected using single band or index, suggesting that predictions were improved when using models that use a combination of bands or VIs.
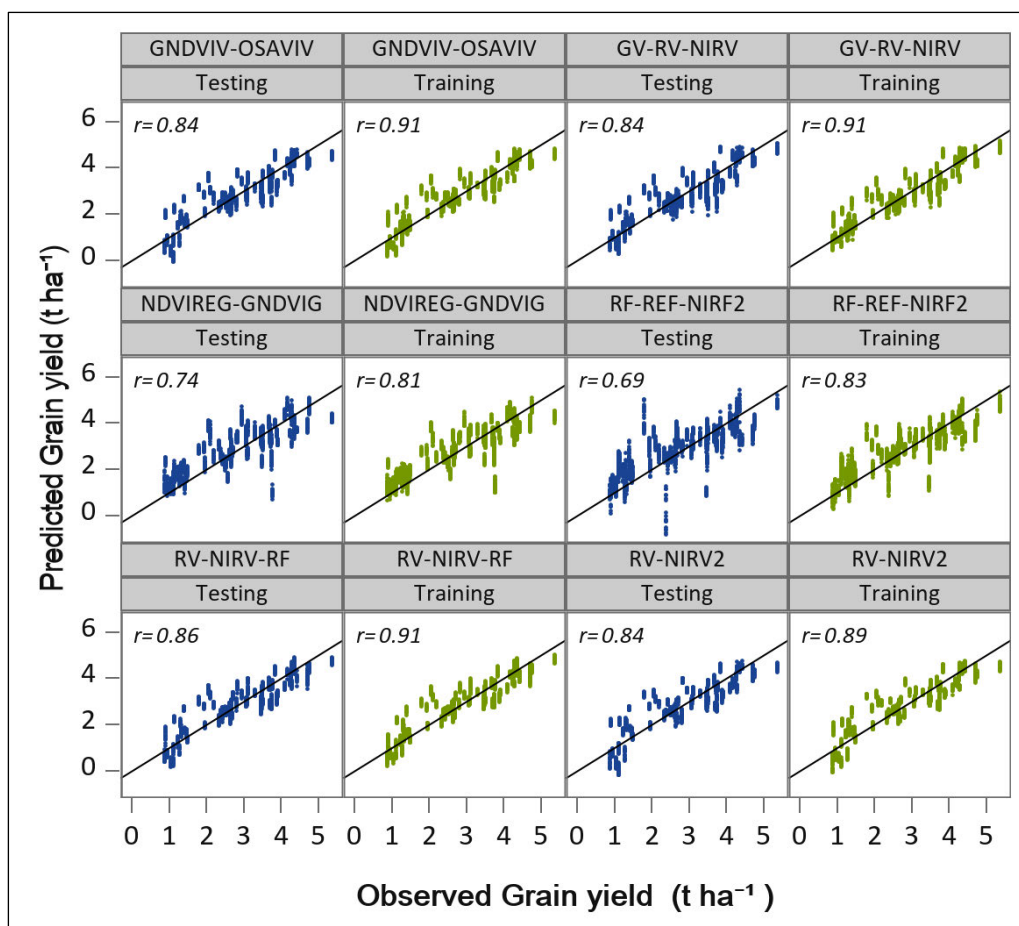
Figure 6.9. Grain yield prediction using the selected models at different phenological stages. GV = Green at vegetative; RV = Red at vegetative; NIRV = Near-infrared at vegetative; RF = Red at flowering; REF = Red-edge at flowering; NIRF = Near-infrared at flowering; NDVIREG = NDVI red-edge at grain filling; GNDVIG = green NDVI at grain filling; GNDVIV = green NDVI at vegetative; OSAVIV = OSAVI at vegetative.

6.4. Discussion

This study set to predict MSV and grain yield using multi-temporal UAV-derived multispectral data measured at different phenological stages. High heritability (H^2) values were obtained for both the spectral and VIs, indicating high level of precision of the UAV-based measurements. In addition, high phenotypic and genotypic correlations were found between indirect traits (spectral and VIs) and MSV and grain yield. This is desirable when using indirect traits for selection. For example, Falconer and Mackay (1996) suggested that the use of indirect selection traits for grain yield is only possible if the H^2 of the indirect traits are higher than that of grain yield itself. In this study most of the potential predictors had higher

149

H^2 than that of grain yield (H^2 = 89%), especially at vegetative stage. This confirms that UAV-based remotely sensed data can provide high precision for field-based maize phenotyping.

Variation among varieties for MSV and grain yield was observed. MSV disease infection in susceptible varieties resulted in significant reduction in grain yield (Figure 6.2). This varietal variation was also detected using spectral reflectance data because MSV disease symptoms on a susceptible variety resulted in changes in color, size and shape. These morpho-physical changes were detected by UAV-based multispectral imaging sensors. This is crucial because in breeding for disease resistance, subtle differences between resistance and susceptibility varieties due to pathogen × genotype interactions need to be efficiently evaluated (Mahlein, 2016). Using UAV-based methods, the disease needs to be quantified with level that is higher or equivalent to the precision and accuracy achieved by visual scoring method – the ground truth data. The use of UAV-based remote sensing in crop evaluation promises to bring phenotyping up to speed with genomics. With easier access to UAVs with reasonable payloads, cheaper, field-based high-throughput plant phenotyping platforms are increasingly becoming useful tools in varietal evaluation in plant breeding to unlock the power of genetic analysis.

6.4.1 Relationship between ground truth and UAV-derived data

The development of maize varieties resistant to MSV is important to adapt to changing climate conditions and to protect the farmers from the effects of the MSV disease on maize. Robust phenotyping is critical in plant breeding and evaluation programs. Our results show significant positive correlations between UAV-derived data and manual scoring (Figure 6.7). Comparison of image-based data with ground truth measurements helped to evaluate the accuracy of UAV-based method used in this study. This agreement between UAV-derived data and ground truth measurements is encouraging and will solve the phenotyping bottleneck currently experienced with manual methods. Our results agree with results reported by other researchers in other crops. For example, good agreements were found between UAV-based and ground truth data in bacterial Huanglongbing (Citrus Greening) disease in citrus trees (Garcia-Ruiz *et al.,* 2013)) and in fire blight disease (*Erwinia amylovora*) in apples (Jarolmasjed *et al.,* 2019). Similarly, Mahlein *et al*. (2013) and Jansen *et al*. (2014) also

reported significant agreements between spectral data and ground truth data in sugarbeet *Cercospora* leaf spot. Our results will form the basis for future refinement of UAV-based remote sensing data in field-based high-throughput phenotyping in maize.

6.4.2 Predicting MSV and grain yield using UAV-derived data

This study predicted maize grain yield using multispectral and derived vegetation indices obtained at three phenological stages (Vegetative, Flowering and Grain filling). Higher MSV and grain yield prediction accuracies were obtained using spectral bands or indices measured at vegetative stage. The modelling results using imaging data from the later phenological stages (Flowering and Grain filling) of maize varieties were less accurate in predicting MSV and grain yield. This is expected given that the study evaluated the utility of phenotyping varietal response to MSV and predicting their final yield. MSV disease symptoms on a susceptible variety result in changes in color, size and shape. Therefore, these morpho-physical changes can be measured accurately using multispectral imaging sensors at the vegetative stage. A further possible explanation could be that measurements after flowering could suffer from masking effects by the flowers (tassels) and old senescing leaves at midgrain filling. Thus, remote sensing at midvegetative stage can improve the accuracy of MSV and yield predictive models. The predictive power of the model increased by addition of one or more predictor variables to the models.

Predictor variables that had low heritability and low phenotypic and genotypic correlations with MSV and grain yield performed poorly in predictions compared to those with high heritability and high phenotypic and genotypic correlations with MSV and grain yield. Using variable importance selection method allowed the model to select a few important predictor variables and to drop non-important variables while improving model performance. Variable importance method is also important in reducing multicollinearity between predictors. The selected variables (Figure 6.4) were combined in the model and addition of highly predictive variables increased the final prediction accuracy. This is evident in our results (Figure 6.9), where all selected models used more than one index or spectral bands. In addition, the effects of individual predictor traits (spectral bands or indices) on the model performance were examined. This is important in assessing which predictor traits may be suitable for future

high-throughput studies and data collection. However, no model using individual predictor trait resulted in significant improvement in the prediction accuracy compared to pooled predictors, suggesting that these predictor traits could work in an additive fashion. These findings provide evidence for measuring multiple phenotypic traits for variety evaluation purposes because accurate prediction results were obtained using multi-trait models. This agrees with Crain *et al*. (2018) who found similar results in wheat.

Examining the spectral data in the models provides an opportunity to see which bands were frequently selected in predicting MSV and grain yield. Of the six models selected (Figure 6.9), four included the NIR and Red bands. In addition, combining NIR band with Red band gave significantly higher prediction or improved the explanatory power of the models. This was also true with the selected indices. Thus, not all indices or bands measure the same aspect of biophysical parameters or crop productivity. Combining them increased the joint predictive power, thus increased complementarity. For example, the NIR band is known to be sensitivity to chlorophyll content and therefore useful for detection of crop health and productivity modelling. NIR senses photosynthesis better than the Red or Green bands (Ollinger, 2011; Mariotto *et al*., 2013). The Red and Green bands saturate at the first leaf layer because 95% of signal tends to be absorbed at this stage, yet in maize more leaf layers with considerable amount of chlorophyll are below the canopy (Gitelson, 2011). The NIR and far-near-infrared (FNIR) are the only remote sensing bands that can sense the middle layer of the canopy due to multiple scattering effects in the NIR (Gitelson, 2011). Thus NIR can sense much more valuable information for crop productivity modelling.

The ability to predict maize grain yield before harvesting will assist breeders and agronomists in the efficient selection and advancement of high yielding varieties resistant to biotic stresses. Furthermore, yield prediction using UAV-derived data can assist in plant breeding by speeding up selections that can be crossed at flowering, instead of waiting until the crop reaches physiological maturity and yield is processed. Early grain yield prediction models based on UAV-derived data could assist in early decision making, time saving and reduce costs in breeding and varietal phenotyping programs. Continuous improvements in yield prediction models and increased data generation capabilities will reduce selection bottlenecks and increase genetic gain.

6.4.3 Field-based high-throughput imaging of maize and the big data challenge

UAV-based phenotyping is becoming an attractive alternative to labor-intensive manual phenotyping. It offers convenient operation, high spatio-temporal and reasonable spectral resolution data (Sankaran *et al.*, 2015), and is able to quantify within-plot variability in field-based crop phenotyping (Araus *et al.*, 2014; Zaman-Allah *et al.*, 2015; Han *et al.*, 2019). This has the potential to revolutionize varietal evaluation in plant breeding programs. However, while UAVs are becoming smart alternatives to labor-intensive manual phenotyping in plant breeding, the massive volume, variety, and velocity of data produced by these platforms result in a 'big data problem' (Mahlein, 2016; Singh *et al.*, 2016; Hickey *et al.*, 2019). To improve our phenotyping ability, the voluminous data produced by real-time UAV-based remote sensing need to be efficiently achieved and retrieved for analysis. Retrieving, analyzing and interpreting image-based data is still a challenge within the plant breeding and phenotyping community (Minervini *et al.*, 2017). Extraction of patterns and features from such a huge corpus of data derived from UAV and other sensor platforms requires powerful analytical tools including machine learning algorithms to derive meaningful phenotypic information. However, the ensuing advantages brought by image-based data makes it a promising approach for addressing phenotyping bottleneck in planting breeding. Therefore, to be able to effectively use UAV-based remotely sensed data for disease phenotyping, advanced statistical and data analysis methods are important (Mahlein, 2016). In this study, we evaluated different methods to analyze UAV-derived multispectral data, in line with future vision that high-throughput phenotyping will become routine in varietal evaluation. Our results show that UAV-derived multispectral remotely sensed data can be used in high-throughput phenotyping of MSV disease with high accuracy.

6.5. Conclusion

Accelerating crop genetic improvement to sustain food production to meet the expected population growth requires significant improvement in phenotyping ability to achieve the needed genetic gain in major food crops like maize. UAVs are becoming a new platform for getting high spatio-temporal resolution data for high-throughput phenotyping in plant breeding and varietal evaluation. This study evaluated the utility of UAV-derived

multispectral data in predicting maize streak virus (MSV) disease and grain yield using UAV-derived multispectral imaging data and identify the most ideal phenological stage for MSV and grain yield prediction. The results show that UAV-based method is a useful and reliable tool for phenotyping and predicting maize yield under artificial MSV inoculation. We conclude that:

1. The vegetative stage appears to be the ideal phenological stage for quantifying MSV and grain yield prediction using UAV-derived multispectral data;
2. The results showed the importance of Red and NIR bands as these were frequently selected in most of the models that gave the highest precision values for grain yield prediction;
3. High spacio-temporal resolution UAV-derived imagery at key phenological stages can be used to predict MSV and grain yield with reasonable accuracy, and therefore, have great potential for use as a selection tool in maize breeding and varietal evaluation;
4. Combining spectral bands and vegetation indices significantly improve model predictions, and the methodology used in this study has demonstrated the utility of image-based high-throughput phenotyping to relieve the breeding community of phenotyping bottlenecks;
5. The methodology used in the study could be applicable to other disease stresses that affect maize, and possibly to other crops to accelerate crop genetic improvement and varietal selection, thereby addressing the current phenotyping bottleneck.

The results obtained in this study represent the successful use of UAV-derived multispectral data for effective and efficient evaluation of maize varieties for MSV resistance. Consequently, UAV-based remote sensing data can be useful for high-throughput phenotyping of maize to identify resistant varieties and to discriminate them under field conditions. However, the prediction models and methodology used in this study need to be further examined in other diseases and abiotic stresses. In addition, yield related variables like leaf area index can be incorporated into the models to see if this can improve maize grain yield prediction accuracy. In this study, we used multispectral data. However, detection of subtle plant disease symptoms may be lost at coarser spectral resolution. Future investigations should look into inter-comparison of hyperspectral versus multispectral sensors.

154

CHAPTER 7: UAV AND FIELD SPECTROMETER BASED REMOTE SENSING OF MAIZE: A SYNTHESIS

7.1 Introduction

The challenges associated with maize production to meet food security in Africa keep evolving. Improving food security in Africa requires robust early warning systems informed by accurate and up-to-date information, especially croplands and yield estimates of the staple food crops. In addition, to address the ever-evolving diseases due to climate change, there is an urgent need to develop and deploy improved and disease-resistant maize varieties using modern tools by combining genomics, high-throughput phenotyping, and GIS-based decision support tools in order to build resilience and adaptive capacity of the resource-poor farmers in tropical Africa. In Africa, crop yield information is updated through farmer communication or farm surveys of selected fields by government agricultural extension officers. However, these conventional methods are error-prone due to discrepancies in declarations (farmer self-reported data) and are time-consuming and expensive. Furthermore, extension agents lack modern instruments to accurately estimate yield. Options to use remotely sensed data are available but are rarely being used despite being proven to be reliable and cost-effective for estimating yields across large areas, providing accurate and timely information required for early warning systems. The use of remotely sensed data for high-throughput phenotyping has been an area of active research because phenotyping of phenomes associated with grain yield is presently a major bottleneck to crop improvement. Few studies have been conducted on phenotyping maize diseases, and no studies have been conducted on maize streak disease phenotyping and yield prediction using remotely sensed data. The need for spatial analysis, estimating yields, and phenotyping maize varieties in crop improvement to address the food security challenges formed the basis of this study.

The aim of this study was to model spatial suitability for maize production and explore the utility of remotely sensed data in maize varietal discrimination, high-throughput phenotyping, and yield prediction.

7.2 Challenges

Large-scale yield estimation of crops is a problem to which the use of remotely sensed data has been able to contribute considerably in certain places. However, while remote sensing can be very useful for crops grown in countries where field sizes are large compared with the available satellite sensors' footprint (instantaneous field of view), there are problems for countries where field sizes are small and cropping systems are diverse and sometimes different crops are mixed in the same field. In addition, the use of remotely sensed data in discriminating different varieties within crop species can be a challenge due to many factors that easily alter the signatures of the target varieties. These factors include the inherent spectral similarities, intercropping culture, experimental or environmental factors, crop growth stage, bio-stressors, spectral collection methodology, and resolutions of sensors used. Furthermore, the options of using remote sensing in disease phenotyping have to take into consideration the practical limitations due to the presence of a complex of different diseases on the same leaf or canopy. The available vegetation indices are not disease-specific, and therefore can only quantify levels of infestation or damage with no ability to distinguish the different types of diseases present in the area of interest.

7.3 The main findings

The use of remotely sensed data in estimating maize yields compared to conventional ground-based survey methods was reviewed. The results showed that the use of remotely sensed data in estimating maize grain yield in Africa is very limited and fraught with challenges. Yet evidence from advanced agricultural systems shows increasing use of satellite-based remote sensing methods in estimating maize yields as a cost-effective option capable of generating accurate data for early warning systems. The results established that when applying satellite-based remote sensing in the African agricultural context, researchers should take into account the intrinsic low-resolution limitations of current sensors in replicating these methodologies in fragmented and highly heterogeneous African agricultural systems. Significant improvements in the accuracy of yield estimates in these fragmented and highly heterogeneous environments are expected from new sensors (e.g. Sentinel 2, Landsat 8 OLI, WV, Dove, etc.), whose pixel sizes are several times smaller than the field sizes prevalent in

these heterogeneous cropping systems. Nonetheless, mixed pixels (pixels with digital numbers representing the mean reflectance from dissimilar surfaces found in the area represented by these pixels) remain a major challenge where maize is intercropped with other crop types, a common practice with African maize farmers.

The results of land suitability modeling using GIS, AHP, and multi-criteria evaluation have shown the feasibility of using modern spatial analysis tools in assessing land suitability for targeting location-specific interventions. These can serve as decision support tools for policymakers and land-use planners regarding maize production and varietal placement. Assessing land suitability for maize production in a developing country like Zimbabwe is important for food security planning, decision making, and land use planning at the national level. This study integrates GIS, AHP, and a multi-criterion evaluation to derive a land suitability map for maize production in Zimbabwe using the methodology that builds on sound concepts and earlier studies by Saaty (1977) and subsequently used recently by other scholars (Akinci *et al*., 2013; Zhang *et al*., 2015; Mu and Pereyra-Rojas, 2017). The relative importance of the factors was validated using expert knowledge and results of modeling maize suitability classification were validated using long-term maize grain yield. The study demonstrates satisfactorily the strength of using GIS and AHP for land suitability mapping, critical for decision support in crop placement. Combining GIS and remote sensing in land suitability analysis and yield forecasting provides powerful analytical tools for decision support systems. In addition, the ability to discriminate individual varieties within crops remotely through unique spectral signatures will increase our understanding of African agriculture and improve food security through early warning systems and crop improvement through breeding.

The ability to discriminate maize varieties using remotely sensed data represents a breakthrough that has many and huge implications in breeding new varieties, monitoring their spread, understanding adaptation, and preparing for a changing world. The results of this study have demonstrated the capability of hyperspectral data in accurately discriminating maize varieties at certain phenological stages. The analysis further shows that, by using appropriate pre-processing transformations like auto-scaling and generalized least squares weighting, the accuracy of discriminating maize varieties using hyperspectral data can be

improved significantly. In addition, using multi-temporal hyperspectral data, our results showed that flowering and onset of senescence are the most ideal phenological stages for discriminating maize varieties at field level. The analysis further identified 10 optimal hyperspectral bands out of the 101 hyperspectral bands in the VIS and NIR spectral range of 400 to 900nm as the most ideal for maize varietal discrimination. It is important that this varietal discrimination ability moves from proximal to distant-discrimination levels using satellite- or aerial-based sensors for commercial purposes in precision agriculture and plant phenotyping and yield prediction in crop genetic improvement.

Plant phenotyping using platforms with high-throughput capabilities remains a major bottleneck in plant breeding. This study evaluated the utility of aerial-based sensors using UAV-derived multispectral data for field-based plant phenotyping. Combining UAV-derived multispectral data and the random forest algorithm, the analysis achieved an accurate classification of 25 different maize varieties into susceptible, moderately resistant, and highly resistant types. The results showed that UAV-based multispectral data combined with the RF classifier is useful in field-based high-throughput maize phenotyping. In this study, not only were the optimal bands and indices identified but also the vegetative stage was identified as the ideal phenological growth stage for accurate MSV disease phenotyping.

Further analysis was performed using multi-temporal UAV-derived multispectral data to predict MSV and grain yield at different phenological stages. Most of the potential predictors (spectral bands and VIs) had higher H^2 than that of grain yield (H^2 = 89%), which is desirable when indirect selection traits for grain yield are being used for selection in plant breeding (see Falconer and Mackay, 1996). Higher MSV (r = 0.77 – 0.84) and grain yield (r = 0.69 – 0.86) prediction accuracies were obtained using spectral bands or indices measured at vegetative stage. In addition, no model using individual predictor traits resulted in significant improvement in the prediction accuracy compared to pooled predictors, suggesting that these predictor traits could work in an additive fashion. Spectral bands measured at the vegetative growth stage were the most ideal for predicting MSV. For grain yield prediction, six models comprising a combination of either bands or indices measured at vegetative were selected as ideal for prediction. This further confirms the utility of UAV-based multispectral remotely

159

sensed data reliability in phenotyping MSV disease and grain yield prediction, an important development in addressing phenotyping bottlenecks in crop improvement.

7.4 Overall conclusions

The key focus of this study was to model spatial land suitability for maize production using GIS and explore the utility of remotely sensed data in maize varietal discrimination, high-throughput phenotyping, and yield prediction. The results have demonstrated that spatial analysis can accomplish land suitability mapping using several environmental factors. In addition, the results of this thesis have demonstrated that remote sensing can be useful in maize varietal discrimination and field-based high-throughput phenotyping. Therefore, we concluded the following.

1. It is possible to forecast maize yield in highly fragmented and heterogeneous African agricultural landscapes if data from high spatial, temporal and spectral resolution multispectral sensors is used together with appropriate classification algorithms and accurate ground truth data.

2. Integrating GIS and AHP in a MCE in land suitability analysis can convert data layers into information that transform and add value to the original data, which in its original form may not be useful for decision support systems.

3. Using proximal sensing (field spectrometer-based) combined with appropriate pre-processing algorithms, maize varieties can be accurately discriminated using hyperspectral data at certain phenological stages.

4. UAV-based remotely sensed data provides a step-change towards data availability and turn-around time in varietal high-throughput plant phenotyping in maize breeding. Spectral data, measured at the vegetative stage appear to be the most important information for the classification of maize varieties and yield prediction under artificial MSV inoculation.

5. The agreement between UAV-derived remotely sensed data and ground truth measurements confirm the utility of a UAV-based approach in field-based high-

160

throughput phenotyping in breeding programs. This will reduce selection bottlenecks associated with manual phenotyping and offers decision support tools for large-scale varietal screening.

6. UAV-based MSV and yield prediction methodology used in the study could be applicable to other disease stresses that affect maize, and possibly to other crops to accelerate crop genetic improvement and varietal selection, thereby addressing the current phenotyping bottleneck.

7.5 Implications for future research

The results reported in this thesis show the capability of geospatial technology (GIS and remote sensing) in modeling land suitability for maize production and the utility of remotely sensed data in discriminating and phenotyping maize varieties. However, further research gaps have been identified.

1. The GIS-based spatial analysis of land suitability facilitates our ability to match the target crop and variety with land suitability. The future focus should extend the method used in this study to quantify genetic correlations of different varietal maturity in terms of growing degree days (GDD) and the land suitability classes. The ultimate objective is to add more GIS data layers for complete land suitability modeling. Such data layers include socio-economic factors, aspect, relief, elevation, day length, soil nutrients, pH, growing degree days, among others.

2. In addition, the results of chapter three may be analyzed using actual historical rainfall and temperature data to assess if the classification accuracy can be improved, higher percentages of variability explained, and separate growing regions in more detail.

3. The results of chapter four explored the use of multi-temporal hyperspectral data and multivariate techniques in discriminating maize varieties as well as identifying optimal spectral bands and phenological stages for varietal discrimination. Future studies should include in the analysis morphological and developmental quantification and qualification determinations to increase discrimination accuracy.

4. The study demonstrated the utility of UAV-derived multispectral data in phenotyping maize varieties under artificial MSV inoculation with good accuracy and therefore can be deployed for multiple varieties evaluation in plant breeding. However, future research should focus on developing and testing disease-specific vegetation indices.

Research should focus on developing ways that will permit image analysis to differentiate diseases on the same leaf or canopy using remotely sensed data and machine learning algorithms.

5. In this study, we used a multispectral sensor mounted on a UAV. However, the detection of subtle plant disease symptoms may be lost at coarser multispectral resolution. Therefore, as phenotyping science evolves, future work should investigate the comparison of hyperspectral versus multispectral imaging for quantifying disease severity in crop improvement and precision agriculture.

6. Many other parts of the electromagnetic spectrum (ultra-violet, mid- and far-infrared), including the thermal bands needs further exploration, and may offer better discrimination in differentiating and quantification of diseases in pant phenotyping using hyperspectral imaging.

References

Abdel-Rahman, E.M., Mutanga, O., Adam, E., Ismail, R. 2014. Detecting Sirex noctilio grey-attacked and lightning-struck pine trees using airborne hyperspectral data, random forest and support vector machines classifiers. *ISPRS J. Photogramm. Remote Sens.* 88, 48-59.

Adam, E., Mutanga, O. 2009. Spectral discrimination of papyrus vegetation (Cyperus papyrus L.) in swamp wetlands using field spectrometry. *ISPRS J. Photogramm. Remote Sens.* 64, 612–620.

Adam, E., Mutanga, O., Rugege, D. 2010. Multispectral and hyperspectral remote sensing for identification and mapping of wetland vegetation: a review. *Wetlands Ecol. Manag.* 18, 281-296.

Adam, E. M., Mutanga, O., Rugege, D., Ismail. R. 2012. Discriminating the papyrus vegetation (*Cyperus papyrus* L.) and its co-existent species using random forest and hyperspectral data resampled to HYMAP. *Inter. J. Remote Sens.* 33(2), 552-569. http://dx.doi.org/10.1080/01431161.2010.543182

Adelabu, S., Mutanga, O., Adam, E. 2014. Evaluating the impact of rededge band from Rapideye image for classifying insect defoliation levels. *ISPRS J. Photogram. Remote Sens.* 95, 34-41.

Adelabu, S., Mutanga, O., Adam, E., Sebego, R. 2014. Spectral discrimination of insect defoliation levels in mopane woodland using hyperspectral data. *IEEE J. Sel. Top. Appl. Earth Obs. Remote Sens.* 7(1), 177–186.

Adjorlolo, C, Botha, J.O., Mhangara, P., Mutanga, O. 2014. Integrating remote sensing and conventional grazing/browsing models for modelling carrying capacity in southern African rangelands, Proc. SPIE 9239, Remote Sensing for Agriculture, Ecosystems, and Hydrology XVI, 92390B (November 11, 2014); doi:10.1117/12.2066330; http://dx.doi.org/10.1117/12.2066330.

Adjorlolo, C., Cho, M.A., Mutanga, O., Ismail, R. 2012. Optimizing spectral resolutions for the classification of C3 and C4 grass species, using wavelengths of known absorption features. *J. Applied Remote Sens.* 6, 063560-063561-063560-063515.

Akıncı, H., Özalp, A.Y., Turgut, B. 2013. Agricultural land use suitability analysis using GIS and AHP Technique. *Comp. Electron. Agric. 97*, 71-82.

Alemu, D., Ayele, G., Behute, B., Beyone, Y., Dewana, R., Fedaku, B., Vergas, H.R., Minot, N., Rashid,

S. Taffesse, A. Tefera, S. 2008. Development of a spatial equilibrium modelling approach to study the impact of policy intervention on cereals availability (JRC Scientific and Technical Report), Cereals availability study in Ethiopia, 2008, JRC, Ispra, Italy.

Alheit, K.V., Busemeyer, L., Liu, W., Maurer, H.P., Gowda, M., Hahn, V., Weissmann, S., Ruckelshausen, A., Reif, J.C., Würschum, T. 2014. Multiple-line cross QTL mapping for biomass yield and plant height in triticale (×Triticosecale Wittmack). *Theor. Appl. Genet.* 127, 251–260.

Alston, J.M., Beddow, J.M., Pardey, P.G. 2009. Agricultural research, productivity, and food prices in the long run. *Science* 325, 1209–1210.

Albaji, M., Naseri, A., Papan, P., Nasab, S.B. 2009. Qualitative evaluation of land suitability for principal crops in the West Shoush Plain, Southwest Iran. *Bulgarian J. Agric. Sci.* 15, 135-145.

Al-Shalabi, M.A., Mansor, S.B., Ahmed, N.B., Shiriff, R. 2006. GIS based multicriteria approaches to housing site suitability assessment', in XXIII FIG Congress, Shaping the Change, Munich, Germany, October, pp. 8-13.

Anderssen, E. Dyrstad, K., Westad, F., Martens, H. 2006. Reducing over-optimism in variable selection by cross-model validation. *Chemometr. Intell. Lab.* 84(1-2), 69–74.

Andrade-Sanchez, P., Gore, M.A., Heun, J.T., Thorp, K.R., Carmo-Silva, A.E., French, A.N., Salvucci, M.E., White. J.W. 2014. Development and evaluation of a field-based high-throughput phenotyping platform. *Funct. Plant Biol.* 41(1): 68–79. http://dx.doi.org/10.1071/FP13126

Anthony, D., Detweiler, C. 2017. UAV Localization in Row Crops. *J. Field Robotics* 00 (0): 1–22.

Apan, A., Held, A., Phinn, S., Markley, J. 2004. Detecting sugarcane 'orange rust' disease using EO-1 Hyperion hyperspectral imagery. *Inter. J. Remote Sens.* 25, 489– 98.

Araus, J.L., Cairns, J.E. 2014. Field high-throughput phenotyping: The new crop breeding frontier. *Trends Plant Sci.* 19(1), 52– 61. https://doi.org/10.1016/j.tplants.2013.09.008

Araus, J.L., Kefauver, S.C., Zaman-Allah, M., Olsen, M.S., Cairns, J.E. 2018. Translating high-throughput phenotyping into genetic gain. *Trends Plant Sci.* 23, 451–466.

Araus, J.L., Slafer, G.A., Reynolds, M.P., Royo, C. 2002. Plant breeding and drought in C3 cereals: What should we breed for? *Annals Bot.* 89(7), 925–940. https://doi.org/10.1093/aob/mcf049

Aronoff, S. 2005. Satellite-based sensors operating in the visible and infrared wavelengths. Remote sensing for GIS managers. ESRI Press, California.

Asner, G.P. 1998. Biophysical and biochemical sources of variability in canopy reflectance. *Remote Sens. Environ.* 64, 234-253.

Atzberger, C. 2013. Advances in remote sensing of agriculture: Context description, existing operational monitoring systems and major information needs. *Remote Sens.* 5, 949-981.

Avery, T.E., Berlin, G.L. 1992. Fundamentals of remote sensing and airphoto interpretation. Prentice Hall. 540 p.

Bachlava, E., Taylor, C.A., Tang, S., Bowers, J.E., Mandel, J.R., Burke, J.M., Knapp, S.J. 2012. SNP discovery and development of a highdensity genotyping array for sunflower. *PLoS ONE.* http://dx.doi.org/10.1371/journal.pone.0029814

Báez-González, A.D., Chen, P., Tiscareño-López, M., Srinivasan, R. 2002. Using satellite and field data with crop growth modeling to monitor and estimate maize yield in Mexico. *Crop Sci.* 42, 1943-1949.

Báez-González, A.D., Kiniry, J.R., Maas, S.J., Tiscareno, M.L., Macias, C., Mendoza, J.L., Richardson, C.W., Salinas, G., Manjarrez, J.R. 2005. Large-area maize yield forecasting using leaf area index based yield model. *Agron. J.* 97, 418-425.

Bagheri, M., Sulaiman, W.N.A., Vaghefi, N. 2013. Application of geographic information system technique and analytical hierarchy process model for land-use suitability analysis on coastal area. *J. Coastal Conserv.* 17, 1-10.

Bagherzadeh, A., Mansouri Daneshvar, M.R. 2011. Physical land suitability evaluation for specific cereal crops using GIS at Mashhad Plain, Northeast of Iran. *Front. Agric. China* 5(4), 504-513.

Banai, R. 1993. Fuzziness in geographical information systems: contributions from the analytic hierarchy process. *Inter. J. Geographic. Inform. Sci.* 7(4), 315-329.

Bandyopadhyay, S., Jaiswal, R., Hegde, V., Jayaraman, V. 2009. Assessment of land suitability potentials for agriculture using a remote sensing and GIS based approach. *Inter. J. Remote Sens.* 30, 879-895.

Barbagallo, R.P., Oxborough, K. Pallett, K.E. and Baker, N.R. 2003. Rapid, non-invasive screening for perturbations of metabolism and plant growth using chlorophyll fluorescence imaging. *Plant Physiology* 132 (2), 485 – 493.

Barbedo, J.G.A. 2013. Digital image processing techniques for detecting, quantifying and classifying plant diseases. *SpringerPlus* 2, 660.

Barbedo, J.G.A. 2014. An automatic method to detect and measure leaf disease symptoms using digital image processing. *Plant Dis.* 98, 1709–16.

Barbedo, J.G.A. 2016. A novel algorithm for semi-automatic segmentation of plant leaf disease symptoms using digital image processing. *Trop Plant Pathol.* 41, 210–24.

Baret, F., Guyot, G. 1991. Potentials and limits of vegetation indices for LAI and APAR assessment. *Remote Sens. Environ.* 35, 161–173.

Basnyat, P., McConkey, B. 2001. Using remote sensing information to identify in-field crop productivity. http://paridss.usask.ca/precisionfarm/factsheets/fs17.pdf.

Barton, C.V.M. 2012. Advances in remote sensing of plant stress. *Plant Soil* 354: 41–44. http://dx.doi.org/10.1007/s11104-011-1051-0

Battude, M., Al Bitar, A., Morin, D., Cros, J., Huc, M., Sicre, C.M., Le Dantec, V., Demarez, V., 2016. Estimating Maize Biomass and Yield over Large Areas Using High Spatial and Temporal Resolution Sentinel-2 like Remote Sensing Data. *Remote Sens. Environ.* 184, 668– 681.

Bauriegel, E., Giebel, A., Geyer, M., Schmidt, U., Herppich, W.B. 2011. Early detection of Fusarium infection in wheat using hyper-spectral imaging. *Comp. Electron. Agric.* 75, 304–312.

Bausch, W.C., Diker, K. 2001. Innovative remote sensing techniques to increase nitrogen use efficiency of corn. *Comm. Soil Sci. Plant Anal.* 32(7-8), 1371–1390.

Bausch, W.C., Duke, H.R. 1996. Remote sensing of plant nitrogen status in corn. *Trans. ASAE* 39(5), 1869–1875.

Becker-Reshef, I., Vermote, E., Lindeman, M., Justice, C. 2010. A generalized regression-based model for forecasting winter wheat yields in Kansas and Ukraine using MODIS data. *Remote Sens. Environ.* 114, 1312-1323.

Beek, K.J., Buirough, P.A., MaCormack, D.E. (eds.). 1987. Quantified Land Evaluation Procedures. Proceedings of the International Workshop on Quantified Land Evaluation Procedures, held in Washmgton, DC 27 April-2 May 1986. International Institute for Aerospace Survey and Earth Sciences (TTC) Publication No. 67 ITC, Enschede, the Netherlands.

Belward, A.S., Skøien, J.O. 2015. Who launched what, when and why; trends in global land-cover observation capacity from civilian earth observation satellites. *ISPRS J. Photogram. Remote Sens.* 103, 115-128.

Benedetti, R., Rossini, P. 1993. On the use of NDVI profiles as a tool for agricultural statistics: the case study of wheat yield estimate and forecast in Emilia Romagna. *Remote Sens. Environ.* 45, 311-326.

Berger, B., Parent, B., Tester, M. 2010. High-throughput shoot imaging to study drought responses. *J Exp. Bot.* 61, 3519–28.

Bilder, R.M., Sabb, F.W., Cannon, T.D, London, E.D, Jentsch, J.D, Parker, D.S, Poldrack, R.A, Evans, C Freimer, N.B. 2009. Phenomics: The systematic study of phenotypes on a genome-wide scale. *Neuroscience* 164 (1), 30–42

Biradar, C.M., Xiao, X. 2011. Quantifying the area and spatial distribution of double-and triple-cropping croplands in India with multi-temporal MODIS imagery in 2005. *Inter. J. Remote Sens.* 32, 367-386.

Blackburn, G.A. 1998. Quantifying chlorophylls and caroteniods at leaf and canopy scales: An evaluation of some hyperspectral approaches. *Remote Sens. Environ.* 66, 273–285.

Bock, K.R., Guthrie, E.J., Woods, R.D. 1974. Purification of maize streak virus and its relationship to viruses associated with streak diseases of sugar cane and Panicum maximum. *Ann. Appl. Biol.* 77, 289-296.

Bock, K.R., Guthrie, E.J. Meredith, G. 1977. RNA and protein components of maize streak and cassava latent viruses. *Ann. Appl. Biol.* 85, 305-308.

Bock, C.H., Parker, P.E., Cook, A.Z., Gottwald, T.R. 2008. Characteristics of the perception of different severity measures of citrus canker and the relationships between the various symptom types. *Plant Dis.* 92, 927–39.

Bock, C.H., Poole, G.H., Parker, P.E., Gottwald, T.R. 2010. Plant disease severity estimated visually, by digital photography and image analysis, and by hyperspectral imaging. *Crit. Rev. Plant Sci.* 29, 59–107.

Bock, C.H., Nutter, F.W. Jr. 2011. Detection and measurement of plant disease symptoms using visible-wavelength photography and image analysis. *CAB Rev.* 2011;6: 1–15

Bock, C.H., Barbedo, J.G.A., Del Ponte, E.M., Bohnenkamp, D., Mahlein, A-K. 2020. From visual estimates to fully automated sensor-based measurements of plant disease severity: status and challenges for improving accuracy. *Phytopathology Res.* 2, 9.

Bondeau, A., Smith, P.C., Zaehle, S., Schaphoff, S., Lucht, W., Cramer, W., Gerten, D., LOTZE-CAMPEN, H., Müller, C., Reichstein, M. 2007. Modelling the role of agriculture for the 20th century global terrestrial carbon balance. *Global Change Biol.* 13, 679-706.

Bosque-Pérez, N.A. 2000. Eight decades of maize streak virus research. *Virus Research* 71, 107–121. https:// doi.org/10.1016/S0168-1702(00)00192-1

Braimoh, A.K., Vlek, P.L., Stein, A. 2004. Land evaluation for maize based on fuzzy set and interpolation. *Environ. Managem.* 33, 226-238

Bravo, C., Moshou, D., West, J., McCartney, A., Ramon, H. 2003. Early disease detection in wheat fields using spectral reflectance. *Biosyst Eng.* 84, 137–45.

Breiman, L. 2001. Random forests. *Machine Learning* 45(1), 5–32.

Breiman, L., Cutler, A. 2007. Random forests-classification description. [Online], 2007. Available: http://www.stat.berkeley.edu/~breiman/RandomForests/cc_home.htm, accessed on May 1, 2020.

Broadhurst, D.I., Kell, D.B. 2006. Statistical strategies for avoiding false discoveries in metabolomics and related experiments. *Metabolomics* 2(4) 171-196.

Burke, M., Lobell, D.B., 2017. Satellite-based assessment of yield variation and its determinants in smallholder African systems. Proceedings of the National Academy of Sciences 114(9): pp.2189-2194.

Calderón, R., Navas Cortés, J.A., Lucena León, C., Zarco-Tejada, P.J. 2013. High resolution airborne hyperspectral and thermal imagery for early detection of Verticillium wilt using fluorescence, temperature and narrowband spectral indices. *Remote Sens. Environ.* 139, 231-245.

Campbell, J.B., Wynne, R.H. 2011. Introduction to Remote Sensing. Fifth Edition. The Guilford Press. New York. 667 p.

Carletto, C., Jolliffe, D., Banerjee, R. 2015. From tragedy to renaissance: improving agricultural data for better policies. *The J. Develop. Stud.* 51, 133-148. doi:10.1080/ 00220388.2014.968140.

Carter, G.A. 1994. Ratios of leaf reflectance's in narrow wavebands as indicators of plant stress. *Inter. J. Remote Sens.* 15, 697-703.

Carver, S.J. 1991. Integrating multi-criteria evaluation with geographical information systems. *Inter. J. Geographic. Inform. Syst.* 5(3) 321-339.

Carvalho, S., Schlerf, M., van der Putten, W. H., Skidmore, A. K. 2013. Hyperspectral reflectance of leaves and flowers of an outbreak species discriminates season and successional stage of vegetation. *Inter. J. Applied Earth Obs. Geoinform.* 24, 32-41 .

Casadesús, J., Kaya, Y., Bort, J., Nachit, M. M., Araus, J. L., Amor, S., Ferrazzano, G., Maalouf, F., Maccaferri, M., Martos, V., Ouabbou, H., Villegas, D. 2007. Using vegetation indices derived from conventional digital cameras as selection criteria for wheat breeding in water-limited environments. *Ann. Appl. Biol.* 150: 227–236. http://dx.doi.org/10.1111/j.1744-7348.2007.00116.x

Challinor, A., Wheeler, T., Craufurd, P., Slingo, J., Grimes, D. 2004. Design and optimisation of a large-area process-based model for annual crops. *Agricu. Forest Meteorol.* 124, 99-120.

Chan, J.C-W., Paelinckx, D. 2008. Evaluation of Random Forest and Adaboost tree-based ensemble classification and spectral band selection for ecotope mapping using airborne hyperspectral imagery. *Remote Sens. Environ.* 112, 2999-3011.

Chang, J., Clay, D. A., Dalsted, K., Clay, S., O'Neill, M. 2003. Corn (*Zea mays* L.) Yield Prediction using Multispectral and Multidate Reflectance. *Agron. J.* 95 (6), 1447–1453.

Chapman, S.C., Merz, T., Chan, A., Jackway, P., Hrabar, S., Dreccer, M.F., Holland, E., Zheng, B., Ling, T.J., Jimenez-Berni, J.A. 2014. Pheno-Copter: A low-altitude, autonomous remote-sensing robotic helicopter for high-throughput field-based phenotyping. *Agron.* 4, 279–301.

Chemura, A., Mutanga, O., Dube, T. 2016. Separability of coffee leaf rust infection levels with machine learning methods at Sentinel-2 MSI spectral resolutions. *Precision Agric.* http://dx.doi.org/ 10.1007/s11119-016-9495-0

Cheriyadat, A., Bruce, L.M. 2003. Why principal component analysis is not an appropriate feature extraction method for hyperspectral data. In Proc. 2003 IEEE Geoscience and Remote Sensing Symposium 6, 3420-3422.

Cho, M.A., Skidmore, A., Corsi, F., van Wieren, S.E., Sobhan, I. 2007. Estimation of green grass/herb biomass from airborne hyperspectral imagery using spectral indices and partial least squares regression. *Int. J. Appl. Earth Obs. Geoinf.* 9, 414–424.

Clark, R.N. 1999. Spectroscopy of rocks and minerals, and principles of spectroscopy. *Manual Remote Sens.* 3, 3-58.

Clément, A., Verfaille, T., Lormel, C., Jaloux, B. 2015. A new color vision system to quantify automatically foliar discoloration caused by insect pests feeding on leaf cells. *Biosyst Eng.* 133,

128–40.

Clevers, J.G.P.W. 1999. The use of imaging spectrometry for agricultural applications. *ISPRS J. Photogram. Remote Sens.* 54 (5-6), 299-304.

Coakley, S.M, Scherm, H., Chakraborty, S. 1999. Climate change and plant disease management. *Annual Rev. Phytopathol.* 37, 399–426.

Cobb, J.N., DeClerck, G., Greenberg, A., Clark, R., McCouch, S. 2013. Next-generation phenotyping: requirements and strategies for enhancing our understanding of genotype–phenotype relationships and its relevance to crop improvement. *Theor. Appl. Genet.* 126: 867–887.

Cochrane, M. 2000. Using vegetation reflectance variability for species level classification of hyperspectral data. *Inter. J Remote Sens.* 21, 2075-2087.

Collins, M.G., Steiner, F.R., Rushman, M.J. 2001. Land-use suitability analysis in the United States: historical development and promising technological achievements. *Environ. Manag* 28, 611-621.

Condorelli, G.E., Maccaferri, M., Newcomb, M., Andrade-Sanchez, P., White, J.W., French, A. N., Sciara, G., Ward, R. Tuberosa, R. 2018. Comparative aerial and ground based high-throughput phenotyping for the genetic dissection of NDVI as a Proxy for drought adaptive traits in durum wheat. *Front. Plant Sci.* 9, 893.

Congalton, R., 1991. A review of assessing the accuracy of classification of remotely sensed data. *Remote Sens. Environ.* 37, 35–46

Congalton, R.G., K. Green, 2009. Assessing the Accuracy of Remotely Sensed Data: Principles and Practices, Second edition, CRC press, 183 p.

Crain, J., Mondal, S., Rutkoski, J., Singh, R.P. Poland, J. 2018. Combining high-throughput phenotyping and genomic information to increase prediction and selection accuracy in wheat breeding. *Plant Genome* 2018, 11.

Crain, J.L., Reynolds, M.P., Poland, J.A. 2017. Utilizing high-throughput phenotypic data for improved phenotypic selection of stress adaptive traits in wheat. *Crop Sci.* 57, 648–659. http://dx.doi.org/10.2135/cropsci2016.02.0135

Crain, J.L., Wei, Y., Barker, J., Thompson, S.M., Alderman, P.D., Reynolds, M.P., Zhang, N., Poland, J. 2016. Development and deployment of a portable field phenotyping platform. *Crop. Sci.* 56, 965–975. http://dx.doi.org/10.2135/cropsci2015.05.0290.

Dabrowski, Z.T. 1987. Cicadulina Ghaurii (Hem., Euscelidae): Distribution, Biology and Maize Streak Virus (MSV) Transmission. *J. Appl. Entomol.* 103, 489–496.

Dammer, K. H., Möller, B., Rodemann, B., Heppner, D. 2011. Detection of head blight (*Fusarium* ssp.) in winter wheat by color and multispectral image analyses. *Crop Protection* 30, 420–428.

Datt, B., McVicar, T.R., Van Niel, T.G., Jupp, D.L., Pearlman, J.S. 2003. Preprocessing EO-1 Hyperion hyperspectral data to support the application of agricultural indexes. *IEEE Trans. Geosci. Remote Sens.* 41, 1246-1259.

de Almeida, M. R., Correa, D. N., Rocha, W. F. C., Scafi, F. J. O., Poppi, R. J. 2013. Discrimination between authentic and counterfeit banknotes using Raman spectroscopy and PLS-DA with uncertainty estimation. *Microchemical J.* 109, 170–177.

Deery, D., Jimenez-Berni, J., Jones, H., Sirault, X., Furbank, R. 2014. Proximal remote sensing buggies and potential applications for field-based phenotyping. *Agron.* 4, 349–379.

Delrue, J., Bydekerke, L., Eerens, H., Gilliams, S., Piccard, I., Swinnen, E. 2013. Crop mapping in countries with small-scale farming: A case study for West Shewa, Ethiopia. *Int. J. Remote Sens.* 34, 2566–2582.

Dent, D., Young, A. 1981, Soil survey and land evaluation. George Allen and Unwin, London. UK. 278 p.

Dhau, I., Adam, E., Mutanga, O., Ayisi, K. K. 2018. Detecting the severity of maize streak virus infestations in maize crop using in situ hyperspectral data. *Trans. Royal Soc. S. Africa* 73(1), 8–15.

Dhondt, S., Wuyts, N., Inzé, D. 2013. Cell to whole-plant phenotyping: the best is yet to come. *Trends Plant Sci.* 18, 428–439.

Díaz-Uriarte, R., Alvarez de Andrés, S. 2006. Gene selection and classification of microarray data using random forest. *BMC Bioinformatics*, 7: 1–13.

Dixon, B.L., Hollinger, S.E., Garcia, P., Tirupattur, V. 1994. Estimating corn yield response models to predict impacts of climate change. *J. Agric. Resource Econ.* 19(1), 58-68.

Doraiswamy, P.C., Moulin, S., Cook, P.W., Stern, A. 2003. Crop yield assessment from remote sensing. *Photogram. Engineer. Remote Sens.* 69, 665-674.

Dorigo, W.A. Zurita-Milla, R., de Wit, A.J.W., Brazile, J., Singh, R., Schaepman, M.E. 2007. A review on reflective remote sensing and data assimilation techniques for enhanced agro-ecosystem modelling. *Int. J. Appl. Earth Obs.* 9, 165 –219.

Dorward, A., Chirwa, E. 2011. The Malawi agricultural input subsidy programme: 2005/06 to 2008/09. *Inter. J. Agric. Sustain.* 9(1), 232-247.

Dorward, A., Chirwa, E., Slater, R. 2010. Evaluation of the 2008/9 Agricultural Input Subsidy Malawi: Preliminary Report on Programme Impact. London, School of Oriental African Studies (SOAS).

Drusch, M., Gascon, F., Berger, M. 2010. GMES Sentinel-2 mission requirements document. ESA EOP-SM1163MR-Dr2, 42.

Dube, T., Mutanga, O., Abdel-Rahman, E.M., Ismail, R., Slotow, R. 2015. Predicting Eucalyptus spp. stand volume in Zululand, South Africa: an analysis using a stochastic gradient boosting regression ensemble with multi-source data sets. *Inter. J. Remote Sens.* 36, 3751-3772.

Dube, T., Mutanga, O., Elhadi, A., Ismail, R. 2014. Intra-and-inter species biomass prediction in a plantation forest: testing the utility of high spatial resolution spaceborne multispectral rapideye sensor and advanced machine learning algorithms. *Sensors* 14, 15348-15370.

Duc, T.T. 2006. Using GIS and AHP technique for land-use suitability analysis', International symposium on geoinformatics for spatial infrastructure development in earth and allied sciences, *Citeseer*. http://dx.doi.org/10.1.1.468.4502

Duddu, H.S.N., Johnson, E.N., Willenborg, C.J., Shirtliffe, S.J. 2019. High-throughput UAV image-based method is more precise than manual rating of herbicide tolerance. *Plant Phenomics*, Volume 2019, Article ID 6036453, 9 p.

Dupuis, L., Dumas, C. 1990. Influence of temperature stress on in vitro fertilization and heat shock of protein synthesis in maize (*Zea mays* L.) reproductive systems. *Plant Physiol.* 94, 665-670.

Duro, D.C., Franklin, S.E., Dubé, M.G. 2012. A comparison of pixel-based and objectbased image analysis with selected machine learning algorithms for the classification of agricultural landscapes using SPOT-5 HRG imagery. *Remote Sens. Environ.* 118, 259–272.

Eastman, J.R. 2012, IDRISI Selva Manual; Clark University: Worcester, MA, USA.

Eastman, J.R., Jin, W, Kyem, PAK, Toledano, J. 1995. Raster Procedures for Multi-Criteria/Multi-Objective Decisions. *Photogram. Engineer. Remote Sens.* 61(5), 539-547.

Efron, Y., Kim, S.K., Fajemisin, J.M., Mareck, J.H., Tang, C.Y., Dabrowski, Z.T., Rossel, H.W., Thottappilly, G., Buddenhagen, I.W. 1989. Breeding for resistance to maize streak virus:a

multidisciplinary team approach. *Plant Breed.* 103, 1–36.

Elsheikh, R., Shariff, A.R.B.M., Amiri, F., Ahmad, N.B., Balasundram, S.K., Soom, M.A.M. 2013. Agriculture Land Suitability Evaluator (ALSE): A decision and planning support tool for tropical and subtropical crops. *Comput. Electron. Agric.* 93, 98-110.

Elshire, R.J., Glaubitz, J.C., Sun, Q., Poland, J.A., Kawamoto, K., Buckler, E.S., Mitchell, S.E. 2011. A robust, simple genotyping-by-sequencing (GBS) approach for high diversity species. *PLoS ONE* 6:e19379

Engelbrecht, A.H.P. 1982. Chloroplast development in streak infected *Zea mays. South African Journal of Botany* 1(3), 80.

Erives, H., Fitzgerald, G.J. 2005. Automated registration of hyperspectral images for precision agriculture. *Comput. Electron. Agric.* 47: 103-119.

Ezeh, A.C., Bongaarts, J., Mberu, B. 2012. Global population trends and policy options. *The Lancet* 380, 142-148.

FAO 1976, A framework for land evaluation. Soils bulletin 32. Food and Agriculture Organization of the United Nations, Rome.

FAO. 2010. FAOSTAT. http://faostat.fao.org/.

FAO. 2012. FAOSTAT: http://faostat.fao.org/.

Fahlgren, N., Gehan, M. A., Baxter, I., 2015. Lights, camera, action: high-throughput plant phenotyping is ready for a close-up. *Current Opinion in Plant Biology* 24, 93–99.

Fajemisin, J.M., Kim, S.K., Efron, Y., Alam, M.S. 1984. Breeding for durable disease resistance in tropical maize with special reference to maize streak virus. FAO Plant Production and Protection Paper, 55, 71 pp.

Fang, H., Liang, S., Hoogenboom, G., Teasdale, J., Cavigelli, M. 2008. Corn-yield estimation through assimilation of remotely sensed data into the CSM-CERES-Maize model. *Inter. J. Remote Sens.* 29 (10), 3011–3032.

Farmaha, B.S., Lobell, D.B., Boone, K.E., Cassman, K.G., Yang, H.S., Grassini, P. 2016. Contribution of persistent factors to yield gaps in high-yield irrigated maize. *Field Crops Res.* 186, 124-132.

Fassnacht, K. S., Gower, S. T., MacKenzie, M. D., Nordheim, E. V., Lillesand, T. M. 1997. Estimating the leaf area index of north central Wisconsin forests using the Landsat Thematic Mapper. *Remote Sens. Environ.* 61, 229–245.

Feizizadeh, B., Blaschke, T. 2013. Land suitability analysis for Tabriz County, Iran: a multi-criteria evaluation approach using GIS. *J. Environ. Planning Management* 56(1) 1-23.

Fensholt, R., Sandholt, I. 2005. Evaluation of MODIS and NOAA AVHRR vegetation indices with in situ measurements in a semi-arid environment. *Inter. J. Remote Sens.* 26, 2561-2594.

Ferencz, Cs., Bognar, P., Lichtenberger, J., Hamar, D., Tarcsai, Gy., Timar, G., Molnar, G., Pasztor, Sz., Steinbach, P., Szekely, B., Ferencz, O. E., Ferencz-Arkos. I. 2004. Crop yield estimation by satellite remote sensing. *Inter. J. Remote Sens.* 25 (20), 4113-4149.

Ferguson, M.E., Hearne, S.J., Close, T.J., Wanamaker, S., Moskal, W.A., Town, C.D., de Young, J., Marri P.R., Rabbi, I.Y., de Villiers, E.P. 2011. Identification, validation and high-throughput genotyping of transcribed gene SNPs in cassava. *Theor Appl Genet.*

Fiorani, F., Schurr, U. 2013. Future scenarios for plant phenotyping. *Annual Reviews in Plant Biology* 64: 267–291.

Fischer, R. A., Rees, D., Sayre, K. D., Lu, Z.-M., Condon, A. G., Larque Saavedra, A. 1998. Wheat yield progress associated with higher stomatal conductance and photosynthetic rate, and

cooler canopies. *Crop Sci.* 38, 1467-1475.

Fortes, C., Demattê, J. A. M. 2006. Discrimination of sugarcane varieties using Landsat 7, ETM+ spectral data. *Int. J. Remote Sens*. 27, 1395–1412.

Frank, L., Norbert, K., David, S., Achim, W., Andreas, H. 2015. Remote, aerial phenotyping of maize traits with a mobile multi-sensor approach Andreas. *Plant Methods* 11, 9

Franklin, P., Pearlstine, L., Dewitt, B., Smith ,S., Watts A., Ifju, P. 2006. Autonomus unmanned aerial vehicle (UAV) for ecological research.http://www.wec.ufl.edu/coop/print/posters/2006watts.pdf.

Freund, J.T. 2005. Estimating Crop Production in Kenya: A Multi-Temporal Remote Sensing Approach. PhD Dissertation, University of California, Santa Barbara, USA.

Fritz, S., See, L., McCallum, I., You, L., Bun, A., Moltchanova, E., Duerauer, M., Albrecht, F., Schill, C., Perger, C., Havilk, P. *et al*. 2015. Mapping global cropland and field size. *Global Change Biology* 21(5), 1980-1992.

Furbank, R.T., Tester, M. 2011. Phenomics – technologies to relieve the phenotyping bottleneck. *Trends Plant Sci.* 16: 635–644.

Galvão, L. S., Formaggio, A.R., Tissot, D.A. 2005. Discrimination of sugarcane varieties in Southeastern Brazil with EO-1 Hyperion data. *Remote Sens. Environ.* 94, 523–534.

Galvão, L. S., Formaggio, A.R., Tissot, D.A. 2006. The influence of spectral resolution on discriminating Brazilian sugarcane varieties. *Inter. J. Remote Sens.* 27 (4), 769–777.

Galvão, L. S., Roberts, D. A., Formaggio, A.R., Numata, I., Breunig, F.M. 2009. View angle effects on the discrimination of soybean varieties and on the relationships between vegetation indices and yield using off-nadir Hyperion data. *Remote Sens. Environ.* 113, 846–856.

Gao, X., Huete, A.R., Ni, W., Miura, T. 2000. Optical–biophysical relationships of vegetation spectra without background contamination. *Remote Sens. Environ.* 74, 609-620.

Garcia-Ruiz, F., Sankaran, S., Maja, J.M., Lee, W.S., Rasmussen, J., Ehsani, R. 2013. Comparison of two aerial imaging platforms for identification of Huanglongbing-infected citrus trees. *Comput. Electron. Agric.* 91, 106–115.

Garrett, K.A, Dendy, S.P, Frank, E.E, Rouse, M.N, Travers, S.E. 2006. Climate change effects on plant disease: genomes to ecosystems. *Annual Rev. Phytopathol.* 44, 489–509.

Geipel, J., Link, J., Wirwahn, J., Claupein, W. 2016. A programmable aerial multispectral camera system for in-season crop biomass and nitrogen content estimation. *Agriculture* 6(1), 4. https://doi.org/10.3390/agriculture6010004.

Ghanem, M.E., Marrou, H., Sinclair, T.R. 2015. Physiological phenotyping of plants for crop improvement. *Trends in Plant Science* 20 (3), 139-144

Ghimire, B., Rogan, J., Rodríguez-Galiano, V., Panday, P., Neeti, N. 2012. An evaluation of bagging, boosting, and random forests for land-cover classification in Cape Cod, Massachusetts, USA. *GIScience Remote Sens.* 49 (5), 623–643. http://dx.doi.org/10.2747/1548-1603.49.5.623.

Gholizadeh, A., Boruvka, L., Saberioon, M., Vašát, R. 2013. Visible, near-infrared, and mid-infrared spectroscopy applications for soil assessment with emphasis on soil organic matter content and quality: Stateof-the-art and key issues. *Appl. Spectroscopy* 67, 1349–1362.

Gislason, P.O., Benediktsson, J.A., Sveinsson, J.R. 2004. Random forest classification of multisource remote sensing and geographic data. In: Geoscience and remote sensing symposium, 2004 (IGARSS'04) (Vol 2, pp. 1049–1052). Piscataway: IEEE International

Gitelson, A.A. 2011. Remote Sensing Estimation of Crop Biophysical Characteristics at Various Scales.

pp 329 - 358. In: Thenkabail, A., Lyon, P.S., Huete, J.G. (Eds), Hyperspectral remote sensing of vegetation. CRC Press. CRC Press, Taylor and Francis Group. New York. 782 p.

Gitelson, A.A., Kaufman, Y.J., Merzlyak, M.N. 1996. Use of a green channel in remote sensing of global vegetation from EOS-MODIS. *Remote Sens. Environ.* 58, 289–298.

Gitelson, A.A.. Merzlyak, M.N. 1994. Quantitative estimation of chlorophyll-a using reflectance spectra: Experiments with autumn chestnut and maple leaves. *J. Photochem. Photobiology B: Biology* 22(3). 247–252.

Gitelson, A.A., Peng, Y., Masek, J.G., Rundquist, D.C., Verma, S., Suyker, A., Baker, J.M., Hatfield, J.L., Meyers, T. 2012. Remote estimation of crop gross primary production with Landsat data. *Remote Sens. Environ.* 121, 404-414.

Gitelson, A.A., Viná, A., Ciganda, V., Rundquist, D.C., Arkebauer, T.J. 2005. Remote estimation of canopy chlorophyll content in crops. *Geophysical Res. Letters* 32, L08403.

Godfray, H.C.J., Beddington, J.R., Crute, I.R., Haddad, L., Lawrence, D., Muir, J.F., Pretty, J., Robinson, S., Thomas, S.M., Toulmin, C. 2010. Food security: the challenge of feeding 9 billion people. *Science* 327, 812–818.

Gommes, R. 1998. Overview of variables used agrometeorological crop forecasting tools. pp 323-326. In: Rijks, D., Terres, J.M., Vossen, P. (Eds.), Agrometeorological application for regional crop monitoring and production assessment. Space Research Institute, EC Joint Research Centre, Italy, European Commission, 516 p.

Gong, P., Wang, J., Yu, L., Zhao, Y.C., Zhao, Y.Y., Liang, L., Niu, Z.G. *et al*. 2013. Finer Resolution Observation and Monitoring of Global Land Cover: First Mapping Results with Landsat TM and ETM+ Data. *Inter. J. Remote Sens.* 34 (7), 2607–2654. http://dx.doi.org/10.1080/01431161.2012.748992.

Govender, M., Chetty, K., Bulcock, H. 2007. A review of hyperspectral remote sensing and its application in vegetation and water resource studies. *Water SA* 33, 145-151.

Grenzdörffer, G.J., Engelb, A., Teichert, B. 2008. The photogrammetric potential of low-cost UAVs in forestry and agriculture. *The International Archives of the Photogrammetry, Remote Sensing and Spatial Information Sciences*. Vol. XXXVII. Part B1. Beijing, 2008

Groten, S. 1993. NDVI—crop monitoring and early yield assessment of Burkina Faso. *Remote Sens.* 14, 1495-1515.

Guan, J., Nutter, F.W. Jr. 2003. Quantifying the intrarater repeatability and interrater reliability of visual and remote sensing disease-assessment methods in the alfalfa foliar pathosystem. *Canadian J. Plant Pathology* 25 (2), 143–149.

Guanter, L., Kaufmann, H., Segl, K., Foerster, S., Rogass, C., Chabrillat, S., Kuester, T., Hollstein, A., Rossner, G., Chlebek, C., Straif, C., *et al*. 2015. The EnMAP spaceborne imaging spectroscopy mission for earth observation. *Remote Sens.* 7(7), 8830-8857.

Guindin-Garcia, N. 2010. Estimating maize grain yield from crop biophysical parameters using remote sensing. Theses, Dissertations, and Student Research in Agronomy and Horticulture. Paper 21. http://digitalcommons.unl.edu/agronhortdiss/21

Guthrie, E.J., 1978. Measurement of yield losses caused by maize streak disease. *Plant Dis. Reptr*. 62 (10), 839-840.

Haghighattalab, A., Crain, J., Mondal, S., Rutkoski, J., Singh, R.P., Poland, J. 2017. Application of geographically weighted regression to improve grain yield prediction from unmanned aerial system imagery. *Crop Sci.* 57(5), 2478–2489. https://doi.org/10.2135/cropsci2016.12.1016

Haghighattalab, A., Pérez, L. G., Mondal2, S., Singh, D., Schinstock, D., Rutkoski, J., Ortiz-Monasterio, I., Singh, R.P., Goodin, D., Poland, J. 2016. Application of unmanned aerial systems for high throughput phenotyping of large wheat breeding nurseries. *Plant Methods* 12, 35 https://doi.org/10.1186/s13007-016-0134-6

Hairmansis, A., Berger, B., Tester, M., Roy, S. J. 2014. Image-based phenotyping for non-destructive screening of different salinity tolerance traits in rice. *Rice* 7, 16. https://doi.org/10.1186/s12284-014-0016-3

Han, L., Yang, G., Dai, H., Xu, B., Yang, H., Feng, H., Li, Z., Yang, X. 2019. Modeling maize above-ground biomass based on machine learning approaches using UAV remote-sensing data. 2019. *Plant Methods* 15, 10. https://doi.org/10.1186/s13007-019-0394-z

Hannerz, F., Lotsch, A. 2008. Assessment of remotely sensed and statistical inventories of African agricultural fields. *Inter. J. Remote Sens* 29, 3787-3804.

Hansen, P. M., Schjoerring, J.K. 2003. Reflectance measurement of canopy biomass and nitrogen status in wheat crops using normalized difference vegetation indices and partial least squares regression. *Remote Sens. Environ.* 86, 542–553.

Hatfield, J.L., Prueger, J.H. 2015. Temperature extremes: effect of plant growth and development', *Weather and Climate Extremes* 10, 4 - 10.

Hayes, M., Decker, W. 1996. Using NOAA AVHRR data to estimate maize production in the United States Corn Belt. *Remote Sens.* 17, 3189-3200.

Herrero, M.P., Johnson, R.R. 1980. High temperature stress and pollen viability in maize. *Crop Sci.* 20, 796 - 800.

Herrmann, I. Shapira, U., Kinast, S., Karnieli, A., Bonfil, D.J. 2013. Ground-level hyperspectral imagery for detecting weeds in wheat fields. *Precision Agric*. Published online: 13 June 2013. https://doi.org/10.1007/s11119-013-9321-x

Hickey, L.T, Hafeez, A.N., Robinson, H., Jackson, S.A., Leal-Bertioli, S.C.M., Tester, M. Gao, C., Godwin I.D., Hayes, B.J., Wulff, B.H. 2019. Breeding crops to feed 10 billion. *Nature Biotechnology* 37, 744–754. https://doi.org/10.1038/s41587-019-0152-9.

Hinton, G.E., Salakhutdinov, R.R. 2006. Reducing the dimensionality of data with neural networks. *Science* 313, 504 - 507.

Hobro, A. J., Kuligowski, J., Doll, M., Lendl, B. 2010. Differentation of walnut wood species and stem treatment using ATR-FTIR and partial least square discriminant analysis (PLS-DA). *Analytical and Bioanalytical Chemistry* 398 (6), 2713 – 2722.

Hoffer, N.V., Coopmans, C., Jensen A.M., Chen, Y-Q. 2014. A Survey and Categorization of Small Low-Cost Unmanned Aerial Vehicle System Identification. *J. Intell. Robot Syst.* 74, 129–145 http://dx.doi.org/10.1007/s10846-013-9931-6

Hosoi, F., Omasa, K. 2009. Estimating vertical plant area density profile and growth parameters of a wheat canopy at different growth stages using three dimensional portable lidar imaging. *ISPRS J. Photogramm. Remote Sens*. 64, 151–158. https://doi.org/10.1016/j.isprsjprs.2008.09.003

Houle, D., Govindaraju, D.R., Omholt, S. 2010. Phenomics: the next challenge. *Nat. Rev. Genet.* 11, 855–866

Hu, Y., Knapp, S., Schmidhalter, U. 2020. Advancing High-Throughput Phenotyping of Wheat in Early Selection Cycles. *Remote Sens.* 12, 574. https://doi.org/10.3390/rs12030574

Huajun, T, Van Ranst, E. 1992. Testing of fuzzy set theory in land suitability assessment for rainfed grain maize production. *Pedologie* 52, 129-147.

Huang, C., Davis, L.S., Townshend, J.R.G. 2002. An Assessment of Support Vector Machines for Land Cover Classification. *International Journal of Remote Sensing* 23 (4): 725–749. https://doi.org/10.1080/01431160110040323.

Huang, W., Lamb, D.W., Niu, Z., Zhang, Y., Liu, L., Wang, J. 2007. Identification of yellow rust in wheat using in-situ spectral reflectance measurements and airborne hyperspectral imaging. *Precis. Agric.* 8, 187–197.

Huang, X., Pan, W., Park, S., Han, X., Miller L.W., Hall, J. 2004. Modeling the relationship between LVAD support time and gene expression changes in the human heart by penalized partial least squares. *Bioinformatics* 20 (6), 888–894.

Huete, A.R. 1988. A soil adjusted vegetation index (SAVI). *Int. J. Remote Sens.* 9, 295–309.

Huete, A., Didan, K., Miura, T., Rodriguez, E.P., Gao, X., Ferreira, L.G. 2002. Overview of the radiometric and biophysical performance of the MODIS vegetation indices. *Remote Sens. Environ.* 83, 195-213.

Hunt, E., Hively, W.D., Daughtry, C.S., McCarty, G.W., Fujikawa, S.J., Ng, T., Tranchitella, M., Linden, D.S., Yoel, D.W. 2008. Remote sensing of crop leaf area index using unmanned airborne vehicles. In: Proceedings of the Pecora 17 Symposium, Denver, CO.

Hurvich, C.M., Tsai, C.L. 1989. Regression and time series model selection in small samples *Biometrika* 76, 297–307.

Hyten, D., Song, Q., Fickus, E., Quigley, C., Lim, J., Choi, I., Hwang, E., Pastor-Corrales, M., Cregan, P. 2010. High-throughput SNP discovery and assay development in common bean. *BMC Genomics*. https://doi.org/10.1186/1471-2164-11-475

IBP Breeding Management System, Version 10. 2018. The Integrated Breeding Platform. https://www.integratedbreeding.net/breeding-management-system. October 2018.

Ilker, E., Tonk, F.A., Tosun, M., Tatar, O. 2013. Effects of direct selection process for plant height on some yield components in common wheat (Triticum aestivum) genotypes. *Int. J. Agric. Biol.* 15, 795–797.

IPCC. 2007. Fourth assessment report: synthesis. 2007. http://www.ipcc.ch/ pdf/assessment-report/ar4/syr/ar4_syr.pdf.

IPCC. 2014. Climate change: Synthesis report. In Contribution of Working Groups I, II and III to the Fifth Assessment Report of the Intergovernmental Panel on Climate Change; Pachauri, R.K., Meyer, L.A., Eds.; IPCC: Geneva, Switzerland, 2014.

Ismail, R., Mutanga, O. 2010. A comparison of regression tree ensembles: Predicting Sirex noctilio induced water stress in Pinus patula forests of KwaZulu-Natal, South Africa. *Inter. J. Applied Earth Obs. Geoinform.* 12 S45-S51.

Jackson, R., Slater, P., Pinter, P. 1983. Discrimination of growth and water stress in wheat by various vegetation indices through clear and turbid atmospheres. *Remote Sens. Environ.* 13, 187-208.

Jansen, M. Bergsträsser, S. Schmittgen, S. Müller-Linow, M., Rascher, U. 2014. Non-invasive spectral phenotyping methods can improve and accelerate cercospora disease scoring in sugar beet breeding. *Agriculture* 4 (2), 147–158.

Jarolmasjed, S., Sankaran, S., Marzougui, A., Kostick, S., Si, Y., Quirós Vargas, J.J., Evans, K. (2019) High-Throughput Phenotyping of Fire Blight Disease Symptoms Using Sensing Techniques in Apple. *Front. Plant Sci.* 10, 576. https://doi.org/10.3389/fpls.2019.00576

Jayne, T.S., Rashid, S. 2010. The value of accurate crop production forecasts. MSU International

Development Working Paper 108. October 2010. Department of Agricultural, Food and Resources Economics, Michigan State University, East Lansing, Michigan 48824-1039, USA. 13p.

Jenks, G. F. 1977. Optimal data classification for chloropleth maps. Occasional paper No. 2. Lawrence, Kansas: University of Kansas, Department of Geography.

Jensen, J.R. 1996. Introductory Digital Image Processing: A Remote Sensing Perspective, Pearson Prentice Hall, New Jersey, USA.

Jensen, J.R. 2009. Remote sensing of the environment: An earth resource perspective 2/e. Pearson Education India. 608 p.

Jiang, Z., Huete, A.R., Didan, K., Miura, T. 2008. Development of a two-band enhanced vegetation index without a blue band. *Remote Sens. Environ*. 112: 3833–3845.

Jimenez-Berni, A., Zarco-Tejada, P.J., Suárez, L., Fereres, E. 2009. Thermal and narrowband multispectral remote sensing for vegetation monitoring from an unmanned aerial vehicle. *IEEE Trans. Geosci. Remote Sens.* 47: 722–738.

Jin, X., Liu, S., Baret, F., Hemerlé, M.. Comar, A. 2017. Estimates of plant density of wheat crops at emergence from very low altitude UAV imagery. *Remote Sens. Environ*. 198: 105–114.

Johnson, D.M. 2014. An assessment of pre-and within-season remotely sensed variables for forecasting corn and soybean yields in the United States. *Remote Sens. Environ.* 141, 116-128.

Jones, J., Keating, B., Porter, C. 2001. Approaches to modular model development. *Agric. Systems* 70, 421-443.

Jones, R.J., Ouattar, S., Crookston, R.K. 1984. Thermal environment during endosperm cell division and grain filling in maize: effects on kernel growth and development in vitro. *Crop Sci*. 24, 133-137.

Jourdan-Ruf, C., Marchand, J.L., Peterschmitt, M., Reynaud, B., Dintinger. J. 1995. Maize streak, maize stripe and maize mosaic virus diseases in the tropics (Africa and islands in the Indian Ocean). *Agriculture et développement, Special Issue* (December 1995), 1995, 55-69

Juliana, P., Montesinos-López, O.A., Crossa, J., Mondal, S., González Pérez, L., Poland, J., Huerta-Espino, J., Crespo-Herrera, L., Govindan, V., Dreisigacker, S., Shrestha, S., Pérez-Rodríguez, P., Pinto Espinosa, F., Singh, R. P. 2018. Integrating genomic-enabled prediction and high-throughput phenotyping in breeding for climate-resilient bread wheat. *Theor. Appl. Genet.* 2018, 132, 177–194.

Justice, C., Townshend, J., Vermote, E., Masuoka, E., Wolfe, R., Saleous, N., Roy, D., Morisette, J. 2002. An overview of MODIS Land data processing and product status. *Remote Sens. Environ.* 83, 3-15.

Keshavarzi, A., Sarmadian, F., Heidari, A., Omid, M. 2010. Land suitability evaluation using fuzzy continuous classification: a case study - Ziaran region. *Modern Applied Sci.* 4, 72.

Kinoshita, R., Moebius-Clune, B.N., van Es, H.M., Hively, W.D., Bilgilis, A.V. 2012. Strategies for soil quality assessment using visible and near-infrared reflectance spectroscopy in a Western Kenya chronosequence. *Soil Sci. Soc. Amer. J.* 76, 1776–1788.

Khot, L.R., Sankaran, S., Cummings, T., Johnson, D., Carter, A.H., Serra, S., Musacchi, S., 2014. Applications of unmanned aerial system in Washington state agriculture, Paper No. 1637. In: 12th International Conferenceon Precision Agriculture, Sacramento, CA, July 20–23.

Kloppers, F. 2005. Maize diseases: reflection on the 2004/2005 season. 2005. Available at: http://saspp.org/index2.php?option=com_content&do_ pdf=1&id=2

Kogan, F. 1990. Remote sensing of weather impacts on vegetation in non-homogeneous areas.

Inter. J. Remote Sens. 11, 1405-1419.

Kuri, F., Murwira, A., Murwira, K.S., Masocha, M. 2014. Predicting maize yield in Zimbabwe using dry dekads derived from remotely sensed Vegetation Condition Index. *Inter. J. Applied Earth Obs. Geoinformation* 33, 39-46. http://dx.doi.org/10.1016/j.jag.2014.04.021

Kuska, M., Wahabzada, M., Leucker, M., Dehne, H-W., Kersting, K., Oerke, E-C., Steiner, U., Mahlein, A-K. 2015. Hyperspectral phenotyping on the microscopic scale: towards automated characterization of plant-pathogen interactions. *Plant Methods* 11, 28.

Laliberte A., Rango A., Slaughter A. 2006. Unmanned Aerial Vehicle (UAVs) for rangeland remote sensing. Proc. 3rd Annual Symposium research insights in semiarid ecosystems RISE. USDA-ARS Walnut Experimental Watershed.

Lamelas, M., Marinoni, O., Riva, J., Hoppe, A. 2012. Comparison of multi-criteria analysis techniques for environmental decision making on industrial location. In C. Jao (Ed.), Decision support systems (pp. 197–221). Vukova: InTech Publisher.

Lamb, D., Brown, R. 2001. PA—precision agriculture: Remote-sensing and mapping of weeds in crops. *J. Agric. Engineer. Res* 78: 117-125.

Lawrence, R.L., Wood, S.D., Sheley, R.L. 2006. Mapping invasive plants using hyperspectral imagery and Breiman Cutler classifications (Random Forest). *Remote Sens. Environ.* 100, 356-362.

Lebedev, A.V., Westman, E., Van Westen, G.J.P., Kramberger, M.G., Lundervold, A., Aarsland, D., Soininen, H., Kłoszewsk, I., Mecocci P., Tsolaki, M., Vellas. B., Lovestone, S., Simmons, A. 2014. Random Forest ensembles for detection and prediction of Alzheimer's disease with a good between cohort robustness. *NeuroImage: Clinical* 6, 115–125.

Lelong, C.C.D., Burger, P., Jubelin, G., Roux, B., Labbé, S., Baret, F. 2008. Assessment of Unmanned Aerial Vehicles Imagery for Quantitative Monitoring of Wheat Crop in Small Plots. *Sensors* 8, 3557-3585

Leroux, L., Jolivot, A., Bégué, A., Seen, D.L., Zoungrana, B. 2014. How reliable is the MODIS land cover product for crop mapping Sub-Saharan agricultural landscapes? *Remote Sens.* 6, 8541-8564.

Lewis, J., Rowland, J., Nadeau, A. 1998. Estimating maize production in Kenya using NDVI: some statistical considerations. *Inter. J. Remote Sens.* 19, 2609-2617.

Liaw, A., Wiener, M. 2002. Classification and regression by random forest. *R News*, 2/3: 18–22.

Li, C., Wang, J., Wang, L., Hu, L., Gong. P. 2014. Comparison of Classification Algorithms and Training Sample Sizes in Urban Land Classification with Landsat Thematic Mapper Imagery. *Remote Sens.* 6 (2), 964–983. doi:10.3390/rs6020964.

Li, X-L. Yi, S-L., He, S-L., Lv, Q., Xie, R-J., Zheng Y-Q., Deng, L. 2016. Identification of pummelo cultivars by using Vis/NIR spectra and pattern recognition methods. *Prec. Agric.* 17(3), 365–374.

Li, Y., Zhou, Q., Zhou, J., Zhang, G., Chen, C., Wang, J. 2014. Assimilating remote sensing information into a coupled hydrology-crop growth model to estimate regional maize yield in arid regions. *Ecological Modelling* 291, 15-27.

Liebisch, F., Kirchgessner, N., Schneider, D., Walter, A., Hund, A. 2015. Remote, aerial phenotyping of maize traits with a mobile multi-sensor approach. *Plant Methods* 11(9) 1-20. https://doi.org/10.1186/s13007-015-0048-8

Lillesand, T., Kiefer, R.W., Chipman, J. 2014. Remote sensing and image interpretation. John Wiley and Sons. 7th Edition. West Sussex. 720 p.

Lin, W.S. Yang, C.M., Kuo, B-J. 2012. Classifying cultivars of rice (Oryza sativa L.) based on corrected

canopy reflectance spectra data using the orthogonal projections to latent structures (O-PLS) method. *Chemometr. Intell. Lab. Syst.* 115, 25–36.

Lin, X., L. Sun, Y. Li, Z. Guo, Y. Li, K. Zhong, Q. Wang, X. Lu, Y. Yang, G. Xu. 2010. A Random Forest of combined features in the classification of cut tobacco based on gas chromatography fingerprinting. *Talanta*, *82 (4),* 1571–1575. https://doi.org/10.1016/j. talanta.2010.07.053

Livingstone, G, Schonberger, S., Delaney, S. 2011. Sub-Saharan Africa: The State of Smallholders in Agriculture. Paper presented at the IFAD Conference on New Directions for Smallholder Agriculture, 24–25 January 2011, Rome: International Fund for Agricultural Development.

Liu, J., Pattey, E., Miller, J.R., McNairn, H., Smith, A., Hu, B. 2010. Estimating crop stresses, aboveground dry biomass and yield of corn using multi-temporal optical data combined with a radiation use efficiency model. *Remote Sens. Environ.* 114, 1167-1177.

Lobell, D.B. 2013. The use of satellite data for crop yield gap analysis. *Field Crops Res.* 143, 56-64.

Lobell, D.B., Asner, G.P., Ortiz-Monasterio, J.I., Benning, T.L. 2003. Remote sensing of regional crop production in the Yaqui Valley, Mexico: estimates and uncertainties. *Agric. Ecosystems Environ.* 94: 205-220.

Lobell, D.B., Ortiz-Monasterio, J.I., Asner, G.P., Naylor, R.L., Falcon, W.P. 2005. Combining field surveys, remote sensing, and regression trees to understand yield variations in an irrigated wheat landscape. *Agron. J.* 97, 241-249.

Los, S.O. 1998. Linkages between global vegetation and climate: an analysis based on noaa advanced very high resolution data. Ph.D. Thesis, Vrije Universiteit, Amsterdam, The Netherlands.

Lu, D., Weng, Q. 2007. A Survey of Image Classification Methods and Techniques for Improving Classification Performance. *Intern. J. Remote Sens.* 28 (5), 823– 870. http://dx.doi.org/10.1080/01431160600746456.

Luo, W., Huan, S., Fu, H., Wen, G., Cheng, H., Zhou, J, Wu, H., Shen, G., Yu, R. 2011. Preliminary study on the application of near infrared spectroscopy and pattern recognition methods to classify different types of apple samples, *Food Chem.* 128 (2), 555-561.

Luo, Y., Teng, P.S, Fabellar, N.G, TeBeest, D.O. 1998. The effects of global temperature change on rice leaf blast epidemics: a simulation study in three agroecological zones. *Agric. Ecosystems Environ.* 68, 187–96.

Lynch, A.L., Holt, M.T., Gray, A.W. 2007. Modeling Technical Change in Midwest Corn Yields, 1895-2005: A Time Varying-Regression Approach. In, 2007 Annual Meeting, July 29-August 1, 2007, Portland, Oregon TN: American Agricultural Economics Association (New Name 2008: Agricultural and Applied Economics Association).

Maas, S.J., 1988. Use of remotely-sensed information in agricultural crop growth models. *Ecol. Mod.* 41, 247–268.

Madden, H. 1978. Comments on the Savitzky–Golay convolution method for least-squares fit smoothing and differentiation of digital data. *Anal. Chem.* 50 (9), 1383–1386.

Madden, L.V., Hughes, G., van den Bosch, F. 2007. The study of plant disease epidemics. St Paul: APS Press; 2007.

Mahlein, A-K. 2016. Plant disease detection by imaging sensors – parallels and specific demands for precision agriculture and plant phenotyping. *Plant Dis.* 100, 241–251. http://dx.doi.org/10.1094/pdis-03-15-0340-fe

Mahlein, A-K., Oerke, E-C., Steiner, U. Dehne, H-W. 2012. Recent advances in sensing plant diseases

for precision crop protection. *Eur J Plant Pathol* 133, 197–209. https://doi.org/10.1007/s10658-011-9878-z

Mahlein, A-K., Rumpf, T., Welke, P., Dehne, H.W., Plümer, L., Steiner, U., Oerke, E.C. 2013. Development of spectral indices for detecting and identifying plant diseases. *Remote Sens. Environ*. 128: 21–30.

Mahlein, A.K., Steiner, U., Dehne, H.W., Oerke, E.C. 2010. Spectral signatures of sugar beet leaves for the detection and differentiation of diseases. *Precis. Agric*. 11, 413–431.

Malczewski, J. 2004. GIS-based land-use suitability analysis: a critical overview. *Progress in Planning* 62(1) 3 – 65.

Malczewski, J. 2006a. GIS-based multicriteria decision analysis: a survey of the literature. *Inter. J. Geo. Inform. Sci.* 20(7), 703-726.

Malczewski, J. 2006b. Ordered weighted averaging with fuzzy quantifiers: GIS-based multicriteria evaluation for land-use suitability analysis. *Intern. J. Applied Earth Obs. Geoinform.* 8(4), 270-277.

Maimaitijiang, M., Ghulam, A., Sidike, P., Hartling, S., Maimaitiyiming, M., Peterson, K., Shavers, E., Fishman, J., Peterson, J., Kadam, S., , Burken, J., Fritschi, F. 2017. Unmanned Aerial System (UAS)-based phenotyping of soybean using multi-sensor data fusion and extreme learning machine. *ISPRS J. Photogramm. Remote Sens.* 134, 43–58.

Major, D., Baret, F., Guyot, G. 1990. A ratio vegetation index adjusted for soil brightness. *Inter. J. Remote Sens.* 11, 727-740.

Malahlela, O., Cho, M.A., Mutanga, O. 2014. Mapping canopy gaps in an indigenous subtropical coastal forest using high-resolution WorldView-2 data. *Inter. J. Remote Sens.* 35, 6397-6417.

Manatsa, D., Nyakudya, I.W., Mukwada, G., Matsikwa, H. Maize yield forecasting for Zimbabwe farming sectors using satellite rainfall estimates. *Nat. Hazards* 59, 447–463. https://doi.org/10.1007/s11069-011-9765-0

Marinoni, O. 2005. A stochastic spatial decision support system based on PROMETHEE. *Inter. J. Geographical Information Science* 19(1), 51-68.

Mariotto, I., Thenkabail, P.S., Huete, A., Slonecker, E.T., Platonov, A. 2013. Hyperspectral versus multispectral crop-productivity modeling and type discrimination for the HyspIRI mission. *Remote Sens. Environ.* 139, 291–305 .

Martin, D.P., Rybicki, E.P. 1998. Microcomputer-based quantification of maize streak virus symptoms in *Zea mays*. *Phytopathology* 88, 422–7.

Martin, D.P, Shepherd, D.N. 2009. The epidemiology, economic impact and control of maize streak disease. *Food Sec.* 1, 305–315. https://doi.org/10.1007/s12571-009-0023-1

Maselli, F., Conese, C., Petkov, L., Gilabert, M-A. 1992. Use of NOAA-AVHRR NDVI data for environmental monitoring and crop forecasting in the Sahel. Preliminary results. *Inter. J. Remote Sens.* 13, 2743-2749.

Maselli, F., Romanelli, S., Bottai, L., Maracchi, G. 2000. Processing of GAC NDVI data for yield forecasting in the Sahelian region. *Inter. J. Remote Sens.* 21, 3509-3523.

Masuka, B., Araus, K.J., Sonder, L. Das, B., Cairns, J.E. 2012. Deciphering the code: successful abiotic stress phenotyping for molecular breeding. *J. Integr. Plant Biol.* 54, 238–249.

Masuka, B., Magorokosho, C., Olsen, M., Atlin, G. N., Bänziger, M., Pixley, K. V., Vivek, B. S., Labuschagne, M., Matemba-Mutasa, R., Burgueño, J., Macrobert, J., Prasanna, B. M., Das, B., Makumbi, D., Tarekegne, A., Crossa, J., Zaman-Allah, M., van Biljon, A., Cairns, J. E. 2016.

Gains in Maize Genetic Improvement in Eastern and Southern Africa: II. CIMMYT Open-Pollinated Variety Breeding Pipeline. *Crop Sci.* 57 (1), 180–191.

Maxwell, A. E., Warner, T. A., Fang, F. 2018. Implementation of machine-learning classification in remote sensing: an applied review. *Inter. J. Remote Sens.* 39(9), 2784–2817 https://doi.org/10.1080/01431161.2018.1433343

Mendas, A., Delali, A. 2012. Integration of MultiCriteria Decision Analysis in GIS to develop land suitability for agriculture: Application to durum wheat cultivation in the region of Mleta in Algeria', *Computers Electron. Agric.* 83, 117-126.

Menze, B.H., Kelm, B.M., Masuch, R., Himmelreich, U., Bachert, P., Petrich, W., Hamprecht. F.A. 2009. A comparison of random forest and its Gini importance with standard chemometric methods for the feature selection and classification of spectral data. *BMC Bioinformatics* 10, 213.

Meroni, M., Atzberger, C., Vancutsem, C., Gobron, N., Baret, F., Lacaze, R., Eerens, H., Leo, O. 2013. Evaluation of agreement between space remote sensing SPOT-VEGETATION fAPAR time series. *IEEE Trans. Geoscience Remote Sens.* 51, 1951-1962.

Minervini, M., Giuffrida. M.V., Perata, P., Tsaftaris, S.A. 2017. Phenotiki: an open software and hardware platform for affordable and easy image-based phenotyping of rosette-shaped plants. *Plant J.* 90(1), 204–216. https :// doi.org/10.1111/tpj.13472

Mingwei, Z., Qingbo, Z., Zhongxin, C., Jia, L., Yong, Z., Chongfa, C. 2008. Crop discrimination in northern China with double cropping systems using Fourier analysis of time-series MODIS data. *Int. J. Appl. Earth Obs. Geoinf.* 10, 476–485.

Misra, G. 2012. Mapping specific cops and their phenology – multi sensor and temporal approach. MSc Thesis, University of Twente.

Mkhabela, M.S., Mkhabela, M.S., Mashinini, N.N. 2005. Early maize yield forecasting in the four agro-ecological regions of Swaziland using NDVI data derived from NOAA's-AVHRR. *Agric. Forest Meteorol.* 129, 1-9.

Moore, G.K. 1979. What is a picture worth? A history of remote sensing. *Hydrological Sci. Bulletin* 24(4), 477 – 485. https :// doi.org/10.1080/02626667909491887

Mu, E., Pereyra-Rojas, M. 2017. Practical decision making. Springer Briefs in Operations Research. http://dx.doi.org/10.1007/978-3-319-33861-3_2

Muchow, R.C, Sinclair, T.R., Bennett, J.M. 1990. Temperature and solar-radiation effects on potential maize yield across locations. *Agron. J.* 82, 338-343.

Munns, R., James, R.A., Sirault, X.R.R., Furbank, R.T., Jones, H.G. 2010. New phenotyp- ing methods for screening wheat and barley for beneficial responses to water deficit. *J. Exp. Bot.* 61, 3499–507.

Mutanga, O., Adam, E., Adjorlolo, C., Abdel-Rahman, E.M. 2015. Evaluating the robustness of models developed from field spectral data in predicting African grass foliar nitrogen concentration using WorldView-2 image as an independent test dataset. *Inter. J. Applied Earth Obs. Geoinform.* 34, 178-187.

Mutanga, O., Dube, T., Ahmed, F. 2016. Progress in remote sensing: vegetation monitoring in South Africa. *S. A. Geographical J.* 98, 461-471.

Mutanga, O., Skidmore, A.K. 2004. Narrow band vegetation indices overcome the saturation problem in biomass estimation. *Inter. J. Remote Sens.* 25, 3999-4014.

Mutanga, O., Skidmore, A.K., van Wieren, S. 2003. Discriminating tropical grass (Cenchrus ciliaris)

canopies grown under different nitrogen treatments using spectroradiometry. *ISPRS J. Photogram. Remote Sens.* 57: 263-272.

Mutka, A.M., Bart, R.S. 2015. Image-based phenotyping of plant disease symptoms. *Front. Plant Sci.* 5, 734.

Naik, H. S., Zhang, J., Lofquist, A., Assefa, T., Sarkar, S., Ackerman, D., Singh, A., Singh, A. K., Ganapathysubramanian, B. 2017. A real-time phenotyping framework using machine learning for plant stress severity rating in soybean. *Plant Methods* 13, 23. http://dx.doi.org/10.1186/s13007-017-0173-7

Nebiker, S., Annen, A., Scherrer, M., Oesch, D. 2008. A light-weight multispectral sensor for micro UAV– opportunities for very high resolution airborne remote sensing. *Int. Arch. Photogram. Remote Sens. Spat. Inf. Sci.* 37: 1193–1200.

Nichol, C.J., Huemmrich, K.F., Black, T.A., Jarvis, P.J., Walthall, C.L., Grace, J., Hall, F.J. 2000. Remote sensing of photosynthetic-light- use efficiency of boreal forest. *Agric. Forest Meteorol.* 101(2-3), 131-142.

Nikolakopoulos, K.G., Tsombos, P.I. 2009. Ameliorating the spatial resolution of high resolution satellite data for use in urban areas. In: Kerk, A., Rumor, M., Zlatanova, S., Fendel, E.M. (Eds). Urban and Regional Data Management, CRS Press. pp 399 - 408.

Nitze, I. Schulthess , U., Asche, H. 2012. Comparison of machine learning algorithms random forest, artificial neural network and support vector machine to maximum likelihood for supervised crop type classification. In: R.Q. Feitosa, G.A.O.P. Costa, C. M. Almeida, L. M. G. Fonseca, H.J.H. Kux (Eds.) Proceedings of the 4th GEOBIA (pp. 35–40). Rio de Janeiro, Brazil: Brazilian National Institute for Space Research.

Njogu, N.W., Kimurto, P., Kamau, A., Towett, B., Mulwa, R.M., Sharma, H.C., Gaur, P., Gangarao, R.N., Silim, S., Varshney, R. 2014. Genotypic performance and principal component analysis of yield and yield components of selected advanced chickpea (*Cicer arietinum* L.) breeding lines. *Egerton Univ. Res. Week Publ*. 5.

Njuguna, J.A.M., Kendera, J.G., Muriithi, L.M.M., Songa, S., Othiambo, R.B. 1990. Overview of maize diseases in Kenya. In: Maize Review Workshop in Kenya, Kenya Agricultural Reseatch Institute, Nairobi, Kenya. 52-62.

Nutter, F.W. Jr., Gleason, M.L. Jeneo, J.H., Christians, N.C. 1993. Assessing the Accuracy, Intra-rater Repeatability, and Inter-rater Reliability of Disease Assessment Systems. *Phytopathology* 83 (8), 806–812.

Nyamapfene, K. 1992. A geographical overview of the soils of Zimbabwe and their agricultural Potential. *Geographical Education Magazine (GEM)* 15(1), 63-73.

Oerke, E-C., Mahlein, A-K., Steiner, U. 2014. Proximal sensing of plant diseases. In: Gullino M., Bonants P. (eds) Detection and diagnostics of plant pathogens. Plant pathology in the 21st Century (Contributions to the 9th International Congress), vol 5. Springer, Dordrecht. https://doi.org/10.1007/978-94-017-9020-8_4

Osborne, S.L., Schepers, J.S., Francis, D.D., Schlemmer, M.R. 2002. Use of spectral radiance to estimate in-season biomass and grain yield in nitrogen and water stressed corn. *Crop Sci.* 42, 165–171.

Oumar, Z., Mutanga, O. 2013. Using WorldView-2 bands and indices to predict bronze bug (Thaumastocoris peregrinus) damage in plantation forests. *Intern. J. Remote Sens.* 34, 2236-2249.

Oumar, Z., Mutanga, O. 2014. Integrating environmental variables and WorldView-2 image data to

improve the prediction and mapping of Thaumastocoris peregrinus (bronze bug) damage in plantation forests. *ISPRS J. Photogram. Remote Sens.* 87, 39-46.

Pal, M. 2005. Random forest classifier for remote sensing classification. *Inter. J. Remote Sens* 26 (1), 217–222.

Pal, M., Foody, G. M. 2010. Feature selection for classification of hyperspectral data by SVM. *IEEE Trans. Geosci. Remote Sens.* 48(5), 2297–2307.

Pauli, D., Chapman, S.C. Bart, R., Topp, C.N., Lawrence-Dill, C.J., Poland, J., Gore, M.A. 2016. The quest for understanding phenotypic variation via integrated approaches in the field environment. *Plant Physiol.* 172, 622 – 634.

Peerbhay, K. Y., Mutanga, O., Ismail, R. 2013. Commercialtreespeciesdiscrimination using airborne AISA eagle hyperspectral imagery and partial least squares discriminant analysis (PLS-DA) in KwaZulu–Natal, South Africa. *ISPRS J. Photogram. Remote Sens.* 79, 19–28.

Pender, J., Place, F., Ehui, S. 2006. Strategies for sustainable land management in the East African highlands. Washington D.C.: International Food Policy Research Institute. http://dx.doi.org/10.2499/0896297578.

Perry, E.M., Brand, J. Kant, S., Fitzgerald, G.J. 2012. Field-based rapid phenotyping with unmanned aerial vehicles (UAV), Proceedings of the 16th Australian Agronomy Conference 2012, URL: http://www. regional.org.au/au/asa/2012/precision-a

Petropoulos, G.P., Kalaitzidisz, C. 2012. Multispectral vegetation indices in remote sensing: an overview. *Ecological Modeling* 2, 15-39.

Pillai, K.C.S. 1955. Some new test criteria in multivariate analysis. *Annals Mathemat. Stat.* 26 (1), 117 – 121.

Pfeiffer, T.W. 1996. Choosing soybean varieties from yield trials: multiple maturity groups and yield variability. *J. Production Agric.* 9(3), 371–376.

Phillips, R.L. 2010. Mobilizing science to break yield barriers. *Crop Sci.* 50, S-99–S-108. https://doi.org/10.2135/cropsci2009.09.0525

Pinter Jr, P.J., Hatfield, J.L., Schepers, J.S., Barnes, E.M., Moran, M.S., Daughtry, C.S.T., Upchurch, D.R. 2003. Remote sensing for crop management. Publications from USDA-ARS / UNL Faculty. Paper 1372. http://digitalcommons.unl.edu/usdaarsfacpub/1372

Pinter, Jr, P., Jackson, R.D., Gausman, H.D. 1985. Sun-angle and canopy-architecture effects on the spectral reflectance of six wheat cultivars. *Inter. J. Remote Sens.* 6, 1813–1825.

Pinter Jr, P., Jackson, R., Idso, S., Reginato, R. 1981. Multidate spectral reflectance as predictors of yield in water stressed wheat and barley. *Inter. J. Remote Sens.* 2, 43-48.

Poland, J. 2015. Breeding-assisted genomics. *Curr. Opin. Plant Biol.* 24,119–124. https://doi.org/10.1016/j.pbi.2015.02.009

Pontius, R. G., Millones, M. 2011. Death to Kappa: Birth of quantity disagreement and allocation disagreement for accuracy assessment. *Int. J. Remote Sens.* 32, 4407–4429.

Prasad, A.K., Chai, L., Singh, R.P., Kafatos, M. 2006. Crop yield estimation model for Iowa using remote sensing and surface parameters. *Inter. J. Applied Earth Obs. Geoinform.* 8, 26-33.

Prashar, A., Jones, H.G. 2014. Infra-red thermography as a high-throughput tool for field phenotyping. *Agron.* 4, 397–417.

Price, J.C. 1994. How unique are spectral signatures? *Remote Sens. Environ.* 49, 181-186.

Prince, S.D. 1990. High temporal frequency remote sensing of primary production using NOAA

AVHRR. pp 169–183. In: Steven, M.D., Clark, J.A. (Eds), Applications of remote sensing in agriculture, Butterworths: London, UK.

Prospere, K., McLaren, K., Wilson, B. 2014. Plant species discrimination in a tropical wetland using in situ hyperspectral data. *Remote Sens.* 6, 8494-8523.

Quarmby, N., Milnes, M., Hindle, T., Silleos, N. 1993. The use of multi-temporal NDVI measurements from AVHRR data for crop yield estimation and prediction. *Inter. J. Remote Sens.* 14, 199-210.

R Core Team. 2019. R: A language and environment for statistical computing. R Foundation for Statistical Computing, Vienna, Austria. http://www.r-project.org/index.html

Rajah, P., Odindi, J., Abdel-Rahman, E.M., Mutanga, O., Modi, A. 2015. Varietal discrimination of common dry bean (Phaseolus vulgaris L.) grown under different watering regimes using multi-temporal hyperspectral data. *J. Applied Remote Sens.* 9, 1931-3195

Rao, N.R. 2008. Development of a crop-specific spectral library and discrimination of various agricultural crop varieties using hyperspectral imagery. *Inter. J. Remote Sens.* 29 (1), 131–144.

Rasmussen, M.S. 1992. Assessment of millet yields and production in northern Burkina Faso using integrated NDVI from the AVHRR. *Inter. J. Remote Sens.* 13, 3431-3442.

Ray, D.K., Mueller, N.D., West, P.C., Foley, J.A. 2013. Yield trends are insufficient to double global crop production by 2050. *PLoS ONE* 8(6). https://doi.org/10.1371/journal.pone.0066428

Ray, D.K, Ramankutty,N., Mueller, N.D., West, P.C, Foley, J. A. 2012. Recent patterns of crop yield growth and stagnation. *Nature Communi.* 3, 1293. https://doi.org/10.1038/ncomms2296

Rembold, F., Atzberger, C., Savin, I., Rojas, O. 2013. Using low resolution satellite imagery for yield prediction and yield anomaly detection. *Remote Sens.* 5, 1704-1733.

Reshmidevi, T, Eldho, T., Jana, R 2009. A GIS-integrated fuzzy rule-based inference system for land suitability evaluation in agricultural watersheds. *Agric. Systems* 101, 101-109.

Roberts, M.J., Schlenker, W., Eyer, J. 2012. Agronomic weather measures in econometric models of crop yield with implications for climate change. *American J. Agric. Econ.* 95(2), 236–243; http://dx.doi.org/10.1093/ajae/aas047.

Rodier, A., Assié, J., Marchand, J.L., Hervé, Y. 1995. Breeding maize lines for complete and partial resistance to maize streak virus (MSV). *Euphytica* 81, 57–70. https://doi.org/10.1007/BF00022459

Rodríguez-Galiano, V. F., B. Ghimire, J. Rogan, M. Chica-Olmo, J. P. Rigol-Sanchez. 2012. An assessment of the effectiveness of a random forest classifier for land-cover classification. *ISPRS J. Photogram. Remote Sens.* 67, 93–104. http://dx.doi.org/10.1016/j. isprsjprs.2011.11.002.

Rogan, J., Franklin, J., Stow, D., Miller, J., Woodcock, C., Roberts, D. 2008. Mapping land-cover modifications over large areas: a comparison of machine learning algorithms. *Remote Sens. Environ.* 112 (5), 2272–2283.

Rojas, O. 2007. Operational maize yield model development and validation based on remote sensing and agro-meteorological data in Kenya. *Inter. J. Remote Sens.* 28, 3775-3793.

Römer, C., Bürling, K., Hunsche, M., Rumpf, T., Noga, G., Plümer, L. 2011. Robust fitting of fluorescence spectra for pre-symptomatic wheat leaf rust detection with support vector machines. *Comput. Electron. Agric.* 79, 180–188. http://dx.doi.org/10.1016/j.compag.2011.09.011

Rondeaux, G., Steven, M., Baret, F. 1996. Optimization of soil-adjusted vegetation indices. *Remote Sens. Environ.* 55, 95–107.

Rose, D.J.W. 1978. Epidemiology of Maize Streak Disease. *Annu. Rev. Entomol.* 23, 259–282.

Rossel, H.W., Thottappilly, G. 1985. Virus Diseases of Important Food Crops in Tropical Africa. pp. 61. Ibadan: International Institute of Tropical Agriculture (IITA).

Rossiter, D.G. 1990. ALES: A framework for land evaluation using a microcomputer. *Soil Use and Management* 6(1), 7-20.

Rotbart, N, Schmilovitch, Z., Cohen, Y., Alchanatis, V., Erel, R., Ignat, T., Shenderey, C., Dag, A., Yermiyahu, U. 2013. Estimating olive leaf nitrogen concentration using visible and near-infrared spectral reflectance. *Biosyst. Eng.* 114, 426–434.

Rouse Jr, J.W., Haas, R., Schell, J., Deering, D. 1974. Monitoring vegetation systems in the Great Plains with ERTS. NASA Special publication 351, 309-317. Washington D.C.: Goddard Space Flight Center.

Rozenstein, O., Paz-Kagan, T., Salbach, C., Karnieli, A. 2014. Comparing the effect of preprocessing transformations on methods of land-use classification derived from spectral soil measurements. *IEEE J. Sel. Top. Appl. Earth Obs. Remote Sens.* 99, 1–12.

Rudorff, B., Batista, G. 1990. Spectral response of wheat and its relationship to agronomic variables in the tropical region. *Remote Sens. Environ.* 31, 53-63.

Rukuni, M. Tawonezvi, C.K. Eicher, Munyki-Hungwe, M., Matondi, P.M. (Eds). 2006. Zimbabwe's Agricultural Revolution Revisited. University of Zimbabwe Publications, Harare. 728 p.

Rumpf, T., Mahlein, A.K., Steiner, U., Oerke, E.C., Dehne, H.W., Pluemer, L. 2010. Early detection and classification of plant diseases with support vector machines based on hyperspectral reflectance. *Comput. Electron. Agric.* 74, 91–99.

Rutkoski, J., Poland, J., Mondal, S., Autrique, E. González Pérez, L., Crossa, J., Reynolds, J., Singh, R. 2016. Canopy temperature and vegetation indices from high-throughput phenotyping improve accuracy of pedigree and genomic selection for grain yield in wheat. *G3: Genes, Genomes, Genetics* 6, 2799-2808. https://doi.org/10.1534/g3.116.032888/-/DC1

Saaty, T.L. 1977. A scaling method for priorities in hierarchical structures. *J. Mathemat. Psychology* 15(3), 234-281.

Saaty, T.L 1983. Priority setting in complex problems. *IEEE Trans. Engineer. Managem.* 30(3) 140-155.

Saaty, T.L. 1987. How to handle dependence with the analytic hierarchy process. *Mathematical Modelling* 9(3 – 5), 369-376.

Saaty, T.L. 1996. The analytic network process. Pittsburgh: RWS Publications.

Saaty, T., L. 2002. Decision making with the analytic hierarchy process. *Scientia Iranica* 9(3), 215-229.

Saaty, T.L. 2008. Decision making with the analytic hierarchy process. *Inter. J. Services Sci.* 1(1), 83-98.

Saaty, T.L. 2012. Decision Making for Leaders: The Analytic Hierarchy Process for Decisions in a Complex World. Third Revised Edition. Pittsburgh: RWS Publications. 343 p.

Saaty, T.L., Tran, L.T. 2007. On the invalidity of fuzzifying numerical judgments in the Analytic Hierarchy Process. *Mathematical Comp. Modelling* 46(7), 962-975.

Saeys, Y., Inza, I., Larrañaga, P. 2007. A review of feature selection techniques in bioinformatics. *Bioinformatics*, 23(19): 2507–2517.

Sakamoto, T., Gitelson, A.A., Arkebauer, T.J. 2013. MODIS-based corn grain yield estimation model incorporating crop phenology information. *Remote Sens. Environ.* 13, 215-231.

Sankaran, S., Khot, L.R., Carter, A.H., Garland-Campbell, K. 2014. Unmanned aerial systems based imaging for field-based crop phenotyping: winter wheat emergence evaluation, Paper No. 1914284. In: 2014 ASABE Annual International Meeting, Montreal, Quebec, Canada, July 13–14.

Sankaran, S., Khot, L.R., Espinoza, C.Z., Jarolmasjed, S., Sathuvalli, V.R., Vandemark, G.J., Miklas, P.

N., Carter, A.H., Pumphrey, M.O., Knowles, N.R., Pavek, M.J. 2015. Low-altitude, high-resolution aerial imaging systems for row and field crop phenotyping: A review. *European J. Agron.* 70, 112–123.

Sankaran, S., Maja, J.M., Buchanon, S., Ehsani, R. 2013. Huanglongbing (Citrus Greening) Detection Using Visible, Near-infrared and Thermal Imaging Techniques. *Sensors* 13, 2117-2130. http://dx.doi.org/10.3390/s130202117

Sankaran, S. Mishra, A. Ehsani, R., Davis, C. 2010. A review of advanced techniques for detecting plant diseases. *Comp. Electron. Agric.* 72, 1 –13.

Savary, S., Bregaglio, S., Willocquet, L., Gustafson, D., Mason D'Croz, D., Sparks, A., Castilla, N., Djurle, A. Allinne, C., Sharma, M., Rossi V., Amorim, L., Bergamin, A., Yuen, J., Esker, P., McRoberts, N., Avelino, J., Duveiller, E., Koo, J., Garrett, K. 2017 Crop health and its global impacts on the components of food security. *Food Secur.* 9, 311–27.

Savary, S., Ficke, A., Aubertot, J-N, Hollier, C. 2012. Crop losses due to diseases and their implications for global food production losses and food security. *Food Secur.* 4, 519–37.

Savitzky, A., Golay, M. J. 1964. Smoothing and differentiation of data by simplified least squares procedures. *Anal. Chem.* 36, 1627–1639.

Shanahan, J. F., Schepers, J. S., Francis, D. D., Varvel, G. E., Wilhelm, W. W., Tringe, J. M., Schlemmer, M. R., Major, D. J. 2001. Use of remote-sensing imagery to estimate corn grain yield. *Agron. J.* 93, 583–589.

Shepherd, D. N, Martin, D. P, Van Der Walt E, Dent K, Varsani A, Rybicki EP. 2010. Maize streak virus: an old and complex 'emerging' pathogen. *Molecular Plant Pathol.* 11, 1–12. https://doi.org/10.1111/j.13643703. 2009.00568.x

Sibanda, M., Murwira, A. 2012. The use of multi-temporal MODIS images with ground data to distinguish cotton from maize and sorghum fields in smallholder agricultural landscapes of Southern Africa. *Inter. J. Remote Sens.* 33(16), 4841-4855.

Sibanda, M. Mutanga, O., Rouget, M., Odindi, J. 2015. Exploring the potential of in situ hyperspectral data and multivariate techniques in discriminating different fertilizer treatments in grasslands. *J. Applied Remote Sens.* 9, 2015. http://dx.doi.org/10.1117/1.JRS.9.096033

Simko, I., Jimenez-Berni, J.A., Sirault, X.R.R. 2017. Phenomic approaches and tools for phytopathologists. *Phytopathology* 107, 6–17.

Schepers, J.S., Blackmer, T.M., Wilhelm, W.W., Resende, M. 1996. Transmittance and reflectance measurements of corn leaves from plants with different nitrogen and water supply. *J. Plant Physiol.* 148, 523-529.

Schlenker, W., Roberts, M.J. 2006. Nonlinear effects of weather on corn yields. *Rev. Agric. Econ.* 28(3), 391-398.

Schmidt, K. S., Skidmore, A.K. 2001. Exploring spectral discrimination of grass species in African rangelands. *Inter. J. Remote Sens.* 22 (17), 3421–3434.

Schmidt, K. S., Skidmore, A. K. 2003. Spectral discrimination of vegetation types in a coastal wetland. *Remote Sens. Environ* 85(1), 92-108.

Schoper, J.B., Lambert, R.J., Vasilas, B.L., Westgate, B.M. 1987. Plant factors affecting seed set in maize. *Plant Physiol.* 83, 121-125.

Schwartz, G. Ben-Dor, E., Eshel, G. 2013. Quantitative assessment of hydrocarbon contamination in soil using reflectance spectroscopy: A "Multipath" Approach. *Appl Spectrosc* 67(11), 1323-31. http://dx.doi.org/10.1366/13-07053.

See, L., Fritz, S., You, L., Ramankutty, N., Herrero, M., Justice, C., Becker-Reshef, I., Thomton, P., Erb, K., Gong, P., Tang, H., Velde van der, M., Ericksen, P., McCallum, I., Kraxner, F., Obersteiner, M. 2015. Improved global cropland data as an essential ingredient for food security. *Global Food Secur.* 4, 37-45.

Sellers, P.J. 1985. Canopy reflectance, photosynthesis and transpiration. *Inter. J. Remote Sens.* 6, 1335-1372.

Shanahan, J.F., Schepers, J.S., Francis, D.D., Varvel, G.E., Wilhelm, W.W., Tringe, J.M., Schlemmer, M.R., Major, D.J. 2001. Use of remote-sensing imagery to estimate corn grain yield. *Agron. J* 93. 583-589.

Shaw, D.T., Malthus, T.J., Kupiec, J.A. 1998. High-spectral resolution data for monitoring Scots pine (*Pinus sylvestris* L.) regeneration. *Inter. J. Remote Sens.* 19 (13), 2601-2608.

Sibanda, M. Mutanga, O., Rouget, M., Odindi, J. 2015. Exploring the potential of in situ hyperspectral data and multivariate techniques in discriminating different fertilizer treatments in grasslands. *J. Applied Remote Sens.* 9, 1931-3195.

Simone, G., Farina, A., Morabito, F.C., Serpico, S.B., Bruzzone, L. 2002. Image fusion techniques for remote sensing applications. *Information Fusion* 3: 3-15.

Singh, Q., Ganaparthysubramanian, B., Singh, A. K., Sarkar, S. 2016. Machine learning for high throughput stress phenotyping in plants. *Trends Plant Sci.* 21(2), 110 – 124.

Smith, A. M., Blackshaw, R. E. 2003. Weed-crop discrimination using remote sensing: a detached leaf Experiment. *Weed Technol.* 17, 811-820.

Sobhan, I. 2007. Species discrimination from hyperspectral perspective. PhD Dissertation. ISBN: 978-90-8504-809-1. International Institute for Geo-information Science and Earth Observation, Enschede, the Netherlands (ITC) ITC Dissertation Number: 150

Stafford, J.V. 2000. Implementing precision agriculture in the 21st century. *J. Agric. Engineer. Res* 76, 267-275.

Stanley, J., Boulton, M.I., Davies, J.W. 1999. Geminiviridae. In: Embryonic encyclopedia of Life Sciences. Nature Publishing Group, London. http://www.els.net/elsonline/html/

Steiner, F., McSherry, L., Cohen, J. 2000. Land suitability analysis for the upper Gila River watershed. *Landscape Urban Plan.* 50, 199-214.

Storey, H.H., 1925. The transmission of streak disease of maize by the leafhopper, Balclutha mbila Naude. *Ann. Appl. Biol.* 12, 422.

Storey, H.H., 1924. The transmission of a new plant virus disease by insects. *Nature* 114(2859), 245.

Storey, H.H., 1928. Transmission of maize streak disease. *Ann. Appl. Biol.* 15, 1-25.

Story, M., Congalton, R. 1986. Accuracy assessment: a user's perspective. *Photogram. Engineer. Remote Sens.* 52, 397 – 399.

Sugiura, R., Noguchi, N., Ishii, K. 2005. Remote-sensing technology for vegetation monitoring using an unmanned helicopter. *Biosyst. Eng*. 90, 369–379.

Svotwa, E., Masuka, J., Maasdorp, B., Murwira, A. 2013. Spectral indices: In-season dry mass and yield relationship of flue-cured tobacco under different planting dates and fertiliser levels. *ISRN Agron.* 2013. http://dx.doi.org/10.1155/2013/816767.

Swain, P.H. Fundamentals of pattern recognition in remote sensing. In Remote Sensing: The Quantitative Approach; Swain, P.H., Davis, S.M., Eds.; McGraw Hill: New York, NY, USA, 1978; pp. 136–187.

Swain, K.C., Zaman, Q.U. 2012. Rice Crop Monitoring with Unmanned Helicopter Remote Sensing

Images. In: Remote Sensing of Biomass - Principles and Applications, Lola Fatoyinbo (Ed.), ISBN: 978-953-51-0313-4, InTech. 322 p. Available from:
http://www.intechopen.com/books/remote-sensing-of-biomassprinciples-and-applications/rice-crop-monitoring-with-unmanned-helicopter-remote-sensing-images.

Sweeney, S., Ruseva, T., Estes, L., Evans, T. 2015. Mapping cropland in smallholder-dominated savannas: integrating remote sensing techniques and probabilistic modeling. *Remote Sens.* 7, 15295-15317.

Tanabata, T., Shibaya, T., Hori, K., Ebana, K., and Yano, M. 2012. Smart Grain: high-throughput phenotyping software for measuring seed shape through image analysis. *Plant Physiol.* 160, 1871–1880. http://dx.doi.org/10.1104/pp.112.205120

Tannura, M.A., Irwin, S.H., Good, D.L. 2008. Weather, Technology, and Corn and Soybean Yields in the U.S. Corn Belt. Marketing and Outlook Research Report 2008-01, Department of Agricultural and Consumer Economics, University of Illinois at Urbana-Champaign, February 2008. [http://www.farmdoc.uiuc.edu/marketing/morr/morr_archive.html].

Tardieu, F., Cabrera-Bosquet, L., Pridmore, T., Bennett, M. 2017. Plant Phenomics, From Sensors to Knowledge. *Current Biol.* 27 (15), R770-R783

Tattaris, M., Reynolds, M.P., Chapman S.C. 2016. A direct comparison of remote sensing approaches for high-throughput phenotyping in plant breeding. *Front. Plant Sci.* 7, 1131. http://dx.doi.org/10.3389/fpls.2016.01131

Thenkabail, P.S., Enclona, E.A., Ashton, M.S., Van Der Meer, B. 2004. Accuracy assessments of hyperspectral waveband performance for vegetation analysis applications. *Remote Sens. Environ.* 91(3), 354-376.

Thenkabail, P.S., Huete, A. J.G., Lyon, J.G., (Eds). 2011. Hyperspectral remote sensing of vegetation. CRC Press. CRC Press, Taylor and Francis Group. New York. 782 p.

Thenkabail, P.S., Gumma, M.K., Teluguntla, P., Mohammed, I.A. 2014. Hyperspectral remote sensing of vegetation and agricultural crops. *Photogram. Engineer. Remote Sens. (PE&RS)* 80, 697-723.

Thenkabail, P.S., Smith, R.B., De Pauw, E. 2000. Hyperspectral vegetation indices and their relationships with agricultural crop characteristics. *Remote Sens. Environ.* 71, 158–182 (2000).

Thenkabail, P.S., Smith, R. B., De Pauw, E. 2002. Evaluation of narrowband and broadband vegetation indices for determining optimal hyperspectral wavebands for agricultural crop characterization. *Photogram. Engineer. Remote Sens.* 68 (6), 607-621.

Thenkabail,P.S., Ward, A.D., Lyon, J.G. 1994. Landsat-5 Thematic Mapper models of soybean and corn crop characteristics. *Int. J. Remote Sens.* 15, 49–61.

Thompson, J.G. 1965. The soils of Rhodesia and their classification. Unpublished PhD thesis, Department of Soil Science Faculty of Agriculture, University of Natal, Pietermaritzburg, South Africa. 135 p.

Thompson, L.M. 1969. Weather and technology in the production of corn in the US corn belt. *Agron. J.* 61, 453-456

Thompson, L.M. 1970. Weather and technology in the production of soybeans in the central United States. *Agron J.* 62, 232-236.

Thompson, L.M. 1988. Effects of changes in climate and weather variability on the yields of corn and soybeans. *J. Production Agric.* 1, 20-27.

Tilman, D., Balzer, C., Hill, J., Befort, B.L. 2011. Global food demand and the sustainable intensification of agriculture. Proc. Natl. Acad. Sci. U.S.A. 108 (50), 20260–20264

Trachsel, S., Kaeppler, S. M., Brown, K. M., Lynch, J. P. 2011. Shovelomics: high-throughput phenotyping of maize (*Zea mays* L.) root architecture in the field. *Plant Soil* 341, 75–87. http://dx.doi.org/10.1007/s11104-010-0623-8

Triantafilis, J, Ward, W., McBratney, A. 2001. Land suitability assessment in the Namoi Valley of Australia, using a continuous model. *Soil Res*. 39, 273-289.

Tsai, F., Philpot, W. 1998. Derivative analysis of hyperspectral data. *Remote Sens. Environ.* 66, 41–51.

Tubiello, F. 2012. Climate change adaption and mitigation: challenges and opportunities in the food sector; Natural Resources Management and Environment Department: Rome, Italy

Tucker, C.J. 1979. Red and photographic infrared linear combinations for monitoring vegetation. *Remote Sens. Environ.* 8, 127-150.

Tucker, C.J. 1980. Remote sensing of leaf water content in the near infrared. *Remote Sens. Environ.* 10, 23-32.

Tung, C., Zhao, K., Wright, M.H., Ali, M.L., Jung, J., Kimball, J., Tyagi, W., Thomson. M.J., McNally, K., Leung, H., Kim, H., Ahn, S., Reynolds, A., Scheffler, B., Eizenga, G., McClung, A., Bustamante, C., McCouch, S.R. 2010. Development of a research platform for dissecting phenotype–genotype associations in Rice (Oryza spp.). *Rice* 3, 205–217. http://dx.doi.org/10.1007/s12284-010-9056-5

Turner, W., Spector, S., Gardiner, N., Fladeland, M., Sterling, E., Steininger, M. 2003. Remote sensing for biodiversity science and conservation. *Trends Ecol. Evolut*. 18, 306-314.

Uganda Bureau of Statistics (UBOS). 2007. Uganda National Household Survey, 2005/2006. Report on the agricultural module. Uganda Bureau of Statistics. Kampala, Uganda. 225 p.

Underwood, E., Ustin, S., DiPietro, D. 2003. Mapping non-native plants using hyperspectral imagery. *Remote Sens. Environ.* 86(2), 150-16.

Unganai, L.S., Kogan, F.N. 1998. Drought monitoring and corn yield estimation in Southern Africa from AVHRR data. *Remote Sens. Environ.* 63, 219-232.

Van Lanen, H.A.J. 1991. Qualitative and quantitative physical land evaluation: an operational approach, Unpublished PhD thesis, Agricultural University Wageningen, The Netherlands, 196 p.

Van Lanen, H.A.J., Bouma, J. 1989. Assessment of soil moisture deficit and soil aeration by quantitative evaluation procedures as opposed to qualitative methods. Symposium organized by the International Society of Soil Science (ISSS), Wageningen (Netherlands), 22-26 Aug 1988, Pudoc.

Van Ranst, E., Tang, H., Groenemam, R., Sinthurahat, S. 1996. Application of fuzzy logic to land suitability for rubber production in peninsular Thailand. *Geoderma* 70, 1-19.

Vincent, V., Thomas, R.G. 1960. An agricultural survey of Southern Rhodesia, Part 1, Agroecological Survey, Government Printer, Salisbury, 124 p.

Voogd, H. 1983. Multi-criteria evaluation for urban and regional planning. In: Zeleny, M. (Ed.), *Multiple Criteria Decision-making*, Springer, Berlin.

Wang, D., Kurle, J., De Jensen, C.E., Percich, J. 2004. Radiometric Assessment of Tillage and Seed Treatment Effect on Soybean Root Rot Caused by Fusarium spp. in Central Minnesota. *Plant Soil* 258, 319–331, http://dx.doi.org/10.1023/b:plso.0000016561.58742.93.

Wang, F. 1994. The use of artificial neural networks in a geographical information system for agricultural land-suitability assessment. *Environ. Planning* 26(2), 265-284.

Vaiphasa, C., Ongsomwang, S., Vaiphasa, T., Skidmore, A.K. 2005. Tropical mangrove species

discrimination using hyperspectral data: A laboratory study. *Estuarine, Coastal and Shelf Science* 65, 371-379.

Vaiphasa, C., Skidmore, A. K., de Boer W.F., Vaiphasa, T. 2007. A hyperspectral band selector for plant species discrimination. *ISPRS J. Photogram. Remote Sens.* 62, 225-235.

Valin, H., Sands, R.D., van der Mensbrugghe, D., Nelson, G.C., Ahammad, H., Blanc, E., Bodirsky, B., Fujimori, S., Hasegawa, T., Havlik, P., Heyhoe, E., Kyle, P., Mason-D'Croz, D., Paltsev, S., Rolinski, S., Tabeau, A., van Meijl, H., von Lampe, M., Willenbockel, D. 2013. The future of food demand: Understanding differences in global economic models. *Agric. Econ.* 45(1), 1–17.

Van Niel, T.G., McVicar, T.R. 2004. Determining temporal windows for crop discrimination with remote sensing: a case study in south-eastern Australia. *Comput. Electron. Agric.* 45, 91–108.

Vancutsem, C., Marinho, E., Kayitakire, F., See, L., Fritz, S. 2013. Harmonizing and combining existing Land Cover/Land Use datasets for cropland area monitoring at the African continental scale. *Remote Sens.* 5, 19–41.

Velásquez, A.C., Castroverde, C.D.M., He, S.Y. 2018. Plant-Pathogen Warfare under Changing Climate Conditions. *Curr. Boil.* 28, R619–R634.

Vergara-Díaz, O., Zaman-Allah, M.A., Masuka, B., Hornero, A., Zarco-Tejada, P., Prasanna, B.M., Cairns, J.E., Araus, J.L. 2016. A novel remote sensing approach for prediction of maize yield under different conditions of nitrogen fertilization. *Front. Plant Sci.* 18 May 2016 https://doi.org/10.3389/fpls.2016.00666

Vrindts, E., De Baerdemaeker, J. 1997. Optical discrimination of crop, weed and soil for on-line weed detection. In: Precision Agriculture '97, Proceedings of the First European Conference on Precision Agriculture, J. Stafford (ed.), BIOS Scientific Publishers, Oxford, 2: Technology, IT and Management, 537-544.

Vrindts, E. De Baerdemaeker, J., Ramon, H. 2002. Weed detection using canopy reflection. *Precis. Agric.* 3 (1), 63–80.

Wahab, I., Hall, O., Jirström, M. 2018. Remote Sensing of Yields: Application of UAV Imagery-Derived NDVI for Estimating Maize Vigor and Yields in Complex Farming Systems in Sub-Saharan Africa. *Drones* 2, 28. https://doi.org/10.3390/drones2030028

Wahabzada, M., Mahlein A-K., Bauckhage, C., Steiner, U., Oerke, E-C., Kersting, K. 2015. Metro maps of plant disease dynamics--automated mining of differences using hyperspectral images. *PloS One* 10, e0116902.

Waldner, F., Fritz, S., DiGregorio, A., Defourny, P. 2015. Mapping priorities to focus cropland mapping activities: fitness assessment of existing global, regional and national cropland maps. *Remote Sens.* 7, 7959-7986.

Walker, P.J.C., 1989. Famine Early Warning Systems. Earthscan Publications Ltd, London. 196 p.

Walsh, O.S., Klatt, A., Solie, J., Godsey, C., Raun, W. 2013. Use of soil moisture data for refined GreenSeeker sensor based nitrogen recommendations in winter wheat (Triticum aestivum L.). *Preci. Agric.* 14, 343-356.

Walter, A., Studer, B., Kölliker, R. 2012. Advanced phenotyping offers opportunities for improved breeding of forage and turf species. *Ann. Bot.*, mcs026.

Wang, D., Kurle, J.E., Estevez de Jensen, C., Percich, J.A. 2004. Radiometric assessment of tillage and seed treatment effect on soybean root rot caused by *Fusarium* spp. in central Minnesota. *Plant and Soil*, 258, 319 –331.

Wang, C., Fritschi, F.B., Stacey, G., Yang, Z.W. 2011. Phenology-based assessment of perennial energy crops in North American tallgrass prairie. *Annals Assoc. American Geographers* 101 (4), 742–751.

Wardlow, B.D., Egbert, S.L. 2008. Large-area crop mapping using time-series MODIS 250 m NDVI data: An assessment for the U.S. Central Great Plains. *Remote Sens. Environ.* 112, 1096–1116.

Webb, M.B., 1987. Species recognition in Cicadulina leaflaoppers (Hemiptera: Cicadellidae), vectors of pathogens of Gramineae. *Bull. Ent. Res*. 77, 683-712.

Weber, V.S., Araus, J.L., Cairns, J.E., Sanchez, C., Melchinger, A.E., Orsini, E. 2012. Prediction of grain yield using reflectance spectra of canopy and leaves in maize plants grown under different water regimes. *Field Crops Res*. 128, 82–90. http://dx.doi.org/10.1016/j.fcr.2011.12.016

Wei, X., Xu, J., Guo, H., Jiang, L., Chen, S., Yu, C., Zhou, Z., Hu, P., Zhai, H., Wan, J. 2010. DTH8 suppresses flowering in rice, influencing plant height and yield potential simultaneously. *Plant Physiol*. 153, 1747–1758.

Westerhuis, J.A., Hoefsloot, H.C.J., Smit, S., Vis, D.J., Smilde, A.K., van Velzen, E.J.J., van Duijnhoven, J.P.M., van Dorsten, F.A. 2008. Assessment of PLSDA cross validation. *Metabolomics* 4 (1), 81-89.

White, J.W., Andrade-Sanchez, P., Gore, M.A., Bronson, K.F., Coffelt, T.A., Conley, M.M., Feldmann, K.A., French, A.N., Heun, J.T. Hunsaker, D.J. 2012. Field-based phenomics for plant genetics research. *Field Crops Res.* 133, 101–112.

Wiegand, C., Gerbermann, A., Gallo, K., Blad, B., Dusek, D. 1990. Multisite analyses of spectral-biophysical data for corn. *Remote Sens. Environ.* 33, 1-16.

Wiegand, C.L., Richardson, A.J. 1990. Use of spectral vegetation indices to infer leaf area, evapotranspiration and yield: I. Rationale. *Agron. J.* 82, 623–629.

Wiegand, C.J., Richardson, A.J., Escobar, D.E., Gerbermann, A.H. 1991. Vegetation indices in crop assessments. *Remote Sens. Environ*. 35, 105–119.

Wiegand, C.L., Richardson, A.J., Jackson, R.D., Pinter, P.J., Aase, J.K., Smika, D.E., Lautenschlager, L.F., McMurtrey, J. 1986. Development of agrometeorological crop model inputs from remotely sensed information. *IEEE Trans. Geosci. Remote Sens.* GE-24(1), 90-98.

Wilks, S.S. 1935. On the independence of k sets of normally distributed statistical variables. *Econometrika* 3 (3), 309-326.

Wilson, J.H. Zhang, C., Kovaes, J.M. 2014. Separating crop species in north-eastern Ontario using hyperspectral data. *Remote Sens.* 6, 925–945.

Wise, B.M., Gallagher, N.B., Bro, R., Shaver, J.M., Windig, W., Koch, R.S. 2006. Chemometris Tutorial for PLS_Toobox and Solo. Eigenvector Research, Inc., 3905 West Eaglerock Drive, Wenatchee, WA 98801 USA, 2006.

Wójtowicz, M., Wójtowicz, A., Piekarczyk, J. 2016. Application of remote sensing methods in agriculture. *Comm. Biometry Crop Sci.* 11, 31-50.

Wold, S., Sjöström, M., Eriksson, L. 2001. PLS-regression: A basic tool of chemometrics. *Chemom. Intell. Lab. Syst.* 58, 109–130.

World Bank. 2010. Global strategy to improve agricultural and rural statistics. Economic Sector Work No. 56719-GLB. Washington DC: The International Bank for Reconstruction and Development / The World Bank

Worley, B., Powers, R. 2013. Multivariate analysis in metabolomics. *Current Metabolomics* 1, 92-107.

Wu, C., Wang, L., Niu, Z., Gao, S., Wu, M. 2010. Nondestructive estimation of canopy chlorophyll content using Hyperion and Landsat/TM images. *Inter. J. Remote Sens.* 31, 2159-2167.

Wulder, M.A., Masek, J.G., Cohen, W.B., Loveland, T.R., Woodcock, C.E. 2012. Opening the archive:

How free data has enabled the science and monitoring promise of Landsat. *Remote Sens. Environ.* 122, 2-10

XLSTAT. 2013. Complete Data Analysis Software System and Statistics Add-in for MS Excel, Version 2014, 2nd ed., Statistical Innovations, Belmont, United States (2013).

Yang, W., Guo, Z., Huang, C., Duan, L., Chen, G., Jiang, N., Fang, W., Feng, H., Xie, W., Lian, X., Wang, G., Luo, Q., Zhang, Q., Liu, Q., Xiong, L. 2014. Combining high-throughput phenotyping and genome-wide association studies to reveal natural genetic variation in rice. *Nat. Commun*. 5, 5087. http://dx.doi.org/10.1038/ncomms6087

Yue, J., Feng, H., Jin, X., Yuan, H., Li, Z., Zhou, C., Yang, G., Tian, Q. 2018. A comparison of crop parameters estimation using images from UAV-mounted snapshot hyperspectral sensor and high-definition digital camera. *Remote Sens*. 10, 1138. http://dx.doi.org/10.3390/rs10071138

You, L., Wood, S.R., Wood-Sichra, U. 2007. Generating plausible crop distribution maps for sub-Saharan Africa using a spatial allocation model. *Information Develop.* 23 (2-3), 151-159.

Zaman-Allah, M.,Vergara, O., Araus, J., Tarekegne, A., Magorokosho, C., Zarco-Tejada, P., Hornero, A., Albà, A. H., Das, B., Craufurd, P. 2015. Unmanned aerial platform based multi-spectral imaging for field phenotyping of maize. *Plant Methods* 11, 35. https://doi.org/10.1186/s13007-015-0078-2

Zarco-Tejada, P.J., Catalina, A., González, M.R., Martín, P. 2013. Relationships between net photosynthesis and steady-state chlorophyll fluorescence retrieved from airborne hyperspectral imagery. *Remote Sens Environ* 136, 247–258.

Zarco-Tejada, P. J., González-Dugo, V., Jimenez-Berni, A. 2012. Fluorescence, temperature and narrow-band indices acquired from a UAV platform for water stress detection using a micro-hyperspectral imager and a thermal camera. *Remote Sens. Environ*. 117, 322–337.

Zhang, C., Kovacs, J.M. 2012. The application of small unmanned aerial systems for precision agriculture: a review. *Precis. Agric*. 13: 693–712.

Zhang, H., Lan, Y., Suh, C.P., Westbrook, J.K., Lacey, R., Hoffmann, W.C. 2012. Differentiation of cotton from other crops at different growth stages using spectral properties and discriminant analysis. *Am. Soc. Agric. Biol. Eng.* 55(4), 1623–1630.

Zhang, J., Su, Y., Wu, J., Liang, H. 2015. GIS based land suitability assessment for tobacco production using AHP and fuzzy set in Shandong province of China. *Comp. Electron. Agric.* 114, 202-211

Zhao, Y., Gong, P., Yu, L., Hu, L., Li, X, Li, C, Zhang, H., Zheng, Y., Wang, J., Zhao, Y., Cheng, Q., Liu, C., Liu., S., Wang, Z. 2014. Towards a common validation sample set for global land-cover mapping. *Inter. J. Remote Sens.* 35 (13), 4795-4814.

Zhou, X., Zheng, H.B., Xu, X.Q., He, J.Y., Ge, X.K., Yao, X., Cheng, T., Zhu, Y., Cao, W.X., Tian, Y.C. 2017. Predicting grain yield in rice using multi-temporal vegetation indices from UAV-based multispectral and digital imagery. *ISPRS J. Photogram. Remote Sens.* 130, 246–255. http://dx.doi.org/10.1016/j.isprsjprs.2017.05.

Zwiggelaar, R. 1998. A review of spectral properties of plants and their potential use for crop/ weed discrimination in row-crops. *Crop Protect.* 17, 189–206.